Copyright is owned by the Author of the thesis. Permission is given for a copy to be downloaded by an individual for the purpose of research and private study only. The thesis may not be reproduced elsewhere without the permission of the Author.

Modelling Infectious Diseases in Multiple Species.

A thesis presented in partial fulfilment of the requirements for the degree of

Doctor of Philosophy
in
Applied Mathematics

at Massey University, Albany
New Zealand.

Andrea Babylon

July 3, 2019

Abstract

Leptospirosis is an infectious disease caused by bacteria in the genus *Leptospira* and is considered as the disease of interest in this thesis. It is the highest occurring occupational disease in New Zealand and the country has one of the highest (per capita) incidences of human leptospirosis in the world. Transmission commonly occurs by contact with infectious animals, or materials contaminated by them. The disease is the cause of great financial losses to the country due to both the medical cost of treating infectious individuals, as well as due to production losses in the farming industry. As such, studying the dynamics of infection and possible control measures for the disease in animals, which also minimises exposure to humans, is an important area of research.

This thesis aims to develop New Zealand specific models demonstrating the dynamics of leptospirosis infection within and between multiple host species, specifically rats and sheep, thus contributing towards an understanding of not only how ecological exchanges between different host populations influence the spreading of the disease, but also how the incidence of leptospirosis may be diminished. This is achieved with the use of compartmental SI type models of increasing complexity, with simpler models used as building blocks in constructing the more advanced systems.

The models presented involving only rats consider an age structure within the population, with different behaviours and infection risks associated with each age class. Models involving only sheep focus on the periodic forcing implemented on the host population by the farmer, and also include an age structure, albeit a somewhat simpler one than the one in the rat models. The seasonal forcing on the livestock population results in a cyclical system which is displayed using limit cycle diagrams. This behaviour is mirrored in the model considering both host species in concert. Each model presents a variety of results, including bifurcation diagrams and quasi-basic reproduction numbers which display the behaviour of the system. The effect of varying various parameter values on the system is explored, and how these may change in relation to climate change is discussed. Parameter values used in numerical results demonstrating analytical ones are New Zealand specific and the model is used to predict conditions under which the infection will persist in the population.

Acknowledgements

This thesis was supported by an INMS, Massey University PhD scholarship and The New Zealand Federation of Graduate Women (Inc), North Shore Branch.

To my supervisor, Professor Mick Roberts, for making me a better writer, researcher and mathematician. Your firm but gentle honesty and guidance meant I always knew where I stood. I couldn't have done this without your unwavering calm and support.

To my co-supervisor, Professor Emeritus Graeme Wake, for challenging me by nudging me in directions I didn't always want to go, you have made me a better mathematician and researcher. Thank you for your kindness and support throughout this endeavour.

To the thesis examiners, Professor Larry Forbes, Dr Tammy Lynch and Professor Michael Plank, I am humbled by the care and effort you went into examining the manuscript. Your comments and constructive criticisms have made for a better thesis. Thank you.

To my partner, Mr Jarod Young, for your all-encompassing support. Finally, to the many colleagues, friends and family that have contributed along the way. You know who you are. Thank you.

A paper, based on section 3.1 of the thesis, has been published in the following.

A.M. Babylon, M.G. Roberts and G.C. Wake, Modelling leptospirosis in livestock, Theoretical Population Biology, 2018, 121, p26-32

Contents

List of Figures

List of Tables

Chapter 1

Introduction

1.1 What is Leptospirosis and Why Study It?

Leptospirosis is an infectious disease caused by the bacteria *Leptospira*. Being a zoonosis, it can be passed from animals to humans, and it is of particular importance in New Zealand due to the high rates experienced in the population [1, 2]. The per capita rates of human leptospirosis in New Zealand are among the highest in the world and akin to lesser developed countries such as Uruguay, Cuba and Nicaragua [2, 3]. It is the highest occurring occupational disease in the country, believed to be largely due to the subtropical climate paired with the importance of the livestock industry [4–6]. This results in an environment which is ideal for the survival of the bacteria outside the host, a large population of animal hosts and a large at-risk population of human hosts with frequent contact with animal hosts.

Several *Leptospira* pathogen types (serovars sv) exist. Six out of the 250 known serovars are present in New Zealand: Hardjo, Pomona, Ballum, Coppenhageni, Balcanica and Tarassovi [1, 4]. In New Zealand, human cases are most commonly caused by Hardjobovis and Pomona, both of which infect livestock, as well as by serovar Ballum [4, 5]. Every serovar tends to have a preferred host species and almost every mammal has a serovar that can infect it [1, 5]. The bacteria can still infect other species which they are less adapted to; however, and which are possibly more resistant to it [5]. If they have access to water, leptospira can survive in the environment for a significant amount of time [7]. This, coupled with their ability to infect a wide variety of host species that then shed the

bacteria in their urine for prolonged periods of time, makes leptospirosis a difficult disease to control and one impossible to eradicate [8].

Hosts become infected when the bacteria, or material contaminated with the bacteria, is ingested internally or comes into contact with broken skin or mucus membranes [1, 9]. Transplacental and sexual transmission may also be possible routes of transmission [10]. Once infected, the bacteria reproduce throughout the body over the course of which there may be a phase during which the host displays signs of infection [1]. After the infection stage is over, the bacteria colonise the kidneys and are then shed out through the urine [1]. This is one of the main infectious substances humans are exposed to [1]. Farmers, veterinarians and meat workers frequently come into contact with urine due to close contact with livestock. Abattoir workers working at the start of the slaughtering process are at particular risk, as many animals spray during the stunning process. This urine can not only directly infect workers at the beginning of the slaughter line, but may also contaminate the carcass, which is handled by workers further down the production line. Abattoir workers handling internal organs, such as the liver, kidney or reproductive organs, are also likely to become exposed [5]. Strict personal hygiene practices are very important in these lines of work. Hands and other items contaminated with urine not properly washed before coming into contact with the mouth, eyes or nose (as in eating, smoking, rubbing ones eyes or blowing ones nose) can cause a person to become infected. Other occupations likely to experience risk are bush working, timber working and pest control. Individuals in these lines of work are likely to come into contact with contaminated material originating from wildlife such as rats and possums. Infection can also be gained through leisure activities such as swimming or kayaking in natural bodies of water such a lakes and streams [7]. This would most likely occur due to the ingestion of contaminated water, but potentially also through skin weakened by prolonged water exposure and, of course, through cuts or grazes [11]. Flooding can increase environmental transmission rates as well by transporting contaminated material into the paths of humans who may not possess the proper attire to clean up safely without becoming exposed [5].

The range of symptoms humans experience once infected are broad and can range from asymptomatic (no symptoms) to fatal. Flu like symptoms are common, resulting in an average of six weeks absence from work [5, 12]. Due to the broad range of symptoms, the disease is often

misdiagnosed or the patient does not seek medical attention, thus leading to underreporting. In New Zealand 60% of reported cases are hospitalised [13]. The human impacts of the disease have both financial as well as personal costs associated with them, with long term health consequences being common. These are covered in further detail in chapter 5.

The disease causes a financial burden on the country due to infection in livestock as well. It is believed that leptospiral infection causes abortions and decreased weight gain in farmed animals, both of which negatively impact production and thus the bottom line for farmers [14]. Altogether, it is estimated that the disease costs the country millions of dollars each year due to medical expenses, lost productivity in the work place, and decreased yield for farmers [15].

The disease is not transmissible between humans and there are presently no human vaccines available, so the impact of reducing infection rates in animals in order to protect people needs to be investigated as a control mechanism. One such method may be the use of animal vaccines, which also have the potential to increase stock yields (this has been shown in studies involving deer and pigs). Vaccination during pregnancy in particular can provide some immunity to young once suckling and this is explored in the multiple age class livestock models (section 3.2, section 3.3 and section 3.4) in the thesis [5].

The human and financial effects of the disease are not the only reasons it is necessary to research leptospirosis. As we enter an age of antibiotic resistance, alternative treatment or preventative measures for not only leptospirosis, but other bacterial diseases also, are imperative. By limiting the use of antibiotics, the progression of resistance of bacteria to antibiotics may be slowed, thus buying more time to create new solutions to bacterial infections not only in livestock, but also in humans, for which antibiotics can be lifesaving in severe leptospirosis cases [16].

1.2 The Mathematics

While there are many models for leptospirosis overseas, there do not appear to be any specific to New Zealand. Traditional studies in modelling the spread of infectious diseases have involved simple predator-prey type models involving only one infectious agent and one host. Multiple species

models typically involve hosts of the same disease where transmission can take place. They do not usually include ecological exchanges, such as consumer resource-relations (feeding relations) and competition, between or even within species. There has been a shift in the theoretical literature, however, as studies have implied that ecological exchanges have large effects on the dynamics of wildlife communities even if the interaction is not related to the transmission of the agent. Hathaway, for example, found that the infection of Balcanica in the common brushtail possum appears to have an age structure [17]. Mature adult possums were found to have a higher incidence of infection than juveniles [17]. Multiple studies suggest that an age structure may exist in leptospirosis infection as well.

The dynamics of the spread of leptospirosis among multiple host species is not known. How the bacteria changes the dynamics of the host populations needs to be explored, as well as how the interaction of the disease between different animal species changes the disease dynamics. This would help to describe the spread of infectious diseases within wildlife communities and its impact on the population of different species which could eventually result in increased, or even new, transmission to humans. A strategic model of leptospirosis has been constructed by Heuer et al., while Roberts and Heesterbeek developed an analytical model of multi-host pathogen transmission [14, 18]. There is a clear need for the strategic and analytical models to be combined.

This thesis develops a multi-species mathematical model to describe the spreading and interaction of leptospirosis between multiple animal host species and is parameterised with data appropriate for leptospirosis in New Zealand. Three chapters are used to cover three main mathematical models, one each for wildlife, livestock and combined wildlife-livestock. Each model chapter progresses through various stages, beginning with a simple base model, before moving to a more complicated one. This allows for a gentle introduction for the reader into each model type and the various mathematical techniques used in each.

There are multiple methods and models that can be used to describe the spreading of an infectious disease. A popular approach, and the one used here, is called a compartmental model. This method divides the population(s) of interest into categories according to their infectious state and/or other characteristics. For example, in an SI type model, susceptible individuals are included in the S compartment, while infectious

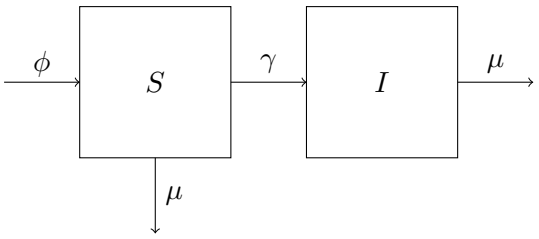

Figure 1.1: *Schematic of a simple, compartmental, SI type model.*

individuals are included in the I compartment. Other compartments, such as E for exposed, and R for recovered or removed, can also be included. When combined, compartments in a model sum to the population total. Differential equations are used to describe the movement of individuals into and out of each compartment. As an example, in an SI type model, an individual may be born into the susceptible compartment at rate ϕ, before becoming infected via density dependent contacts and moving into the infectious compartment at rate γ. Once an individual is infected, it remains infected for the duration of its life. Individuals from both compartments may leave the system via death at rate μ. This simple system is demonstrated in the schematic in figure 1.1 and represented mathematically by the equations 1.1-1.2. Note that the sum of the two compartments equates to the total population, that is, $S + I = N$.

$$\dot{S} = \phi N - \gamma S \frac{I}{N} - \mu S, \tag{1.1}$$

$$\dot{I} = \gamma S \frac{I}{N} - \mu I. \tag{1.2}$$

In compartmental models involving multiple infectious compartments (such as a model involving multiple age classes) the next generation matrix is used to describe the expected number of infections produced in each compartment caused by an infectious individual in each other compartment. That is, each entry $K(i, j)$ in the matrix describes the expected number of infections in population i caused by an infectious individual in population j. This matrix can be constructed in one of two ways; either by using a "recipe", which is described in further detail in section 2.1, or by using biological interpretation. This matrix can then be used to calculate the basic reproduction number, R_0, simply by calculating its spectral radius (dominant eigenvalue). The basic reproduction number is an important measure in that it provides a threshold quantity for the

spreading of an infection. It is defined as "the expected number of secondary cases produced by a typical infected individual during its entire period of infectiousness in a completely susceptible population" [19]. So, when $R_0 < 1$, an initial infectious individual is expected to infect fewer than one other individual, and as such, infection within the population is not expected to take off. Conversely, when $R_0 > 1$, an initial infectious individual is expected to infect more than one other individual and the infection is expected to spread within the population.

1.2.1 Wildlife Model

The first mathematical chapter in the thesis uses a model presented by Holt et. al. for a rodent in Tanzania to construct a model for rats in New Zealand [20]. Rats are a good choice of wildlife host species for the model in terms of the interaction likely to occur between the wildlife host and the livestock host and also due to the respective serovars adapted to each host.The model is an SI type model considering multiple age classes and transmission types within the host species and a free living leptospire compartment. Rather than have a susceptible compartment, this model includes a compartment for the total number of rats per hectare, N_a, in each age class a. This allows the exploration of infection in the host species as the total population varies over time. The usual infectious compartment, I_a, for each age class is also included. Where possible, the model here finds analytical solutions to the system, thus improving on the Holt model, which uses parameter values that may or may not be correct. The model by Holt considers a pulse in the rat population as a result of seasonal trends in breeding, whereas all parameters in the model presented here are considered constant due to the location's temperate climate. In the multiple species model later in the thesis, seasonal variation is introduced via season dependent livestock management practices (discussed in further detail below). The rat chapter is broken up into sections depending on the number of age classes considered, with the first, second and third sections corresponding to one, two and three age classes respectively. Each sub-model is further broken up into five simplifications by setting various parameters equal to zero, or by reducing the number of differential equations. This allows the analysis of each submodel to build up in complexity over the course of the chapter. The model also stands as inspiration for the livestock model in the chapter to follow. Two main components are carried over. These are the differential equation for free living leptospires, and a non-linear saturation term for environmental

transmission to the host. The equation describing the change in leptospiral population includes a shedding (by the host) component, which changes depending on which and how many host species are present in the model. It also includes a leptospire death component, which is used as a control parameter. The non-linear saturation term $\frac{L}{L+H}$, where L is the free living leptospire population per hectare and H is the density of leptospires per hectare at which transmission rate from the environment is half the transmission coefficient, allows infection transmission to increase as free living leptospires increase, while at the same time limiting the effect of transmission to the host as the density of free living leptospires becomes large.

1.2.2 Livestock Model

The second mathematical chapter in the thesis uses components of the wildlife model to build a model for sheep. Sheep are not only a commonly farmed animal in New Zealand, but are believed to be an emerging reservoir of importance, particularly for abattoir workers [5]. In this chapter, a flock of sheep is introduced into a field (an area in which livestock are confined) at the beginning of each year. The host population density is now set to be fixed and so the model considers both susceptible and infectious compartments for the host. The chapter is again broken up by section, with submodels building up to include multiple age classes, as well as other components in the model such as the number of fields, and potential immunity in particular age classes. Sheep are removed from the field after some time depending on their age class and either removed from the system completely, to be replaced with a new cohort of sheep, or potentially moved to another field. This is done in accordance to local farming practices (C. Heuer, personal communication, 2014). As for the wildlife model, a compartment for free living leptospires is included in the model for each field and the leptospire death rate is used as a control parameter. Each field remains empty for some portion of the year, allowing it to recover from infection as the free living leptospires die off. The seasonal forcing incorporated into the model demonstrates how incentives by the farmer can impact on infection rates within a flock. This model structure is also influenced by research showing that infection rates of paratuberculosis (caused by Mycobacterium avium subspecies paratuberculosis) in red deer can be decreased by 50% by moving the deer to different grazing locations on a regular basis, rather than grazing them permanently on the same pasture [21]. While this method resulted in

higher grazing rates of the used fields (for three months at a time), the field was then left ungrazed for a period of time (one month, in this particular study) which not only allowed it to recover, but prevented infection to other livestock by allowing enough time to elapse for the free living leptospires in the environment to die.

1.2.3 Combined Model

The third and final mathematical chapter in the thesis combines the wildlife and livestock models to demonstrate how the indirect interaction between the two host species influences infection rates in each population. Here, the field hosting the sheep is assumed to be bordered by New Zealand native forest (bush) from which rats enter the field in order to drink from the watering trough. In this way, the field becomes contaminated by leptospires shed into the field by the rats and the rats become infected by leptospires shed by the sheep. These models are more than just the sum of their respective parts. New aspects must be incorporated into the system as a result of the interaction between the two host species. The birth rate for rats is now included as a control parameter along with the leptospire death rate. This pair of parameters is used to simulate the effects of climate change on the system, demonstrating the effects extreme weather events may have on infection rates in the future. The proportion of time spent by rats in various environments is introduced into the system as a new parameter and is explored in concert with the climate change parameter pair; however, it is difficult to predict how these proportions may change is response to severe climatic events and so they are not coupled with the climate change parameters directly. None-the-less, the models, building up from the most simple pairing of the single species models, to the most complex, demonstrating the relationship between the two host species and its effect on infection rates in both populations.

1.2.4 Risk to Humans

The final chapter in the thesis discusses in further detail the implications the disease has on New Zealanders, not only on a personal level, but also on an economic one. New Zealand specific risk factors, serovars, prevention strategies and exacerbating factors are discussed. How the models presented in the thesis relate to human infection is deliberated in this chapter as well as in the conclusion.

Chapter 2

The Wildlife Model

This chapter is based on a paper by Holt et. al. which presents a numerical SI model of leptospirosis in an African rodent [20]. The model includes three age classes, resulting in six differential equations for the rodent, as well as one equation for free living leptospires. In order to consider the distinct dry season observed in the location of the study, during which breeding in the local rat population does not occur, the model includes seasonality. New Zealand, however, has a temperate climate and rats can breed year round [22–25]. Breeding behaviour in NZ forest rats does exhibit seasonal trends and these effects may be at least partially due to decreased access to water during certain times of year. However, as the focus here is on rats on farms with constant access to water via watering troughs provided for livestock, it is assumed that birth pulses in the local rat population are unlikely to occur and so are not included [23, 25–28].

As in the Holt model, infectious rats are considered to have the same mortality rate as susceptible rats. This is due to the serovar chosen in future chapters being host adapted. As such, the infectious rats are assumed to be asymptomatic [14, 29–31].

Three variations of the Holt model are explored here. The first model involves only one age class, the second involves two and the last involves all three age classes. Each age class consists of one equation for the total rat population and one for the infectious rat population.

Each age class model is also broken down into five simplifications (refer to the chapter's three sub-chapters section 2.1, section 2.2 and section 2.3

for model equations):
Simplification 1: The environmental transmission coefficient $\gamma = 0$. This eliminates environmental transmission from the model and decouples the system of equations. Leptospirosis is transmitted through sexual transmission only and the problem is one-dimensional.
Simplification 2: Sexual transmission $\beta = 0$ and the rate of change of the free living leptospire population $\dot{L} = 0$. This eliminates sexual transmission from the model and keeps the leptospire population constant. In this simplification, the time scale of $\dot{I}$, the infectious rat population, is much slower than that of $\dot{L}$, the free living leptospire population. Leptospirosis is transmitted through environment transmission only and the problem is one-dimensional.
Simplification 3: Sexual transmission $\beta \neq 0$ and the rate of change of the free living leptospire population $\dot{L} = 0$. Both sexual and environmental transmission occur, the leptospire population remains constant and the problem is one-dimensional.
Simplification 4: Sexual transmission $\beta = 0$ and the rate of change of the free living leptospire population $\dot{L} \neq 0$. This eliminates sexual transmission and allows the leptospire population to vary. Leptospirosis is transmitted through the environment only. The system is now coupled and the problem is two-dimensional.
Simplification 5: Sexual transmission $\beta \neq 0$ and the rate of change of the free living leptospire population $\dot{L} \neq 0$. This is the full model as in [20]. Both sexual and environmental transmission occur and the leptospire population can vary with time. The problem is two-dimensional.

Unless needing to be calculated numerically, for each simplification, fixed points and the conditions under which they are feasible are found, stability is analysed, a bifurcation diagram is produced and the next generation matrix, K, and basic reproduction number, R_0 are found. Also, where possible, trapping regions and Dulac's criterion are used to show that models are well posed, biologically feasible and that no periodic solutions exist. To be considered "feasible", for biological reasons, a model's (including simplifications) fixed points must be real and positive.

In each model, the dynamics of the infection free system (the equations considering the total rat population including both susceptible and infectious rats) is independent of the infectious system (the equations considering the infectious rat populations only and the free living leptospire population). As such, it can be assumed that the total rat

populations for each age class have reached a steady state. These steady state values, indicated with a superscript $*$ (ie. N_J^*, N_S^* or N_A^* where N_{ac} is the total rat density of age class ac in a given area), can then be used as constants when solving the infectious system for fixed points.

The true trivial steady state (when all population densities are zero) exists for all simplifications of all models. If the total rat population for every age class in a model is equal to zero, there are no potential hosts in that population to become infectious and due to the nature of the leptospire life cycle, this population then also reaches zero. This steady state is not mentioned in the analysis of the models/simplifications.

Semi-trivial steady states occur when total rat population densities are positive, yet infectious rat population densities are zero. These semi-trivial steady states are referred to as trivial steady states in upcoming analysis as they are trivial steady states of the infectious subsystems of the models.

Note that the term "steady state" is referred to as both the solution to individual equations (derivatives set to zero), as well as to the set of solutions for the whole system being referred to.

Figures and numerical solutions are produced using parameter values from the original paper by Holt et. al. [20]. Several of these values are amended to reflect New Zealand specific conditions in the combined wildlife-livestock model covered in chapter section 4.1.

Lemma 1

In some cases, the fixed point for the infectious rat population, I^* (where I^* is either I_J^*, I_S^* or I_A^*, with subscripts denoting the age class) is found by solving a quadratic equation. The following lemma is given to help determine which, if any, solutions are feasible. The total rat population density, N, is either N_J, N_S or N_A, with subscripts denoting the age class.

Call $F(I) = AI^2 + BI + C$ the quadratic equation needing to be solved in order to find the fixed points of $\dot{I}$. Let $A > 0$. This fixes the graph of the quadratic equation (a parabola) to be concave up, with a minimum, rather than a maximum. As only physically feasible (positive and real) solutions in the region $0 \leq I \leq N$ are of interest, $F(I)$ is evaluated at these end points and the signs at the endpoints are used to assist in determining

the roots of $F(I)$ and the conditions under which they exist. In general there are five different possibilities
1. $F(0) \leq 0, F(N) > 0$.
2. $F(0) \geq 0, F(N) < 0$.
3. $F(0) < 0, F(N) \leq 0$.
4. $F(0) > 0, F(N) \geq 0$.
5. $F(0) = 0, F(N) = 0$.

Cases 1 and 2 When $F(0)$ and $F(N)$ have opposite signs there is only one solution. In case 1 the graph is increasing, so the solutions is on the right hand side of the parabola, ie. $I^* = \dfrac{-B + \sqrt{B^2 - 4AC}}{2A}$. In case 2, the graph is decreasing and the solution is on the left hand side of the parabola, ie. $I^* = \dfrac{-B - \sqrt{B^2 - 4AC}}{2A}$. In either case, both $C < 0$ and $\dfrac{B^2}{4AC} > 1$ are needed for the solution to be in the feasible region.

If $F(0) = 0$, then clearly $I^* = 0$ is one solution. Another, non-trivial solution, $I^* = \dfrac{-B}{A}$, exists and is feasible if $B < 0$.

Cases 3 and 4 When $F(0)$ and $F(N)$ have the same sign there are either 0, 1 or 2 solutions. As the quadratic equation is set to be concave up, no solutions exist for case 3. For case 4, no solutions exist if $\min(F(I)) > 0$, one solution exists if $\min(F(I)) = 0$ and two solutions exist if $\min(F(I)) < 0$.

The minimum of $F(I)$ occurs when $F'(I) = 2AI + B = 0$, so $I_{\min} = \dfrac{-B}{2A}$. Now for $I_{\min}$ to be in the feasible region, $B < 0$ is needed. Then, $F(I_{\min}) = A\left(\dfrac{-B}{2A}\right)^2 + B\left(\dfrac{-B}{2A}\right) + C = \dfrac{-B^2}{4A} + C$. If $\dfrac{B^2}{4AC} = 1$, then only one solution exists. If $\dfrac{B^2}{4AC} > 1$, then two solutions exist: $I^* = \dfrac{-B \pm \sqrt{B^2 - 4AC}}{2A}$. If $\dfrac{B^2}{4AC} < 1$, then no (feasible) solutions exist.

Case 5 Case 5 already has two solutions, both of which are zero. As $F(I)$ is a polynomial of degree two, no more solutions exist.

Stability

For one dimensional systems the stability of each fixed point is found by substituting the fixed point into $\frac{d\dot{I}}{dI}$ and examining the sign of the result. For two dimensional systems the fixed point is substituted into the Jacobian matrix of the system and the signs of the corresponding trace and determinant are examined. For systems of three or more dimensions the signs of the eigenvalues of the Jacobian at each fixed point can be examined [32]. An easier way of determining stability in three dimensional systems than actually computing eigenvalues, however, is to use the Routh-Hurwitz condition.

Routh-Hurwitz condition for a three-dimensional system
Let $\{a_n\}$ be the coefficients of the characteristic polynomial, ie, $\det(J - \lambda I_n) = \lambda^3 + a_1\lambda^2 + a_2\lambda + a_3 = 0$, where I_n here is the identity matrix of dimension n and J is the Jacobian matrix evaluated at the fixed point in question. Now, if $a_1 > 0$, $a_2 > 0$, $a_3 > 0$ and $a_1 a_2 > a_3$, then all three of the eigenvalues are negative and the fixed point is stable. Otherwise it is unstable [33].

The Next Generation Matrix (K) and Basic Reproduction Number (R_0)

The next generation matrix can be found either through biological interpretation or by using a 'recipe' [34]. The 'recipe' method is used here.

The equations of the system that "describe the production of new infections and changes in state among infectious individuals " is referred to as the infectious subsystem [34]. This subsystem is linearised about the infection free steady state (the "trivial" steady state). In some cases, this is done by taking the first term of the Taylor series expansion of the subsystem. Note that at the infection free steady state, the density of infectious rats, as well as leptospires, is zero, and so the density of susceptible rats is the same as the total rat density.

Next, the linearised infection subsystem at the infection-free steady state is divided into two matrices, the transmission matrix T, containing all the entries relating to transmission, and the transition matrix Σ, containing everything else. So $J = T + \Sigma$. Then, the next generation matrix is $K = -T\Sigma^{-1}$, where each entry $K_{i,j}$ is the number of individuals

of type i that a typical individual of type j will infect within its lifetime. When the next generation matrix is two dimensional, the basic reproduction number can be found using the following formula: $R_0 = \frac{1}{2}(\text{trace}(K) + \sqrt{\text{trace}^2(K) - 4\det(K)})$. Substituting the fixed point threshold into this expression should result in $R_0 = 1$.

2.1 Rat Model: Single Age Class

The single age class rat model considers just the adults of the Holt. et al model in the following set of differential equations:

$$\frac{dN}{dt} = \sigma e^{-cN} N - \mu N, \tag{2.1}$$

$$\frac{dI}{dt} = \frac{\beta(N-I)I}{N} + \frac{\gamma(N-I)L}{L+H} - \mu I, \tag{2.2}$$

$$\frac{dL}{dt} = \alpha I - \rho L. \tag{2.3}$$

Here N is the density of the total rat population, I the density of the infectious rat population and L the density of free living leptospires, all in a given area. Entry into the total rat population occurs at rate σe^{-cN}, where σ is the maximum rat maturation rate and c is the shape parameter for density dependence in maturation. Note that in this instance σ acts as a birth rate into the population, while e^{-cN} causes the total rat population to increase more slowly as it gets larger. Rats, regardless of whether they are infectious or susceptible, leave the population via death at rate μ. Rats become infectious via density dependent sexual contacts at rate β, as well as via the environment. The environmental transmission co-efficient γ is paired with the non-linear saturation term $\frac{L}{L+H}$, where H is the density of leptospires at which transmission rate from the environment is 0.5γ. This term is used in the Holt. et al model to limit the effect of transmission to rats as free living leptopsire values become large, while still allowing infection transmission to increase as free living leptospires increase [20]. Leptospires are shed into the environment by infectious rats at rate α and leave the environment via death or removal at rate ρ.

Note that the equation describing the total rat population (equation 2.1) can be decoupled from the rest of the system (equations 2.2-2.3). Therefore, the total rat population density, N, can be assumed to be constant, with N

Symbol	Description	Units
N	Density of the rat population in a given area	ha^{-1}
I	Density of the infectious rat population in a given area	ha^{-1}
L	Free living leptospires in a given area	ha^{-1}
σ	Maturation rate of rats	day^{-1}
c	Shape parameter for density dependence in rat maturation	
μ	Rat death rate	day^{-1}
β	Sexual transmission co-efficient for rats	day^{-1}
γ	Environmental transmission co-efficient for rats	day^{-1}
H	Number of leptospires at which transmission rate from the environment is 0.5γ	ha^{-1}
α	Number of leptospires shed per infectious rat	day^{-1}
ρ	Leptospire death rate	day^{-1}

Table 2.1: *Nomenclature for the single age class rat model*

being set to its constant equilibrium value N^* (defined in subsection 2.1.1 to follow). This quasi-stationary approach effectively reduces the model to a two dimensional system on the (I, L) phase plane.

2.1.1 Fixed Points

Fixed points occur when $\dot{N} = 0, \dot{I} = 0$ and $\dot{L} = 0$. In each of the simplifications covered, the solutions to $\dot{N} = 0$ and $\dot{L} = 0$ are the same, so these are solved first.

$\dot{N} = 0$ when either $N = 0$ or $N = \frac{1}{c}\log(\frac{\sigma}{\mu})$. The fixed point $N^* = \frac{1}{c}\log(\frac{\sigma}{\mu})$ is positive, and hence feasible, only if $\frac{\sigma}{\mu} > 1$. This condition is necessary for all fixed points of the infectious system.

Next, $\dot{L} = 0$ when $L^* = \frac{\alpha I}{\rho}$.

The fixed point I^* is found on a case by case basis.

2.1.2 Trapping Region and Dulac's Criterion

Biologically, $N \geq I$. That is, the total number of rats is greater than or equal to the number of infectious rats. It can be shown that this condition is incorporated in the model by demonstrating that a trapping region exists.

From equation 2.2, when $I = 0$ and $L > 0, \dot{I} = \frac{\gamma L N}{L + H} > 0$, and when $I = N$ and $L > 0, \dot{I} = -\mu I < 0$.

From equation 2.3, when $L = 0$ and $I > 0, \dot{L} = \alpha I > 0$, and when $L = \frac{\alpha N}{\rho}$ and $I < N, \dot{L} = \alpha(I - N) < 0$.

The above can be summarised in figure 2.1.

Clearly, a trapping region exists. So, if I and L start positive, then I and L can not become negative and the set of equations 2.1-2.3 is well posed.

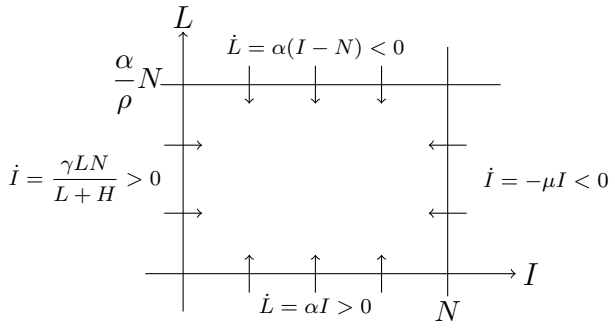

Figure 2.1: *Trapping region for the single age class rat model.*

Now, by using Dulac's Criterion, it can be shown that no periodic solutions exist. Let $g(I, L) = \dfrac{1}{IL}$. Then

$$\nabla \cdot g\begin{pmatrix} \dot{I} \\ \dot{L} \end{pmatrix} = \frac{\partial}{\partial I}\left(g\dot{I}\right) + \frac{\partial}{\partial L}\left(g\dot{L}\right) = -\frac{\beta}{NL} - \frac{\gamma N}{I^2(L+H)^2} - \frac{\alpha}{L^2} < 0.$$

Since the sign of $\nabla \cdot g\begin{pmatrix} \dot{I} \\ \dot{L} \end{pmatrix}$ doesn't change (in particular, the sign doesn't change within the trapping region in figure 2.1), by Dulac's criterion it can be concluded that a closed orbit can not exist in that region [32].

2.1.3 Simplification 1 ($\gamma = 0$)

When $\gamma = 0$, equation 2.2 becomes

$$\dot{I} = \frac{\beta(N - I)I}{N} - \mu I. \tag{2.4}$$

The system of equations 2.1-2.3 is uncoupled, so the problem is one dimensional, with focus on $\dot{I}$.

The fixed points of equation 2.4 are $I^* = 0$ and $I^* = N^*(1 - \dfrac{\mu}{\beta})$. So the fixed points of the system are $(N^*, I^*, L^*) = (N^*, 0, 0)$ and $(N^*, I^*, \dfrac{\alpha}{\rho}I^*)$, where the non-trivial fixed point is positive, and hence feasible, only if $\dfrac{\beta}{\mu} > 1$.

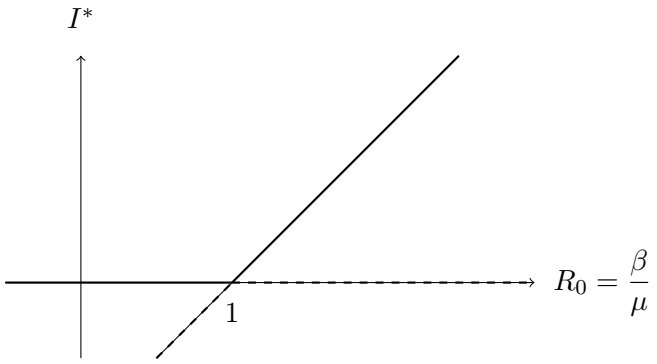

Figure 2.2: *Bifurcation diagram for simplification one of the single age class rat model. Bifurcation at* $R_0 = 1$.

Now, each fixed point must be substituted into $\frac{d\dot{I}}{dI}$, the sign of which is used to determine stability.

$$\frac{d\dot{I}}{dI} = \beta - \mu - \frac{2\beta I}{N}. \tag{2.5}$$

Substituting the fixed point $(N^*, 0, 0)$ into equation 2.5 gives:
$\frac{d\dot{I}}{dI} = \beta - \mu < 0$ if $\frac{\beta}{\mu} < 1$, and the fixed point is stable.
$\frac{d\dot{I}}{dI} = \beta - \mu > 0$ if $\frac{\beta}{\mu} > 1$, and the fixed point is unstable.

If $\frac{\beta}{\mu} < 1$ then the fixed point $(N^*, 0, 0)$ is the only fixed point and (biologically speaking) one would expect this fixed point to be stable. If $\frac{\beta}{\mu} > 1$ then another fixed point exists, which one would expect to be stable, while the other is unstable.

Substituting the fixed point $(N^*, I^*, \frac{\alpha}{\rho} I^*)$ into equation 2.5 gives:
$\frac{d\dot{I}}{dI} = -(\beta - \mu) < 0$ since $\frac{\beta}{\mu} > 1$ and the fixed point is stable.

The infection subsystem in a small neighbourhood of the infection-free steady state is

$$\dot{I} = \beta I - \mu I.$$

The Jacobian is then

$$J = \left[\beta - \mu\right] \text{ and so } T = \left[\beta\right] \text{ and } \Sigma = \left[-\mu\right].$$

Then the next generation matrix is

$$K = -T\Sigma^{-1} = \left[\frac{\beta}{\mu}\right] = R_0.$$

2.1.4 Simplification 2 ($\beta = 0$ and $\dot{L} = 0$)

Since $\dot{L} = 0$, $L = \frac{\alpha}{\rho}I$ and $\frac{\gamma L}{L+H} = \frac{\gamma\frac{\alpha I}{\rho}}{\frac{\alpha I}{\rho}+H} = \frac{\gamma I}{I+\frac{H\rho}{\alpha}} = \frac{\gamma I}{I+\tilde{H}}$ where $\tilde{H} = \frac{\rho}{\alpha}H$. Equation 2.2 now becomes

$$\dot{I} = \frac{\gamma(N-I)I}{I+\tilde{H}} - \mu I. \tag{2.6}$$

The system of equations 2.1-2.3 is uncoupled, so the problem is again one dimensional with focus on $\dot{I}$.

The fixed points of equation 2.6 are $I^* = 0$ and $I^* = \frac{\gamma N^* - \mu\tilde{H}}{\gamma+\mu}$. So the fixed points of the system are $(N^*, I^*, L^*) = (N^*, 0, 0)$ and $(N^*, I^*, \frac{\alpha}{\rho}I^*)$, the latter of which is feasible if $\frac{\gamma N^*}{\mu\tilde{H}} > 1$.

Now

$$\frac{d\dot{I}}{dI} = -\frac{\gamma I^2 + 2\gamma\tilde{H}I - \tilde{H}\gamma N}{(I+\tilde{H})^2} - \mu. \tag{2.7}$$

Substituting the fixed point $(N^*, 0, 0)$ into equation 2.7 gives:
$\frac{d\dot{I}}{dI} = \frac{\gamma N^*}{\tilde{H}} - \mu < 0$ if $\frac{\gamma N^*}{\mu\tilde{H}} < 1$ and the fixed point is stable.
$\frac{d\dot{I}}{dI} = \frac{\gamma N^*}{\tilde{H}} - \mu > 0$ if $\frac{\gamma N^*}{\mu\tilde{H}} > 1$ and the fixed point is unstable.

Substituting the fixed point $(N^*, I^*, \frac{\alpha}{\rho}I^*)$ into equation 2.7 gives:
$\frac{d\dot{I}}{dI} = -\frac{(\gamma N - \mu\tilde{H})^2 + 2\tilde{H}(\gamma N - \mu\tilde{H})(\gamma+\mu) + \tilde{H}N(\gamma+\mu)^2}{\gamma(N+\tilde{H})^2} + \mu < 0$ since

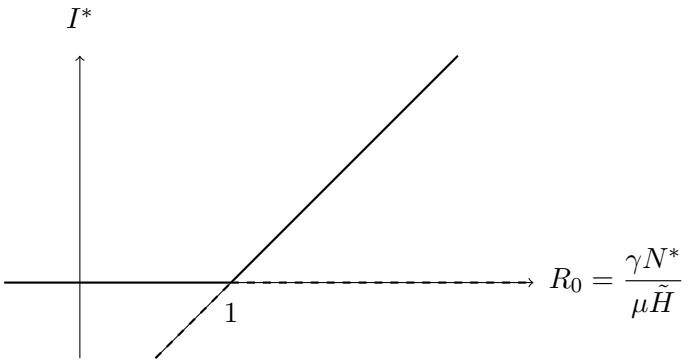

Figure 2.3: *Bifurcation diagram for simplification two of the single age class rat model. Bifurcation at* $R_0 = 1$.

$\frac{\gamma N^*}{\mu \tilde{H}} > 1$, so the fixed point is stable.

The infection subsystem in a small neighbourhood of the infection-free steady state is

$$\dot{I} = \frac{\gamma I N}{I + \tilde{H}} - \mu I.$$

The Taylor series expansion of this subsystem, keeping the first order terms only, in matrix form is

$$J = \left[\frac{\gamma N}{\tilde{H}} - \mu\right] \text{ and so } T = \left[\frac{\gamma N}{\tilde{H}}\right] \text{ and so } \Sigma = \left[-\mu\right].$$

Then the next generation matrix is

$$K = -T\Sigma^{-1} = \left[\frac{\gamma N}{\mu \tilde{H}}\right] = R_0.$$

2.1.5 Simplification 3 ($\beta \neq 0$ and $\dot{L} = 0$)

This simplification is similar to simplification 2 except now $\beta \neq 0$. Equation 2.2 becomes

$$\dot{I} = \frac{\beta(N - I)I}{N} + \frac{\gamma(N - I)I}{I + \tilde{H}} - \mu I. \tag{2.8}$$

$I^* = 0$ is clearly a solution. After setting equation 2.8 to zero and dividing by I, the following quadratic equation remains to be solved in order to find the remaining fixed point of equation 2.8.

$$F(I) = \beta I^2 + I(\beta \tilde{H} + N(\gamma + \mu - \beta)) + N(\mu \tilde{H} - \beta \tilde{H} - \gamma N) = 0.$$

Now $F(0) = N(\mu\tilde{H} - \beta\tilde{H} - \gamma N)$ and $F(N) = \mu N(N + \tilde{H}) > 0$ so cases 1 and 4 of lemma 1 are considered.

Case 1 $F(0) < 0$ when $\mu\tilde{H} < \beta\tilde{H} + \gamma N$. In this case only one positive root exists. The solution is

$$I^* = -\frac{1}{2\beta}\Big(\beta(\tilde{H} - N) + N(\gamma + \mu)\Big) + \frac{1}{2\beta}\sqrt{\Big(\beta(\tilde{H} - N) + N(\gamma + \mu)\Big)^2 - 4\beta N\Big(\mu\tilde{H} - \beta\tilde{H} - \gamma N\Big)}.$$

Case 4 $F(0) > 0$ when $\mu\tilde{H} > \beta\tilde{H} + \gamma N$. $F(I)$ has real positive roots if $\min(F(I)) = 2\beta I + \beta\tilde{H} + N(\gamma + \mu - \beta) < 0$. Now $F(0) > 0 \Rightarrow$ $\mu\tilde{H} > \beta\tilde{H} + \gamma N \Rightarrow \mu - \frac{\gamma N}{\tilde{H}} > \beta \Rightarrow \mu > \beta \Rightarrow \min(F(I)) > 0$. So there is a contradiction. That is, $F(0) > 0 \Rightarrow \mu > \beta \Rightarrow \min(F(I)) > 0$, but $\min(F(I)) \not< 0$ if $\mu > \beta$ and so this case is not possible.

So the fixed points of the system are $(N^*, I^*, L^*) = (N^*, 0, 0)$ and $(N^*, I^*, \frac{\alpha}{\rho}I^*)$, the latter of which is feasible if $\frac{\beta\tilde{H} + \gamma N}{\mu\tilde{H}} > 1$.

Now

$$\frac{d\dot{I}}{dI} = \beta - \mu - \frac{2\beta I}{N} - \frac{\gamma I^2 + 2\gamma\tilde{H}I - \tilde{H}\gamma N}{(I + \tilde{H})^2}. \tag{2.9}$$

Substituting the fixed point $(N^*, 0, 0)$ into equation 2.9 gives:
$\frac{d\dot{I}}{dI} = \beta - \mu + \frac{\gamma N^*}{\tilde{H}} < 0$ if $\frac{\beta\tilde{H} + \gamma N^*}{\mu\tilde{H}} < 1$ and the fixed point is stable.
$\frac{d\dot{I}}{dI} = \beta - \mu + \frac{\gamma N^*}{\tilde{H}} > 0$ if $\frac{\beta\tilde{H} + \gamma N^*}{\mu\tilde{H}} > 1$ and the fixed point is unstable.

Since substituting the fixed point $(N^*, I^*, \frac{\alpha}{\rho}I^*)$ into $\frac{d\dot{I}}{dI}$ results in a fairly complicated expression, some simplifications are made. $\frac{d\dot{I}}{dI}$ needs to be evaluated at the solution to $\beta - \mu - \frac{\beta I}{N} + \frac{\gamma(N - I)}{I + \tilde{H}} = 0$. This is just the right hand side of equation 2.8 divided by I as explained above. Note that this equation has terms in common with equation 2.9 and if $\beta - \mu - \frac{\beta I}{N} +$

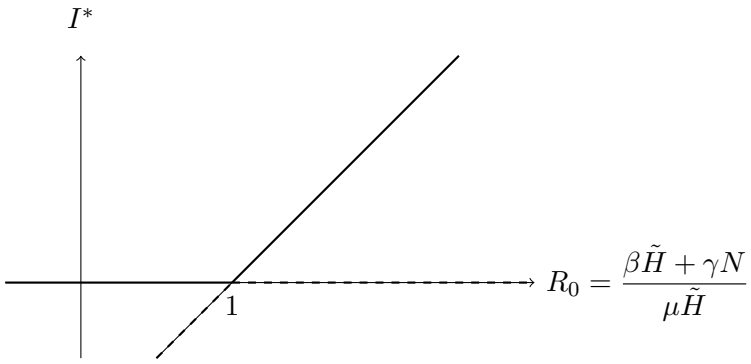

Figure 2.4: *Bifurcation diagram for simplification three of the single age class rat model. Bifurcation at* $R_0 = 1$.

$\frac{\gamma(N-I)}{I+\tilde{H}} = 0$ is subtracted from equation 2.9 then $\frac{d\dot{I}}{dI}$ becomes

$$\left.\frac{d\dot{I}}{dI}\right|_{I=I^*} = -\frac{\beta I^*}{N^*} - \frac{(N+\tilde{H})I^*}{(I^*+\tilde{H})^2} < 0$$

and the fixed point $(N^*, I^*, \frac{\alpha}{\rho}I^*)$ is stable when it exists.

The infection subsystem in a small neighbourhood of the infection-free steady state is

$$\dot{I} = \beta I + \frac{\gamma I N}{I+\tilde{H}} - \mu I.$$

The Taylor series expansion of this subsystem, keeping the first order terms only, in matrix form is

$$J = \left[\beta + \tfrac{\gamma N}{\tilde{H}} - \mu\right] \text{ and so } T = \left[\beta + \tfrac{\gamma N}{\tilde{H}}\right] \text{ and } \Sigma = \left[-\mu\right].$$

Then the next generation matrix is

$$K = -T\Sigma^{-1} = \left[\tfrac{\beta\tilde{H}+\gamma N}{\mu\tilde{H}}\right] = R_0.$$

2.1.6 Simplification 4 ($\beta = 0$ and $\dot{L} \neq 0$)

When $\beta = 0$, but $\frac{dL}{dt} \neq 0$ the problem becomes two dimensional. Equation 2.3 is included in the analysis and equation 2.2 becomes equation 2.10 below

$$\begin{aligned} \dot{I} &= \frac{\gamma(N-I)L}{(L+H)} - \mu I, \\ \dot{L} &= \alpha I - \rho L. \end{aligned} \tag{2.10}$$

First, the fixed point L^*, as found in section 2.1.1, is substituted into equation 2.10 before it is solved for fixed points, resulting in the equation below

$$\dot{I} = \frac{\gamma\alpha I}{(\alpha I + H\rho)}(N-I) - \mu I. \tag{2.11}$$

The solutions to equation 2.11 are $I^* = 0$ and $I^* = \frac{\gamma\alpha N^* - \mu H\rho}{\alpha(\gamma+\mu)}$. So the fixed points of the system are $(N^*, I^*, L^*) = (N^*, 0, 0)$ and $(N^*, I^*, \frac{\alpha}{\rho}I^*)$, the latter of which is feasible if $\frac{\gamma\alpha N^*}{\mu H\rho} > 1$.

As the problem is now two dimensional, rather than substituting each fixed point into $\frac{d\dot{I}}{dI}$, the fixed points are substituted into the Jacobian.

The Jacobian for this system is

$$J = \begin{bmatrix} -\frac{\gamma L}{L+H} - \mu & \frac{\gamma H}{(L+H)^2}(N-I) \\ \alpha & -\rho \end{bmatrix}. \tag{2.12}$$

Substituting the fixed point $(N^*, 0, 0)$ into the Jacobian (equation 2.12) gives:

$$J_{(N^*,0,0)} = \begin{bmatrix} -\mu & \frac{\gamma N^*}{H} \\ \alpha & -\rho \end{bmatrix}.$$

The corresponding trace and determinant are:

$$\begin{aligned} \tau &= -(\mu + \rho), \\ \Delta &= \mu\rho - \frac{\alpha\gamma N^*}{H}. \end{aligned}$$

$\tau < 0$ so the fixed point is either a saddle or a stable point.

$\Delta < 0$ if $\dfrac{\gamma\alpha N^*}{H\mu\rho} > 1$, which suggests a saddle.
$\Delta > 0$ if $\dfrac{\gamma\alpha N^*}{H\mu\rho} < 1$, which suggests a stable point.

If $\Delta < 0$ then $\tau^2 - 4\Delta = (\mu - \rho)^2 + \dfrac{4\alpha\gamma N^*}{H} > 0$, and the fixed point is a stable node.

Substituting the fixed point $(N^*, I^*, \dfrac{\alpha}{\rho}I^*)$ into the Jacobian (equation 2.12) doesn't produce a 'nice' determinant that relates well to either the conditions used for the previous fixed points, or to the existence of the fixed point. A simplification to the determinant of the general Jacobian matrix can be made to show that the non-trivial fixed point is stable when it exists.

The trace and determinant of the general Jacobian (equation 2.12) are:

$$\begin{aligned} \tau &= -\left(\frac{\gamma L}{L+H} + \mu + \rho\right), \\ \Delta &= \rho\frac{\gamma L}{L+H} + \rho\mu - \frac{\gamma H\alpha}{(L+H)^2}(N-I). \end{aligned}$$

$\tau < 0$, so the fixed point is either a saddle or a stable point.

The sign of the determinant isn't clear; however $\dot{L} = 0 \Rightarrow \dfrac{I}{L} = \dfrac{\rho}{\alpha}$ and $\dot{I} = 0 \Rightarrow \dfrac{\gamma(N-I)}{L+H} = \dfrac{\mu I}{L} = \dfrac{\mu\rho}{\alpha}$. Making these substitutions into the determinant gives $\Delta = \dfrac{\rho L(\gamma+\mu)}{L+H} > 0$. So the fixed point is stable when it exists.

Now $\tau^2 - 4\Delta = (\mu - \rho)^2 + \dfrac{4H\mu^2\rho^2}{\gamma\alpha} > 0$, so the fixed point is a stable node.

The infection subsystem in a small neighbourhood of the infection-free

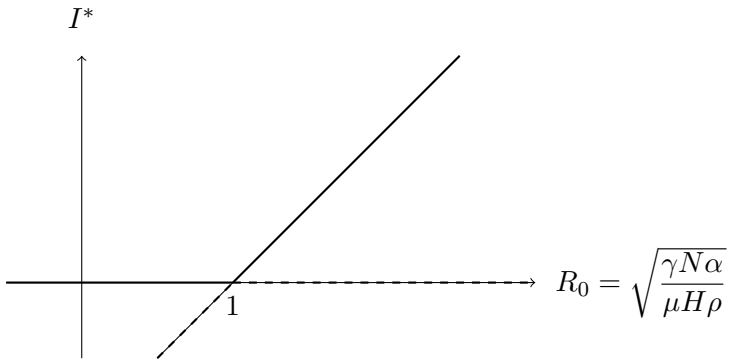

Figure 2.5: *Bifurcation diagram for simplification four of the single age class rat model. Bifurcation at* $R_0 = 1$.

steady state is

$$\begin{aligned} \dot{I} &= \frac{\gamma N L}{L+H} - \mu I, \\ \dot{L} &= \alpha I - \rho L. \end{aligned}$$

The Taylor series expansion of this subsystem, keeping the first order terms only, in matrix form is

$$J = \begin{bmatrix} -\mu & \frac{\gamma N}{H} \\ \alpha & -\rho \end{bmatrix} \text{ and so } T = \begin{bmatrix} 0 & \frac{\gamma N}{H} \\ \alpha & 0 \end{bmatrix} \text{ and } \Sigma = \begin{bmatrix} -\mu & 0 \\ 0 & -\rho \end{bmatrix}.$$

Then the next generation matrix is

$$K = -T\Sigma^{-1} = \begin{bmatrix} 0 & \frac{\gamma N}{H\rho} \\ \frac{\alpha}{\mu} & 0 \end{bmatrix} \text{ and } R_0 = \sqrt{\frac{\gamma N \alpha}{\mu H \rho}}.$$

2.1.7 Simplification 5

Recall equations 2.1-2.3, where no simplifications are made to the system.

The fixed point L^* is substituted into equation 2.2 before it is solved for fixed points, resulting in the equation below

$$\dot{I} = \frac{\beta(N-I)I}{N} + \frac{\gamma(N-I)\alpha I}{(\alpha I + H\rho)} - \mu I. \tag{2.13}$$

One solution is $I^* = 0$. After setting equation 2.13 to zero and dividing by I, the following quadratic equation remains to be solved.

$$F(I) = \beta\alpha I^2 + (\beta H\rho + N\alpha(\mu - \beta + \gamma))\, I + NH\rho(\mu - \beta) - N^2\alpha\gamma = 0.$$

Now $F(0) = N\,(H\rho(\mu - \beta) - N\alpha\gamma)$ and $F(N) = N\mu(N\alpha + H\rho) > 0$. So cases 1 and 4 of lemma 1 are considered.

Case 1 $F(0) < 0$ when $H\rho\mu < H\rho\beta + N\alpha\gamma$. The solution is then

$$I^* = -\frac{1}{2\beta\alpha}\big(\beta(H\rho - N\alpha) + N\alpha(\mu + \gamma)\big) + \frac{1}{2\beta\alpha}\sqrt{\big(\beta(H\rho - N\alpha) + N\alpha(\mu + \gamma)\big)^2 - 4\beta N\alpha\,(H\rho\mu - H\rho\beta - N\alpha\gamma)}.$$

Case 4 $F(0) > 0$ when $H\rho\mu > H\rho\beta + N\alpha\gamma$. $F(I)$ has real positive roots if $\min(F(I)) = 2\beta\alpha I + \beta H\rho + N\alpha(\mu - \beta + \gamma) < 0$. Now $H\rho\mu > H\rho\beta + N\alpha\gamma \Rightarrow H\rho(\mu - \beta) > N\alpha\gamma \Rightarrow \mu > \beta$ so $\min(F(I)) > 0$ and therefore no roots exist.

So, the fixed points of the system are $(N^*, I^*, L^*) = (N^*, 0, 0)$ and $(N^*, I^*, \frac{\alpha}{\rho}I^*)$, the latter of which is feasible if $\dfrac{H\rho\beta + N\alpha\gamma}{H\rho\mu} > 1$.

The Jacobian for this system is

$$J = \begin{bmatrix} \beta - \frac{2\beta I}{N} - \frac{\gamma L}{L+H} - \mu & \frac{H\gamma(N-I)}{(L+H)^2} \\ \alpha & -\rho \end{bmatrix}. \tag{2.14}$$

Substituting the fixed point $(N^*, 0, 0)$ into the Jacobian (equation 2.14) gives:

$$J_{(N^*,0,0)} = \begin{bmatrix} \beta - \mu & \frac{\gamma N}{H} \\ \alpha & -\rho \end{bmatrix}.$$

The corresponding trace and determinant are:

$$\begin{aligned} \tau &= \beta - \mu - \rho, \\ \Delta &= \rho(\mu - \beta) - \frac{\gamma N\alpha}{H}. \end{aligned}$$

$\tau < 0$ if $\dfrac{\beta}{\mu + \rho} < 1$, which suggests that the fixed point is either a saddle or a stable point.

$\tau > 0$ if $\dfrac{\beta}{\mu+\rho} > 1$, which suggests that the fixed point is either a saddle or an unstable point.

$\Delta < 0$ if $\dfrac{H\rho\beta + \gamma N\alpha}{\rho H\mu} > 1$, which suggests a saddle.
$\Delta > 0$ if $\dfrac{H\rho\beta + \gamma N\alpha}{\rho H\mu} < 1$, which suggests either a stable or an unstable point.

Since $\tau^2 - 4\Delta = (\beta - \mu + \rho)^2 + 4\dfrac{\gamma N\alpha}{H} > 0$, the fixed point is either a stable or an unstable node.

If $\dfrac{H\rho\beta + \gamma N\alpha}{\rho H\mu} > 1$ and the non-trivial fixed point exists, then the trivial fixed point is unstable regardless of the sign of τ. If $\dfrac{H\rho\beta + \gamma N\alpha}{\rho H\mu} < 1$, then $\dfrac{\beta}{\mu+\rho} < 1$ and the fixed point is stable.

As for simplification 4, the general Jacobian is used for the stability analysis of the fixed point $(N^*, I^*, \dfrac{\alpha}{\rho}I^*)$.

The trace and determinant of the general Jacobian (equation 2.14) are:

$$\begin{aligned} \tau &= \beta - \mu - \frac{2\beta I}{N} - \frac{\gamma L}{L+H} - \rho, \\ \Delta &= \rho(\mu - \beta) + \frac{2\beta\rho I}{N} + \frac{\rho\gamma L}{L+H} - \frac{\gamma H\alpha(N-I)}{(L+H)^2}. \end{aligned}$$

Now, the condition for the fixed point to exist is $\dfrac{\beta H\rho + \gamma N\alpha}{\mu H\rho} > 1 \Rightarrow \dfrac{\gamma N\alpha}{H\rho(\mu-\beta)} > 1 \Rightarrow \dfrac{\mu}{\beta} > 1$ so:

$\tau < 0$ and the fixed point is either a saddle or a stable point.

The sign of the determinant of the general Jacobian isn't immediately deducible, but $\dot{I} = 0$ together with $\dot{L} = 0 \Rightarrow \dfrac{\gamma(N-I)}{L+H} = \dfrac{\mu\rho}{\alpha} - \dfrac{\beta(N-I)\rho}{N\alpha}$. Substituting this into the determinant gives:

$\Delta = \dfrac{\rho L(\mu - \beta + \gamma)}{L+H} + \dfrac{\beta\rho I(2L+H)}{N(L+H)} > 0$, so the fixed point is stable when it exists.

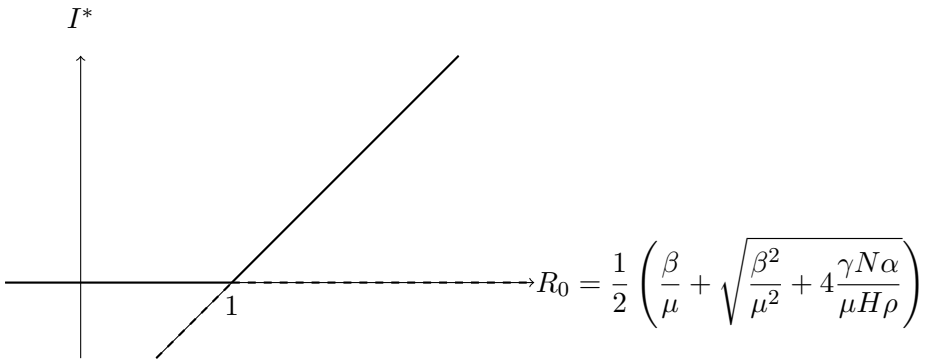

Figure 2.6: *Bifurcation diagram for simplification five of the single age class rat model. Bifurcation at* $R_0 = 1$.

The infection subsystem in a small neighbourhood of the infection-free steady state is

$$\begin{aligned} \dot{I} &= \beta I + \frac{\gamma N L}{L+H} - \mu I, \\ \dot{L} &= \alpha I - \rho L. \end{aligned}$$

The Taylor series expansion of this subsystem, keeping the first order terms only, in matrix form is

$$J = \begin{bmatrix} \beta - \mu & \frac{\gamma N}{H} \\ \alpha & -\rho \end{bmatrix} \text{ and so } T = \begin{bmatrix} \beta & \frac{\gamma N}{H} \\ \alpha & 0 \end{bmatrix} \text{ and } \Sigma = \begin{bmatrix} -\mu & 0 \\ 0 & -\rho \end{bmatrix}.$$

Then the next generation matrix is

$$K = -T\Sigma^{-1} = \begin{bmatrix} \frac{\beta}{\mu} & \frac{\gamma N}{H\rho} \\ \frac{\alpha}{\mu} & 0 \end{bmatrix} \text{ and } R_0 = \frac{1}{2}\left(\frac{\beta}{\mu} + \sqrt{\frac{\beta^2}{\mu^2} + 4\frac{\gamma N\alpha}{\mu H\rho}}\right).$$

The basic reproduction number is now a little more complex than for the previous simplifications and it is not immediately clear the $R_0 = 1$ at the stability threshold of the fixed points. The stability threshold is $\frac{\beta}{\mu} + \frac{\gamma N\alpha}{\mu H\rho} = 1$. Rearranging this gives $\frac{\gamma N\alpha}{\mu H\rho} = 1 - \frac{\beta}{\mu}$. Substituting this into R_0 gives $R_0 = \frac{1}{2}\left(\frac{\beta}{\mu} + \sqrt{\frac{\beta^2}{\mu^2} + 4(1 - \frac{\beta}{\mu})}\right) = \frac{1}{2}\left(\frac{\beta}{\mu} + \sqrt{(2 - \frac{\beta}{\mu})^2}\right) = 1$. So R_0 is indeed the bifurcation parameter.

2.2 Rat Model: Two Age Classes

The rat model covered in the previous sub-chapter is now expanded to include an extra age class. N in the single age class model is now renamed N_A, with the subscript A denoting the adult class. The additional age class, N_J, indicates the juvenile category. The birth rate is now ϕ, while the birth rate in the single age class model becomes the maturation rate of juvenile rats to adult rats. Pseudo-vertical transmission, that is, transmission of leptospirosis from infectious mothers to offspring via suckling, is also introduced into the model at rate ν. Note that in this model, juvenile rats do not become infectious via the environment, nor do they shed into it. This is due to the assumption that juveniles are nest bound, meaning that they do not venture outside the nest and are hence not exposed to, nor contribute to, environmental bacterial exposures. Consider the following set of differential equations:

$$\frac{dN_J}{dt} = \phi N_A - \sigma e^{-cN_A} N_J - \mu N_J, \tag{2.15}$$

$$\frac{dN_A}{dt} = \sigma e^{-cN_A} N_J - \mu N_A, \tag{2.16}$$

$$\frac{dI_J}{dt} = \nu\phi I_A - \sigma e^{-cN_A} I_J - \mu I_J, \tag{2.17}$$

$$\frac{dI_A}{dt} = \sigma e^{-cN_A} I_J + \frac{\beta(N_A - I_A)I_A}{N_A} + \frac{\gamma(N_A - I_A)L}{L + H} - \mu I_A, \tag{2.18}$$

$$\frac{dL}{dt} = \alpha I_A - \rho L. \tag{2.19}$$

The preliminary analysis of the two age class model is divided into two parts; one for the infection free subsystem and the other for the infectious subsystem. Note that the former decouples from the latter and so, during the analysis of the infectious subsystem, the total rat population densities N_J and N_A can be assumed to be at their constant equilibrium values of N_J^* and N_A^* respectively, both of which are defined in subsection 2.2.1.1 below. This quasi-stationary approach reduces simplifications 1-3 of the model to two dimensional systems on the (I_J, I_A) phase plane, while simplifications 4-5 remain three dimensional. Each part of the model (infection free and infectious) finds the fixed points of its respective subsystem, constructs a trapping region and uses Dulac's criterion to exclude the existence of periodic solutions.

Symbol	Description	Units
N_J	Density of the juvenile rat population in a given area	ha^{-1}
N_A	Density of the adult rat population in a given area	ha^{-1}
I_J	Density of the infectious juvenile rat population in a given area	ha^{-1}
I_A	Density of the infectious adult rat population in a given area	ha^{-1}
L	Free living leptospires	ha^{-1}
ϕ	Rat birth rate	day^{-1}
σ	Maturation rate of juvenile rats to adult rats	day^{-1}
c	Shape parameter for density dependence in rat maturation	
μ	Rat death rate	day^{-1}
ν	Probability of pseudo vertical transmission in rats	
β	Sexual transmission co-efficient for rats	day^{-1}
γ	Environmental transmission co-efficient for rats	day^{-1}
H	Number of leptospires at which transmission rate from the environment is 0.5γ	ha^{-1}
α	Number of leptospires shed per infectious rat	day^{-1}
ρ	Leptospire death rate	day^{-1}

Table 2.2: *Nomenclature for the two age class rat model*

2.2.1 Infection-free System

2.2.1.1 Fixed Points

The infection free subsystem is made up of equations 2.15 and 2.16, $\dot{N}_J$ and $\dot{N}_A$ respectively. Fixed points occur when $\dot{N}_J = 0$ and $\dot{N}_A = 0$.

The fixed point for $\dot{N}_J$ occurs when $N_J^* = \dfrac{\phi}{\sigma e^{-cN_A} + \mu} N_A$.

To solve $\dot{N}_A = 0$, N_J^* must first be substituted into $\dot{N}_A = 0$ to give $\dot{N}_A = \dfrac{\left(\sigma e^{-cN_A}(\phi - \mu) - \mu^2\right)}{\sigma e^{-cN_A} + \mu} N_A = 0$. The solutions to this are $N_A^* = 0$ and $N_A^* = \dfrac{1}{c} \log \dfrac{\sigma(\phi - \mu)}{\mu^2}$. So the fixed points of the infection free system are $(N_J^*, N_A^*) = (0, 0)$ and (N_J^*, N_A^*), the latter of which is positive and hence feasible only if $\dfrac{\sigma(\phi - \mu)}{\mu^2} > 1$. This condition is necessary for all fixed points of the infectious system.

2.2.1.2 Local Stability

The stability of each fixed point is determined by examining the sign of $\dfrac{d\dot{N}_A}{dN_A}$ after the fixed point has been substituted into it.

$$\frac{d\dot{N}_A}{dN_A} = \frac{\sigma e^{-cN_A}\phi}{\sigma e^{-cN_A} + \mu} - \frac{c\mu\sigma e^{-cN_A}}{(\sigma e^{-cN_A} + \mu)^2}\phi N_A - \mu. \tag{2.20}$$

Substituting the trivial fixed point into equation 2.20 gives:
$\dfrac{d\dot{N}_A}{dN_A} = \dfrac{\sigma\phi}{\sigma + \mu} - \mu < 0$ if $\dfrac{\sigma(\phi - \mu)}{\mu^2} < 1$ and the fixed point is stable.
$\dfrac{d\dot{N}_A}{dN_A} = \dfrac{\sigma\phi}{\sigma + \mu} - \mu > 0$ if $\dfrac{\sigma(\phi - \mu)}{\mu^2} > 1$ and the fixed point is unstable.

Substituting the non-trivial fixed point (N_J^*, N_A^*) into equation 2.20 gives:
$\dfrac{d\dot{N}_A}{dN_A} = -\dfrac{c\mu}{\phi} N_A^*(\phi - \mu) < 0$, so the fixed point is stable when it exists, that is when $\dfrac{\sigma(\phi - \mu)}{\mu^2} > 1$.

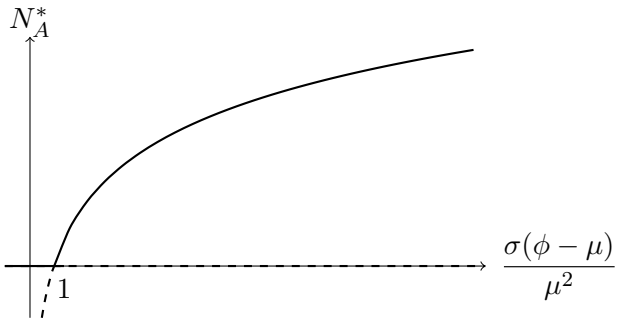

Figure 2.7: *Bifurcation diagram for the infection-free subsystem of the two age class rat model. Bifurcation at* $\frac{\sigma(\phi-\mu)}{\mu^2} = 1$.

Note that the bifurcation parameter $\frac{\sigma(\phi-\mu)}{\mu^2}$ is found by rearranging $\frac{d\dot{N}_A}{dN_A} < 0$.

2.2.1.3 Trapping Region and Dulac's Criterion

A trapping region is shown to exist as follows.

From equations 2.15 and 2.16, the equations for the nullclines of the system are $N_J = \frac{\phi N_A}{\sigma e^{-cN_A} + \mu}$ for $\dot{N}_J = 0$ and $N_J = \frac{\mu N_A}{\sigma e^{-cN_A}}$ for $\dot{N}_A = 0$.

Now $\frac{\phi N_A}{\sigma e^{-cN_A} + \mu} < \frac{\mu N_A}{\sigma e^{-cN_A}}$ (found by rearranging $N_A > N_A^*$) for all $N_A > N_A^*$. Note that when $\frac{\sigma(\phi-\mu)}{\mu^2} < 1$ then $N_A^* < 0$ and $N_A > N_A^*$ is true for all N_A in the positive quadrant.

Now, when $N_J = 0$ then $\dot{N}_J = \phi N_A > 0$ for $N_A > 0$ and when $N_A = 0$ then $\dot{N}_A = \sigma N_J > 0$ for $N_J > 0$.

Let $\bar{N_A} > N_A^*$. Then $\dot{N}_A\big|_{N_A=\bar{N_A}} < 0 \implies N_J < \frac{\mu \bar{N_A}}{\sigma e^{-c\bar{N_A}}}$ (found by rearranging $\dot{N}_A\big|_{N_A=\bar{N_A}} < 0$).

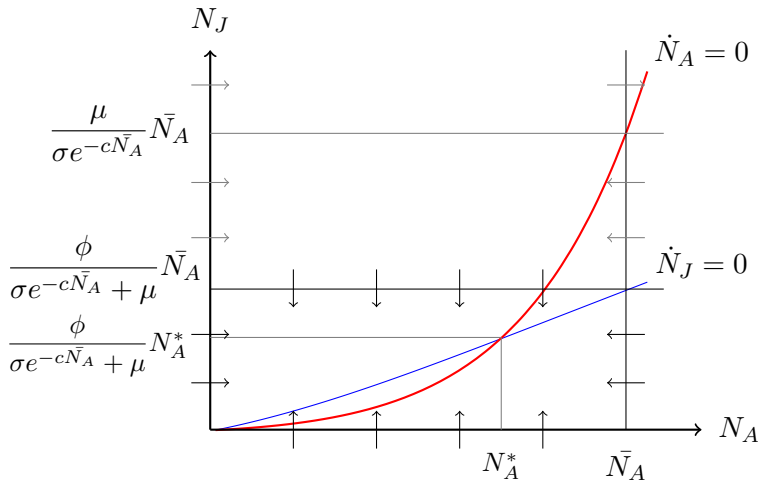

Figure 2.8: *Trapping region for the infection-free subsystem of the two age class rat model.*

Now, since $\bar{N}_A > N_A^*$, then $\dfrac{\phi\bar{N}_A}{\sigma e^{-c\bar{N}_A}+\mu} < \dfrac{\mu\bar{N}_A}{\sigma e^{-c\bar{N}_A}}$ and so if $N_J < \dfrac{\phi\bar{N}_A}{\sigma e^{-c\bar{N}_A}+\mu}$ then $N_J < \dfrac{\mu\bar{N}_A}{\sigma e^{-c\bar{N}_A}}$ also.

Next $\dot{N}_J\Big|_{N_J=\frac{\phi\bar{N}_A}{\sigma e^{-c\bar{N}_A}+\mu}} < 0$ when $\dfrac{\phi N_A}{\sigma e^{-cN_A}+\mu} < \dfrac{\phi\bar{N}_A}{\sigma e^{-c\bar{N}_A}+\mu}$, which is true when $N_A < \bar{N}_A$.

The above results are summarised in figure 2.8.

Clearly, a trapping region exists. So if N_J and N_A start positive, then N_J and N_A can not become negative and the set of equations 2.15-2.16 is well posed.

Now, by using Dulac's criterion, it can be shown that no periodic solutions exist. Let $g(N_J, N_A) = \dfrac{1}{N_J N_A}$.

Then

$$\begin{aligned}\nabla \cdot g\begin{pmatrix} \dot{N}_J \\ \dot{N}_A \end{pmatrix} &= \frac{\partial}{\partial N_J}(g\dot{N}_J) + \frac{\partial}{\partial N_A}(g\dot{N}_A) \\ &= -\left(\frac{\phi}{N_J^2} + \frac{\sigma e^{-cN_A}(1+cN_A)}{N_A^2}\right) < 0.\end{aligned}$$

Now, as the sign of $\nabla \cdot g\begin{pmatrix} \dot{N}_J \\ \dot{N}_A \end{pmatrix}$ doesn't change within the trapping region in figure 2.8, by Dulac's criterion it can be concluded that a closed orbit can not exist in that region [32].

2.2.2 Infectious System

2.2.2.1 Fixed Points

The infectious subsystem is made up of equations 2.17, 2.18 and 2.19, $\dot{I}_J, \dot{I}_A$ and $\dot{L}$ respectively. Fixed points occur when $\dot{N}_J = 0, \dot{N}_A = 0, \dot{I}_J = 0, \dot{I}_A = 0$ and $\dot{L} = 0$. In each of the cases covered, the solutions to $\dot{N}_J = 0, \dot{N}_A = 0, \dot{I}_J = 0$ and $\dot{L} = 0$ are the same, so these are solved first.

The dynamics of N_J and N_A are independent of the dynamics of I_J, I_A and L, so it is assumed that N_J and N_A are at the non-trivial steady state values of N_J^* and N_A^* as found in section 2.2.1.1. Then, simply by substituting N_A^*, several simplifications can be made to the calculations in this section:

$$\sigma e^{-cN_A^*} = \frac{\mu^2}{\phi - \mu}, \quad \sigma e^{-cN_A^*} + \mu = \frac{\phi\mu}{\phi - \mu} \quad \text{and} \quad \frac{\sigma e^{-cN_A^*}}{\sigma e^{-cN_A^*} + \mu} = \frac{\mu}{\phi}.$$

Now, the solution to $\dot{I}_J = 0$ is $I_J^* = \dfrac{\nu\phi}{\sigma e^{-cN_A} + \mu} I_A = \dfrac{\nu(\phi - \mu)}{\mu} I_A$.

The solution to $\dot{L} = 0$ is $L^* = \dfrac{\alpha}{\rho} I_A$.

The solutions to $\dot{I}_A = 0$ are discussed on a case by case basis.

2.2.2.2 Trapping Region and Dulac's Criterion

Biologically $N_J \geq I_J$ and $N_A \geq I_A$. It can be shown, by constructing a trapping region, that this condition is included in the models.

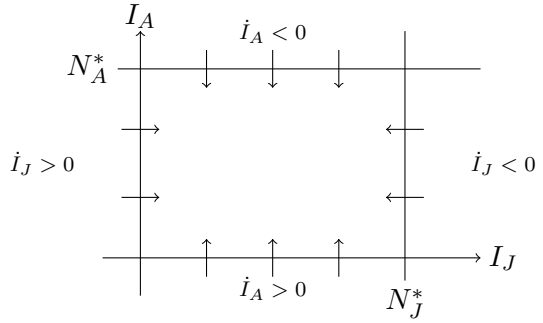

Figure 2.9: *Trapping region for the infection subsystem, involving I_A and I_J of the two age class rat model.*

From equation 2.17, when $I_J = 0$ and $I_A > 0$, then $\dot{I}_J = \nu\phi I_A > 0$.

When $I_J = N_J^*$, then $\dot{I}_J = \nu\phi I_A - (\sigma e^{-cN_A^*} + \mu)N_J^*$ and $\dot{I}_J\big|_{I_J=N_J^*} < 0$ when $I_A < \dfrac{\sigma e^{-cN_A^*} + \mu}{\nu\phi} N_J^* = \dfrac{1}{\nu} N_A^*$ and $\dfrac{1}{\nu} N_A^* > N_A^*$ since $0 \leq \nu \leq 1$.

Next consider simplification 3,

$$\dot{I}_A = \sigma e^{-cN_A^*} I_J + \frac{\beta(N_A^* - I_A)I_A}{N_A^*} + \frac{\gamma(N_A^* - I_A)I_A}{I_A + \tilde{H}} - \mu I_A.$$

When $I_A = 0$ and $I_J = 0$, then $\dot{I}_A = \sigma e^{-cN_A^*} I_J > 0$.

When $I_A = N_A^*$, then $\dot{I}_A = \sigma e^{-cN_A^*} I_J - \mu N_A^*$ and $\dot{I}_A\big|_{I_A=N_A^*} < 0$ when $I_J < \dfrac{\mu}{\sigma e^{-cN_A^*}} N_A^* = N_J^*$.

The above results are summarised in figure 2.9.

Clearly a trapping region exists. So if I_J and I_A start positive, then I_J and I_A can not become negative and for simplification 3, the set of equations 2.15-2.19 is well posed.

Now, by using Dulac's criterion, it can be shown that no periodic solutions exist. Let $g(I_J, I_A) = \dfrac{1}{I_J I_A}$. Then, again using simplification 3,

$$\begin{aligned}\nabla \cdot g\begin{pmatrix} \dot{I}_J \\ \dot{I}_A \end{pmatrix} &= \frac{\partial}{\partial I_J}\left(g\dot{I}_J\right) + \frac{\partial}{\partial I_A}\left(g\dot{I}_A\right) \\ &= -\left(\frac{\sigma e^{-cN_A}}{I_A^2} + \frac{\beta}{N_A I_J} + \frac{\gamma(\tilde{H}+N_A)}{I_J(I_A+H)^2} + \frac{\nu\phi}{I_J^2}\right) < 0.\end{aligned}$$

Now, as the sign of $\nabla \cdot g\begin{pmatrix} \dot{I}_J \\ \dot{I}_A \end{pmatrix}$ doesn't change within the trapping region in figure 2.9, by Dulac's criterion it can be concluded that a closed orbit can not exist in that region [32].

As none of the above results depend on either γ or β, they can be generalised to the first two simplifications of the model as well, but not to simplifications 4 and 5.

2.2.3 Simplification 1 ($\gamma = 0$)

When $\gamma = 0$, equations 2.17 and 2.18 become:

$$\begin{aligned}\frac{dI_J}{dt} &= \nu\phi I_A - \sigma e^{-cN_A^*} I_J - \mu I_J, \\ \frac{dI_A}{dt} &= \sigma e^{-cN_A^*} I_J + \frac{\beta(N_A^* - I_A)I_A}{N_A^*} - \mu I_A\end{aligned}$$

and the problem is two dimensional.

Solving $\dot{I}_J = 0$ and $\dot{I}_A = 0$ simultaneously gives the fixed points $(I_J^*, I_A^*) = (0,0)$ and $\left(\frac{\nu(\phi-\mu)}{\mu}N_A^*\left(1-\frac{\mu}{\beta}(1-\nu)\right), N_A^*\left(1-\frac{\mu}{\beta}(1-\nu)\right)\right)$ the latter of which is positive, and hence feasible, only if $\dfrac{\beta}{\mu(1-\nu)} > 1$.

The Jacobian for the system is

$$J = \begin{bmatrix} -\sigma e^{-cN_A^*} - \mu & \nu\phi \\ \sigma e^{-cN_A^*} & \beta - 2\frac{\beta I_A}{N_A *} - \mu \end{bmatrix} = \begin{bmatrix} -\frac{\phi\mu}{\phi-\mu} & \nu\phi \\ \frac{\mu^2}{\phi-\mu} & \beta - 2\frac{\beta I_A}{N_A^*} - \mu \end{bmatrix}. \quad (2.21)$$

Substituting the trivial fixed point $(I_J^*, I_A^*) = (0,0)$ into the Jacobian (equation 2.21) gives:

$$J = \begin{bmatrix} -\frac{\phi\mu}{\phi-\mu} & \nu\phi \\ \frac{\mu^2}{\phi-\mu} & \beta - \mu \end{bmatrix}.$$

The corresponding trace and determinant are:

$$\begin{aligned}\Delta &= \frac{\phi\mu}{\phi-\mu}\left(\mu(1-\nu)-\beta\right),\\ \tau &= \beta-\mu-\frac{\phi\mu}{\phi-\mu}.\end{aligned}$$

$\Delta < 0$ when $\dfrac{\beta}{\mu(1-\nu)} > 1$ and the fixed point is a saddle.

$\Delta > 0$ when $\dfrac{\beta}{\mu(1-\nu)} < 1$ and the fixed point is either a stable or an unstable node. Now $\dfrac{\phi-\mu}{2\phi-\mu} < 1$ and $\dfrac{\beta}{\mu} < \dfrac{\beta}{\mu(1-\nu)} < 1$, so $\dfrac{\beta}{\mu}\dfrac{\phi-\mu}{2\phi-\mu} < 1 \Rightarrow \tau < 0$ and the fixed point is a stable node.

Substituting the non-trivial fixed point (I_J^*, I_A^*) into the Jacobian (equation 2.21) gives:

$J = \begin{bmatrix} -\frac{\phi\mu}{\phi-\mu} & \nu\phi \\ \frac{\mu^2}{\phi-\mu} & -\beta+\mu-2\nu\mu \end{bmatrix}$.

The corresponding trace and determinant are:

$$\begin{aligned}\Delta &= \frac{\phi\mu}{\phi-\mu}\left(\beta-\mu(1-3\nu)\right),\\ \tau &= -\beta-2\nu\mu-\frac{\mu^2}{\phi-\mu}.\end{aligned}$$

$\tau < 0$ and the fixed point is either a saddle or a stable node.

$\Delta > 0$ since $\dfrac{\beta}{\mu(1-\nu)} > 1 \Rightarrow \beta > \mu(1-\nu) > \mu(1-3\nu)$ and the fixed point is stable when it exists.

The infection subsystem in a small neighbourhood of the infection-free steady state is

$$\begin{aligned}\dot{I}_J &= \nu\phi I_A - \sigma e^{-cN_A^*} I_J - \mu I_J,\\ \dot{I}_A &= \sigma e^{-cN_A^*} I_J + \beta I_A - \mu I_A.\end{aligned}$$

The Jacobian is

$$J = \begin{bmatrix} -\sigma e^{-cN_A^*} - \mu & \nu\phi \\ \sigma e^{-cN_A^*} & \beta-\mu \end{bmatrix} \text{ and so } T = \begin{bmatrix} 0 & \nu\phi \\ \sigma e^{-cN_A^*} & \beta \end{bmatrix} \text{ and}$$

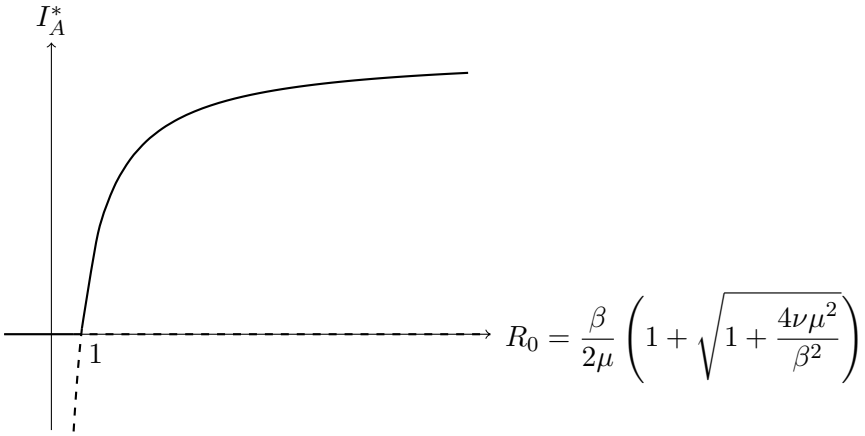

Figure 2.10: *Bifurcation diagram for simplification one of the two age class rat model. Bifurcation at* $R_0 = 1$.

$$\Sigma = \begin{bmatrix} -\sigma e^{-cN_A^*} - \mu & 0 \\ 0 & -\mu \end{bmatrix}.$$

The next generation matrix is

$$K = -T\Sigma^{-1} = \begin{bmatrix} 0 & \frac{\nu\phi}{\mu} \\ \frac{\sigma e^{-cN_A^*}}{\mu+\sigma e^{-cN_A^*}} & \frac{\beta}{\mu} \end{bmatrix} \text{ and}$$

$$R_0 = \frac{1}{2}\left(\frac{\beta}{\mu} + \sqrt{\frac{\beta^2}{\mu^2} + 4\frac{\nu\phi\sigma e^{-cN_A^*}}{\mu(\mu+\sigma e^{-cN_A^*})}}\right) = \frac{1}{2}\left(\frac{\beta}{\mu} + \sqrt{\frac{\beta^2}{\mu^2} + 4\nu}\right).$$

The stability threshold for the fixed point is $\dfrac{\beta}{\mu(1-\nu)} = 1$. Rearranging this gives $\dfrac{\beta}{\mu} = 1-\nu$. Substituting this into $R_0 = \frac{1}{2}\left(1-\nu+\sqrt{(1+\nu)^2}\right) = 1$. So R_0 is indeed the bifurcation parameter.

2.2.4 Simplification 2 ($\beta = 0$ and $\dot{L} = 0$)

When $\beta = 0$ and $\dot{L} = 0$, equations 2.17 and 2.18 become:

$$\begin{aligned} \frac{dI_J}{dt} &= \nu\phi I_A - \sigma e^{-cN_A^*} I_J - \mu I_J, \\ \frac{dI_A}{dt} &= \sigma e^{-cN_A^*} I_J + \frac{\gamma I_A (N_A^* - I_A)}{I_A + \tilde{H}} - \mu I_A, \end{aligned}$$

where $\tilde{H} = \dfrac{\rho}{\alpha} H$, and the problem is two dimensional.

Solving $\dot{I}_J = 0$ and $\dot{I}_A = 0$ simultaneously gives the fixed points $(I_J^*, I_A^*) = (0,0)$ and $\left(\dfrac{\nu(\phi-\mu)}{\mu} \dfrac{\mu\tilde{H}(1-\nu) - \gamma N_A^*}{\mu(\nu-1)-\gamma}, \dfrac{\mu\tilde{H}(1-\nu) - \gamma N_A^*}{\mu(\nu-1)-\gamma} \right)$, the latter of which is positive, and hence feasible, only if $\dfrac{\gamma N_A^*}{\mu\tilde{H}(1-\nu)} > 1$.

The Jacobian for the system is

$$\begin{aligned} J &= \begin{bmatrix} -\sigma e^{-cN_A^*} - \mu & \nu\phi \\ \sigma e^{-cN_A^*} & \frac{\tilde{H}\gamma N_A^* - \gamma I_A^2 - 2\gamma I_A \tilde{H}}{(I_A+\tilde{H})^2} - \mu \end{bmatrix} \\ &= \begin{bmatrix} -\frac{\phi\mu}{\phi-\mu} & \nu\phi \\ \frac{\mu^2}{\phi-\mu} & \frac{\tilde{H}\gamma N_A^* - \gamma I_A^2 - 2\gamma I_A \tilde{H}}{(I_A+\tilde{H})^2} - \mu \end{bmatrix}. \end{aligned} \tag{2.22}$$

Substituting the trivial fixed point $(I_J^*, I_A^*) = (0,0)$ into the Jacobian (equation 2.22) gives:

$$J = \begin{bmatrix} -\frac{\phi\mu}{\phi-\mu} & \nu\phi \\ \frac{\mu^2}{\phi-\mu} & \frac{\gamma N_A^*}{\tilde{H}} - \mu \end{bmatrix}.$$

The corresponding trace and determinant are:

$$\begin{aligned} \Delta &= \frac{\phi\mu}{\phi-\mu} \left(\mu(1-\nu) - \frac{\gamma N_A^*}{\tilde{H}} \right), \\ \tau &= \frac{\gamma N_A^*}{\tilde{H}} - \frac{\mu(2\phi-\mu)}{(\phi-\mu)}. \end{aligned}$$

$\Delta < 0$ when $\dfrac{\gamma N_A^*}{\mu\tilde{H}(1-\nu)} > 1$ and the fixed point is a saddle.

$\Delta > 0$ when $\dfrac{\gamma N_A^*}{\mu\tilde{H}(1-\nu)} < 1$ and the fixed point is either a stable or an unstable node. Now $\dfrac{\phi-\mu}{2\phi-\mu} < 1$ and $\dfrac{\gamma N_A^*}{\tilde{H}\mu} < \dfrac{\gamma N_A^*}{\mu\tilde{H}(1-\nu)} < 1$ since $0 \leq \nu \leq 1$ and so $\dfrac{\gamma N_A^*}{\mu\tilde{H}}\dfrac{\phi-\mu}{2\phi-\mu} < 1 \Rightarrow \tau < 0$ and the fixed point is stable.

Substituting the non-trivial fixed point (I_J^*, I_A^*) into the Jacobian (equation 2.22) gives:

$$J = \begin{bmatrix} -\frac{\phi\mu}{\phi-\mu} & \nu\phi \\ \frac{\mu^2}{\phi-\mu} & -\mu + \frac{(1-\nu)^2\mu^2\tilde{H}+2(1-\nu)\mu\gamma\tilde{H}-\gamma^2 N_A^*}{\gamma(N_A^*+\tilde{H})} \end{bmatrix}.$$

The corresponding trace and determinant are:

$$\begin{aligned} \Delta &= \frac{\phi\mu}{\gamma(\phi-\mu)(N_A^*+\tilde{H})}\left(\gamma+\mu(1-\nu)\right)\left(\gamma N_A^* - \mu\tilde{H}(1-\nu)\right), \\ \tau &= (\gamma+\mu)(\phi-\mu)\left(\mu\tilde{H}(1-\nu) - \gamma N_A^* - \mu\nu\tilde{H}\right) - \phi(N_A^*+\tilde{H}). \end{aligned}$$

$\Delta > 0$ so the fixed point is either stable or unstable when it exists.

$\tau < 0$ so the fixed point is a stable node.

The infection subsystem in a small neighbourhood of the infection-free steady state is

$$\begin{aligned} \dot{I}_J &= \nu\phi I_A - \sigma e^{-cN_A^*} I_J - \mu I_J, \\ \dot{I}_A &= \sigma e^{-cN_A^*} I_J + \frac{\gamma N_A^*}{\tilde{H}} I_A - \mu I_A. \end{aligned}$$

The Jacobian is then

$$J = \begin{bmatrix} -\sigma e^{-cN_A^*} - \mu & \nu\phi \\ \sigma e^{-cN_A^*} & \frac{\gamma N_A^*}{\tilde{H}} - \mu \end{bmatrix} \text{ and so } T = \begin{bmatrix} 0 & \nu\phi \\ \sigma e^{-cN_A^*} & \frac{\gamma N_A}{\tilde{H}} \end{bmatrix} \text{ and}$$

$$\Sigma = \begin{bmatrix} -\sigma e^{-cN_A^*} - \mu & 0 \\ 0 & -\mu \end{bmatrix}.$$

Then the next generation matrix is

$$K = -T\Sigma^{-1} = \begin{bmatrix} 0 & \frac{\nu\phi}{\mu} \\ \frac{\sigma e^{-cN_A^*}}{\mu+\sigma e^{-cN_A^*}} & \frac{\gamma N_A^*}{\mu\tilde{H}} \end{bmatrix} \text{ and}$$

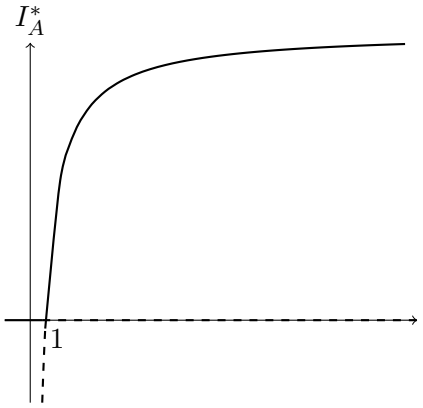

$$R_0 = \frac{1}{2}\frac{\gamma N_A^*}{\mu\tilde{H}}\left(1+\sqrt{1+4\nu\frac{\mu^2\tilde{H}^2}{\gamma^2 N_A^{*2}}}\right)$$

Figure 2.11: *Bifurcation diagram for simplification two of the two age class rat model. Bifurcation at* $R_0 = 1$.

$$R_0 = \frac{1}{2}\left(\frac{\gamma N_A^*}{\mu\tilde{H}}+\sqrt{\frac{\gamma^2 N_A^{*2}}{\mu^2\tilde{H}^2}+4\frac{\nu\phi\sigma e^{-cN_A^*}}{\mu(\mu+\sigma e^{-cN_A^*})}}\right) = \frac{1}{2}\left(\frac{\gamma N_A^*}{\mu\tilde{H}}+\sqrt{\frac{\gamma^2 N_A^{*2}}{\mu^2\tilde{H}^2}+4\nu}\right).$$

The stability threshold for the fixed point is $\frac{\gamma N_A^*}{\mu\tilde{H}(1-\nu)} = 1$. Rearranging this gives $\frac{\gamma N_A^*}{\mu\tilde{H}} = 1-\nu$. Substituting this into $R_0 = \frac{1}{2}\left(1-\nu+\sqrt{(1+\nu)^2}\right) = 1$.

2.2.5 Simplification 3 ($\beta \neq 0$ and $\dot{L} = 0$)

When $\beta \neq 0$ and $\dot{L} = 0$, equations 2.17 and 2.18 become:

$$\begin{aligned}\frac{dI_J}{dt} &= \nu\phi I_A - \sigma e^{-cN_A^*} I_J - \mu I_J,\\ \frac{dI_A}{dt} &= \sigma e^{-cN_A^*} I_J + \frac{\beta I_A(N_A^* - I_A)}{N_A^*} + \frac{\gamma I_A(N_A^* - I_A)}{I_A+\tilde{H}} - \mu I_A,\end{aligned}$$

where $\tilde{H} = \frac{\rho}{\alpha}H$ and the problem is two dimensional.

$\dot{I}_J = 0$ and $\dot{I}_A = 0$ need to be solved simultaneously to find the fixed points. One solution is $(I_J^*, I_A^*) = (0,0)$.

Other potential fixed points are given by the roots of

$$\begin{aligned} F(I) &= \beta I_A^2 + \left(\beta\tilde{H} + \gamma N_A^* + \mu N_A^*(1-\nu) - \beta N_A^*\right) I_A \\ &\quad + \mu N_A^* \tilde{H}(1-\nu) - \beta N_A^* \tilde{H} - \gamma N_A^{*2}. \end{aligned}$$

Using lemma 1, $F(0) = N_A^*\left(\mu\tilde{H}(1-\nu) - \beta\tilde{H} - \gamma N_A^*\right)$ and $F(N) = N_A^*\mu(1-\nu)(N_A^* + \tilde{H}) > 0$, so only cases 1 and 4 are possible.

Case 1 $F(0) < 0$ when $\mu\tilde{H}(1-\nu) < \beta\tilde{H} + \gamma N_A^*$, so the solution is

$$\begin{aligned} I_A^* = &\frac{-\left(\beta\tilde{H} + N_A^*(\gamma - \beta + \mu(1-\nu))\right)}{2\beta} \\ &+ \frac{\sqrt{\left(\beta\tilde{H} + N_A^*(\gamma - \beta + \mu(1-\nu))\right)^2 - 4\beta N_A^*\left(\mu\tilde{H}(1-\nu) - \gamma N_A^* - \beta\tilde{H}\right)}}{2\beta}. \end{aligned}$$

Case 4 $F(0) > 0$ when $\mu\tilde{H}(1-\nu) > \beta\tilde{H} + \gamma N_A^* \Rightarrow \tilde{H}\left(\mu(1-\nu) - \beta\right) > \gamma N_A^* \Rightarrow \mu(1-\nu) > \beta$. Now $B = \beta\tilde{H} + \gamma N_A^* + \mu N_A^*(1-\nu) - \beta N_A^* > 0$, so by lemma 1 no feasible solution exists.

Now the fixed points are $(I_J^*, I_A^*) = (0,0)$ and (I_J^*, I_A^*) the latter of which is positive and hence feasible only if $\dfrac{\beta\tilde{H} + \gamma N_A^*}{\mu\tilde{H}(1-\nu)} > 1$.

The Jacobian for this system is

$$\begin{aligned} J &= \begin{bmatrix} -\sigma e^{-cN_A^*} - \mu & \nu\phi \\ \sigma e^{-cN_A^*} & \beta - \frac{2\beta I_A}{N_A^*} + \frac{\tilde{H}\gamma N_A^* - \gamma I_A^2 - 2\gamma I_A \tilde{H}}{(I_A + \tilde{H})^2} - \mu \end{bmatrix} \\ &= \begin{bmatrix} -\frac{\phi\mu}{\phi - \mu} & \nu\phi \\ \frac{\mu^2}{\phi - \mu} & \beta - \frac{2\beta I_A}{N_A^*} + \frac{\tilde{H}\gamma N_A^* - \gamma I_A^2 - 2\gamma I_A \tilde{H}}{(I_A + \tilde{H})^2} - \mu \end{bmatrix}. \end{aligned} \tag{2.23}$$

Substituting the trivial fixed point $(I_J^*, I_A^*) = (0,0)$ into the Jacobian (equation 2.23) gives:

$$J = \begin{bmatrix} -\frac{\phi\mu}{\phi - \mu} & \nu\phi \\ \frac{\mu^2}{\phi - \mu} & \beta + \frac{\gamma N_A^*}{\tilde{H}} - \mu \end{bmatrix}.$$

The corresponding trace and determinant are:

$$\begin{aligned}\Delta &= \frac{\phi\mu}{\phi-\mu}\left(\mu(1-\nu)-\frac{\gamma N_A^*}{\tilde{H}}-\beta\right),\\ \tau &= \frac{\beta\tilde{H}+\gamma N_A^*}{\tilde{H}}-\frac{\mu(2\phi-\mu)}{(\phi-\mu)}.\end{aligned}$$

$\Delta < 0$ when $\dfrac{\beta\tilde{H}+\gamma N_A^*}{\mu\tilde{H}(1-\nu)} > 1$ and the fixed point is a saddle.

$\Delta > 0$ when $\dfrac{\beta\tilde{H}+\gamma N_A^*}{\mu\tilde{H}(1-\nu)} < 1$ and the fixed point is either a stable node or an unstable node. Now $\dfrac{\phi-\mu}{2\phi-\mu} < 1$ and $\dfrac{\beta\tilde{H}+\gamma N_A^*}{\mu\tilde{H}} < \dfrac{\beta\tilde{H}+\gamma N_A^*}{\mu\tilde{H}(1-\nu)} < 1$ so $\dfrac{\beta\tilde{H}+\gamma N_A^*}{\mu\tilde{H}}\dfrac{\phi-\mu}{2\phi-\mu} < 1 \Rightarrow \tau < 0$ and the fixed point is stable.

Substituting the non-trivial fixed point (I_J^*, I_A^*) into the Jacobian (equation 2.23) gives:

$$J = \begin{bmatrix} -\frac{\phi\mu}{\phi-\mu} & \nu\phi \\ \frac{\mu^2}{\phi-\mu} & \beta - \frac{2\beta I_A^*}{N_A^*} + \frac{\gamma(N_A^*\tilde{H} - I_A^{*2} - 2I_A^*\tilde{H})}{(I_A^*+\tilde{H})^2} - \mu \end{bmatrix}.$$

The corresponding trace and determinant are:

$$\begin{aligned}\Delta &= \frac{\phi\mu}{\phi-\mu}[-\beta + \frac{2\beta I_A^*}{N_A^*} - \frac{\gamma\tilde{H}(N_A^*-I_A^*)}{(I_A^*+\tilde{H})^2} + \frac{\gamma I_A^*}{I_A^*+\tilde{H}} + \mu(1-\nu)],\\ \tau &= -\frac{\phi\mu}{\phi-\mu} + \beta - \frac{2\beta I_A^*}{N_A^*} + \frac{\gamma\tilde{H}(N_A^*-I_A^*)}{(I_A^*+\tilde{H})^2} - \frac{\gamma I_A^*}{I_A^*+\tilde{H}} - \mu.\end{aligned}$$

Now let $\Phi(I_J, I_A) = \dot{I}_A$. By adding $\dfrac{\phi\mu}{\phi-\mu}\dfrac{\Phi(I_J^*, I_A^*)}{I_A^*} = 0$ to Δ,

$\Delta = \dfrac{\phi\mu}{\phi-\mu}\left(\dfrac{\beta I_A^*}{N_A^*} + \dfrac{\gamma I_A^*(N_A^*+\tilde{H})}{(I_A^*+\tilde{H})^2}\right) > 0$ and the fixed point is either stable or unstable.

By subtracting $\dfrac{\Phi(I_J^*, I_A^*)}{I_A^*} = 0$ from τ,

$\tau = -\dfrac{\phi\mu}{\phi-\mu} - \dfrac{\beta I_A^*}{N_A^*} - \dfrac{\gamma I_A^*(N_A^*+\tilde{H})}{(I_A^*+\tilde{H})^2} - \mu\nu < 0$, so the fixed point is a stable

node.

The infection subsystem in a small neighbourhood of the infection-free steady state is

$$\begin{aligned}\dot{I}_J &= \nu\phi I_A - \sigma e^{-cN_A^*} I_J - \mu I_J,\\ \dot{I}_A &= \sigma e^{-cN_A^*} I_J + \beta I_A + \frac{\gamma N_A^*}{\tilde{H}} I_A - \mu I_A.\end{aligned}$$

The Jacobian is then

$$J = \begin{bmatrix} -\sigma e^{-cN_A^*} - \mu & \nu\phi \\ \sigma e^{-cN_A^*} & \beta + \frac{\gamma N_A^*}{\tilde{H}} - \mu \end{bmatrix} \text{ and so } T = \begin{bmatrix} 0 & \nu\phi \\ \sigma e^{-cN_A^*} & \beta + \frac{\gamma N_A^*}{\tilde{H}} \end{bmatrix}$$

$$\text{and } \Sigma = \begin{bmatrix} -\sigma e^{-cN_A^*} - \mu & 0 \\ 0 & -\mu \end{bmatrix}.$$

Then the next generation matrix is

$$K = -T\Sigma^{-1} = \begin{bmatrix} 0 & \frac{\nu\phi}{\mu} \\ \frac{\sigma e^{-cN_A^*}}{\mu + \sigma e^{-cN_A^*}} & \frac{\beta}{\mu} + \frac{\gamma N_A^*}{\mu\tilde{H}} \end{bmatrix} \text{ and}$$

$$\begin{aligned} R_0 &= \frac{1}{2}\left(\frac{\beta}{\mu} + \frac{\gamma N_A^*}{\mu\tilde{H}} + \sqrt{\left(\frac{\beta}{\mu} + \frac{\gamma N_A^*}{\mu\tilde{H}}\right)^2 + 4\frac{\sigma e^{-cN_A^*}\nu\phi}{\mu(\sigma e^{-cN_A^*} + \mu)}} \right) \\ &= \frac{1}{2}\left(\frac{\beta}{\mu} + \frac{\gamma N_A^*}{\mu\tilde{H}} + \sqrt{\left(\frac{\beta}{\mu} + \frac{\gamma N_A^*}{\mu\tilde{H}}\right)^2 + 4\nu} \right). \end{aligned}$$

The stability threshold for the fixed point is $\dfrac{\beta\tilde{H} + \gamma N_A^*}{\mu\tilde{H}(1-\nu)} = 1$. Rearranging this gives $\dfrac{\beta}{\mu} + \dfrac{\gamma N_A^*}{\mu\tilde{H}} = 1 - \nu$. Substituting this into $R_0 = \dfrac{1}{2}\left(1 - \nu + \sqrt{(1+\nu)^2}\right) = 1$.

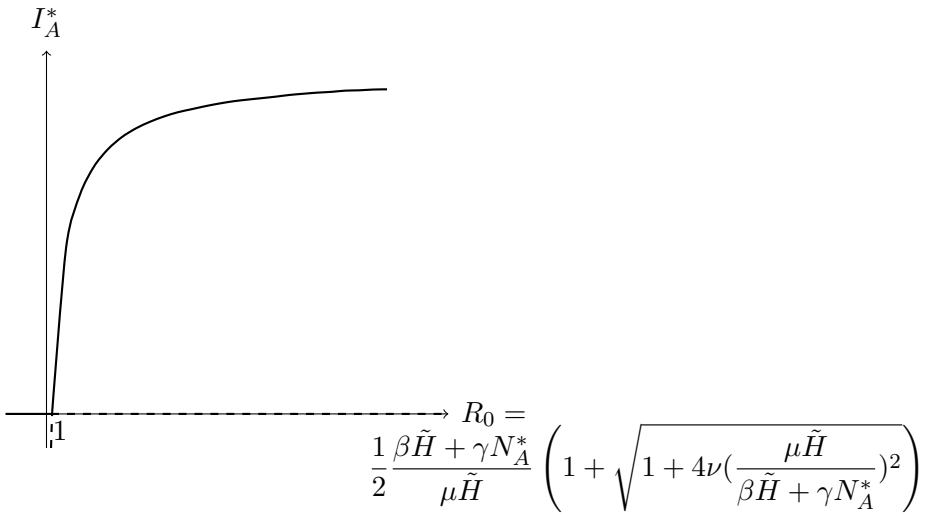

Figure 2.12: *Bifurcation diagram for simplification three of the two age class rat model. Bifurcation at* $R_0 = 1$.

2.2.6 Simplification 4 ($\beta = 0$ and $\dot{L} \neq 0$)

When $\beta = 0$ and $\dot{L} \neq 0$, equations 2.17 and 2.18 become the first two equations below and equation 2.19 is included in the analysis:

$$\begin{aligned}
\frac{dI_J}{dt} &= \nu\phi I_A - \sigma e^{-cN_A^*} I_J - \mu I_J, \\
\frac{dI_A}{dt} &= \sigma e^{-cN_A^*} I_J + \frac{\gamma L(N_A^* - I_A)}{L+H} - \mu I_A, \\
\frac{dL}{dt} &= \alpha I_A - \rho L,
\end{aligned}$$

and the problem is now three dimensional.

Solving $\dot{I}_J = 0, \dot{I}_A = 0$ and $\dot{L} = 0$ simultaneously gives the fixed points $(I_J^*, I_A^*, L^*) = (0,0,0)$ and $\left(\frac{\nu(\phi-\mu)}{\mu} I_A^*, I_A^*, \frac{\alpha}{\rho} I_A^*\right)$ where $I_A^* = \frac{\gamma\alpha N_A^* - \mu H\rho(1-\nu)}{\alpha\left(\gamma+\mu(1-\nu)\right)}$, which is positive and hence feasible if $\frac{\gamma\alpha N_A^*}{\mu H\rho(1-\nu)} > 1$.

The Jacobian for this system is

$$\begin{aligned} J &= \begin{bmatrix} -\sigma e^{-cN_A^*} - \mu & \nu\phi & 0 \\ \sigma e^{-cN_A^*} & -\frac{\gamma L}{L+H} - \mu & \frac{\gamma H(N_A^* - I_A)}{(L+H)^2} \\ 0 & \alpha & -\rho \end{bmatrix} \\ &= \begin{bmatrix} -\frac{\phi\mu}{\phi-\mu} & \nu\phi & 0 \\ \frac{\mu^2}{\phi-\mu} & -\frac{\gamma L}{L+H} - \mu & \frac{\gamma H(N_A^* - I_A)}{(L+H)^2} \\ 0 & \alpha & -\rho \end{bmatrix}. \end{aligned} \tag{2.24}$$

Substituting the trivial fixed point $(I_J^*, I_A^*, L^*) = (0, 0, 0)$ into the Jacobian (equation 2.24) gives:

$$J = \begin{bmatrix} -\frac{\phi\mu}{\phi-\mu} & \nu\phi & 0 \\ \frac{\mu^2}{\phi-\mu} & -\mu & \frac{\gamma N_A^*}{H} \\ 0 & \alpha & -\rho \end{bmatrix}.$$

The Routh-Hurwitz coefficients $\{a_n\}$ are:

$$\begin{aligned} a_1 &= \frac{\phi\mu}{\phi-\mu} + \mu + \rho, \\ a_2 &= \frac{\phi\mu}{H(\phi-\mu)} \left((\phi-\mu)(\mu H\rho - \gamma N_A^*\alpha) + H\mu(1-\nu) + H\rho \right), \\ a_3 &= \frac{\phi\mu}{H(\phi-\mu)} \left(\mu H\rho(1-\nu) - \gamma N_A^*\alpha \right) \end{aligned}$$

and

$$a_1a_2 - a_3 = \frac{\phi\mu}{\phi-\mu} \left(\left(\frac{\phi\mu}{\phi-\mu} + \mu + \rho \right) (\mu(1-\nu) + \rho) + \mu\rho\nu \right) + (\rho+\mu)(\mu\rho - \frac{\gamma N_A^*\alpha}{H}).$$

Now $a_1 > 0, a_2 > 0, a_3 > 0$ and $a_1a_2 > a_3$ when $\dfrac{\gamma\alpha N_A^*}{\mu H\rho(1-\nu)} < 1$ ($\dfrac{\mu}{\phi} < 1$ follows from the feasibility condition for N_A^*) and the fixed point is stable, otherwise it is unstable.

Substituting the non-trivial fixed point (I_J^*, I_A^*, L^*) into the Jacobian (equation 2.24) gives:

$$J = \begin{bmatrix} -\frac{\phi\mu}{\phi-\mu} & \nu\phi & 0 \\ \frac{\mu^2}{\phi-\mu} & -\frac{\gamma L^*}{L^*+H} - \mu - \lambda & \frac{\gamma(N_A^* - I_A^*)H}{(L^*+H)^2} \\ 0 & \alpha & -\rho \end{bmatrix}.$$

The corresponding a_n's are:

$$\begin{aligned}
a_1 &= \frac{\phi\mu}{\phi-\mu}+\frac{\gamma L^*}{L^*+H}+\mu+\rho,\\
a_2 &= \frac{\phi\mu}{\phi-\mu}\left(\mu(1-\nu)+\rho\right)+\frac{\phi\mu}{\phi-\mu}\frac{\gamma\alpha I_A^*}{\alpha I_A^*+H\rho}+\frac{\rho\left(\alpha I_A^*(\mu+\gamma)+H\mu\nu\right)}{\alpha I_A^*+H\rho},\\
a_3 &= \frac{\phi\mu\alpha\rho I_A^*}{(\alpha I_A^*+H\rho)(\phi-\mu)}\left(\gamma+\mu(1-\nu)\right)
\end{aligned}$$

and

$$a_1a_2-a_3=\left(\frac{\gamma I_A^*\alpha}{\alpha I_A^*+H\rho}+\mu+\rho\right)a_2+\left(\frac{\phi\mu}{\phi-\mu}\right)^2\left(\frac{\gamma I_A^*\alpha}{\alpha I_A^*+H\rho}+\mu(1-\nu)+\rho(1+\mu\nu)\right).$$

Now $a_1>0, a_2>0, a_3>0$ and $a_1a_2>a_3$, so the fixed point is stable when it exists.

The infection subsystem in a small neighbourhood of the infection-free steady state is

$$\begin{aligned}
\dot{I}_J &= \nu\phi I_A-\sigma e^{-cN_A^*}I_J-\mu I_J,\\
\dot{I}_A &= \sigma e^{-cN_A^*}I_J+\frac{\gamma N_A^* L}{L+H}-\mu I_A,\\
\dot{L} &= \alpha I_A-\rho L.
\end{aligned}$$

The Taylor series expansion of this subsystem, keeping the first order terms only, in matrix form is

$$J=\begin{bmatrix}-\sigma e^{-cN_A^*}-\mu & \nu\phi & 0\\ \sigma e^{-cN_A^*} & -\mu & \frac{\gamma N_A^*}{H}\\ 0 & \alpha & -\rho\end{bmatrix}\text{ and so }T=\begin{bmatrix}0 & \nu\phi & 0\\ \sigma e^{-cN_A^*} & 0 & \frac{\gamma N_A^*}{H}\\ 0 & \alpha & 0\end{bmatrix}$$

$$\text{and }\Sigma=\begin{bmatrix}-\sigma e^{-cN_A^*}-\mu & 0 & 0\\ 0 & -\mu & 0\\ 0 & 0 & -\rho\end{bmatrix}.$$

Then the next generation matrix is

$$K=-T\Sigma^{-1}=\begin{bmatrix}0 & \frac{\nu\phi}{\mu} & 0\\ \frac{\sigma e^{-cN_A^*}}{\sigma e^{-cN_A^*}+\mu} & 0 & \frac{\gamma N_A^*}{H\rho}\\ 0 & \frac{\alpha}{\mu} & 0\end{bmatrix}\text{ and}$$

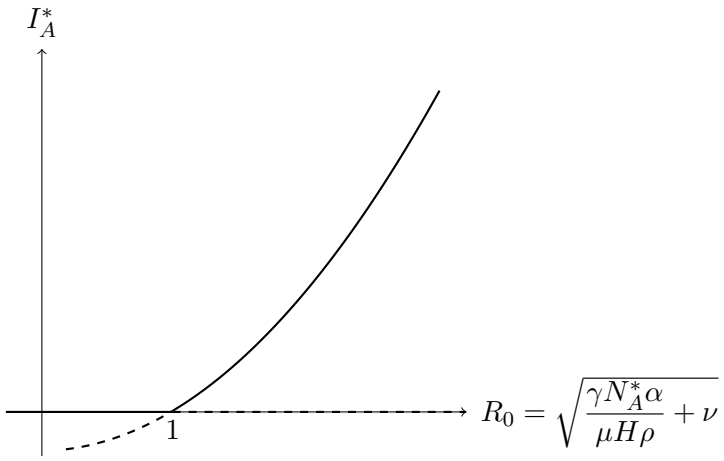

Figure 2.13: *Bifurcation diagram for simplification four of the two age class rat model. Bifurcation at* $R_0 = 1$.

$$R_0 = \sqrt{\frac{\gamma N_A^* \alpha}{\mu H \rho} + \frac{\sigma e^{-cN_A^*} \nu \phi}{\mu(\sigma e^{-cN_A^*} + \mu)}} = \sqrt{\frac{\gamma N_A^* \alpha}{\mu H \rho} + \nu}.$$

The stability threshold for the fixed point is $\frac{\gamma N_A^* \alpha}{\mu H \rho (1-\nu)} = 1$. Rearranging this gives $\frac{\gamma N_A^* \alpha}{\mu H \rho} = 1 - \nu$. Substituting this into $R_0 = \sqrt{1 - \nu + \nu} = 1$.

2.2.7 Simplification 5

Recall equations 2.17-2.19, where no simplifications are made to the system.

$\dot{I}_J = 0, \dot{I}_A = 0$ and $\dot{L} = 0$ need to be solved simultaneously to find the fixed points of the system. One solutions is $(I_J^*, I_A^*, L^*) = (0, 0, 0)$.

Other potential fixed points are given by the roots to

$$F(I) = \beta \alpha I_A^2 + \left(\beta H \rho - \beta N_A^* \alpha + \gamma \alpha N_A^* + \alpha \mu N_A^* (1-\nu)\right) I_A + H \rho N_A^* \mu (1-\nu) - \beta N_A^* H \rho - \gamma \alpha N_A^{*2}.$$

Using lemma 1, $F(0) = N_A^* \left(\mu H \rho (1-\nu) - \beta H \rho - \gamma \alpha N_A^*\right)$ and

$F(N_A^*) = N_A^*\mu(1-\nu)(\alpha N_A^* + H\rho) > 0$, so only cases 1 and 4 are possible.

Case 1 $F(0) = C < 0$ when $\mu H\rho(1-\nu) \leq \beta H\rho + \gamma\alpha N_A^*$, so the solution is $I_A^* = \dfrac{-\left(\beta H\rho + \alpha N_A^*\left(\gamma - \beta + \mu(1-\nu)\right)\right)}{2\alpha\beta}$

$$+\frac{\sqrt{\left(\beta H\rho + \alpha N_A^*\left(\gamma - \beta + \mu(1-\nu)\right)\right)^2 - 4\beta\alpha N_A^*\left(H\rho\left(\mu(1-\nu) - \beta\right) - \gamma\alpha N_A^*\right)}}{2\alpha\beta}.$$

Case 4 $F(0) > 0$ when $\mu H\rho(1-\nu) > \beta H\rho + \gamma\alpha N_A^* \Rightarrow \mu(1-\nu) > \beta$. Now $B = \beta H\rho + \alpha N_A^*\left(\gamma - \beta + \mu(1-\nu)\right)$, but since $\mu(1-\nu) > \beta$, then $B \not< 0$ and by lemma 1, no feasible solution exists.

Now the fixed points are $(I_J^*, I_A^*, L^*) = (0,0,0)$ and (I_J^*, I_A^*, L^*), the latter of which is feasible only if $\dfrac{\beta H\rho + \gamma\alpha N_A^*}{\mu H\rho(1-\nu)} > 1$.

The Jacobian for this system is

$$\begin{aligned} J &= \begin{bmatrix} -\sigma e^{-cN_A^*} - \mu & \nu\phi & 0 \\ \sigma e^{-cN_A^*} & \beta - \frac{2\beta I_A}{N_A^*} - \frac{\gamma L}{L+H} - \mu & \frac{\gamma H(N_A^* - I_A)}{(L+H)^2} \\ 0 & \alpha & -\rho \end{bmatrix} \\ &= \begin{bmatrix} -\frac{\phi\mu}{\phi-\mu} & \nu\phi & 0 \\ \frac{\mu^2}{\phi-\mu} & \beta - \frac{2\beta I_A}{N_A^*} - \frac{\gamma L}{L+H} - \mu & \frac{\gamma H(N_A^* - I_A)}{(L+H)^2} \\ 0 & \alpha & -\rho \end{bmatrix}. \end{aligned} \tag{2.25}$$

Substituting the trivial fixed point $(I_J^*, I_A^*, L^*) = (0,0,0)$ into the Jacobian (equation 2.25) gives:

$$J = \begin{bmatrix} -\frac{\phi\mu}{\phi-\mu} & \nu\phi & 0 \\ \frac{\mu^2}{\phi-\mu} & \beta - \mu & \frac{\gamma N_A^*}{H} \\ 0 & \alpha & -\rho \end{bmatrix}.$$

The Routh-Hurwitz coefficients $\{a_n\}$ are:

$$\begin{aligned}
a_1 &= \frac{\phi\mu}{\phi-\mu} + \rho + \mu - \beta, \\
a_2 &= \frac{\phi\left(\mu H\rho - \gamma\alpha N_A^* - \beta H\rho\right) + \frac{\phi\mu}{\rho}\left(\mu H\rho(1-\nu) - \beta H\rho\right)}{H(\phi-\mu)} \\
&\qquad + \frac{\beta H\rho\mu + H\rho\mu(\phi-\mu) + \gamma N_A^*\alpha\mu}{H(\phi-\mu)}, \\
a_3 &= \frac{\phi\mu}{H(\phi-\mu)}\left(\mu H\rho(1-\nu) - \beta H\rho - \gamma N_A^*\alpha\right)
\end{aligned}$$

$$\begin{aligned}
\text{and } a_1a_2 - a_3 = {} & \frac{\phi\mu}{H(\phi-\mu)}\left(\left(\frac{\phi\mu}{\phi-\mu} + \rho\right)H\rho + \left(\mu H\rho\nu + \gamma N_A^*\alpha\right)\right) \\
& + \frac{\phi}{H(\phi-\mu)}\left(\left(\frac{\phi\mu}{\phi-\mu} + \rho + \mu - \beta\right)\left(H\rho(\mu-\beta) - \gamma\alpha N_A^*\right)\right) \\
& + \frac{\mu}{H(\phi-\mu)}\left(\left(\frac{\phi\mu}{\phi-\mu} + \rho + \mu - \beta\right)\left(\phi\left(\mu H(1-\nu) - \beta H\right) + H\rho(\phi-\mu) + \gamma N_A^*\alpha\right)\right).
\end{aligned}$$

Now $a_1 > 0, a_2 > 0, a_3 > 0$ and $a_1a_2 > a_3$ when $\dfrac{\beta H\rho + \gamma\alpha N_A^*}{\mu H\rho(1-\nu)} < 1$ and the fixed point is stable, otherwise it is unstable.

Substituting the non-trivial fixed point (I_J^*, I_A^*, L^*) into the Jacobian (equation 2.25) gives:

$$J = \begin{bmatrix} -\frac{\phi\mu}{\phi-\mu} & \nu\phi & 0 \\ \frac{\mu^2}{\phi-\mu} & \beta - \frac{2\beta I_A^*}{N_A^*} - \frac{\gamma L^*}{L^*+H} - \mu & \frac{\gamma H(N_A^*-I_A^*)}{(L^*+H)^2} \\ 0 & \alpha & -\rho \end{bmatrix}.$$

The corresponding a_n's are:

$$\begin{aligned}
a_1 &= \frac{\phi\mu}{\phi-\mu} + \frac{\gamma\alpha I_A^*}{\alpha I_A^* + H\rho} + \mu + \rho - \beta + \frac{2\beta I_A^*}{N_A^*}, \\
a_2 &= \frac{\phi\mu}{\phi-\mu}\left(\mu(1-\nu) + \rho + \frac{\gamma\alpha I_A^*}{\alpha I_A^* + H\rho} - \beta + \frac{2\beta I_A^*}{N_A^*}\right) \\
&\qquad + \rho\left(\mu + \frac{\gamma\alpha I_A^*}{\alpha I_A^* + H\rho} - \beta + \frac{2\beta I_A^*}{N_A^*} - \frac{\gamma\alpha H\rho(N_A^* - I_A^*)}{(\alpha I_A^* + H\rho)^2}\right)
\end{aligned}$$

and

$$a_3 = \frac{\phi\mu\rho}{\phi-\mu}\left(\mu(1-\nu) + \frac{\gamma\alpha I_A^*}{\alpha I_A^* + H\rho} - \beta + \frac{2\beta I_A^*}{N_A^*} - \frac{\gamma\alpha H\rho(N_A^* - I_A^*)}{(\alpha I_A^* + H\rho)^2}\right).$$

As for simplification 3, let $\Phi(I_J, I_A) = \dot{I}_A$. Then adding $\dfrac{\Phi(I_J^*, I_A^*)}{I_A^*} = 0$ to a_1 gives $a_1 = \dfrac{\phi\mu}{\phi-\mu} + \dfrac{\gamma\alpha N_A^*}{\alpha I_A^* + H\rho} + \mu\nu + \rho + \dfrac{\beta I_A^*}{N_A^*} > 0$.

Adding $\dfrac{\phi\mu}{\phi-\mu}\dfrac{\Phi(I_J^*, I_A^*)}{I_A^*} + \rho\dfrac{\Phi(I_J^*, I_A^*)}{I_A^*} = 0$ to a_2 gives

$$a_2 = \frac{\phi\mu}{\phi-\mu}\left(\rho + \frac{\beta I_A^*}{N_A^*} + \frac{\gamma N_A^*\alpha}{\alpha I_A^* + H\rho}\right) + \rho\left(\frac{\beta I_A^*}{N_A^*} + \mu\nu + \frac{\gamma I_A^*\alpha H\rho}{\alpha I_A^* + H\rho} + \frac{\gamma I_A^*\alpha^2 N_A^*}{(\alpha I_A^* + H\rho)^2}\right) > 0.$$

Adding $\dfrac{\phi\mu\rho}{\phi-\mu}\dfrac{\Phi(I_J^*, I_A^*)}{I_A^*} = 0$ to a_3 gives

$$a_3 = \frac{\phi\mu}{\phi-\mu}\left(\frac{\beta I_A^*}{N_A^*} + \frac{\gamma\alpha(N_A^* + \tilde{H})}{I_A^* + \tilde{H}}\right) > 0.$$

Now, $a_1a_2 - a_3$

$$\begin{aligned}
&= \frac{\phi\mu}{\phi-\mu}\left(\frac{\phi\mu}{\phi-\mu} + \frac{\beta I_A^*}{N_A^*} + \frac{\gamma\alpha N_A^*}{\alpha I_A^* + H\rho} + \mu\nu\right)\left(\rho + \frac{\beta I_A^*}{N_A^*} + \frac{\gamma\alpha N_A^*}{\alpha I_A^* + H\rho}\right) \\
&+\rho\left(\rho + \frac{\beta I_A^*}{N_A^*} + \frac{\gamma\alpha N_A^*}{\alpha I_A^* + H\rho} + \mu\nu\right)\left(\frac{\beta I_A^*}{N_A^*} + \mu\nu + \frac{\gamma\alpha I_A^* H\rho}{\gamma\alpha + H\rho} + \frac{\gamma\alpha^2 N_A^* I_A^*}{(\alpha I_A^* + H\rho)^2}\right) \\
&+\frac{\phi\mu\rho}{\phi-\mu}\left(\mu\nu + \rho + \frac{\beta I_A^*}{N_A^*} + \frac{\gamma\alpha^2 I_A^{*2} H\rho}{(\alpha I_A^* + H\rho)^2}(1 + H\rho N_A^*)\right) \\
&+\frac{\phi\mu\rho}{\phi-\mu}\frac{\gamma\alpha H\rho}{(\alpha I_A^* + H\rho)^2}(N_A^* - I_A^*) > 0.
\end{aligned}$$

Since $a_1 > 0, a_2 > 0, a_3 > 0$ and $a_1a_2 > a_3$, the fixed point is stable when it exists.

The infection subsystem in a small neighbourhood of the infection-free steady state is

$$\begin{aligned}
\dot{I}_J &= \nu\phi I_A - \sigma e^{-cN_A^*} I_J - \mu I_J, \\
\dot{I}_A &= \sigma e^{-cN_A^*} I_J + \beta I_A + \frac{\gamma N_A^* L}{L+H} - \mu I_A, \\
\dot{L} &= \alpha I_A - \rho L.
\end{aligned}$$

The Taylor series expansion of this subsystem, keeping the first order terms only, in matrix form is

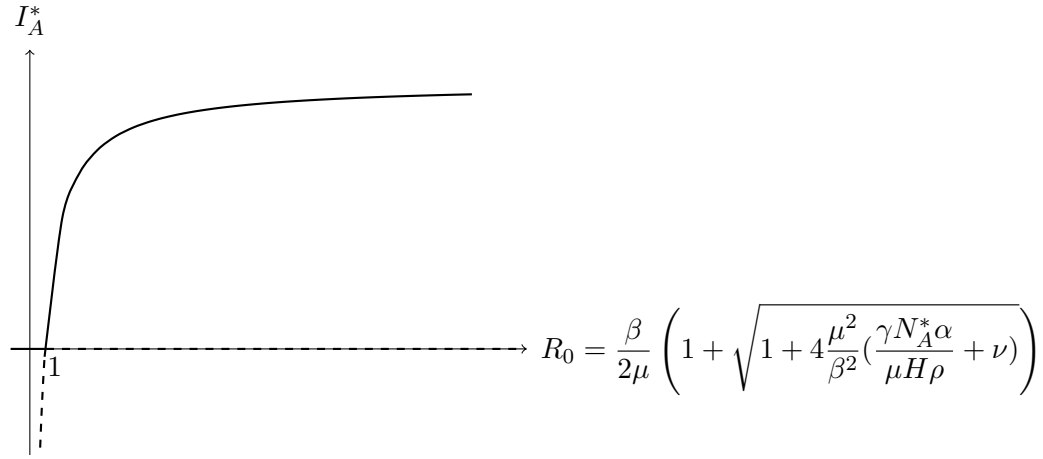

Figure 2.14: *Bifurcation diagram for simplification five of the two age class rat model. Bifurcation at* $R_0 = 1$.

$$J = \begin{bmatrix} -\sigma e^{-cN_A^*} - \mu & \nu\phi & 0 \\ \sigma e^{-cN_A^*} & \beta - \mu & \frac{\gamma N_A^*}{H} \\ 0 & \alpha & -\rho \end{bmatrix} \text{ and so } T = \begin{bmatrix} 0 & \nu\phi & 0 \\ \sigma e^{-cN_A^*} & \beta & \frac{\gamma N_A^*}{H} \\ 0 & \alpha & 0 \end{bmatrix}$$

$$\text{and } \Sigma = \begin{bmatrix} -\sigma e^{-cN_A^*} - \mu & 0 & 0 \\ 0 & -\mu & 0 \\ 0 & 0 & -\rho \end{bmatrix}.$$

The next generation matrix is

$$K = -T\Sigma^{-1} = \begin{bmatrix} 0 & \frac{\nu\phi}{\mu} & 0 \\ \frac{\sigma e^{-cN_A^*}}{\sigma e^{-cN_A^*}+\mu} & \frac{\beta}{\mu} & \frac{\gamma N_A^*}{H\rho} \\ 0 & \frac{\alpha}{\mu} & 0 \end{bmatrix} \text{ and}$$

$$\begin{aligned} R_0 &= \frac{1}{2}\left(\frac{\beta}{\mu} + \sqrt{\frac{\beta^2}{\mu^2} + 4\left(\frac{\gamma N_A^*\alpha}{\mu H\rho} + \frac{\phi\nu}{\mu}\frac{\sigma e^{-cN_A^*}}{\sigma e^{-cN_A^*}+\mu}\right)}\right) \\ &= \frac{1}{2}\left(\frac{\beta}{\mu} + \sqrt{\frac{\beta^2}{\mu^2} + 4\left(\frac{\gamma N_A^*\alpha}{\mu H\rho} + \nu\right)}\right). \end{aligned}$$

The stability threshold for the fixed point is $\frac{\gamma\alpha N_A^* + \beta H\rho}{\mu H\rho(1-\nu)} = 1$. Rearranging this gives $\frac{\gamma N_A^* \alpha}{\mu H\rho} = 1 - \nu - \frac{\beta}{\mu}$. Substituting this into $R_0 = \frac{1}{2}\left(\frac{\beta}{\mu} + \sqrt{\left(2 - \frac{\beta}{\mu}\right)^2}\right) = 1$.

2.3 Rat Model: Three Age Classes

The final age class model considers the full model as in [20]. The model includes all three age classes: juvenile, sub-adult and adult. While the adult classes between the two age class model and the current model remain the same, the juvenile class in the two age class model now becomes the sub-adult class, and the juvenile age class (in the current model) is assigned a new differential equation. Juveniles are introduced into the system at birth rate ϕ and transition from the juvenile class into the sub-adult class at maturation rate ψ. Once a juvenile transitions into the sub-adult class, it is able to leave the nest and hence contribute to, and become infectious by, environmental leptospira. However, it is assumed that they are not yet sexually mature and hence do not pick up infection via sexual contacts. Maturation of sub-adults to sexually mature adults is dependent on adult rat population density. As for all age and infection classes, rats die at rate μ. Take the following set of differential equations:

$$\frac{dN_J}{dt} = \phi N_A - \psi N_J - \mu N_J, \tag{2.26}$$

$$\frac{dN_S}{dt} = \psi N_J - \sigma e^{-cN_A} N_S - \mu N_S, \tag{2.27}$$

$$\frac{dN_A}{dt} = \sigma e^{-cN_A} N_S - \mu N_A, \tag{2.28}$$

$$\frac{dI_J}{dt} = \nu\phi I_A - \psi I_J - \mu I_J, \tag{2.29}$$

$$\frac{dI_S}{dt} = \psi I_J - \sigma e^{-cN_A} I_S + \frac{\gamma(N_S - I_S)L}{L+H} - \mu I_S, \tag{2.30}$$

$$\frac{dI_A}{dt} = \sigma e^{-cN_A} I_S + \frac{\beta(N_A - I_A)I_A}{N_A} + \frac{\gamma(N_A - I_A)L}{L+H} - \mu I_A, \tag{2.31}$$

$$\frac{dL}{dt} = \alpha(I_A + I_S) - \rho L. \tag{2.32}$$

Symbol	Description	Value	Units
N_J	Density of the juvenile rat population in a given area		ha^{-1}
N_S	Density of the sub-adult rat population in a given area		ha^{-1}
N_A	Density of the adult rat population in a given area		ha^{-1}
I_J	Density of the infectious juvenile rat population in a given area		ha^{-1}
I_S	Density of the infectious sub-adult rat population in a given area		ha^{-1}
I_A	Density of the infectious adult rat population in a given area		ha^{-1}
L	Free living leptospires		ha^{-1}
ϕ	Rat birth rate	0.28	day^{-1}
ψ	Maturation rate of juvenile rats to sub-adult rats	0.04	day^{-1}
μ	Rat death rate	0.013	day^{-1}
σ	Maturation rate of sub-adult rats to adult rats	0.01	day^{-1}
c	Shape parameter for density dependence in maturation of sub-adult rats to adult rats	0.04	
ν	Probability of pseudo vertical transmission in rats	0.01	
β	Sexual transmission co-efficient for rats	0.01	day^{-1}
γ	Environmental transmission co-efficient for rats	0.005	day^{-1}
H	Number of leptospires at which transmission rate from the environment is 0.5γ	10^6	ha^{-1}
α	Number of leptospires shed per infectious rat	10^3	day^{-1}
ρ	Leptospire death rate	0.05	day^{-1}

Table 2.3: *Nomenclature and parameter values for the three age class rat model*

2.3.1 Numerical Results

For simplifications 2-5, non-trivial fixed points are found numerically using Matlab. Parameter values, shown in table 2.3, are chosen from those in the Holt model. Each fixed point found, as well as the trivial fixed point, is substituted into the Jacobian matrix of its system. The eigenvalues of the corresponding Jacobian matrix are used to determine stability. If the real part of all the eigenvalues is negative, then the fixed point is stable, otherwise it is unstable. The basic reproduction number, R_0, which is just the dominant eigenvalue of the next generation matrix, must also be calculated numerically. The information is summarised in a numerically plotted bifurcation diagram.

2.3.2 Infection-free System

2.3.2.1 Fixed Points

The infection free subsystem is made up of equations 2.26, 2.27 and 2.28, $\dot{N}_J$, $\dot{N}_S$ and $\dot{N}_A$ respectively. Fixed points occur when $\dot{N}_J = 0$, $\dot{N}_S = 0$ and $\dot{N}_A = 0$.

The fixed point for $\dot{N}_J$ occurs when $N_J^* = \dfrac{\phi}{\psi + \mu} N_A$.

The fixed point for $\dot{N}_S$ occurs when $N_S^* = \dfrac{\psi}{\sigma e^{-cN_A} + \mu} N_J$.

To solve $\dot{N}_A = 0$, N_J^* must be substituted into N_S^* and N_S^* substituted into $\dot{N}_A$ to give $\dot{N}_A = \dfrac{\sigma e^{-cN_A} \psi \phi}{(\sigma e^{-cN_A} + \mu)(\psi + \mu)} N_A - \mu N_A$.

The solutions to this are $N_A^* = 0$ and $N_A^* = \dfrac{1}{c} \log \dfrac{\sigma(\phi\psi - \mu\psi - \mu^2)}{\mu^2(\psi + \mu)}$. So the fixed points of the infection free system are $(N_J^*, N_S^*, N_A^*) = (0, 0, 0)$ and (N_J^*, N_S^*, N_A^*), the latter of which is positive and hence feasible if $\dfrac{\sigma(\phi\psi - \mu\psi - \mu^2)}{\mu^2(\psi + \mu)} > 1$. This condition is necessary for all non-trivial fixed points of the infectious system.

2.3.2.2 Local Stability

The stability of each fixed point is determined by substituting the fixed point into the Jacobian matrix of the system and using the Routh-Hurwitz

condition to determine stability.

The Jacobian for the system is

$$J = \begin{bmatrix} -\psi - \mu & 0 & \phi \\ \psi & -\sigma e^{-cN_A} - \mu & cN_S\sigma e^{-cN_A} \\ 0 & \sigma e^{-cN_A} & -cN_S\sigma e^{-cN_A} - \mu \end{bmatrix}. \tag{2.33}$$

Substituting the trivial fixed point into the Jacobian (equation 2.33) gives:

$$J = \begin{bmatrix} -\psi - \mu & 0 & \phi \\ \psi & -\sigma - \mu & 0 \\ 0 & \sigma & -\mu \end{bmatrix}.$$

The Routh-Hurwitz coefficients $\{a_n\}$ are:

$$\begin{aligned} a_1 &= \sigma + 3\mu + \psi, \\ a_2 &= \mu(2\sigma + 3\mu + 2\psi) + \psi\sigma, \\ a_3 &= \mu^2(\psi + \mu) - \sigma(\phi\psi - \mu\psi - \mu^2) \end{aligned}$$

and

$$a_1a_2 - a_3 = (\sigma + 2\mu + \psi)(2\mu\sigma + 4\mu^2 + \psi\sigma + 2\psi\mu) + \psi\sigma\phi.$$

Now $a_1 > 0, a_2 > 0, a_3 > 0$ and $a_1a_2 > a_3$ when $\dfrac{\sigma(\phi\psi - \mu\psi - \mu^2)}{\mu^2(\psi + \mu)} < 1$ and the fixed point is stable, otherwise it is unstable.

The Routh-Hurwitz coefficients of the Jacobian at the non-trivial fixed point (I_J^*, I_A^*, L^*) are:

$$\begin{aligned} a_1 &= \sigma e^{-cN_A^*}(1 + cN_S^*) + 3\mu + \psi, \\ a_2 &= \sigma e^{-cN_A^*}(\psi + 2\mu)(1 + cN_S^*) + \mu(2\psi + 3\mu), \\ a_3 &= \mu cN_S^*\sigma e^{-cN_A^*}(\psi + \mu) \end{aligned}$$

and

$$\begin{aligned} a_1a_2 - a_3 &= \left(\sigma e^{-cN_A^*}(1 + cN_S^*) + \psi\right)\left(\sigma e^{-cN_A^*}(\psi + 2\mu)(1 + cN_S^*) + \mu(2\psi + 3\mu)\right) \\ &\quad + 3\mu\left(\sigma e^{-cN_A^*}(\psi + 2\mu) + \mu(2\psi + 3\mu)\right) + \mu cN_S^*\sigma e^{-cN_A^*}(2\psi + 5\mu). \end{aligned}$$

Now $a_1 > 0, a_2 > 0, a_3 > 0$ and $a_1a_2 > a_3$, so the fixed point is stable when it exists.

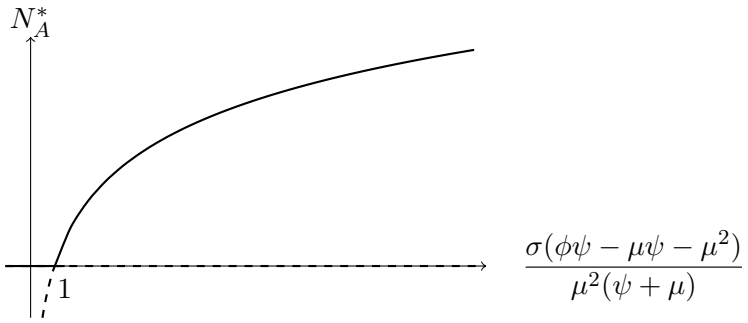

Figure 2.15: *Bifurcation diagram for the infection-free subsystem of the three age class rat model. Bifurcation at* $\frac{\sigma(\phi\psi - \mu\psi - \mu^2)}{\mu^2(\psi + \mu)} = 1$.

2.3.3 Infectious System

2.3.3.1 Fixed Points

The infectious subsystem is made up of equations 2.29, 2.30, 2.31 and 2.32, $\dot{I}_J$, $\dot{I}_S$, $\dot{I}_A$ and $\dot{L}$ respectively. Fixed points occur when $\dot{N}_J = 0$, $\dot{N}_S = 0$, $\dot{N}_A = 0$, $\dot{I}_J = 0$, $\dot{I}_S = 0$, $\dot{I}_A = 0$ and $\dot{L} = 0$. In each of the cases covered, the solutions to $\dot{N}_J = 0, \dot{N}_S = 0, \dot{N}_A = 0, \dot{I}_J = 0$ and $\dot{L} = 0$ are the same, so these are solved first.

The dynamics of N_J, N_S and N_A are independent of the dynamics of I_J, I_S, I_A and L, so it is assumed that N_J, N_S and N_A are at the non-trivial steady state values of N_J^*, N_S^* and N_A^* as found in section 2.3.2.1. Now, several simplifications can be made to the calculations in this section:

$$\sigma e^{-cN_A^*} = \frac{\mu^2(\psi + \mu)}{\phi\psi - \mu\psi - \mu^2}, \quad \sigma e^{-cN_A^*} + \mu = \frac{\phi\psi\mu}{\phi\psi - \mu\psi - \mu^2}$$

and

$$\frac{\sigma e^{-cN_A^*}}{\sigma e^{-cN_A^*} + \mu} = \frac{\mu(\psi + \mu)}{\phi\psi}.$$

Also, let $\sigma e^{-cN_A^*}$ be denoted σ_a.

Then, the solution to $\dot{I}_J = 0$ is $I_J^* = \frac{\nu\phi}{\psi + \mu} I_A$.

The solution to $\dot{L} = 0$ is $L^* = \frac{\alpha}{\rho}(I_S + I_A)$.

The solutions to $\dot{I}_S = 0$ and $\dot{I}_A = 0$ are discussed on a case by case basis.

The existence of a trivial fixed point for $\dot{I}_S = 0$ and $\dot{I}_A = 0$ is easy to prove analytically simply by substituting the the fixed point into $\dot{I}_S$ and $\dot{I}_A$. However, in some cases, analytically proving the existence of a non-trivial fixed point is not possible, so the fixed point is found numerically. This is done by first analytically solving $\dot{I}_S = 0$ with respect to I_A. Values of I_A in the range $0 < I_A < N_A$ are then substituted into the solution for $\dot{I}_S = 0$, which are in turn substituted into $I_A^{**} = \frac{1}{\mu}\left(\sigma e^{-cN_A} I_S + \frac{\beta(N_A - I_A)I_A}{N_A} + \frac{\gamma(N_A - I_A)L}{L + H}\right)$ (derived from $\dot{I}_A = 0$). I_A^{**} can then be plotted together with I_A over the range $0 < I_A < N_A$. The intersection of the two curves is a fixed point. Parameter values from [20] are used in calculations.

2.3.4 Simplification 1 ($\gamma = 0$)

When $\gamma = 0$, equations 2.29, 2.30 and 2.31 become:

$$\begin{aligned}
\frac{dI_J}{dt} &= \nu\phi I_A - \psi I_J - \mu I_J, \\
\frac{dI_S}{dt} &= \psi I_J - \sigma_a I_S - \mu I_S, \\
\frac{dI_A}{dt} &= \sigma_a I_S + \frac{\beta(N_A^* - I_A)I_A}{N_A^*} - \mu I_A.
\end{aligned}$$

Solving $\dot{I}_J = 0$, $\dot{I}_S = 0$ and $\dot{I}_A = 0$ simultaneously gives the fixed points $(I_J^*, I_S^*, I_A^*) = (0, 0, 0)$ and $\left(\frac{\nu\phi}{\psi + \mu} I_A^*, \frac{\psi}{\sigma_a + \mu}\frac{\nu\phi}{\psi + \mu} I_A^*, I_A^*\right)$ where $I_A^* = N_A^*\left(1 - \frac{\mu}{\beta}(1 - \nu)\right)$, which is positive, and hence feasible, only if $\frac{\beta}{\mu(1 - \nu)} > 1$.

The Jacobian for this system is

$$J = \begin{bmatrix} -\psi - \mu & 0 & \nu\phi \\ \psi & -\sigma_a - \mu & 0 \\ 0 & \sigma_a & \beta - 2\frac{\beta I_A}{N_A} - \mu \end{bmatrix}. \tag{2.34}$$

Substituting the trivial fixed point $(I_J^*, I_S^*, I_A^*) = (0, 0, 0)$ into the Jacobian (equation 2.34) gives:

$$J = \begin{bmatrix} -\psi - \mu & 0 & \nu\phi \\ \psi & -\sigma_a - \mu & 0 \\ 0 & \sigma_a & \beta - \mu \end{bmatrix}.$$

The corresponding Routh-Hurwitz coefficients are:

$$\begin{aligned} a_1 &= \psi + \mu + \sigma_a - \beta, \\ a_2 &= \psi\sigma_a + (\psi + \sigma_a + 2\mu)(2\mu - \beta) + \mu(\mu - \beta) \\ a_3 &= (\psi + \mu)(\sigma_a + \mu)\,(\mu(1 - \nu) - \beta) \end{aligned}$$

and

$$\begin{aligned} a_1 a_2 - a_3 &= (\psi + \sigma_a)\,(\psi\sigma_a + (2\mu - \beta)(\psi + \sigma_a + 2\mu) + \mu(\mu - \beta)) \\ &\quad + (\mu - \beta)^2(3\mu + \psi + \sigma_a + \mu^2) + \psi\sigma_a\nu\phi. \end{aligned}$$

Now $a_1 > 0, a_2 > 0, a_3 > 0$ and $a_1 a_2 > a_3$ when $\dfrac{\beta}{\mu(1-\nu)} < 1$ and the fixed point is stable, otherwise it is unstable.

Substituting the non-trivial fixed point (I_J^*, I_S^*, I_A^*) into the Jacobian (equation 2.34) gives:

$$J = \begin{bmatrix} -\psi - \mu & 0 & \nu\phi \\ \psi & -\sigma_a - \mu & 0 \\ 0 & \sigma_a & -\beta + \mu - 2\frac{\nu}{\phi} \end{bmatrix}.$$

The corresponding $a_n's$ are:

$$\begin{aligned} a_1 &= \psi + \mu + \sigma_a + \beta + 2\mu\nu, \\ a_2 &= 2\,(\beta - \mu(1 - \nu))\,(\psi + \mu + \sigma_a) + \psi\sigma_a + 2\mu(\psi + \beta + \mu\nu), \\ a_3 &= (\beta - \mu(1 - \nu) + \mu\nu)\,(\psi + \mu)(\sigma_a + \mu) \end{aligned}$$

and

$$\begin{aligned} a_1 a_2 - a_3 &= 2(\psi + \sigma_a + \beta + \mu + 2\mu\nu)\,(\psi\mu + \psi\,(\beta - \mu(1 - \nu)) + \beta\mu) \\ &\quad + 2\,(\beta - \mu(1 - \nu))\,(\sigma_a + \beta + 2\mu\nu)(\mu + \sigma_a) \\ &\quad + \mu\,(\beta - \mu(1 - \nu))\,(\psi + \sigma_a + \mu) + \mu^2\nu(\psi + \sigma_a + \mu) \\ &\quad + \psi\sigma_a(\psi + \sigma_a + 2\beta + 2\mu\nu) + 2\mu^2\nu(\beta + 2\mu\nu). \end{aligned}$$

Now $a_1 > 0, a_2 > 0, a_3 > 0$ and $a_1 a_2 > a_3$, so the fixed point is stable when it exists.

The infection subsystem in a small neighbourhood of the infection-free steady state is

$$\begin{aligned} \dot{I}_J &= \nu\phi I_A - \psi I_J - \mu I_J, \\ \dot{I}_S &= \psi I_J - \sigma_a I_S - \mu I_S, \\ \dot{I}_A &= \sigma_a I_S + \beta I_A - \mu I_A. \end{aligned}$$

The Taylor series expansion of this subsystem, keeping the first order terms only, in matrix form is

$$J = \begin{bmatrix} -\psi - \mu & 0 & \nu\phi \\ \psi & -\sigma_a - \mu & 0 \\ 0 & \sigma_a & \beta - \mu \end{bmatrix} \text{ and so } T = \begin{bmatrix} 0 & 0 & \nu\phi \\ 0 & 0 & 0 \\ 0 & 0 & \beta \end{bmatrix}$$

$$\text{and } \Sigma = \begin{bmatrix} -\psi - \mu & 0 & 0 \\ \psi & -\sigma_a - \mu & 0 \\ 0 & \sigma_a & -\mu \end{bmatrix}.$$

Then the next generation matrix is

$$K = -T\Sigma^{-1} = \begin{bmatrix} \frac{\psi}{\psi+\mu}\frac{\sigma_a}{\sigma_a+\mu}\frac{\phi\nu}{\mu} & \frac{\sigma_a}{\sigma_a+\mu}\frac{\phi\nu}{\mu} & \frac{\phi\nu}{\mu} \\ 0 & 0 & 0 \\ \frac{\psi}{\psi+\mu}\frac{\sigma_a}{\sigma_a+\mu}\frac{\beta}{\mu} & \frac{\sigma_a}{\sigma_a+\mu}\frac{\beta}{\mu} & \frac{\beta}{\mu} \end{bmatrix} \text{ and}$$

$$R_0 = \frac{\beta}{\mu} + \frac{\nu\phi\sigma_a\psi}{\mu(\sigma_a+\mu)(\psi+\mu)} = \frac{\beta}{\mu} + \nu.$$

The stability threshold for the fixed point is $\dfrac{\beta}{\mu(1-\nu)} = 1$. Rearranging this gives $\dfrac{\beta}{\mu} = 1-\nu$. Substituting this into $R_0 = 1-\nu+\dfrac{\nu\phi\sigma_a\psi}{\mu(\sigma_a+\mu)(\psi+\mu)} = 1-\nu+\nu = 1$.

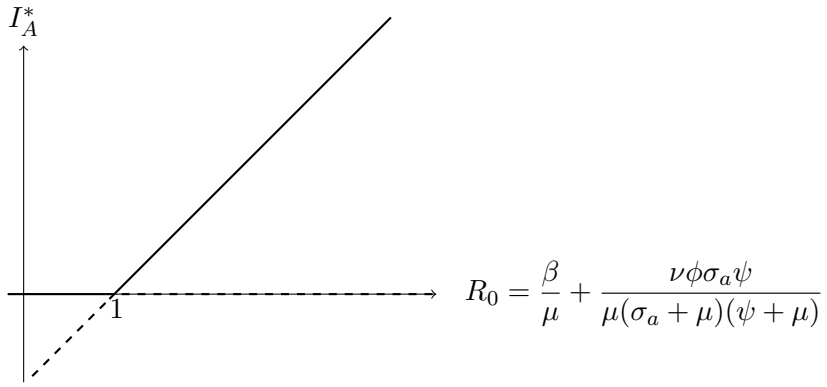

Figure 2.16: *Bifurcation diagram for simplification one of the three age class rat model. Bifurcation at* $R_0 = 1$.

2.3.5 Simplification 2 ($\beta = 0$ and $\dot{L} = 0$)

When $\beta = 0$ and $\dot{L} = 0$, equations 2.29, 2.30 and 2.31 become:

$$\begin{aligned}
\frac{dI_J}{dt} &= \nu\phi I_A - \psi I_J - \mu I_J, \\
\frac{dI_S}{dt} &= \psi I_J - \sigma_a I_S + \frac{\gamma(N_S - I_S)(I_A + I_S)}{I_S + I_A + \tilde{H}} - \mu I_S, \\
\frac{dI_A}{dt} &= \sigma_a I_S + \frac{\gamma(N_A - I_A)(I_A + I_S)}{I_S + I_A + \tilde{H}} - \mu I_A
\end{aligned}$$

where $\tilde{H} = \frac{\rho}{\alpha} H$.

The results for this simplification, as well as simplifications 3, 4 and 5, can not be found analytically and are hence calculated numerically.

Equation 2.35 (shown on page 75) shows the Jacobian for this system used in numerical calculations.

The infection subsystem in a small neighbourhood of the infection-free

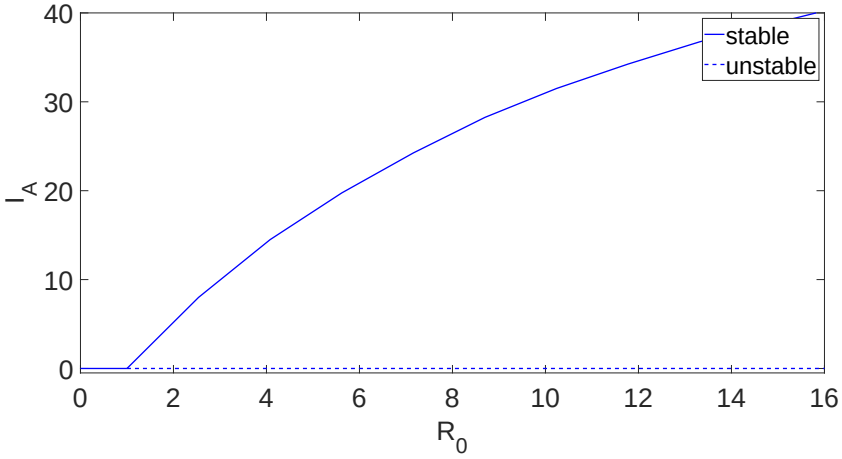

Figure 2.17: *Bifurcation diagram for simplification two of the three age class rat model. Bifurcation at* $R_0 = 1$.

steady state is

$$\begin{aligned}
\dot{I}_J &= \nu\phi I_A - \psi I_J - \mu I_J, \\
\dot{I}_S &= \psi I_J - \sigma_a I_S + \frac{\gamma N_S}{\tilde{H}}(I_S + I_A) - \mu I_S, \\
\dot{I}_A &= \sigma_a I_S + \frac{\gamma N_A}{\tilde{H}}(I_S + I_A) - \mu I_A.
\end{aligned}$$

The Taylor series expansion of this subsystem, keeping the first order terms only, in matrix form is

$$J = \begin{bmatrix} -\psi - \mu & 0 & \nu\phi \\ \psi & \frac{\gamma N_S}{\tilde{H}} + \sigma_a - \mu & \frac{\gamma N_S}{\tilde{H}} \\ 0 & \frac{\gamma N_A}{\tilde{H}} + \sigma_a & \frac{\gamma N_A}{\tilde{H}} - \mu \end{bmatrix} \text{ and so } T = \begin{bmatrix} 0 & 0 & \nu\phi \\ 0 & \frac{\gamma N_S}{\tilde{H}} & \frac{\gamma N_S}{\tilde{H}} \\ 0 & \frac{\gamma N_A}{\tilde{H}} & \frac{\gamma N_A}{\tilde{H}} \end{bmatrix}$$

$$\text{and } \Sigma = \begin{bmatrix} -\psi - \mu & 0 & 0 \\ \psi & -\sigma_a - \mu & 0 \\ 0 & \sigma_a & -\mu \end{bmatrix}.$$

Then the next generation matrix is

$$K = -T\Sigma^{-1} = \begin{bmatrix} \frac{\nu\phi}{\mu}\frac{\psi}{\psi+\mu}\frac{\sigma_a}{\sigma_a+\mu} & \frac{\nu\phi}{\mu}\frac{\sigma_a}{\sigma_a+\mu} & \frac{\phi\nu}{\mu} \\ \frac{\gamma N_S}{\tilde{H}(\sigma_a+\mu)}\frac{\psi}{\psi+\mu}\left(1+\frac{\sigma_a}{\mu}\right) & \frac{\gamma N_S}{\tilde{H}(\sigma_a+\mu)}\left(1+\frac{\sigma_a}{\mu}\right) & \frac{\gamma N_S}{\tilde{H}\mu} \\ \frac{\gamma N_A}{\tilde{H}(\sigma_a+\mu)}\frac{\psi}{\psi+\mu}\left(1+\frac{\sigma_a}{\mu}\right) & \frac{\gamma N_A}{\tilde{H}(\sigma_a+\mu)}\left(1+\frac{\sigma_a}{\mu}\right) & \frac{\gamma N_A}{\tilde{H}\mu} \end{bmatrix}.$$

R_0 is then the dominant eigenvalue of the next generation matrix.

Then, plotting I_A^* against R_0 gives a bifurcation at $R_0 = 1$.

2.3.6 Simplification 3 ($\beta \neq 0$ and $\dot{L} = 0$)

When $\beta \neq 0$ and $\dot{L} = 0$, equations 2.29, 2.30 and 2.31 become:

$$\begin{aligned}
\frac{dI_J}{dt} &= \nu\phi I_A - \psi I_J - \mu I_J, \\
\frac{dI_S}{dt} &= \psi I_J - \sigma_a I_S + \frac{\gamma(N_S - I_S)(I_A + I_S)}{I_S + I_A + \tilde{H}} - \mu I_S, \\
\frac{dI_A}{dt} &= \sigma_a I_S + \frac{\beta(N_A - I_A)I_A}{N_A} + \frac{\gamma(N_A - I_A)(I_A + I_S)}{I_S + I_A + \tilde{H}} - \mu I_A.
\end{aligned}$$

where $\tilde{H} = \dfrac{\rho}{\alpha} H$.

Equation 2.36 (shown on page 75) shows the Jacobian for the system.

The infection subsystem in a small neighbourhood of the infection-free steady state is

$$\begin{aligned}
\dot{I}_J &= \nu\phi I_A - \psi I_J - \mu I_J, \\
\dot{I}_S &= \psi I_J - \sigma_a I_S + \frac{\gamma N_S}{\tilde{H}}(I_S + I_A) - \mu I_S, \\
\dot{I}_A &= \sigma_a I_S + \frac{\gamma N_A}{\tilde{H}}(I_S + I_A) + \beta I_A - \mu I_A.
\end{aligned}$$

The Taylor series expansion of this subsystem, keeping the first order terms only, in matrix form is

$$J = \begin{bmatrix} -\psi - \mu & 0 & \nu\phi \\ \psi & \frac{\gamma N_S}{\tilde{H}} + \sigma_a - \mu & \frac{\gamma N_S}{\tilde{H}} \\ 0 & \frac{\gamma N_A}{\tilde{H}} + \sigma_a & \frac{\gamma N_A}{\tilde{H}} + \beta - \mu \end{bmatrix} \text{ and so } T = \begin{bmatrix} 0 & 0 & \nu\phi \\ 0 & \frac{\gamma N_S}{\tilde{H}} & \frac{\gamma N_S}{\tilde{H}} \\ 0 & \frac{\gamma N_A}{\tilde{H}} & \frac{\gamma N_A}{\tilde{H}} + \beta \end{bmatrix}$$

$$\text{and } \Sigma = \begin{bmatrix} -\psi - \mu & 0 & 0 \\ \psi & -\sigma_a - \mu & 0 \\ 0 & \sigma_a & -\mu \end{bmatrix}.$$

Equation 2.37 shows the next generation matrix for the system.

Jacobian matrix for simplification two of the three age class model.

$$J = \begin{bmatrix} -\phi-\mu & 0 & \nu\phi \\ \psi & -\sigma_a + \frac{\gamma\left(\tilde{H}(N_S-I_A-2I_S)-(I_S+I_A)^2\right)}{(I_S+I_A+\tilde{H})^2} - \mu & \frac{\gamma\tilde{H}(N_S-I_S)}{(I_S+I_A+\tilde{H})^2} \\ 0 & \sigma_a + \frac{\gamma\tilde{H}(N_A+I_A)}{(I_S+I_A+\tilde{H})^2} & \frac{\gamma\left(\tilde{H}(N_A-2I_A-I_S)-(I_S+I_A)^2\right)}{(I_S+I_A+\tilde{H})^2} - \mu \end{bmatrix} \tag{2.35}$$

Jacobian matrix for simplification three of the three age class model.

$$J = \begin{bmatrix} -\phi-\mu & 0 & \nu\phi \\ \psi & -\sigma_a + \frac{\gamma\left(\tilde{H}(N_S-I_A-2I_S)-(I_S+I_A)^2\right)}{(I_S+I_A+\tilde{H})^2} - \mu & \frac{\gamma\tilde{H}(N_S-I_S)}{(I_S+I_A+\tilde{H})^2} \\ 0 & \sigma_a + \frac{\gamma\tilde{H}(N_A+I_A)}{(I_S+I_A+\tilde{H})^2} & \frac{\gamma\left(\tilde{H}(N_A-2I_A-I_S)-(I_S+I_A)^2\right)}{(I_S+I_A+\tilde{H})^2} + \beta - \frac{2*\beta I_A}{N_A} - \mu \end{bmatrix} \tag{2.36}$$

Next generation matrix for simplification three of the three age class model.

$$K = -T\Sigma^{-1} = \begin{bmatrix} \frac{\nu\phi}{\mu}\frac{\psi}{\psi+\mu}\frac{\sigma_a}{\sigma_a+\mu} & \frac{\nu\phi}{\mu}\frac{\sigma_a}{\sigma_a+\mu} & \frac{\phi\nu}{\mu} \\ \frac{\gamma N_S}{\tilde{H}(\sigma_a+\mu)}\frac{\psi}{\psi+\mu}\left(1+\frac{\sigma_a}{\mu}\right) & \frac{\gamma N_S}{\tilde{H}(\sigma_a+\mu)}\left(1+\frac{\sigma_a}{\mu}\right) & \frac{\gamma N_S}{\tilde{H}\mu} \\ \frac{\gamma N_A}{\tilde{H}(\sigma_a+\mu)}\frac{\psi}{\psi+\mu}\left(1+\frac{\sigma_a}{\mu}\right)+\frac{\beta}{\mu}\frac{\sigma_a}{\sigma_a+\mu}\frac{\psi}{\psi+\mu} & \frac{\gamma N_A}{\tilde{H}(\sigma_a+\mu)}\left(1+\frac{\sigma_a}{\mu}\right)+\frac{\beta}{\mu}\frac{\sigma_a}{\sigma_a+\mu} & \frac{\gamma N_A}{\tilde{H}\mu}+\frac{\beta}{\mu} \end{bmatrix} \tag{2.37}$$

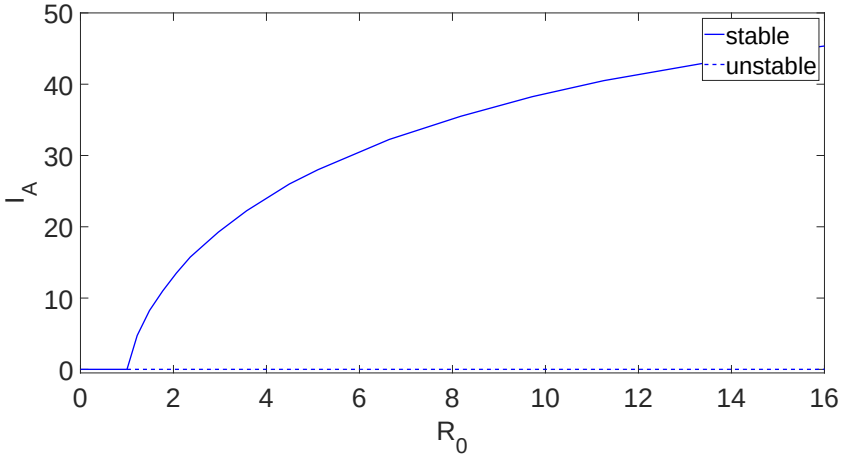

Figure 2.18: *Bifurcation diagram for simplification three of the three age class rat model. Bifurcation at* $R_0 = 1$.

2.3.7 Simplification 4 ($\beta = 0$ and $\dot{L} \neq 0$)

When $\beta = 0$ and $\dot{L} \neq 0$, equations 2.29, 2.30 and 2.31 become the first three equations below and equation 2.32 is included in the analysis.

$$\begin{aligned}
\frac{dI_J}{dt} &= \nu\phi I_A - \psi I_J - \mu I_J, \\
\frac{dI_S}{dt} &= \psi I_J - \sigma_a I_S + \frac{\gamma(N_S - I_S)L}{L+H} - \mu I_S, \\
\frac{dI_A}{dt} &= \sigma_a I_S + \frac{\gamma(N_A - I_A)L}{L+H} - \mu I_A \\
\frac{dL}{dt} &= \alpha(I_S + I_A) - \rho L.
\end{aligned}$$

The Jacobian for the system is

$$J = \begin{bmatrix} -\phi - \mu & 0 & \nu\phi & 0 \\ \psi & -\sigma_a - \frac{\gamma L}{L+H} - \mu & 0 & \frac{\gamma(N_S - I_S)H}{(L+H)^2} \\ 0 & \sigma_a & -\frac{\gamma L}{L+H} - \mu & \frac{\gamma(N_A - I_A)H}{(L+H)^2} \\ 0 & \alpha & \alpha & -\rho \end{bmatrix}.$$

The infection subsystem in a small neighbourhood of the infection-free

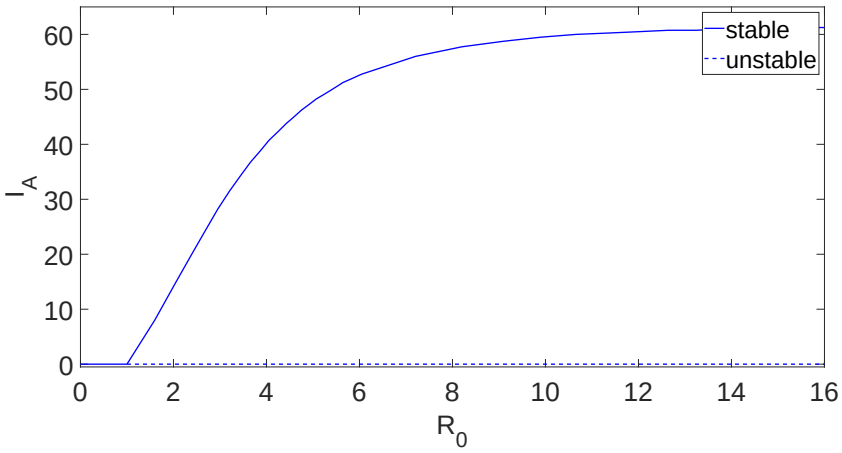

Figure 2.19: *Bifurcation diagram for simplification four of the three age class rat model. Bifurcation at* $R_0 = 1$.

steady state is

$$\begin{aligned}
\dot{I}_J &= \nu\phi I_A - \psi I_J - \mu I_J, \\
\dot{I}_S &= \psi I_J - \sigma_a I_S + \frac{\gamma N_S L}{L+H} - \mu I_S, \\
\dot{I}_A &= \sigma_a I_S + \frac{\gamma N_A L}{L+H} - \mu I_A \\
\dot{L} &= \alpha(I_S + I_A) - \rho L.
\end{aligned}$$

The Taylor series expansion of this subsystem, keeping the first order terms only, in matrix form is

$$J = \begin{bmatrix} -\psi-\mu & 0 & \nu\phi & 0 \\ \psi & -\sigma_a-\mu & 0 & \frac{\gamma N_S}{H} \\ 0 & \sigma_a & -\mu & \frac{\gamma N_A}{H} \\ 0 & \alpha & \alpha & -\rho \end{bmatrix} \text{ and so } T = \begin{bmatrix} 0 & 0 & \nu\phi & 0 \\ 0 & 0 & 0 & \frac{\gamma N_S}{H} \\ 0 & 0 & 0 & \frac{\gamma N_A}{H} \\ 0 & \alpha & \alpha & 0 \end{bmatrix}$$

$$\text{and } \Sigma = \begin{bmatrix} -\psi-\mu & 0 & 0 & 0 \\ \psi & -\sigma_a-\mu & 0 & 0 \\ 0 & \sigma_a & -\mu & 0 \\ 0 & 0 & 0 & -\rho \end{bmatrix}.$$

Then the next generation matrix is

$$K = -T\Sigma^{-1} = \begin{bmatrix} \frac{\nu\phi}{\mu}\frac{\psi}{\psi+\mu}\frac{\sigma_a}{\sigma_a+\mu} & \frac{\nu\phi}{\mu}\frac{\sigma_a}{\sigma_a+\mu} & \frac{\phi\nu}{\mu} & 0 \\ 0 & 0 & 0 & \frac{\gamma N_S}{H\rho} \\ 0 & 0 & 0 & \frac{\gamma N_A}{H\rho} \\ \frac{\psi}{\psi+\mu}\frac{\alpha}{\sigma_a+\mu}\left(1+\frac{\sigma_a}{\mu}\right) & \frac{\alpha}{\sigma_a+\mu}\left(1+\frac{\sigma_a}{\mu}\right) & \frac{\alpha}{\mu} & 0 \end{bmatrix}.$$

2.3.8 Simplification 5

Recall equations 2.29-2.32, where no simplifications are made to the system.
The Jacobian for the system is

$$J = \begin{bmatrix} -\phi-\mu & 0 & \nu\phi & 0 \\ \psi & -\sigma_a - \frac{\gamma L}{L+H} - \mu & 0 & \frac{\gamma(N_S-I_S)H}{(L+H)^2} \\ 0 & \sigma_a & \beta - \frac{2\beta I_A}{N_A} - \frac{\gamma L}{L+H} - \mu & \frac{\gamma(N_A-I_A)H}{(L+H)^2} \\ 0 & \alpha & \alpha & -\rho \end{bmatrix}.$$

The infection subsystem in a small neighbourhood of the infection-free steady state is

$$\begin{aligned} \dot{I}_J &= \nu\phi I_A - \psi I_J - \mu I_J, \\ \dot{I}_S &= \psi I_J - \sigma_a I_S + \frac{\gamma N_S L}{L+H} - \mu I_S, \\ \dot{I}_A &= \sigma_a I_S + \beta I_A + \frac{\gamma N_A L}{L+H} - \mu I_A \\ \dot{L} &= \alpha(I_S + I_A) - \rho L. \end{aligned}$$

The Taylor series expansion of this subsystem, keeping the first order terms only, in matrix form is

$$J = \begin{bmatrix} -\psi-\mu & 0 & \nu\phi & 0 \\ \psi & -\sigma_a-\mu & 0 & \frac{\gamma N_S}{H} \\ 0 & \sigma_a & \beta-\mu & \frac{\gamma N_A}{H} \\ 0 & \alpha & \alpha & -\rho \end{bmatrix} \text{ and so } T = \begin{bmatrix} 0 & 0 & \nu\phi & 0 \\ 0 & 0 & 0 & \frac{\gamma N_S}{H} \\ 0 & 0 & \beta & \frac{\gamma N_A}{H} \\ 0 & \alpha & \alpha & 0 \end{bmatrix}$$

$$\text{and } \Sigma = \begin{bmatrix} -\psi-\mu & 0 & 0 & 0 \\ \psi & -\sigma_a-\mu & 0 & 0 \\ 0 & \sigma_a & -\mu & 0 \\ 0 & 0 & 0 & -\rho \end{bmatrix}.$$

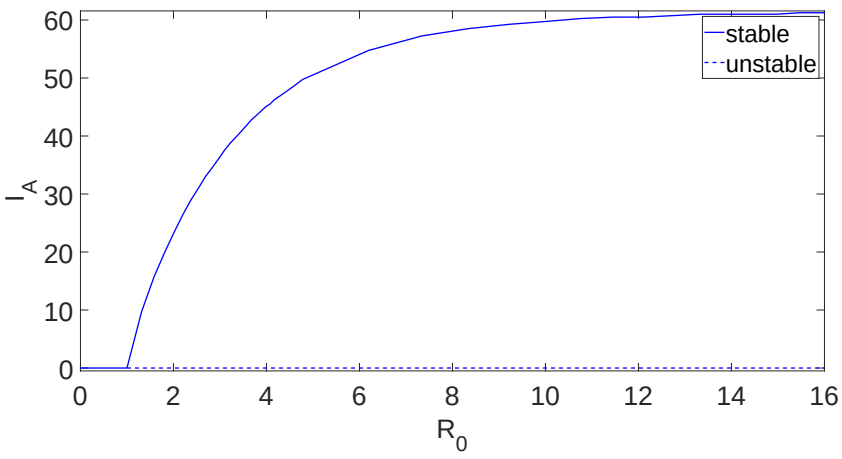

Figure 2.20: *Bifurcation diagram for simplification five of the three age class rat model. Bifurcation at* $R_0 = 1$.

Then the next generation matrix is

$$K = -T\Sigma^{-1} = \begin{bmatrix} \frac{\nu\phi}{\mu}\frac{\psi}{\psi+\mu}\frac{\sigma_a}{\sigma_a+\mu} & \frac{\nu\phi}{\mu}\frac{\sigma_a}{\sigma_a+\mu} & \frac{\phi\nu}{\mu} & 0 \\ 0 & 0 & 0 & \frac{\gamma N_S}{H\rho} \\ \frac{\psi}{\psi+\mu}\frac{\sigma_a}{\sigma_a+\mu}\frac{\beta}{\mu} & \frac{\sigma_a}{\sigma_a+\mu}\frac{\beta}{\mu} & \frac{\beta}{\mu} & \frac{\gamma N_A}{H\rho} \\ \frac{\psi}{\psi+\mu}\frac{\alpha}{\sigma_a+\mu}\left(1+\frac{\sigma_a}{\mu}\right) & \frac{\alpha}{\sigma_a+\mu}\left(1+\frac{\sigma_a}{\mu}\right) & \frac{\alpha}{\mu} & 0 \end{bmatrix}.$$

2.4 Discussion

The most important aspect of the analysis of the rat models is the basic reproduction number, R_0. Several observations can be made about the relationships of the R_0 values between both models and simplifications (see table 2.4).

In the single age class model, the R_0 of simplifications one and two sum to that of simplification three. This can be expected, as both simplifications (one and two) are simple systems which consider each transmission type separately, while in simplification three there is no interaction between transmission types and the equation for free living leptospires is set to zero, ensuring no interaction with a non-constant

variable in the model. As each of these systems is one dimensional and $R_0 = K$, a simple relationship of the basic reproduction number between the simplifications is possible.

Once both $\gamma \neq 0$ and $\dot{L} \neq 0$ in the single age class model, the problem becomes two dimensional. The R_0 of simplification four is the square root of that of simplification two; however, as the basic reproduction number is now the dominant eigenvalue of the next generation matrix (ie. $R_0 = \frac{1}{2}(\text{trace}(K) + \sqrt{\text{trace}^2(K) - 4\det(K)})$), the relationships between the remaining R_0 values in the chapter aren't obviously predictable, although some similarities are apparent.

For the first three simplifications of the two age class model, it can be noted that $K_{1,1} = 0$ and $K_{2,2} = R_0^1$, where R_0^1 is the single age class model basic reproduction number for the corresponding simplification. This is expected, as in this model juvenilles do not transmit infection amongst one another and the equation describing the spreading of infection in the adult class is just the same as the single age class model. The combination of these two facts results in the trace of each simplification being the same as the basic reproduction number for the corresponding simplification in the single age class model. It can also be noted that $K_{1,2} = \frac{\nu\phi}{\mu}$ and $K_{2,1} = \frac{\sigma_a}{\sigma_a + \mu}$ and so the determinant of each simplification (simplifications one to three) is $-\nu$. So for the first three simplifications $R_0^2 = \frac{1}{2}\left(R_0^1 + \sqrt{(R_0^1)^2 + 4\nu}\right)$ where R_0^2 is the basic reproduction number for the two age class model and R_0^1 is the basic reproduction number for the single age class model. It should be expected that R_0^1 makes an appearance in R_0^2 as the single age class model is a component of the two age class model.

As for simplifications one to three (of the two age class model), the next generation matrices of simplifications four and five include the next generation matrices of simplifications four and five of the single age class model, as well as that of simplification one of the two age class model. It should also be pointed out that the basic reproduction numbers of the single age class model can be reached simply by setting the pseudo-vertical transmission probability, ν, in the basic reproduction numbers of the two age class model to zero.

In the three age class model, the majority of the R_0 values are not found analytically at all; however, a comparison of the numerical results of the three age class model with those of the two age class model shows differences between the two models which cannot be generalised through the simplifications.

The differences of the R_0 values between models must be put down to the structured nature of the age classes and the way the spreading of the disease varies amongst age groups. Allowing the free living leptospire class to vary as opposed to holding it constant results in clear differences in the outcomes of the various model simplifications. The major differences in the way the disease spreads in the different model types supports the use of a model with structured age classes and no simplifications. One should keep in mind, however, that the importance of the various transmission routes in the model is not known and these may prove to be insignificant, as field studies provide a greater understanding of the weights various aspects of the model hold in a real life setting.

Simplification	Single Age Class Model	Two Age Class Model	Three Age Class Model
1	$\frac{\beta}{\mu}$	$\frac{1}{2}\left(\frac{\beta}{\mu}+\sqrt{\frac{\beta^2}{\mu^2}+4\nu}\right)$	$\frac{\beta}{\mu}+\frac{\nu\phi\sigma_a\psi}{\mu(\sigma_a+\mu)(\psi+\mu)}$
2	$\frac{\gamma N\alpha}{\mu H\rho}$	$\frac{1}{2}\left(\frac{\gamma N_A^*\alpha}{\mu H\rho}+\sqrt{\left(\frac{\gamma N_A^*\alpha}{\mu H\rho}\right)^2+4\nu}\right)$	Numerical results only
3	$\frac{\beta}{\mu}+\frac{\gamma N\alpha}{\mu H\rho}$	$\frac{1}{2}\left(\frac{\beta}{\mu}+\frac{\gamma N_A^*\alpha}{\mu H\rho}+\sqrt{\left(\frac{\beta}{\mu}+\frac{\gamma N_A^*\alpha}{\mu H\rho}\right)^2+4\nu}\right)$	Numerical results only
4	$\sqrt{\frac{\gamma N\alpha}{\mu H\rho}}$	$\sqrt{\frac{\gamma N_A^*\alpha}{\mu H\rho}+\nu}$	Numerical results only
5	$\frac{1}{2}\left(\frac{\beta}{\mu}+\sqrt{\frac{\beta^2}{\mu^2}+4\frac{\gamma N\alpha}{\mu H\rho}}\right)$	$\frac{1}{2}\left(\frac{\beta}{\mu}+\sqrt{\frac{\beta^2}{\mu^2}+4\left(\frac{\gamma N_A^*\alpha}{\mu H\rho}+\nu\right)}\right)$	Numerical results only

Table 2.4: *Table showing the basic reproduction numbers for all three age class models. Simplifications are as follows:*
Simplification 1: $\gamma = 0$,
Simplification 2: $\beta = 0$ *and* $\frac{dL}{dt} = 0$,
Simplification 3: $\beta \neq 0$ *and* $\frac{dL}{dt} = 0$,
Simplification 4: $\beta = 0$ *and* $\frac{dL}{dt} \neq 0$,
Simplification 5: no simplification.

Chapter 3

The Livestock Model

Introduction

This chapter presents four compartmental, SI type models simulating New Zealand sheep farming practices. The models are cyclical in nature and aim to demonstrate the dynamics of leptospiral infection in farmed livestock, as well as on the farm, and to predict conditions under which the infection will persist in the population.

While numerous compartmental, SI type models for leptospirosis exist, they do not generally include periodic, time varying parameter values, as are incorporated here. Existing models which do include periodic, time varying parameters, usually relate to pulse vaccination, or culling of the host population [35]. While each model presented here does include a culling component, the focus is more on the free living leptospires in the host's environment and how this effects rates of infection in the host from one year to the next. A New Zealand specific compartmental model of paratuberculosis studied by Verdugo explores the free living bacterial aspect of the spreading of infection as well. The model has a similar structure to the ones presented here in that it includes a compartment for free living bacteria, which is considered the most important source of transmission for the disease. Verdugos work is purely numerical due to the complexity of the model, which includes two host species, each of which is divided into four age classes and up to four infection states. The system includes between eight and ten pastures to allow for the separation and periodic grazing of different host types and age classes. The models presented here are somewhat simpler in comparison; however, where possible, results are not only numerical, but also analytical [36].

The main parameter of interest for this chapter is the leptospire death rate, ρ, which is used as a control parameter. While artificially increasing the death rate of leptospires in the environment doesn't currently appear to be in use, it may be an option worth exploring by biologists due to the sensitivity of leptospires to various chemicals such as acids and detergents [37–39]. The effect of climate change on leptospire death rate and its effect on leptospirosis is another consideration, one which is, however, not covered in this chapter. Some other variations in control parameter are included where this is deemed appropriate.

The first model presented is a foundational model and the models following build upon it. The basis of the expanded models is formed on rotational grazing. This is the practice where livestock are moved from one field (pasture) to another, as opposed to stock setting, where the flock or herd remain on the same field permanently. This strategy has been shown to reduce, by 50%, the prevalence of paratuberculosis (caused by *Mycobacterium avium* subspecies *paratuberculosis*) in red deer [21]. The models examine how this farming strategy impacts leptospiral infection in sheep and pasture.

Each of the models in this chapter are SI-type compartmental models. That is, the host population(s) move from one compartment, or category, to another. In the basic cases, these compartments include susceptible and infectious compartments. In two of the extension cases, an immune compartment is also included. Note that the sum of these compartments adds up to the total population density.

Data

The parameter values used for the models are, where possible, based on New Zealand's unique conditions and are derived or calculated from existing published data. Several factors, such as local climate, farming practices and farming conditions, can impact on the spreading of leptospirosis, and these need to be considered when developing a location specific model.

As discussed in the thesis introduction, chapter 1 , climate, for example, will affect the ability of leptospires to survive in the environment

and is considered when selecting the leptospiral death rate, ρ. While the leptospire death rate is used as a control parameter for the livestock models, and hence is made to vary, a default value is useful in demonstrating conditions which occur without any interventions. Several different values of free living leptospire survival times are presented in the literature, ranging from two weeks, to several months and even years [40–42]. The default leptospire death rate, ρ_0, used here, is based on Hellstrom and Marshall [43]. Their study was specific to the Manawatu region of New Zealand and serovar Pomona. Leptospires from livestock fields (paddocks) were found to be culturable and infectious for at least 42 days [43]. Hence $\rho_0 = 1/42 = 0.02381$ day^{-1}. Note that the notation ρ_0 is used to distinguish the default leptospire death rate from the variable leptospire death rate ρ.

Unlike many other countries, livestock in New Zealand are predominantly pasture fed, that is, they spend the majority of their lives outside, eating grass. The stocking density at which they are kept depends on land topography (high, hill or flat country) [44]. New Zealand specific stocking densities range from 0.7 SU ha^{-1} to 25 SU ha^{-1} on high country, to intensive finishing land respectively [44–48]. One stocking unit (SU) is equivalent to one 55kg ewe and her lamb per hectare. For these models, a stocking density of 10 animals per hectare is used. That is, the stocking density refers to single animals only. In the foundational model, which includes only one age class, namely lambs, this means there are 10 lambs in the field. In the model extensions, which include two age classes, lambs and ewes, this stocking density describes 10 ewes and 10 lambs in the field. This value is chosen simply for aesthetic purposes; however, in each situation, it is still within the range described above.

The density of leptospires at which transmission rate from the environment is half the environmental transmission coefficient, H, as well as the density of free living leptospires, L, is scaled by a factor of 1 to 10^3 ha^{-1}. That is, for these models, each unit of H (or L) is equivalent to 10^3 leptospire bacteria per hectare, and so in the nomenclatures the descriptions for L and H begin with, "Density of leptospires ($\times 10^{-3}$)...". In order to achieve this scaling, the "true" number of leptospire bacteria per hectare is divided by 10^3. For example, in the paper by Holt et. al. $H = 10^6$ ha^{-1}. Dividing this by 10^3 gives a scaled H value of 10^3 ha^{-1}, which is the value used in the upcoming models.

The concentration of leptospires in the urine of infectious hosts is available for a variety of different animals. Most studies look at rats, which shed leptospires at a concentration of $10^5 - 10^7$ per ml of urine [31, 49]. Cats shed at a concentration of approximately $400 - 1.6 \times 10^4$ per ml of urine and dogs shed at a concentration of approximately $40 - 1.33 \times 10^6$ per ml of urine [50, 51]. Deer shed approximately 3×10^3 - 1.7×10^6 leptospires (serovar Hardjobovis) per ml of urine and as deer are more similar to sheep and cows than the other animals mentioned, and the study is New Zealand specific, these values are used here [52]. The shedding rate per infectious animal depends on the age class the animal is in and as such is discussed on a case by case basis.

As one might imagine, finding an environmental transmission coefficient, γ, for any environmentally acquired disease, poses a real challenge. As such, these data are not available in the literature. However, Fang in chapter 3 of her thesis compares three different techniques for detecting leptospirosis in cows and sheep [53]. By taking a simplistic approach to the data available for leptospire detection in urine, an environmental transmission coefficient, γ, is estimated. Four trials were conducted, three for sheep and one for cows. Unfortunately, the animals in each trial were different ages, the days on which animals were tested for leptospirosis in each trial were not consistent with the other trials, the strength of challenge differed between trials, as did the serovar used (Hardjobovis and/or Pomona). Therefore, a seperate γ is found for each trial, as the data from each trial can not be pooled. First, data from one detection technique, dark field microscopy (DFM), are ignored, as the findings of the study do not recommend it for detecting leptospires in urine. Each animal was tested for leptospirosis using MAT between 40 and 14 days before the trial and was found to be seronegative. Therefore, animals that were shedding on the first day of the trial, where these data were collected, would have picked up the infection from the field or other animals they were on pasture with (chronic infection with intermittent shedding is another possibility). Taking the proportion of animals in each trial shedding on the first day and dividing by the number of days from first testing (before the trial) to the first data collection (after trial began), gives a separate environmental transmission coefficient for each trial (population density is ignored as this information was not given). These values range from 7.8125×10^{-3} to 0.058 day^{-1}. Each trial was quite small (between 3 and 16 animals, depending on pooling for serovar type), so the validity of these results is in question and as such a numerical approach is

used for finding γ for each variation of the model.

Most of the sheep in trial C (the largest trial, 16 sheep) of Fang's thesis, shed fairly consistently until day 42, the last sampling day. This is used to justify not having a recovery term in the model, as from this trial, sheep appear to shed for at least 42 days [53]. The assumption that livestock continue to shed after 42 days is supported by the literature. In fact, shedding can occur for years [54–56].

Despite recovery not being supported by the literature, for comparison, a small section is included at the end of the presentation of the single age class model (model A, section 3.1), with the parameter value for recovery chosen arbitrarily.

Results

In the main models presented in this chapter, the leptospire death rate, ρ, is used as the control parameter. All figures are produced to demonstrate analytical results. Graphs showing the behaviour of the infectious population(s) and free living leptospires over time are presented, as are the limit cycle and bifurcation diagrams. Graphs are not included for sub-models if the results are similar to that of the main model, unless these are included for comparison purposes.

As the basic reproduction number R_0 itself cannot be found explicitly, it is not presented for the models. However, where possible, a quasi-R_0 value of the system is determined.

3.1 Sheep Model A

3.1.1 Introduction

The model presented in this section includes only one age class of sheep (lambs) and one environment. It is the foundational model for the remaining models in this chapter. A constant density of sheep, N, is introduced into a field contaminated with free living leptospires, L. The sheep become infectious, I, through grazing, at rate γ, and reinfect the field through shedding, at rate α. After a fixed period of time, t_r, the

lambs are removed, allowing the bacteria in the field to die off, at rate ρ. The whole process is repeated at the beginning of the following year with a new flock of susceptible lambs, $S(0) = N$. Note that $N = S + I$. The non-linear saturation term, $L/(L + H)$, as described in chapter 1, is also included in the model.

The system can be described using the following set of differential equations:

The system before removal (phase one: $0 < t < t_r$),

$$\begin{aligned} \frac{dS}{dt} &= -\frac{\gamma SL}{L+H}, && (3.1)\\ \frac{dI}{dt} &= \frac{\gamma SL}{L+H}, && (3.2)\\ \frac{dL}{dt} &= \alpha I - \rho L. \end{aligned}$$

The first and second equations above follow Michaelis-Menten kinetics. They describe the rates at which the susceptible and infectious populations change over time. Note that the right hand side of the first equation is negative, thus describing a decrease in the susceptible population, while the right hand side of the second equation is the same as the first equation, but positive. This means that the rate at which the susceptible population decreases is the same as the rate at which the infectious population increases. Thus, the system can be simplified to a two dimensional system of equations, as equation 3.1 is redundant. First, divide equation 3.2 by equation 3.1 to get $\frac{\dot{I}}{\dot{S}} = \frac{dI}{dS} = -1$. With the initial conditions $S(0) = N$ and $I(0) = 0$, this results in the solution $I = -S + N$. So the three dimensional system of equations above is simplified to the following:

$$\begin{aligned} \frac{dI}{dt} &= \frac{\gamma(N-I)L}{L+H}, && (3.3)\\ \frac{dL}{dt} &= \alpha I - \rho L. && (3.4) \end{aligned}$$

The second equation above, equation 3.4, satisfies constant production and loss rates. It describes the rate of change in the free living leptospire population. The first term on the right hand side is the shedding term and

the second is the death term.

The system after removal (phase two: $t_r < t < t_y$), reduces to

$$\frac{dL}{dt} = -\rho L. \tag{3.5}$$

3.1.2 Data and Parameter Values

The model notation and parameter values used are summarised in Table 3.1 (note that the value of the parameter H is the same as in chapter 2; however, it has now been scaled). This section explains how parameter values are derived.

The shedding rate is determined by calculating the volume of urine shed per lamb and multiplying this by the leptospiral concentration. Lambs weight between 5 and 65 kilograms, with an average weight of 38.9kg, and sheep shed between 10 and 40 ml of urine per kilogram of body weight per day, with a median of 25ml [57, 57, 58, 58]. Hence, on average, each lamb produces approximately one litre of urine per day (38.9kg $\times$ 25ml/kg/day = 972.5ml/day). Multiplying this by the leptospiral concentration in urine (3×10^3 - 1.7×10^6 leptospires per ml of urine), as mentioned in section 3, results in a range of 3×10^6 - 1.7×10^9 leptospires shed per infectious lamb per day. However, not every leptospire shed into the environment will be available to be ingested by the sheep. Some of the bacteria will sink into the soil. Kumar et al found that approximately 50% of leptospira bacteria cells were absorbed into (paddy field) soil [59]. Unfortunately, the paper confirms neither the soil type nor its permeability. Hence, the shedding rate α in the model is less than the number of bacteria each infectious lamb is estimated to shed into the environment. For aesthetic purposes, α is chosen to be 1 day^{-1}. Note that this is the scaled leptospiral value as described in chapter 1, that is, the actual number of leptospires shed per infectious lamb is 10^3 day^{-1}.

In an abattoir in Waikato, New Zealand, it was found that at time of slaughter, approximately 27% of sheep, the majority of which were lambs (78%), from sheep-only suppliers, were shedding leptospires [53]. By specifying the percentage of infectious lambs in the model at time of removal to 27%, a value for γ can be found. In this case, the infection rate

Description	**Symbol**	**Value**	**Units**
Density of the lamb population in a given area (the field)	N	10	SU ha^{-1}
Density of the susceptible lamb population in a given area (the field)	S		SU ha^{-1}
Density of the infectious lamb population in a given area (the field)	I		SU ha^{-1}
Density of the free living leptospires ($\times 10^{-3}$) in a given area (the field)	L		ha^{-1}
Environmental transmission coefficient	γ	0.02477	day^{-1}
Density of leptospires ($\times 10^{-3}$) at which transmission rate from the environment is 0.5γ	H	10^3	ha^{-1}
Number of leptospires ($\times 10^{-3}$) shed per infectious lamb	α	1	day^{-1}
Per capita leptospire death rate	ρ	0.02381	day^{-1}
Time	t		days
Removal date	t_r	335	days
End of year	t_y	365	days
Density of the infectious lamb population in a given area (the field) at the beginning of each year	I_0	0	SU ha^{-1}
Density of the free living leptospires ($\times 10^{-3}$) in a given area (the field) at $t = 0$	L_0	10	ha^{-1}

Table 3.1: *Parameters and initial conditions used for sheep model A.*

γ, obtained to four significant figures, is $\gamma = 0.02477$ day^{-1}, which conveniently is within the range mentioned in the data section at the beginning of the chapter (section 3).

In New Zealand, lambs are generally kept in a single field for 11 months (C. Heuer, personal communication, 2014). In the model, this equates to a removal time of $t_r = 335$ days.

The initial condition for free living leptospira, L_0, is chosen as the small, but arbitrary, value of 10 leptospire units per hectare.

3.1.3 Results

The results, found numerically, of the system of equations 3.3-3.5, are shown in figure 3.1. The first graph shows the density of susceptible and infectious lambs per hectare, while the second graph shows the density of free living leptospires per hectare, all over the same time period. In figure 3.1a the breaks in the curves indicate where the lambs are removed from the system. Note that the number of infectious lambs is reset to zero at the beginning of each year and that the behaviour of the system towards the end of the time period appears to be the same for both lamb and leptospire poulations. This repetitive behaviour is indicative of a limit cycle and is explored in the following sections.

3.1.4 Cobwebbing

A cobweb diagram is a one dimensional map, similar to a Poincaré map, from $L_0(n)$ to $L_0(n+1)$, where $L_0(n)$ is the initial condition for leptospires for year n, and n is a non-negative integer. That is, a cobweb diagram plots a range of initial conditions of free living leptospires, against their corresponding end conditions (the density of leptospires at the end of the year). A steady state can be observed on a cobweb diagram by line of unit slope. Steady states occur where the two curves (the graph and the line of unit slope) intersect. This occurs when $L_0(n) = L_0(n+1)$. That is, the steady state L^* is the value of the initial condition for leptospire density, $L_0(n)$, for which the behaviour of the system repeats itself from one year to the next. See figure 3.2 for a schematic. In other words, L^* is the initial condition that results in a limit cycle for the set of differential equations

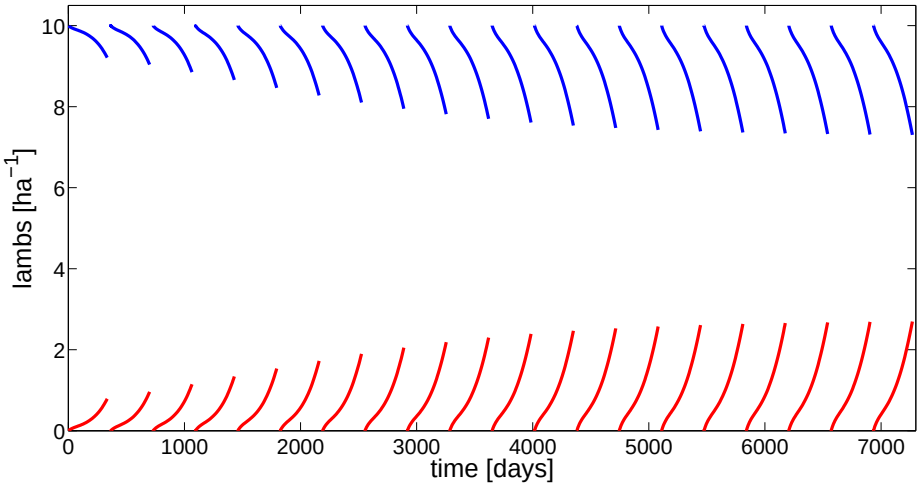

(a) *Density of susceptible and infectious lambs over time (days). Susceptible lambs shown in blue. Infectious lambs shown in red.*

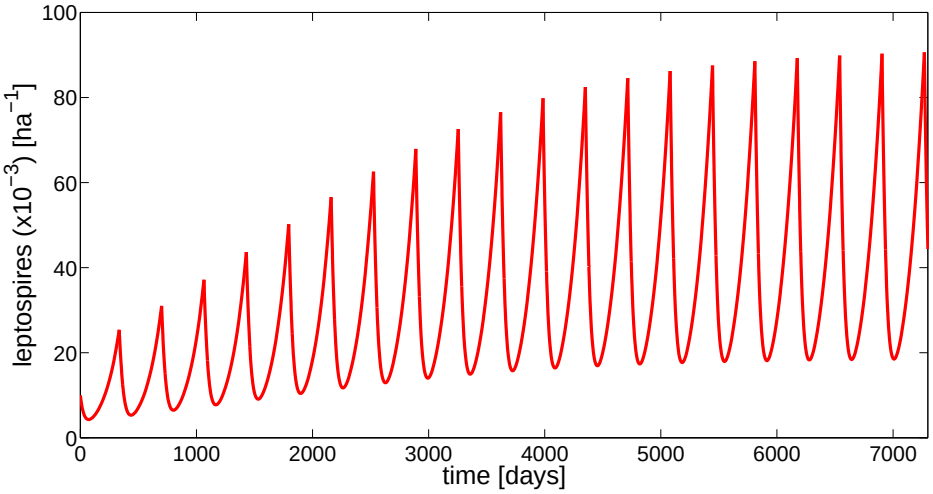

(b) *Density of free-living leptospires over time (days).*

Figure 3.1: *Numerical solutions for sheep model A. All parameter values are as in Table 3.1.*

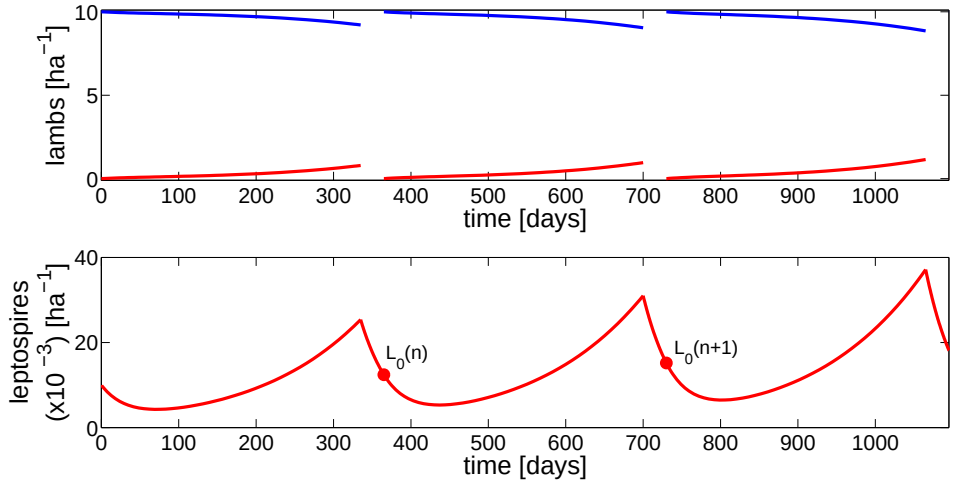

Figure 3.2: *The behaviour of sheep model A in years n (for the graph showing L, this is the curve between the points $L_0(n)$ and $L_0(n+1)$) and $n+1$ (the curve from the point $L_0(n+1)$ to the end of the graph), is not the same. $L_0(n) \neq L_0(n+1)$ and so $L_0(n)$ is not a fixed point. After some time, the behaviour of the model will repeat, however. That is, for some $n \in \mathbb{N}$, $L_0(n) = L_0(n+1)$ and L^* will have been reached.*

3.3-3.5. Hence, $L^* = \lim_{n\to\infty} L(nt_y) = \lim_{n\to\infty} L((n+1)t_y)$ where $L_0(n) = L(nt_y)$.

Cobwebbing can also be used to show that a steady state, in this case a limit cycle, is unique and stable [32]. Stability is determined by drawing a vertical line from some point on the horizontal axis (ie, pick an arbitrary initial condition, $L_0(n)$) up to the graph. From there, drawing a horizontal line to the line of unit slope moves the cobweb over the initial condition for the following year, $L_0(n+1)$. Repeating this process, by moving the cobweb up (or down) to the graph, and then horizontally to the line of unit slope, moves the cobweb towards a stable steady state and away from an unstable one.

As seen in figure 3.3a and 3.3b, using a different leptospire death rate, ρ, produces different results. Figure 3.3a shows a stable and unique, non-trivial fixed point for $\rho = \rho_0$. This is indicated by the non-trivial intersection of the two curves (the graph and line of unit slope), as well as an unstable trivial fixed point indicated by the trivial intersection of the

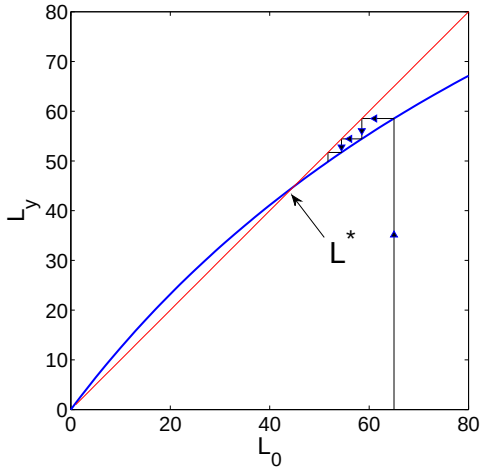

(a) *Cobweb diagram using* $\rho = \rho_0 = 0.02381$ day^{-1} *showing the non-trivial fixed point at* $L^* = 46$ ha^{-1}.

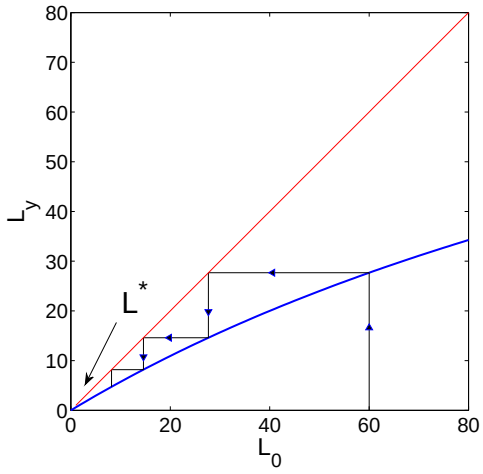

(b) *Cobweb diagram using* $\rho = 0.03$ day^{-1}. *A magnification of the cobweb diagram close to the origin shows that the trivial fixed point is the only fixed point in that region.*

Figure 3.3: *Cobweb diagrams for sheep model A for different values of* ρ.

two curves at the origin. Figure 3.3b, which uses $\rho = 0.3$ day^{-1}, has only a trivial intersection. This is hence a trivial fixed point, which is stable. Note that cobwebbing is not a rigorous proof for the behaviour of the system, but rather a helpful exploratory method in understanding the nature of the solutions.

3.1.5 Bifurcation

A bifurcation diagram is constructed by finding the steady state, L^*, over a range of ρ values. For each value of ρ, using a range of initial condition values, L_0, (in increments of 10), the numerical solution to the system after one year is calculated. The initial and corresponding end conditions are both stored in vectors, the minimum absolute difference of which is used to find the steady state, L^*. This calculation is only made to occur if there is a change in sign in the vector storing the difference of the initial and end condition vectors. These calculations are performed over a range of ρ (in increments of 0.001) values. A vector holding the fixed points of the system for the various ρ values is constructed and used to graph the bifurcation diagram. It is also used to find the bifurcation point, ρ_{crit}. This is done by working through the vector until a trivial fixed point is reached. Any value of L^* less than one is considered a trivial fixed point, as it is assumed that fewer than one units of leptospires is insufficient for infection to take off.

Recall that ρ is the leptospire death rate, therefore, when ρ is large, L is expected to be small and when ρ is small, L is expected to be large. This is observed in the bifurcation diagram below.

The point where the non-trivial fixed point collides with the x-axis is a critical value of ρ (when $\rho > \rho_{crit}$ only the trivial fixed point exists and when $\rho < \rho_{crit}$ both a trivial and a non-trivial fixed point exist) and a threshold for a periodic solution of the system of differential equations 3.3-3.5. In the diagram below (figure 3.4), this occurs at $\rho = 0.0260$ day^{-1}.

3.1.6 Limit Cycle

A limit cycle diagram can be constructed on the (L, I) phase plane by starting at an initial point (L_0, I_0) and following its trajectory over the course of several years. In this way, over time, the apparent repetitive behaviour observed in figure 3.1 can be examined. See figure 3.5 for an

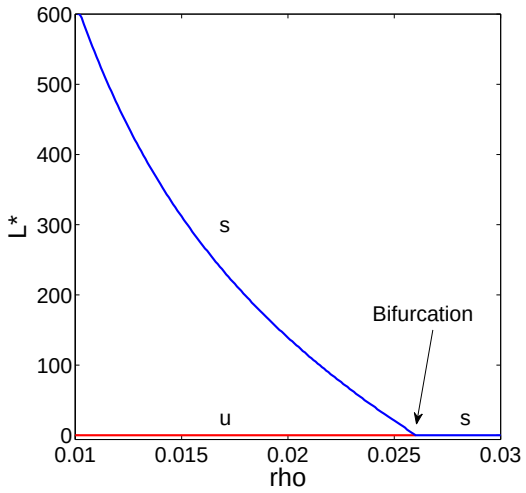

Figure 3.4: *Bifurcation diagram for sheep model A showing the fixed point L^* as ρ is varied from* 0.01 *to* 0.03 day^{-1} *in increments of* 10^{-4} day^{-1}. *For $\rho > \rho_{crit}$, the stable and only fixed point is the trivial fixed point. At $\rho = \rho_{crit}$, the trivial fixed point becomes unstable. A non-trivial stable fixed point exists for $\rho < \rho_{crit}$ as well as the trivial fixed point. In this example, $\rho_{crit} = 0.0260$ day^{-1}. The diagram is not plotted for $\rho <$* 0.01 day^{-1} *as the values of L become very large.*

example of a limit cycle diagram.

First, start at the point $(L, I) = (L_0, 0)$ and follow the streamline for $0 < t < t_r$. Initially, I increases while L decreases. At the nullcline $L = \alpha I/\rho$, $L(t)$ has a minimum, after which both L and I increase. At $t = t_r$ the streamline descends instantly from $(L, I) = (L_r, I_r)$ to the L-axis at $(L, I) = (L_r, 0)$, where it then moves towards the origin, as $\dot{L} = -\rho L < 0$ for $t_r < t < t_y$. At $t = t_y$ the point $(L, I) = (L_y, I_y)$ is reached. This is the end of one "cycle". L_y is the initial condition for L for the following year.

Biologically speaking, the year begins with free living leptospires in the field and no infectious sheep. As the sheep are exposed to the leptospires, the density of infectious sheep increases. However, the rate at which leptospires die is still greater than the rate at which shedding occurs. Eventually, these two rates balance and the density of leptospires starts to increase. When all the sheep are removed from the field, the leptospires in the field die, without being replaced, for the remainder of the year, until a

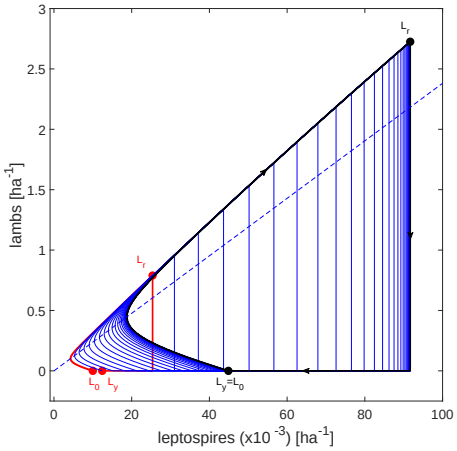

Figure 3.5: *Limit cycle diagram for sheep model A. Phase-plane showing the relationship between leptospires and lambs over time. First year shown in red. Limit cycle shown in black. Intermediate years shown in blue. A nullcline is indicated as a dashed blue line.*

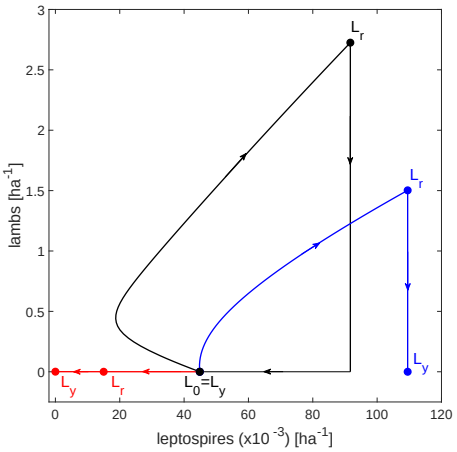

Figure 3.6: *Limit cycle proof streamline demonstration for sheep model A. The figure above demonstrates the three cases mentioned in the limit cycle proof in section 3.1.6. The red curve is the case when ρ is large, the blue curve is the case when $\rho = 0$ day^{-1} and the black curve is the limit cycle case, where the behaviour of the system repeats itself from one year to the next. Note that for demonstration purposes, L_r for ρ large and L_r for $\rho = 0$ are not to scale.*

new cohort of sheep is introduced to the field.

In the limit cycle diagram in figure 3.5, the first year cycle is shown in red, intermediate year cycles are shown in blue and the last (calculated) year cycle is shown in black. The black curve also happens to be a limit cycle. That is, the behaviour of the system repeats from one year to the next.

In the proof of the existence of the limit cycle (below), the following parameters are fixed: γ, H, α and t_r. The dynamics of the system are examined for different values of ρ, as shown in figure 3.6. First, let $\ell_0(n,\rho) = L(nt_y)$ be the initial condition for $L(t)$, $\ell_r(n,\rho) = L(nt_y + t_r)$ be the density of leptospires when the sheep are removed, and $\ell_y(n,\rho) = L((n+1)t_y) = \ell_0(n+1,\rho)$ be the density of leptospires at the end of the year, all for year n.

Proof. Recall equations 3.3 and 3.4 and define $\rho_\infty = \alpha N/L_0$. It is shown that when $\rho = 0$, $\ell_y(n,0) > \ell_0(n,0)$, and when $\rho > \rho_\infty$, $\ell_y(n,\rho) < \ell_0(n,\rho)$. Hence, by continuity, there exists ρ such that $\ell_y(n,\rho) = \ell_0(n,\rho)$.

a) For $0 < t < t_r$, when $\rho = 0$, from equation 3.4, $\dot{L} = \alpha I$. Since $\dot{L} > 0$, then $\ell_r(n,0) > \ell_0(n,0)$. For $t_r < t < t_y$, $\dot{L} = 0$, so $\ell_y(n,0) = \ell_r(n,0)$ and so when $\rho = 0$, $\ell_y(n,0) > \ell_0(n,0)$.

b) Next consider the case when ρ is very large. For $0 < t < t_r$, multiplying equation 3.4 by the integrating factor and rearranging gives

$$\frac{d}{dt}(Le^{\rho t}) = \alpha I e^{\rho t}.$$

Integrating the above gives

$$Le^{\rho t} - L_0 = \alpha \int_0^t I(u)e^{\rho u}du$$

which simplifies to

$$L(t) = L_0 e^{-\rho t} + \alpha e^{-\rho t} \int_0^t I(u)e^{\rho u}du.$$

Then, since $I \leq N$,

$$\begin{aligned} L(t) \leq \tilde{L}(t) &= L_0 e^{-\rho t} + \alpha e^{-\rho t} N \int_0^t e^{\rho u} du \\ &= L_0 e^{-\rho t} + \frac{\alpha N}{\rho}(1 - e^{-\rho t}). \end{aligned}$$

Now, if $\rho > \rho_\infty = \alpha N / L_0$, then $L(t) \leq \tilde{L}(t) < L_0$ for all $0 < t < t_r$, and so $\ell_r(n, \rho) < \ell_0(n, \rho)$.

For $t_r < t < t_y$, $\dot{L} = -\rho L < 0$, so $\ell_y(n, \rho) < \ell_r(n, \rho)$ and $\ell_y(n, \rho) < \ell_0(n, \rho)$.

So when ρ is small, $\ell_y(n, \rho) > \ell_0(n, \rho)$, and when ρ is large ($\rho > \rho_\infty$), $\ell_y(n, \rho) < \ell_0(n, \rho)$. So for some value $\rho = \rho_{crit}$ where $0 < \rho_{crit} < \rho_\infty$, $\ell_y(n, \rho) = \ell_0(n, \rho)$ and a limit cycle exists.

More formally, first recall the intermediate value theorem:

"A function $y = f(x)$ that is continuous on a closed interval $[a, b]$ takes on every value between $f(a)$ and $f(b)$. In other words, if y_0 is any value between $f(a)$ and $f(b)$, then $y_0 = f(c)$ for come c in $[a, b]$ [60]."

Now L is a continuous function. Consider L_y as a function of ρ, continuous on $\rho \in [0, \rho_\infty)$. That is, L_y is the value of L at the end of one year for different values of ρ. If $L_0 \in [L_y(0), L_y(\rho_\infty)]$, then there exists a $\rho_{crit} \in [0, \rho_\infty)$ such that $L_y(\rho_{crit}) = L_0$.

□

Biologically, when the free living leptospire death rate is very small ($\rho = 0$ day^{-1}), the bacteria never die and therefore continue to increase in density. When the free living leptospire death rate is very large, the bacteria die so quickly that they are unable to infect a host. One would expect there to be a death rate in between "very small" and "very large" which would result in a steady state.

If L_y is monotonic decreasing with respect to ρ (see figure 3.7 for an example), then ρ_{crit} is unique and the limit cycle is unique. That is, each

value of L_0 has a unique value of ρ_{crit} which makes it part of a limit cycle. Consider the proof below:

Proof. First, let $L(t) = \ell(t, \rho)$. Then, let $L_1(t) = \ell(t, \rho_1)$, $L_2(t) = \ell(t, \rho_2)$ and $\rho_1 < \rho_2$. At $t = 0$, since $I = 0$, $\dot{L} = -\rho L$, and since $\rho_1 < \rho_2$, then $\dot{L}_2 < \dot{L}_1$ and there exists an interval $[0, t)$ such that $L_2(t) < L_1(t)$.

Now, starting at any point (L_i, I_i) in the (L, I) phase plane,

$$\dot{L}_1 = \alpha I_i - \rho_1 L_i \quad \text{and} \quad \dot{L}_2 = \alpha I_i - \rho_2 L_i,$$

so $\dot{L}_2 < \dot{L}_1$. So the trajectory of the streamline of ρ_2 is always to the left of that of ρ_1. Therefore, the streamlines of ρ_1 and ρ_2, starting at the same initial condition, cannot intersect, and $L_2(t) < L_1(t)$ for $0 < t < t_r$. Therefore, $L_2(t_r) < L_1(t_r)$. After removal, for $t_r < t < t_y$, $L(t) = L(0)e^{-\rho t}$. Initial conditions are $L_1(t_r)$ and $L_2(t_r)$ for $\rho = \rho_1$ and $\rho = \rho_2$ respectively. Since $L_2(t_r) < L_1(t_r)$ and $e^{-\rho_2 t} < e^{-\rho_1 t}$, then $L_2(t_y) < L_1(t_y)$ and L_y is monotonic decreasing in ρ and a unique limit cycle exists.

□

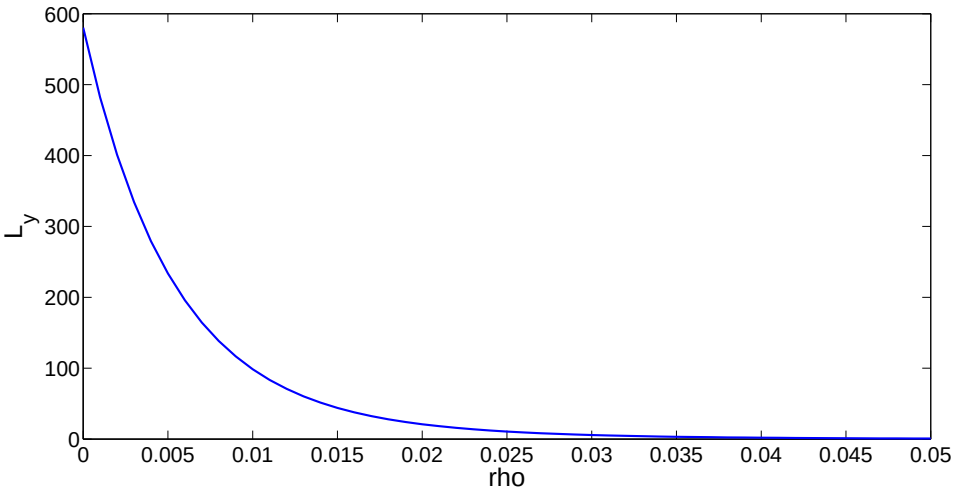

Figure 3.7: *An example of the function $L_y(\rho)$ for sheep model A. It is clear that for the specific parameter values used here, L_y is indeed monotonic decreasing. While the bifurcation curve does get very close to the ρ axis, it never actually reaches it.*

Finally, stability can be confirmed using the Lyapunov exponent. Lyapunov exponents measure the rate at which trajectories near a steady state, in this case, the limit cycle, move away (diverge) from that steady state. A positive Lyapunov exponent (the rate of divergence is greater than 1) indicates an unstable steady state, while a negative Lyapunov exponent (the rate of divergence is less than 1) indicates a stable steady state. Here, the Lyapunov exponent is calculated numerically using the formula $\log_2 \left| \frac{L_0 - L_y}{L_0 - L^*} \right|$, where $L_0 = L^* + \epsilon$ for a range of $\epsilon << 1$. For the parameters in table 3.1, the Lyapunov exponent is negative and of order 10^0, so the limit cycle is stable.

3.1.7 The Quasi-Basic Reproduction Number, R_L

A threshold quantity, R_L, that relates L at the beginning of one year to L at the beginning of the next year, is found. This is not a true R_0, which would require averaging throughout the year and would also be a valid threshold quantity.

To find R_L, first linearise equations 3.3 and 3.4 about the trivial steady state. This results in the system:

$$\begin{aligned} \dot{I} &= \frac{\gamma L N}{H}, \\ \dot{L} &= \alpha I - \rho L, \end{aligned}$$

with the initial conditions $L(0) = L_0$ and $I(0) = 0$.

This system can be solved analytically. One approach is to first differentiate $\dot{I}$ to get $\ddot{I} = \frac{\gamma \dot{L} N}{H}$. Then, substituting $\dot{L}$ into $\ddot{I}$ gives $\ddot{I} = \frac{\gamma N}{H}(\alpha I - \rho L)$. Rearranging $\dot{I}$ for L and substituting into $\ddot{I}$ gives $\ddot{I} = \frac{\gamma N}{H}(\alpha I - \frac{\rho H}{\gamma N}\dot{I}) = \frac{\gamma N \alpha}{H} I - \rho \dot{I}$, which results in the second-order ordinary differential equation $\ddot{I} + \rho \dot{I} - \frac{\gamma N \alpha}{H} I = 0$, the solution to which is $I(t) = \frac{\gamma N L_0}{H \rho h} \left[e^{-\rho(1-h)t/2} + e^{-\rho(1+h)t/2} \right]$, where $h = \sqrt{1 + \frac{4\gamma\alpha N}{H\rho^2}}$. Note that $I(t) = 0$ for $t > t_r$.

Alternatively, one can solve for L. This is the approach used here. Differentiate $\dot{L}$ to get $\ddot{L} = \alpha\dot{I} - \rho\dot{L}$. Then substitute $\dot{I}$ into $\ddot{L}$ to get the second-order ordinary differential equation $\ddot{L} + \rho\dot{L} - \frac{\gamma N\alpha}{H}L = 0$. The solution to this is $L(t) = \frac{L_0}{2h}\left[(1+h)e^{-\rho(1+h)t/2} - (1-h)e^{-\rho(1-h)t/2}\right]$. At $t_r < t < t_y$, the differential equation $\dot{L}$ becomes $\dot{L} = -\rho L$, the general solution to which is $L(t) = ce^{-\rho t}$. The initial condition for this is $L(t_r) = \frac{L_0}{2h}\left[(1+h)e^{-\rho(1+h)t_r/2} - (1-h)e^{-\rho(1-h)t_r/2}\right]$, so the particular solution is $L(t) = \frac{L_0}{2h}\left[(1+h)e^{-\rho(1+h)t_r/2} - (1-h)e^{-\rho(1-h)t_r/2}\right]e^{\rho(t_r-t)}$.

A quasi-R_0 can be found by noting that $R_0 = 1$ when $L(t_y) = L(0)$, or $L_y = L_0$. Define $R_L = L(t_y)/L_(0)$. Then $R_0 > 1$ when $R_L > 1$ and $R_0 < 1$ when $R_L < 1$.

$$\text{Here } R_L = \frac{e^{-\rho t_y}}{2h}\left[(1+h)e^{\rho(1-h)t_r/2} - (1-h)e^{\rho(1+h)t_r/2}\right] \text{ where}$$

$h = \sqrt{1 + \frac{4\gamma\alpha N}{H\rho^2}}$.

R_L is a monotonic increasing function of N, α and γ and a monotonic decreasing function of ρ. This is confirmed by numerical results. See figure 3.8.

Note that R_L is not dependent on the initial condition L_0 and so L_0 can be made as small as one likes, that is, R_L does indeed reflect the behaviour of the system near the trivial fixed point.

$$R_L = \lim_{L_0 \to 0} \frac{L_y}{L_0}\bigg|_{I(0)=0}.$$

Recall that ρ_{crit} is the value of ρ for which the system moves from a limit cycle, to the trivial fixed point. Finding ρ for a particular value of R_L requires solving a transcendental equation. It can, however, be determined numerically, that when $\rho = \rho_{crit}$, as found in section 3.1.5, $R_L = 1$. This is achieved simply by substituting ρ_{crit} for ρ in R_L and checking that $R_L = 1$. For the parameter values used in this case study, $R_L \approx 1.34$. This is to be expected, as the ρ value used is less than ρ_{crit}, and the infection is prevalent in livestock.

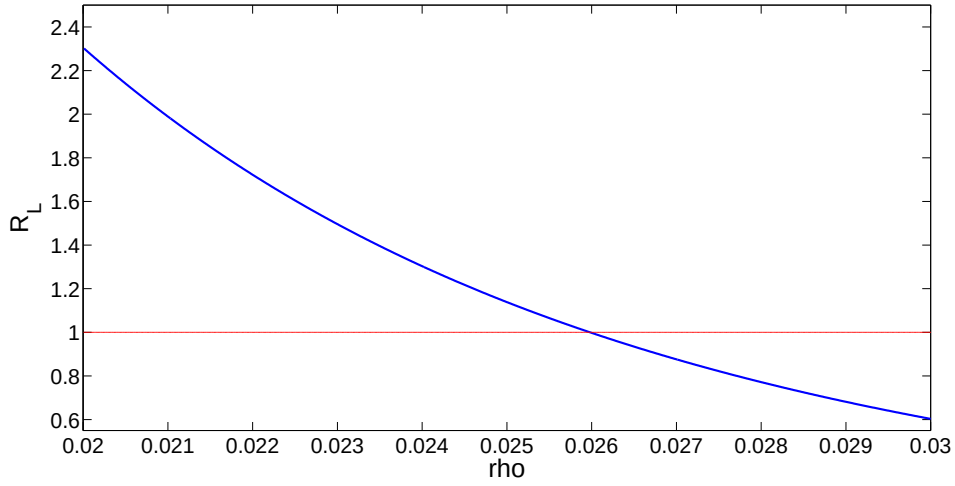

Figure 3.8: *Graph showing R_L as a function of leptospire death rate ρ for sheep model A. $R_L = 1$ is shown with a horizontal red line.*

3.1.8 Recovery

If it is assumed that infectious lambs can become susceptible again after infection (either naturally or through antibiotic treatment), at a rate σ, then the system before removal becomes:

$$\frac{dS}{dt} = -\frac{\gamma SL}{L+H} + \sigma I, \tag{3.6}$$

$$\frac{dI}{dt} = \frac{\gamma SL}{L+H} - \sigma I, \tag{3.7}$$

$$\frac{dL}{dt} = \alpha I - \rho L. \tag{3.8}$$

and the system after removal remains the same (equation 3.5).

In this case, even though the value of the recovery term is quite small ($\sigma = 5 \times 10^{-4}$ day^{-1}, chosen arbitrarily), the density of leptospires is almost halved as compared to the system without recovery (see figure 3.9). The infection in the flock is also reduced.

Cobweb and bifurcation diagrams (figures 3.10 and 3.11) for this variation of the model behave in a similar manner as those for the system without recovery. Note that the non-trivial fixed point in the cobweb

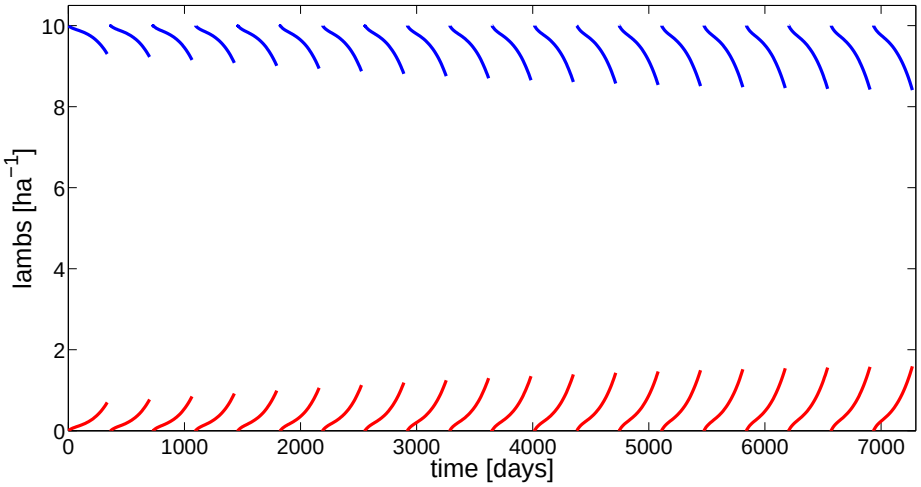

(a) *Density of susceptible and infectious lambs over time (days). Susceptible lambs shown in blue. Infectious lambs shown in red.*

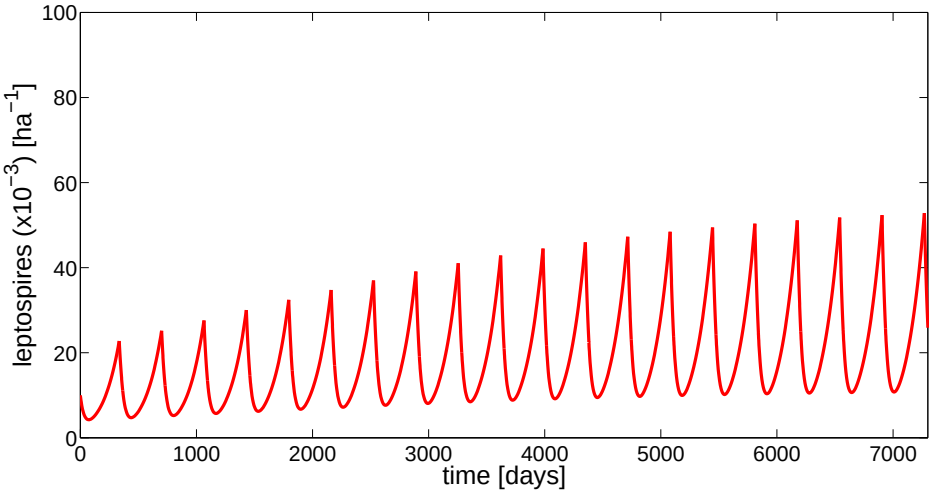

(b) *Density of free-living leptospires over time (days).*

Figure 3.9: *Numerical solutions for sheep model A. All parameter values are as in Table 3.1, except for* $\sigma = 5 \times 10^{-4}$ *day*$^{-1}$.

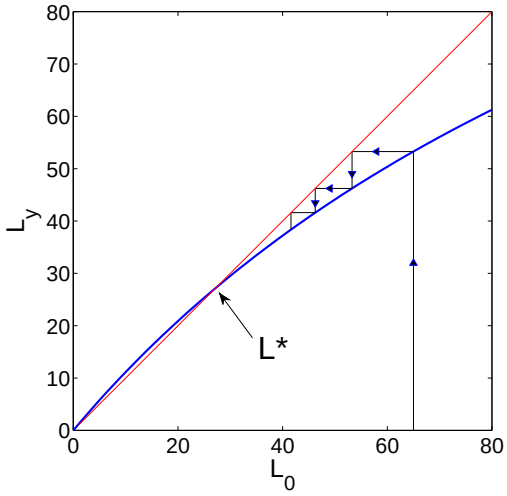

(a) *Cobweb diagram using* $\rho = \rho_0 = 0.02381$ day^{-1} *showing the non-trivial fixed point at* $L^* = 28$ ha^{-1}.

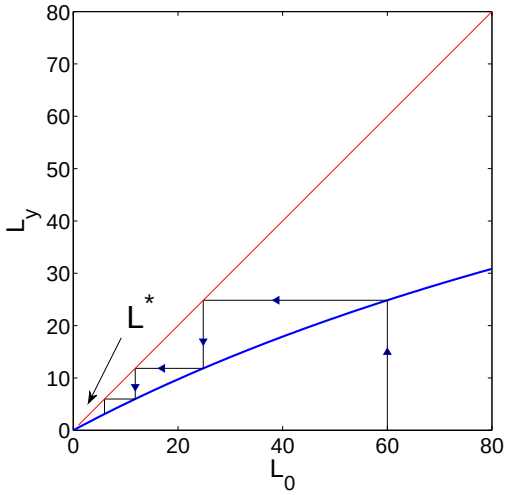

(b) *Cobweb diagram using* $\rho = 0.03$ day^{-1}. *A magnification of the cobweb diagram close to the origin shows that the trivial fixed point is the only fixed point in that region.*

Figure 3.10: *Cobweb diagrams for sheep model A using different values of* ρ. *All parameter values are as in Table 3.1, except for* $\sigma = 5 \times 10^{-4}$ day^{-1}.

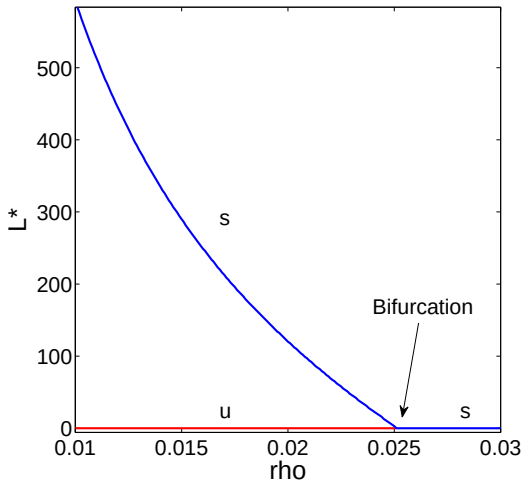

Figure 3.11: *Bifurcation diagram for sheep model A showing the fixed point L^* as ρ is varied from* 0.01 *to* 0.03 *day*$^{-1}$ *in increments of* 10^{-4} *day*$^{-1}$*. For $\rho > \rho_{crit}$, the stable and only fixed point is the trivial fixed point. At $\rho = \rho_{crit}$, the trivial fixed point becomes unstable. A non-trivial stable fixed point exists for $\rho < \rho_{crit}$, as well as the trivial fixed point. In this example, $\rho_{crit} = 0.0251$ day^{-1}. The diagram is not plotted for $\rho < 0.01$ day^{-1} as the values of L become very large. All parameter values are as in Table 3.1, except for $\sigma = 5 \times 10^{-4}$ day^{-1}.*

diagram of the model including recovery at $\rho = 0.02381$ day^{-1} is smaller ($L^* = 28$ ha^{-1}) than that in the model excluding recovery ($L^* = 46$ ha^{-1}). As such, as one may expect, the critical value of ρ for the recovery model, using the same parameter values as for the basic model, is smaller than ρ_{crit} without recovery ($\rho_{crit} = 0.0251$ vs. $\rho_{crit} = 0.0260$ day^{-1} respectively).

3.1.9 Removal Date

Another parameter value of interest, and one that could be easy for farmers to implement, is the removal date. The removal date has a fairly large impact on the behaviour of the system. For the parameter values used here, removing the lambs from the paddock a little over a week early can prevent the infection from taking off at all. Included are a series of graphs demonstrating this behaviour.

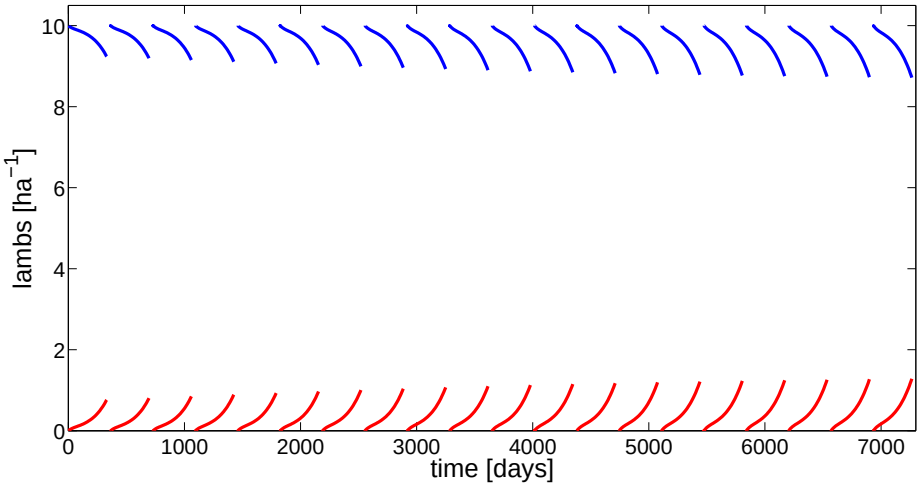

(a) *Density of susceptible and infectious lambs over time (days). Susceptible lambs shown in blue. Infectious lambs shown in red.*

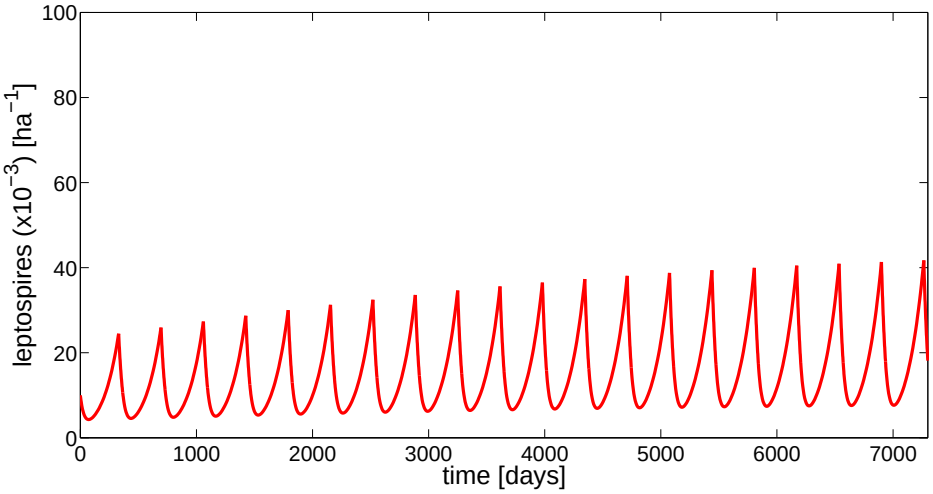

(b) *Density of free-living leptospires over time (days).*

Figure 3.12: *Numerical solutions for sheep model A. All parameter values are as in Table 3.1, except for* $t_r = 330$ *days.*

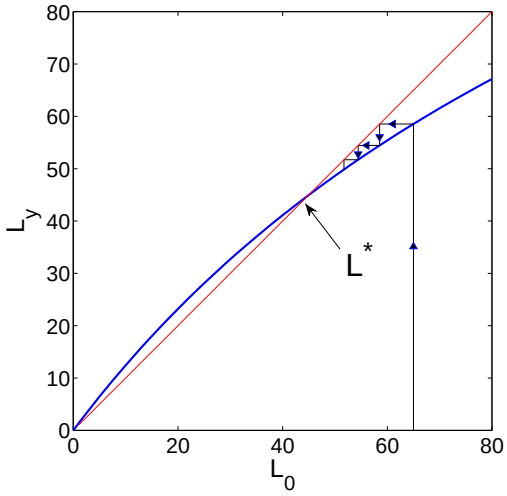

(a) *Cobweb diagram using* $t_r = 335$ *days showing the non-trivial fixed point at* $L^* = 46$ ha^{-1}. *Note this is the same graph as in figure 3.3a.*

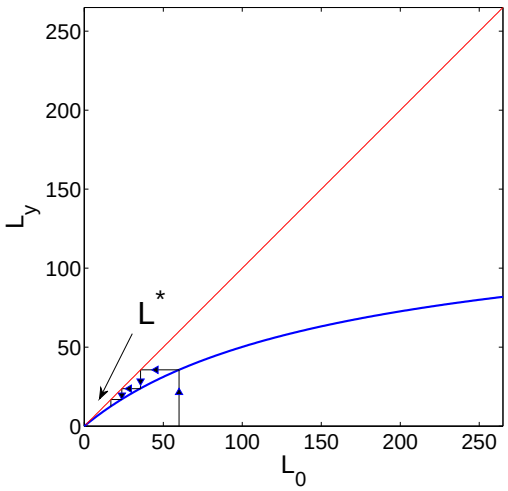

(b) *Cobweb diagram using* $t_r = 320$ *days. A magnification of the cobweb diagram close to the origin shows that the trivial fixed point is the only fixed point in that region.*

Figure 3.13: *Cobweb diagrams for sheep model A for different values of* t_r.

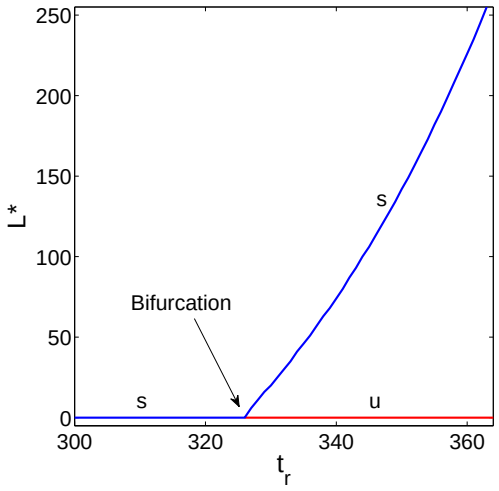

Figure 3.14: *Bifurcation diagram for sheep model A showing the fixed point L^* as removal time, t_r, is varied from 300 to 365 days in increments of 1 day. For $t_r < t_{rcrit}$, the stable and only fixed point is the trivial fixed point. At $t_r = t_{rcrit}$, the trivial fixed point becomes unstable. A non-trivial stable fixed point exists for $t_r > t_{rcrit}$, as well as the trivial fixed point. In this example, $t_{rcrit} = 327$ days.*

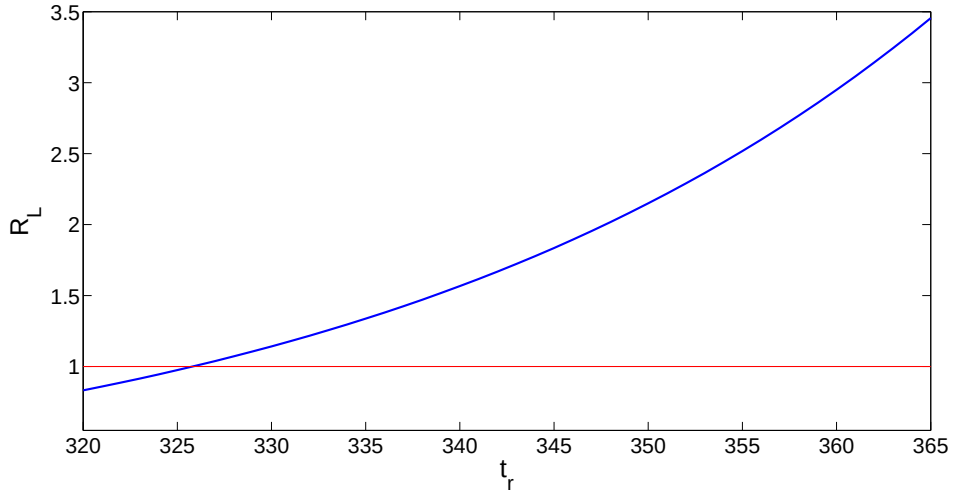

Figure 3.15: *Graph showing R_L as a function of removal date t_r for sheep model A. $R_L = 1$ is shown with a horizontal red line. Note that R_L is an increasing function of t_r.*

Figure 3.12 shows the behaviour of the system over time with a removal date, t_r, of 330 days. Note that the axes are the same as for figure 3.1. The removal date has only been shifted by 5 days, yet the density of leptospires is substantially reduced.

In the cobweb diagrams (figure 3.13), decreasing the variable parameter, t_r, decreases the value of the non-trivial fixed point. This is as opposed to when the variable parameter is ρ, in which case decreasing the parameter increases the value of the non-trivial fixed point. As such, the behaviour of the bifurcation diagram (figure 3.14) is a mirror image of the bifurcation diagram for ρ, with the non-trivial fixed point existing when $t_r > t_{rcrit}$ and only the trivial fixed point existing when $t_r < t_{rcrit}$. The critical value for the removal date is $t_{rcrit} = 327$ days. This is only 8 days less than the fixed value ($t_r = 335$ days) used in the model varying ρ.

Note that the stability of the fixed points remains the same as for when the varying parameter is ρ. That is, when it exists, the non-trivial fixed point is stable while the trivial fixed point is unstable, otherwise the trivial fixed point is stable. The Lyapunov exponents are just the same as those found in section 3.1.6.

The quasi-basic reproduction number, R_L, shown in figure 3.15 also remains the same and the critical value of the removal date can again be confirmed simply by inserting it into R_L. In this case, $R_L(tr_{crit}) = 1.0060$. This is not exactly 1, as one would prefer; however, it is as close as one can get with the units of the removal date being in integer number of days.

3.1.10 Turning the System into a Second Order Non-linear Equation

By using a method similar to what was used to find the quasi-basic reproduction number in 3.1.7, the system of equations 3.3 and 3.4 can be turned into a second order non-linear equation. First, rearranging $\dot{L}$ to solve for I gives $I = \dfrac{\dot{L} + \rho L}{\alpha}$. Then, substituting I into $\dot{I}$ gives $\dot{I}$ as a function of L only, $\dot{I} = \dfrac{\gamma(\alpha N - \dot{L} - \rho L)L}{\alpha(L + H)}$. Next, $\dot{L}$ is differentiated with respect to time to get $\ddot{L} = \alpha\dot{I} - \rho\dot{L}$. Finally, $\dot{I}(L)$ is substituted into $\ddot{L}$ to

give $\ddot{L} = \dfrac{\gamma(\alpha N - \dot{L} - \rho L)L}{(L+H)} - \rho\dot{L}$. The second order non-linear equation is:

$$\ddot{L} + \left(\rho + \frac{\gamma L}{L+H}\right)\dot{L} + \frac{\gamma(\rho L - \alpha N)}{L+H}L = 0. \tag{3.9}$$

This equation is examined, but is not solved analytically. Some simplifications of the equation are also examined.

3.1.11 Turning Point

A turning point for L occurs when $\dot{L} = 0$. The equation 3.9 then becomes

$$\ddot{L} = \frac{\gamma(\alpha N - \rho L)}{L+H}L.$$

Now, since $\dot{L} = \alpha I - \rho L = 0$ and $N \geq I$, then $\alpha N - \rho L \geq 0$. Also, γ, L and $H \geq 0$ and so $\ddot{L} \geq 0$. Hence, the turning point is a minimum. A local maximum is not possible in the system for $0 < t < t_r$; however, a global maximum does occur at the end point $t = t_r$.

3.1.12 What Happens when $H << L$?

H is the density of leptospires at which transmission from the environment is 0.5γ ha^{-1}. That is, when H is very small, only a small density of leptospires is needed for environmental transmission to occur.

When $H << 1$ day^{-1}, then $\dfrac{L}{L+H} \approx \dfrac{L}{L} = 1$ and so

$$\ddot{L} + \left(\rho + \frac{\gamma L}{L+H}\right)\dot{L} + \frac{\gamma(\rho L - \alpha N)}{L+H}L = 0$$

becomes

$$\ddot{L} + (\rho + \gamma)\dot{L} + \gamma(\rho L - \alpha N) = 0,$$

the solution to which is $L = c_1 e^{-\gamma t} + c_2 e^{-\rho t} + \frac{\alpha N}{\gamma\rho}$, where c_1, c_2 are constants determined by initial conditions.

3.1.13 What Happens when $L << H$?

When H is large, a large density of leptospires is needed for environmental transmission to occur. If $L << H$, then it is expected that not much transmission occurs and the free-living leptospires die out. This can be

observed by looking at the model.

First, when $L << H$, then $\frac{L}{L+H} \approx \frac{L}{H} << 1$ and so

$$\frac{dI}{dt} = \frac{\gamma(N-I)L}{L+H} \approx \frac{\gamma(N-I)L}{H} << 1.$$

This means that the rate of change of I is very small. As the system begins with $I = 0$, I is expected to grow very slowly and so $\dot{L} = \alpha I - \rho L$ is expected to tend to zero (assuming ρ is not also very small).

3.1.14 Discussion

This section presents a single age class model of leptospirosis in a flock of lambs. The results demonstrate the behaviour of the system over time using cobweb diagrams and a bifurcation diagram, as well as basic graphs showing the change in infectious agent and host populations over time. These numerical results are used to check analytical ones.

The periodicity of the model is presented using limit cycle diagrams, and a quasi-R_0 value, similar to the one presented in Roberts & Heesterbeek is found [61]. This quasi-R_0 could be used to predict the behaviour of the dynamics of infection.

As described in the chapter (chapter 3) introduction, the main control parameter used for the models in this section is the leptospire death rate, ρ. When this parameter is increased, the incidence of leptospiral infection, and the size of the bacterial population in the environment, decreases.

Including a recovery rate in the model is briefly explored; however, due to lack of supporting evidence of recovery occurring in livestock, this direction is not pursued further.

The removal date parameter, t_r, is another parameter value which could be used as a control measure. Earlier removal of the lambs decreases the density of free living leptospires in the field and subsequently the infection rates in the flock. This removal date, however, is influenced by the size and value of the lambs at time of sale and subsequently impacts on the farmer's profit margins. Lambs could be moved to a different pasture before sale,

allowing the lambs to gain weight before slaughter, as well as to reduce infection rates; however this is not covered here. This model is used as a building block for the models presented in upcoming sections.

3.2 Sheep Model B

3.2.1 Introduction

In the first extension to sheep model A as presented in section 3.1, an extra age class is included in the model and, as a result, the lambs are exposed to an additional transmission type dependant on life stage. Each age class interacts with the pathogen for a different period of time. The model begins with a constant density of susceptible lambs, N_J, in a field, together with their respective mothers, N_A, a proportion of which may be infectious. Note that all terms related to lambs are now denoted with a subscript J (for juvenile) to distinguish them from ewe related terms, which are denoted with a subscript A (for adult). Lambs become infectious via pseudo-vertical transmission (suckling) as well as via the environment, while ewes become infectious only via the environment. Both infectious lambs, I_J, and infectious ewes, I_A, shed leptospires back into the field at rates α_J and α_A respectively. Once the lambs reach a certain stage of maturity, t_m, the ewes are removed from the field. As before, at time $t_r > t_m$ days, the lambs are also removed from the field and the field remains empty for the remainder of the year. This process is repeated after 12 months. Note that $N_J = S_J + I_J$ and $N_A = S_A + I_A$. The system can be described using the following set of differential equations.

The system before the removal of ewes (phase one: $0 < t < t_m$),

$$\begin{aligned} \frac{dI_J}{dt} &= \nu(N_J - I_J)\frac{I_A}{N_A} + \gamma_J(N_J - I_J)\frac{L}{L+H}, \\ \frac{dI_A}{dt} &= \gamma_A(N_A - I_A)\frac{L}{L+H} - \sigma I_A, \\ \frac{dL}{dt} &= \alpha_J I_J + \alpha_A I_A - \rho L. \end{aligned} \tag{3.10}$$

The system after the removal of ewes, but before the removal of lambs (phase two: $t_m < t < t_r$),

$$\begin{aligned} \frac{dI_J}{dt} &= \gamma_J(N_J - I_J)\frac{L}{L+H}, \\ \frac{dL}{dt} &= \alpha_J I_J - \rho L. \end{aligned} \tag{3.11}$$

The system after the removal of lambs (phase three: $t_r < t < t_y$),

$$\frac{dL}{dt} = -\rho L. \tag{3.12}$$

The initial conditions for leptospires can be either $L_0 = 0, 10$ or 10^3. For ewes, the initial conditions are either $I_{A0} = 0$ or $I_{A0} = N_A\eta$, where $0.1 \leq \eta \leq 0.3$ is the proportion of the flock (of ewes) that is infectious. Several combinations of initial condition are considered. Case B1 shows the most basic of scenarios where $L_0 = 10$ and $I_{A0} = 0$ and is the case used (unless otherwise specified) for the majority of the model analysis. Cases B2-4 explore the relationship between the various sizes of L_0 when $I_{A0} = N_A\eta$ with $\eta = 0.2$. Cases B5 and B6 compare the results for different values of η when $L_0 = 10$. Cases B7 and B8 explore what happens when the proportion of infectious ewes is carried over from one year to the next, with and without recovery ($\sigma = 0$ and $\sigma \neq 0$).

Case B1: $L_0 = 10, I_{A0} = 0$,
Case B2: $L_0 = 0, I_{A0} = N_A\eta$,
Case B3: $L_0 = 10, I_{A0} = N_A\eta$,
Case B4: $L_0 = H, I_{A0} = N_A\eta$,
Case B5: $L_0 = 10, I_{A0} = N_A\eta, \eta = 0.1$,
Case B6: $L_0 = 10, I_{A0} = N_A\eta, \eta = 0.3$,
Case B7: $L_0 = H, I_{A0} = N_A\eta, \eta$ carried over,
Case B8: $L_0 = H, I_{A0} = N_A\eta, \eta$ carried over, ewes recover.

A description of the symbols used is included below.

3.2.2 Data and Parameter Values

Where possible, the parameter values used in the current model are borrowed from model A (section 3.1). As explained in the section introduction (section 3.2.1), the stocking density is set at 10 animals per hectare, this is for both age classes og the model. The lamb removal date

Description	Symbol	Value	Units
Density of the total lamb population in a given area (the field)	N_J	10	SU ha^{-1}
Density of the total ewe population in a given area (the field)	N_A	10	SU ha^{-1}
Density of the infectious lamb population in a given area (the field)	I_J		SU ha^{-1}
Density of the infectious ewe population in a given area (the field)	I_A		SU ha^{-1}
Density of the free living leptospires ($\times 10^{-3}$) in a given area (the field)	L		ha^{-1}
Pseudo vertical transmission coefficient	ν	0.01	days^{-1}
Environmental transmission coefficient for lambs	γ_J	0.02477	day^{-1}
Environmental transmission coefficient for ewes	γ_A	0.02359	day^{-1}
Density of leptospires ($\times 10^{-3}$) at which transmission rate from the environment is 0.5γ	H	10^3	ha^{-1}
Ewe recovery rate	σ	0.02	days^{-1}
Number of leptospires ($\times 10^{-3}$) shed per infectious lamb	α_J	1	day^{-1}
Number of leptospires ($\times 10^{-3}$) shed per infectious ewe	α_A	1.6	day^{-1}
Per capita leptospire death rate	ρ	0.02381	day^{-1}
Time	t		days
Proportion of ewes infectious at $t = t_m$	η	$0.1 - 0.3$	
Removal date of ewes	t_m	90	days
Removal date of lambs	t_r	335	days
End of year	t_y	365	days
Density of the infectious ewe population in a given area (the field) at the beginning of each year n	I_{A0}	0 or ηN_A	SU ha^{-1}
Density of the free living leptospires ($\times 10^{-3}$) in a given area (field one) at $t = 0$	L_0	0 or 10 or 10^3	ha^{-1}

Table 3.2: *Parameters and initial conditions used for sheep model B.*

and positive, non-large value of the leptospire initial condition are carried over from model A, as are H and ρ, both of which are taken from the rat model (chapter 2). The parameter values for γ_J and α_J are taken as the γ and α values in model A and the pseudo-vertical transmission value is borrowed from the rat model (chapter 2), as no data are currently available [20]. The remaining parameter values are considered individually below.

Multiple factors should be considered when deciding on a time to wean lambs, including, but not limited to; the age, weight and growth of the lamb; the condition of the ewe; and food availability [62, 63]. Lambs weaned early, at the age of eight weeks, grow slower than those weaned when they are older [62, 64, 65]. This is due to lambs younger than eight weeks getting most of their energy from milk, as opposed to grass [63]. Despite it being more stressful for lambs than if they are weaned at an older age, weaning at eight weeks appears to be a common practice [65, 66]. A weaning age of 90 days is chosen for this model, as it not only improves weight gain in lambs, but also fits within the recommended weaning time frame of between 83 and 122 days [57, 63, 67].

Ideally, the environmental and pseudo vertical transmission rates, as well as the lamb shedding rate, would not be constant for each time period, but instead, varying functions of time. Lambs initially get all their sustenance from milk, via suckling, progressively getting more and more of their food intake from the pasture as they mature. This is likely to influence their shedding rates over time as well. Unfortunately, the relationships of these figures over time are not available in the literature and so any parameters made to be functions of time would be guesses based on infection rates at the end of the year. Thus, for the sake of simplicity, these terms are made to be constant. The environmental transmission coefficient for ewes is made to be 95.24% of that of lambs, as while in the field with the lambs, ewes eat on average 95.24% of the dry matter of that of lambs (lambs eat more, as they are growing). As such, $\gamma_A = 0.9524 \times \gamma_J$ day^{-1}, resulting in a value of 0.02359 day^{-1} [48]. In terms of shedding, ewes are approximately 1.6 times heavier than lambs, so α_A is made to be $1.6 \times \alpha_J = 1.6$ day^{-1} [57].

The initial condition for the infectious ewes is chosen as either the trivial initial condition ($I_{A0} = 0$), or as some fixed proportion of the population, η. The values of η used range from 0.1 to 0.3, with the default value being $\eta = 0.2$ [68].

Case B8 of the model includes ewe recovery, despite lack of evidence to support it. This is done for interest's sake and the recovery rate is chosen arbitrarily. An extra, large value of leptospire initial condition is also chosen for interest and comparison's sake and is set arbitrarily at 10^3 leptospiral units per hectare.

3.2.3 Numerical Results

As for model A, in section 3.1, each system is solved numerically (see table 3.2 for the parameter values used). The solutions for each case are graphed in figures 3.16-3.23, with the first graph showing the density of susceptible and infectious lambs, the second graph showing the density of susceptible and infectious ewes and the last graph showing the density of free living leptospires, all over a period of six years.

In case B1 (see figure 3.16), all ewes are initially susceptible. As the initial condition for leptospires is quite small and the ewes only remain in the field for a short period of time, the proportion of infectious ewes at t_m is quite small. After the ewes are removed, there is a small dip in the graph for leptospires, this is due to a sudden decrease in the shedding load and the fact that the rate at which the lambs are shedding is not enough to counterbalance the leptospire death rate. There is also a bend in the graph for lambs as the decrease in leptospires means that the lambs become infectious at a slower rate. After the lambs are removed, at time t_r, the leptospire graph plummets rapidly, as the bacteria is no longer being shed into the environment at all and as such, the density of leptospires decreases. Much of this behaviour is repeated in the other cases covered.

In case B2 (see figure 3.17), there are initially no leptospires in the field; however, at the beginning of each year a fixed proportion of ewes is infectious. The number of leptospires now initially increases quite rapidly due to ewe shedding and remains high for the same reason. This results in the rate at which both lambs and ewes become infectious to be somewhat larger than in case B1.

In case B3 (see figure 3.18), neither initial condition is trivial. Both the initial density of leptospires and the proportion of infectious ewes at the beginning of each year is positive. As seen in the previous two examples,

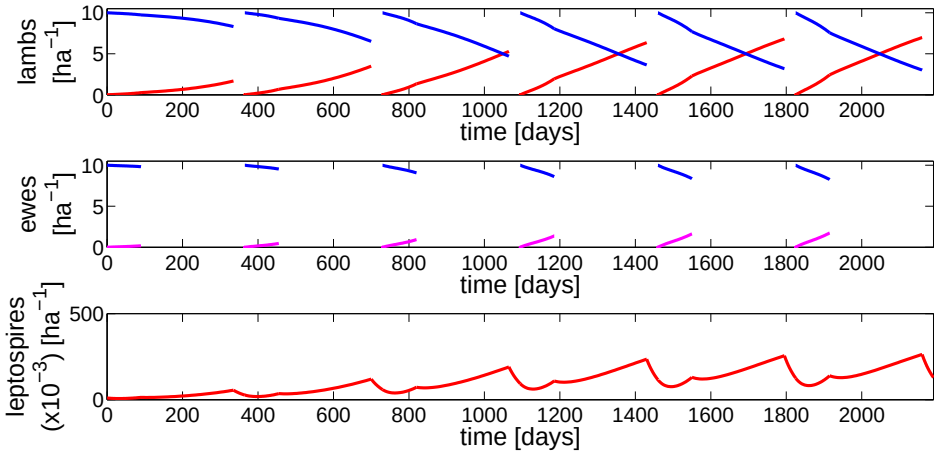

Figure 3.16: *Numerical solutions to sheep model B, case B1: Density of susceptible and infectious lambs (top), density of susceptible and infectious ewes (middle), and density of free-living leptospires (bottom) all over time (days). Susceptible populations shown in blue. Infectious populations shown in either red or purple. The following initial conditions are used:* $I_J(0) = 0, I_A(0) = 0$ *and* $L(0) = 10$.

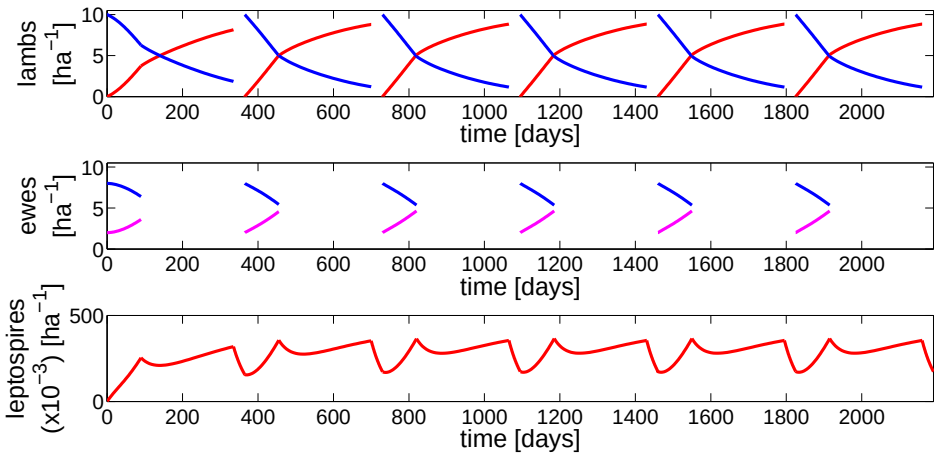

Figure 3.17: *Numerical solutions to sheep model B, case B2: Density of susceptible and infectious lambs (top), density of susceptible and infectious ewes (middle), and density of free-living leptospires (bottom) all over time (days). Susceptible populations shown in blue. Infectious populations shown in either red or purple. The following initial conditions are used:* $I_J(0) = 0, I_A(0) = N_A * 0.2$ *and* $L(0) = 0$.

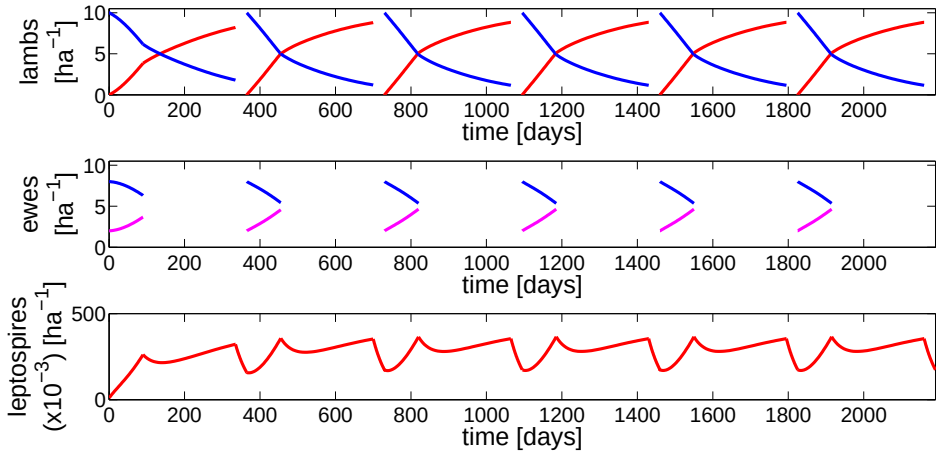

Figure 3.18: *Numerical solutions to sheep model B, case B3: Density of susceptible and infectious lambs (top), density of susceptible and infectious ewes (middle), and density of free-living leptospires (bottom) all over time (days). Susceptible populations shown in blue. Infectious populations shown in either red or purple. The following initial conditions are used:* $I_J(0) = 0, I_A(0) = N_A * 0.2$ *and* $L(0) = 10$.

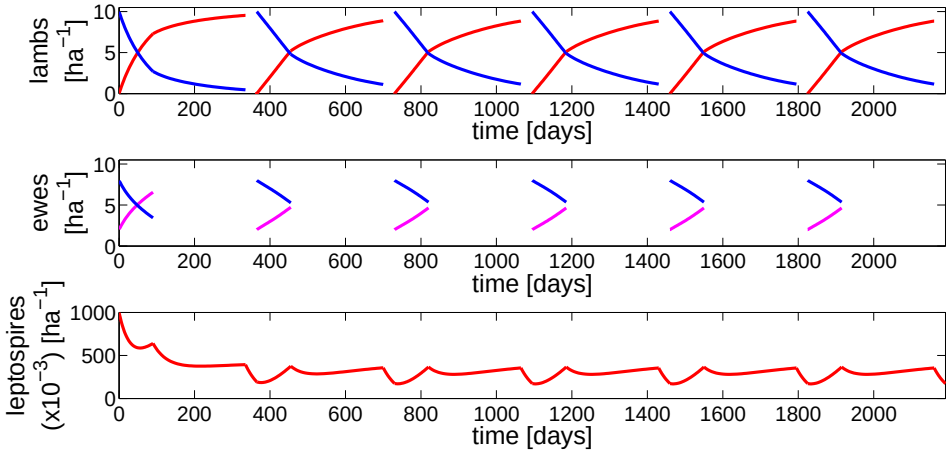

Figure 3.19: *Numerical solutions to sheep model B, case B4: Density of susceptible and infectious lambs (top), density of susceptible and infectious ewes (middle), and density of free-living leptospires (bottom) all over time (days). Susceptible populations shown in blue. Infectious populations shown in either red or purple. The following initial conditions are used:* $I_J(0) = 0, I_A(0) = N_A * 0.2$ *and* $L(0) = 10^3$.

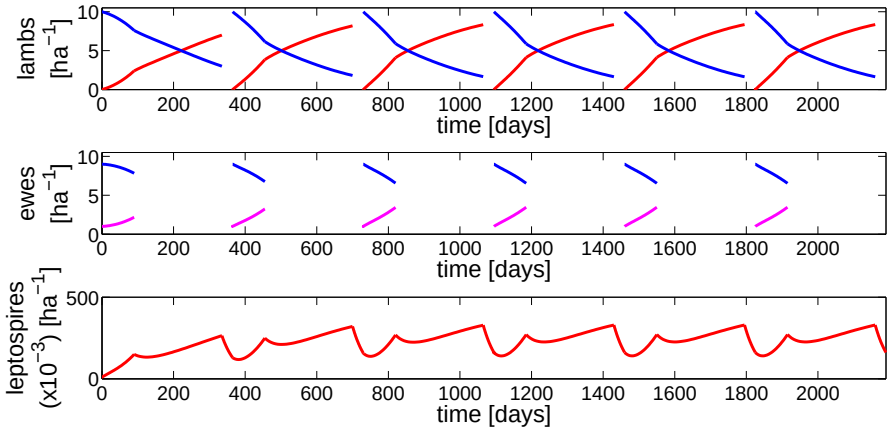

Figure 3.20: *Numerical solutions to sheep model B, case B5: Density of susceptible and infectious lambs (top), density of susceptible and infectious ewes (middle), and density of free-living leptospires (bottom) all over time (days). Susceptible populations shown in blue. Infectious populations shown in either red or purple. The following initial conditions are used:* $I_J(0) = 0, I_A(0) = N_A\eta$ *and* $L(0) = 10$, *where* $\eta = 0.1$.

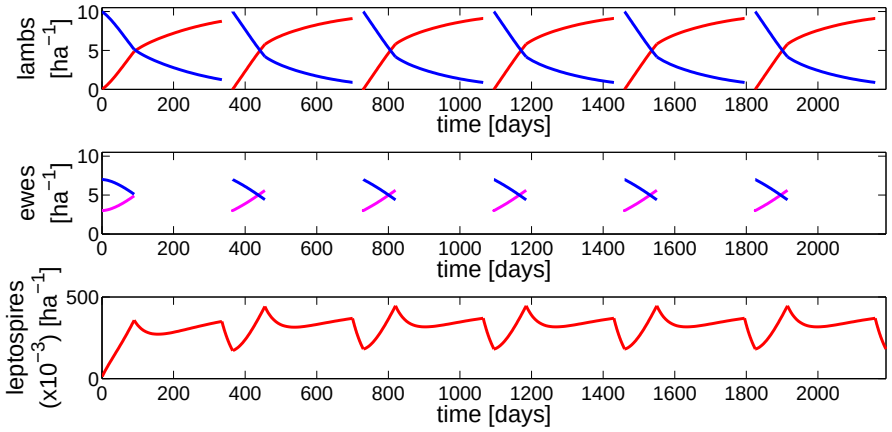

Figure 3.21: *Numerical solutions to sheep model B, case B6: Density of susceptible and infectious lambs (top), density of susceptible and infectious ewes (middle), and density of free-living leptospires (bottom) all over time (days). Susceptible populations shown in blue. Infectious populations shown in either red or purple. The following initial conditions are used:* $I_J(0) = 0, I_A(0) = N_A\eta$ *and* $L(0) = 10$, *where* $\eta = 0.3$.

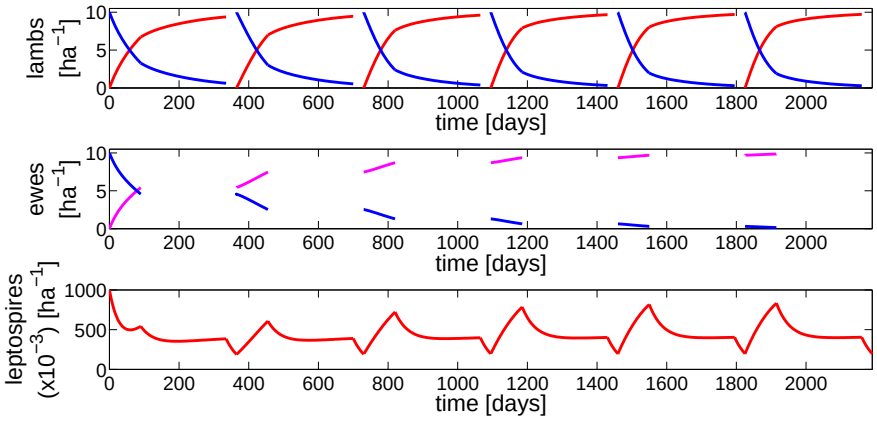

Figure 3.22: *Numerical solutions to sheep model B, case B7: Density of susceptible and infectious lambs (top), density of susceptible and infectious ewes (middle), and density of free-living leptospires (bottom) all over time (days). Susceptible populations shown in blue. Infectious populations shown in either red or purple. The following initial conditions are used:* $I_J(0) = 0, I_A(0) = N_A\eta$ *and* $L(0) = 10$*, where* η *is carried over from the end of one year to the next.*

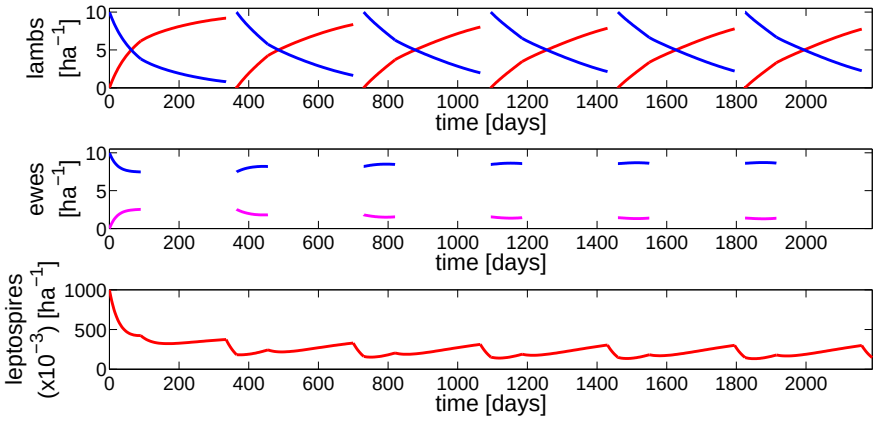

Figure 3.23: *Numerical solutions to sheep model B, case B8: Density of susceptible and infectious lambs (top), density of susceptible and infectious ewes (middle), and density of free-living leptospires (bottom) all over time (days). Susceptible populations shown in blue. Infectious populations shown in either red or purple. The following initial conditions are used:* $I_J(0) = 0, I_A(0) = N_A\eta$ *and* $L(0) = 10$*, where* η *is carried over from the end of one year to the next and ewes can recover,* $\sigma = 0.13$ day^{-1}.

the initial condition for the ewes has a greater effect on the leptospire graph than the initial condition for leptospires. Hence, the graph for case B3 closely resembles that of case B2.

Case B4 explores how case B3 changes when $L(0) >> 1$. The behaviour of the system in case B4 (see figure 3.19) again closely resembles that of cases B2 and B3, except for in the first year. In case B4, both lambs and ewes become infectious faster than in cases B2 and B3. This is due to there being more bactieria in the field. The initial condition for the leptospires is much larger in case B4 than in the previous two cases, but values quickly plummet down to similar values of leptospires as cases B2 and B3. So it would appear that the initial condition for leptospires has little effect on the system over time, as compared to the initial condition for infectious ewes.

Cases B5 and B6 (see figures 3.20 and 3.21) compare the system for values of $\eta = 0.1$ and $\eta = 0.3$. When η, the proportion of infectious ewes, is larger, both lambs and ewes become infectious faster than when η is smaller. The density of leptospires is also larger in case B6 than in case B5.

In case B7 (see figure 3.22), rather than resetting η, the infectious ewe proportion, back to a constant at the beginning of each year, the proportion of infectious ewes is carried over from one year to the next. That is $\eta = \dfrac{I_A(t_m)}{N_A}$ where $I_A(t_m)$ is the density of infectious ewes at the time at which they are removed from the field. The behaviour of the system for the first year is the same as for case B4; however, in subsequent years, the density of infectious ewes continues to increase until it approaches carrying capacity. As a result, the density of leptospires in the field increases at a much faster rate at the beginning of each year. This in turn infects the lambs at a faster rate than in case B4. This behaviour for the ewes in not biologically plausible, as indicated by Dreyfus who found that infection rates in sheep flocks are much lower than 100% [68].

In case B8 (see figure 3.23), recovery is included into the case B7 model. That is, the proportion of infectious ewes is carried from one year to the next; however, ewes can now recover. The value for the recovery rate, σ, is chosen so that the proportion of infectious ewes remains within the biologically feasible boundaries, $0.1 < \eta < 0.3$, as shown in [68]. While the density of infectious lambs still reach carrying capacity, as in case B7,

they become infectious at a slower rate. This is due to there being fewer infectious ewes in the system. There is a slight dip in the curve for infectious ewes at the beginning of each year. This is due to there not being enough leptospires in the field for the ewes to become infectious in comparison to the recovery rate. The ewes overall start to recover for a short period of time before the density of leptospires in the field reach high enough densities to counteract the recovery rate. Infection rates then begins to increase again. As the density of infectious ewes does not reach levels as high as in case B7, neither do the leptospires.

The cyclical behaviour of the system apparent in section 3.1 is again present here and a similar analysis of the model is conducted below.

3.2.4 Cobwebbing

Cobweb diagrams for leptospires, as described in section 3.1, are plotted for each of the two ewe initial conditions (case B1: $I_{A0} = 0$ and case B2: $I_{A0} = N_A\eta$), each for two cases of the leptospire death rate ρ.

Figure 3.24a shows the cobweb for ewe initial condition $I_{A0} = 0$, for $\rho = \rho_0$. Two steady states occur, one is the trivial fixed point (occuring at the origin) and the other is the fixed point for a limit cycle.

In figure 3.24b, ρ is increased to 0.04 day^{-1}. In this cobweb diagram, the trivial fixed point is the only fixed point. This indicates that when ρ is large enough, the bacteria in the field will die out. These results are similar to the results found in model A (section 3.1).

Figure 3.25a shows the cobweb for ewe initial condition $I_{A0} = 0.2N_A$ (for $\eta = 0.1$ and 0.3 the graph of the cobweb moves down and up respectively, when compared to the graph for $\eta = 0.2$), for $\rho = \rho_0$. In this case, only one steady state occurs, the non-trivial steady state.

This is biologically plausible, as even if there are no free-living leptospires in the field, the infectious ewes immediately start shedding them into the environment and so there is little chance for the infection to die out and for a trivial fixed point to occur.

In figure 3.25b, ρ is increased to 0.04 day^{-1}. The behaviour of the cobweb diagram is similar to that of the cobweb at ρ smaller; however, the

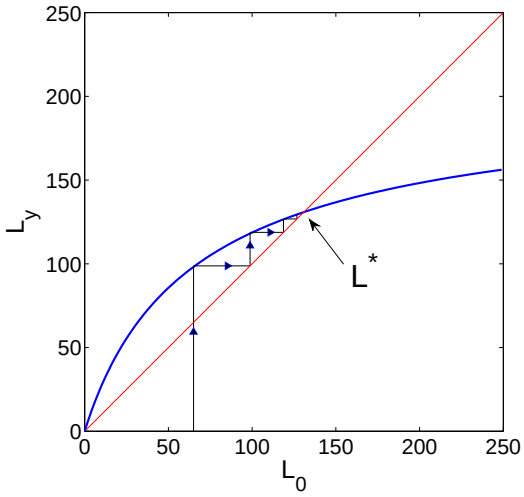

(a) *Cobweb diagram using* $\rho = \rho_0 = 0.02381$ day^{-1} *showing the non-trivial fixed point at* $L^* = 132$ ha^{-1}.

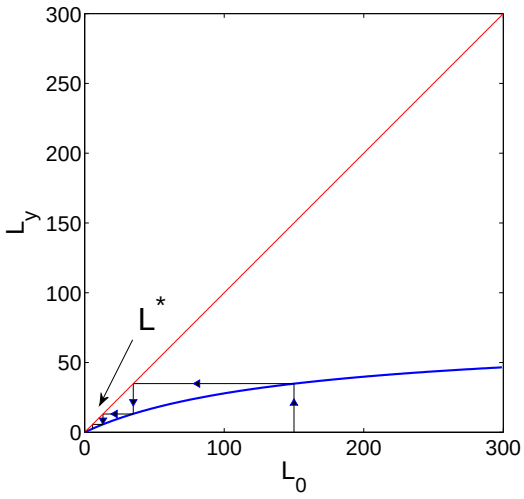

(b) *Cobweb diagram using* $\rho = 0.04$ day^{-1}. *A magnification of the cobweb diagram close to the origin shows that the trivial fixed point is the only fixed point in that region.*

Figure 3.24: *Cobweb diagrams for sheep model B, case B1, using different values of* ρ*, for ewe initial condition* $I_{A0} = 0$.

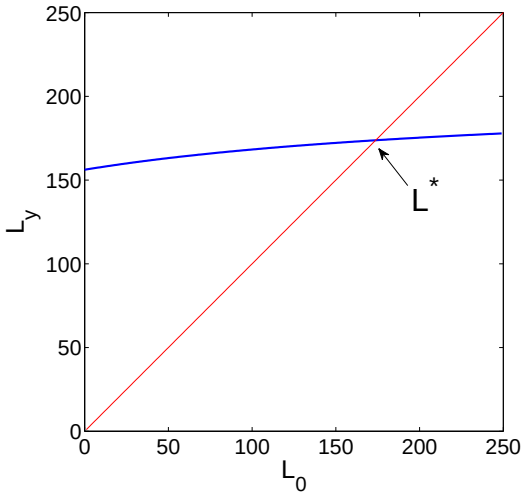

(a) *Cobweb diagram using* $\rho = \rho_0 = 0.02381$ day^{-1} *showing the non-trivial fixed point at* $L^* = 175$ ha^{-1}.

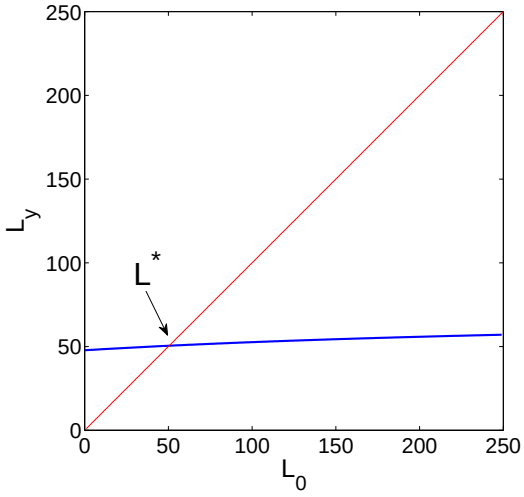

(b) *Cobweb diagram using* $\rho = 0.04$ day^{-1} *showing the non-trivial fixed point at* $L^* = 51$ ha^{-1}. *Note that this is smaller than for* $\rho = 0.02381$ day^{-1}.

Figure 3.25: *Cobweb diagram for sheep model B, case B1, using different values of* ρ, *for ewe initial condition* $I_{A0} = N_A 0.2$. *Cobweb arrows have been excluded from these graphs due to the steepness of the cobweb curve.*

steady state is now smaller.

Note that for visual clarity, due to the steepness of the plots, the "cobwebs" are not included in figures 3.25a and 3.25b.

Cobwebbing shows that in each of the cobweb diagrams, if there is only one steady state, then that steady state is stable and unique, and if there are two steady states, then the non-trivial steady state is stable and unique while the trivial steady state is unstable.

3.2.5 Bifurcation

The bifurcation diagram (figure 3.26) for the trivial ewe initial condition ($I_{A0} = 0$) is similar to that in section 3.1. Here, the critical value of ρ occurs at $\rho = 0.0330$ day^{-1}.

3.2.6 Limit Cycle

The streamlines in the limit cycle diagram of the current model (figure 3.27) follow a similar pattern as for model A (section 3.1); however, there is now an added bend in the curve before it falls to the x-axis. This curve corresponds to the decrease in leptospire density, which occurs as a result of removing the ewes from the field, as is described in section 3.2.3.

The proof for the existence of the limit cycle is again similar to that in model A (section 3.1). Call the initial condition for year n, $\ell_0(n, \rho) = L(nt_y)$, the density of leptospires when the ewes are removed (that is, once the lambs reach a certain level of maturity (m)), $\ell_m(n, \rho) = L(nt_y + t_m)$, the density of leptospires when the lambs are removed, $\ell_r(n, \rho) = L(nt_y + tr)$ and the leptospires at the end of the year, $\ell_y(n, \rho) = L((n + 1)t_y) = \ell_0(n + 1, \rho)$. Then, it is possible to get $\ell_0(n, \rho) = \ell_0(n + 1, \rho)$. That is, the initial condition for the current year is the same as the initial condition for the following year and so the behaviour of the system is repeated. This is proved using ρ as an independent variable. See figure 3.28 for a visual demonstration of the proof.

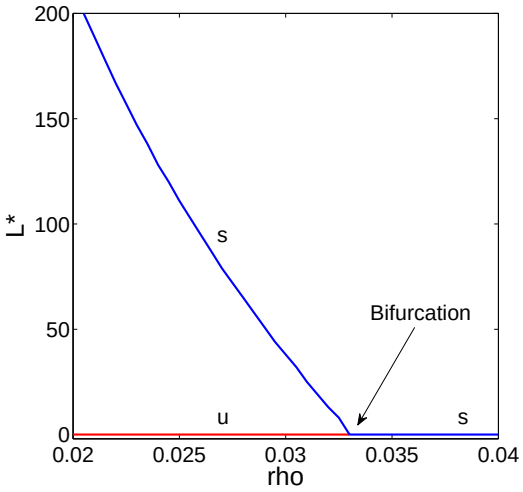

Figure 3.26: *Bifurcation diagram for sheep model B, case B1, showing the fixed point L^* as ρ is varied from 0.02 to 0.03 day^{-1} in increments of 5×10^{-4} day^{-1}. For $\rho > \rho_{crit}$, the stable and only fixed point is the trivial fixed point. At $\rho = \rho_{crit}$, the trivial fixed point becomes unstable. A non-trivial stable fixed point exists for $\rho < \rho_{crit}$ as well as the trivial fixed point. In this example, $\rho_{crit} = 0.0330$ day^{-1}. The diagram is not plotted for $\rho < 0.02$ day^{-1} as the values of L become very large.*

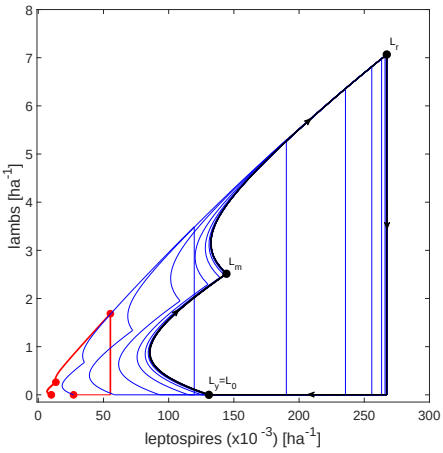

Figure 3.27: *Limit cycle diagram for sheep model B, case B1. Phase-plane showing the relationship between leptospires and lambs over time. First year shown in red. Limit cycle shown in black. Intermediate years shown in blue. A nullcline is indicated as a dashed blue line.*

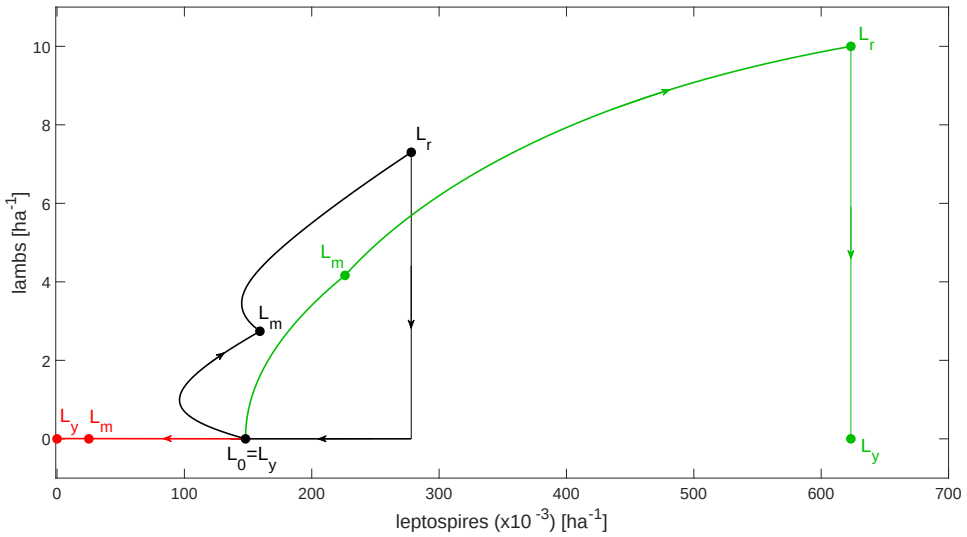

Figure 3.28: *Limit cycle proof streamline demonstration for sheep model B, case B1. The figure above demonstrates the three cases mentioned in the limit cycle proof in section 3.2.6. The red curve is the case when ρ is large, the blue curve is the case when $\rho = 0$ day^{-1} and the black curve is the limit cycle case, where the behaviour of the system repeats itself from one year to the next. Note that for demonstration purposes, L_r for ρ large and L_r for $\rho = 0$ are not to scale.*

Proof. Recall equations 3.10, 3.11 and 3.12. Define $\rho_\infty = \dfrac{\alpha_J N_J + \alpha_A N_A}{L_0}$. It is shown that when $\rho = 0$, $\ell_y(n,0) > \ell_0(n,0)$, and when $\rho > \rho_\infty$, $\ell_y(n,\rho) < \ell_0(n,\rho)$. Hence, by continuity, there exists ρ such that $\ell_y(n,\rho) = \ell_0(n,\rho)$.

a) For $0 < t < t_m$, when $\rho = 0$, from equation 3.10, $\dot{L} = \alpha_J I_J + \alpha_A I_A$. Since $\dot{L} > 0$, then $\ell_m(n,0) > \ell_0(n,0)$.

For $t_m < t < t_r$, when $\rho = 0$, from equation 3.11, $\dot{L} = \alpha_J I_J$. Again $\dot{L} > 0$, so $\ell_r(n,0) > \ell_m(n,0)$.

Finally, for $t_r < t < t_y$, when $\rho = 0$, from equation 3.12, $\dot{L} = 0$, so $\ell_y(n,0) = \ell_r(n,0)$.

In conclusion $\ell_y(n,0) = \ell_r(n,0) > \ell_m(n,0) > \ell_0(n,0)$ and so when

$\rho = 0$, $\ell_y(n,0) > \ell_0(n,0)$.

b) Next consider the case when ρ is very large. For $0 < t < t_m$, multiplying equation 3.10 by the integrating factor and rearranging gives

$$\frac{d}{dt}(Le^{\rho t}) = (\alpha_J I_J + \alpha_A I_A)e^{\rho t}.$$

Integrating the above gives

$$Le^{\rho t} - L_0 = \int_0^t (\alpha_J I_J(u) + \alpha_A I_A(u))\, e^{\rho u} du$$

which simplifies to

$$L(t) = L_0 e^{-\rho t} + e^{-\rho t}\alpha_J \int_0^t I_J(u)e^{\rho u} du + e^{-\rho t}\alpha_A \int_0^t I_A(u)e^{\rho u} du.$$

Now, recall that $I_J \leq N_J$ and $I_A \leq N_A$. So

$$\begin{aligned} L(t) \leq \tilde{L}(t) &= L_0 e^{-\rho t} + e^{-\rho t}\,(\alpha_J N_J + \alpha_A N_A) \int_0^t e^{\rho u} du \\ &= L_0 e^{-\rho t} + \frac{\alpha_J N_J + \alpha_A N_A}{\rho}(1 - e^{-\rho t}). \end{aligned}$$

Now, if $\rho > \rho_\infty = \dfrac{\alpha_J N_J + \alpha_A N_A}{L_0}$, then $L(t) \leq \tilde{L}(t) < L_0$ for all $0 < t < t_m$ and so $\ell_m(n,\rho) < \ell_0(n,\rho)$.

For $t_m < t < t_r$, multiplying equation 3.11 by the integrating factor and rearranging gives

$$\frac{d}{dt}(Le^{\rho t}) = \alpha_J I_J e^{\rho t}.$$

Integrating the above from t_m to t gives

$$Le^{\rho t} - L_m e^{\rho t_m} = \alpha_J \int_{t_m}^t I_J(u)e^{\rho u} du$$

which simplifies to

$$L(t) = L_m e^{\rho(t_m - t)} + e^{-\rho t}\alpha_J \int_{t_m}^{t} I_J(u) e^{\rho u} du.$$

Now $I_J \leq N_J$ and $\rho > \rho_\infty = \dfrac{\alpha_J N_J + \alpha_A N_A}{L_0} \implies L_0 > \dfrac{\alpha_J N_J + \alpha_A N_A}{\rho}$ $> \dfrac{\alpha_J N_J}{\rho}$ and $L_m < L_0$. So

$$\begin{aligned} L(t) \leq \tilde{L}(t) &= L_m e^{\rho(t_m - t)} + e^{-\rho t}\alpha_J N_J \int_{t_m}^{t} e^{\rho u} du \\ &= L_m e^{\rho(t_m - t)} + \frac{\alpha_J N_J}{\rho}\left(1 - e^{\rho(t_m - t)}\right) \\ &< L_0 e^{\rho(t_m - t)} + L_0\left(1 - e^{\rho(t_m - t)}\right) \\ &= L_0. \end{aligned}$$

So, when $\rho > \rho_\infty = \dfrac{\alpha_J N_J + \alpha_A N_A}{L_0}$, then $L(t) \leq \tilde{L}(t) < L_0$ for all $t_m < t < t_r$ and so $\ell_r(n, \rho) < \ell_0(n, \rho)$.

For $t_r < t < t_y$, from equation 3.12, $\dot{L} < 0$ and so $\ell_y(n, \rho) < \ell_r(n, \rho)$.

In conclusion $\ell_y(n, \rho) < \ell_r(n, \rho) < \ell_0(n, \rho)$ and so when $\rho > \rho_\infty = \dfrac{\alpha_J N_J + \alpha_A N_A}{L_0}$, then $\ell_y(n, \rho) < \ell_0(n, \rho)$. As $\ell_y(n, \rho) > \ell_0(n, \rho)$ when ρ is small and $\ell_y(n, \rho) < \ell_0(n, \rho)$ when ρ is large ($\rho > \rho_\infty$), it follows that a limit cycle exists (see section 3.1 for further detail). □

The monotonic decreasing nature of $L_y(\rho)$, as defined in subsection 3.1.6, which shows that the limit cycle is unique, can be proved by following a similar procedure to that in section 3.1. For the set of parameters used here, using the same formula as in subsection 3.2.6, the Lyapunov exponent is negative and approximately equal to $\log_2 10^{-1}$, so the limit cycle is confirmed to be stable.

3.2.7 The Quasi-Basic Reproduction Number, R_L

A quasi-basic reproduction number is found for the predecessor to this model (model A) by linearising the original system of equations (equations

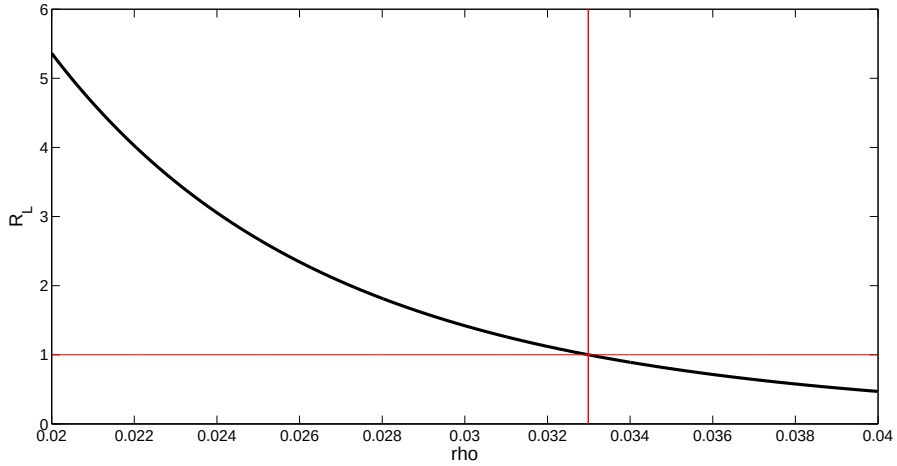

Figure 3.29: *Graph showing R_L as a function of leptospire death rate ρ for sheep model B, case B1. $R_L = 1$ is shown with a horizontal red line. The critical value of ρ (ρ_{crit}) is shown with a vertical red line. The graph shows that $\rho = \rho_{crit}$ and $R_L = 1$ coincide and are in agreement with the bifurcation diagram.*

3.10-3.12) about the trivial fixed point, solving the resulting second order, autonomous, differential equations and dividing the solution for L_y by L_0. That is, the quasi-basic reproduction number, R_L, is defined as $R_L(\rho) = \lim_{L_0 \to 0} \dfrac{L_y(1,\rho)}{L_0}$. Unfortunately, due to the additional age class considered in this model, the system of equations can not be turned into a set of second order linear equations. Linearising the set of equations for $0 < t < t_m$ (equations 3.10) about the trivial fixed point, results in the non-autonomous, second order differential equation

$$\ddot{L} + \rho\dot{L} - \frac{\alpha_A\gamma_A N_A + \alpha_J\gamma_J N_J}{H} L + \left(\alpha_A\sigma - \alpha_J\nu\frac{N_S}{N_A}\right) I_A = 0,$$

with initial conditions $L(0) = L_0$ and $\dot{L}(0) = \alpha_A I_A(0) + \alpha_J I_J(0) - \rho L(0)$ $= -\rho L_0$. This equation can not be solved analytically and so an analytical expression for R_L cannot be found.

One can, however, find a numerical solution for a threshold value using the parameter values selected at the beginning of the section. As before,

$$R_L = \lim_{L_0 \to 0} \frac{L_y}{L_0}\bigg|_{I_J(0)=0, I_A(0)=0}.$$

As such, the graph for R_L (figure 3.29) simply plots $\frac{L_y}{L_0}$ over ρ, with initial conditions $I_J(0) = 0$, $I_A(0) = 0$ and $L(0) << 1$. In this case, $L(0) = 1$. The value of ρ for which $R_L = 1$ is the same as ρ_{crit} as found using the bifurcation diagram. The value of R_L at ρ_0, may also be of interest. For this model $R_L(\rho_0) = 3.1388$. This value is greater than one, which is to be expected, as infection is present in the system.

3.2.8 Discussion

The model presented in this section expands on sheep model A by introducing an additional age class into the host population. It explores the interaction of free living leptospires with both ewes and lambs using several cases of initial conditions.

In case B1 it is seen that when both host populations are initially fully susceptible, environmental contamination is enough to perpetuate the disease within the flock from one generation to the next. Case B1 is also the case used in the rest of the section to demonstrate the repetitive behaviour of the system using cobwebbing, a bifurcation diagram and a limit cycle diagram.

Case B2 shows that the field doesn't need to be contaminated with bacteria initially for the infection to persist, if the disease is initially present within the flock of ewes.

Cases B3 and B4, which both include the non-trivial initial condition for infectious ewes (as in case B2), show that the initial environmental load of leptospires is insignificant over time, with the system reaching the same steady state in both cases. A cobweb diagram for case B3 is used to demonstrate that in this case, only one fixed point for leptospires exists at a time. That is, the non-trivial fixed point does not exist in concert with the trivial fixed point.

Cases B5 and B6 show that the proportion of the ewe flock infected at the beginning of each year impacts on all populations, both host and infectious agent, with the larger proportion of infectious ewes increasing both the density of infectious lambs, as well as the free living leptospire density.

In case B7, the proportion of infectious ewes is passed from one year to the next. Eventually, the whole ewe population is infectious. The rate at which lambs become infected is much faster as compared to case B4 (which is similar to case B7; however the initial infectious ewe population is fixed), and the density of leptospires in the environment is much higher.

Case B8 builds upon case B7 by including a recovery term. This case shows that even a modest rate of recovery has a visible impact on infection rates and suggests that treatment may be an important strategy for disease control.

Overall, by including ewes into the system, this expansion to the model improves its realism and demonstrates how infection in the ewe population impacts on infection rates in lambs.

3.3 Sheep Model C

3.3.1 Introduction

The second extension to sheep model A includes both age classes and all three time phases in sheep model B (section 3.2). In this expansion to the model pseudo-vertical transmission is excluded from the system and an immune compartment for lambs is introduced in its place.

As before, the density of ewes and lambs is constant. The ewe population is considered to be fully susceptible at the beginning of each year, $S_A(0) = N_A$, while lambs are assumed to be immune, $M_J(0) = N_J$. Lambs must first lose maternally derived immunity to become susceptible, S_J, before they can become infectious, I_J. As in the previous models, lambs remain in the field for a total of 11 months before being removed, while ewes are removed after three months. As before, the field remains unoccupied once the lambs are removed, thus allowing it to recover from free living leptospire, L, infection. At the beginning of the next year, the ewes, now again all susceptible, S_A, together with their new offspring, are reintroduced into the field and the process is repeated. It is assumed that the ewes have been treated with antibiotics to remove infection, but have not been vaccinated and so are susceptible at the beginning of the year. Note that $N_A = S_A + I_A$, where the infectious ewes are denoted by I_A.

Similarly, $N_J = S_J + M_J + I_J$. The following set of differential equations is used to model the system.

The system before removal of ewes (phase one: $0 < t < t_m$),

$$\begin{aligned}
\frac{dS_A}{dt} &= -\frac{\gamma_A S_A L}{L+H}, \\
\frac{dI_A}{dt} &= \frac{\gamma_A S_A L}{L+H}, \\
\frac{dM_J}{dt} &= -\nu M_J, \\
\frac{dS_J}{dt} &= \nu M_J - \frac{\gamma_J S_J L}{L+H}, \\
\frac{dI_J}{dt} &= \frac{\gamma_J S_J L}{L+H}, \\
\frac{dL}{dt} &= \alpha_J I_J + \alpha_A I_A - \rho L.
\end{aligned}$$

The system after removal of ewes, but before removal of lambs (phase two: $t_m < t < t_r$ and $S_A = I_A = 0$),

$$\begin{aligned}
\frac{dM_J}{dt} &= -\nu M_J, \\
\frac{dS_J}{dt} &= \nu M_J - \frac{\gamma_J S_J L}{L+H}, \\
\frac{dI_J}{dt} &= \frac{\gamma_J S_J L}{L+H}, \\
\frac{dL}{dt} &= \alpha_J I_J - \rho L.
\end{aligned}$$

The system after removal of both ewes and lambs (phase three: $t_r < t < t_y$ and $S_A = I_A = M_J = S_J = I_J = 0$),

$$\frac{dL}{dt} = -\rho L.$$

3.3.2 Model Components

Pseudo-vertical transmission (transmission via suckling of milk) as is included in model B (section 3.2) is not included in this version of the

model as there is mixed evidence for its occurrence. Several sources claim that leptospirosis may be maintained through vertical transmission, either via the milk, transplacentally, or both; however there are no data available for what a possible transmission coefficient might be [41, 69–74]. Other sources claim that while the bacteria may be present in milk, its survival duration is very short (4-5 minutes) due to the fats, and possibly other components, present in the milk being toxic to the bacteria. Therefore, transmission to offspring may not be possible after all and is excluded from the model [75, 76].

There is mixed evidence for in-utero transmission of infection as well, with some sources claiming that young are born susceptible, while others claim that in-utero transmission is possible and that young can be born infectious [5, 77]. There is definitive evidence of maternal antibodies being passed to young through colostrum however. Colostrum is the fluid produced by mothers and fed to the young via the milk in the first hours after birth [5, 78]. The antibodies present in the colostrum pass through the gut of the offspring and into the bloodstream, providing protection from infection [78–80, 80]. The level of antibodies received by the young depends on the levels in their mother. A ewe may acquired antibodies either via vaccination or by becoming infected [81, 82]. A completely naive ewe which has never been vaccinated (as is assumed in the model), nor been exposed to leptospire bacteria, will not have any antibodies to pass to her lamb. In ewes that do possess antibodies, immunity may fail due to the lamb not consuming enough colostrum. Despite this, for the sake of simplicity, if is assumed that all young do receive antibodies, and so $M_J(0) = N_J$ [83]. The length of immunity depends not only on the antibody half-life, but also on the initial titre [79, 80]. One study claims up to 12 weeks of protection in young if the mother is vaccinated during pregnancy, while another gives antibody half-lives of 6.7 and 6.3 months for Hardjobovis and Pomona serovars respectively [78, 81]. These half-life values are supported by another source which gives a half-life range of three to six months [80].

3.3.3 Data and Parameter Values

The antibody half-life of 6.7 months for Hardjobovis is chosen for the calculation of the loss of immunity parameter value and leads to a rate $\nu = \log(2)/204 = 4.9 \times 10^{-3}$ day^{-1} [81].

Description	Symbol	Value	Units
Density of the total ewe population in a given area (the field)	N_A	10	SU ha^{-1}
Density of the susceptible ewe population in a given area (the field)	S_A		SU ha^{-1}
Density of the infectious ewe population in a given area (the field)	I_A		SU ha^{-1}
Density of the total lamb population in a given area (the field)	N_J	10	SU ha^{-1}
Density of the immune lamb population in a given area (the field)	M_J		SU ha^{-1}
Density of the susceptible lamb population in a given area (the field)	S_J		SU ha^{-1}
Density of the infectious lamb population in a given area (the field)	I_J		SU ha^{-1}
Density of the free living leptospires ($\times 10^{-3}$) in a given area (the field)	L		ha^{-1}
Environmental transmission coefficient for ewes	γ_A	0.02359	day^{-1}
Environmental transmission coefficient for lambs	γ_J	0.02477	day^{-1}
Density of leptospires ($\times 10^{-3}$) at which transmission rate from the environment is 0.5γ	H	10^3	ha^{-1}
Loss of immunity for lambs	ν	3.4×10^{-3}	day^{-1}
Number of leptospires ($\times 10^{-3}$) shed per infectious ewe	α_A	3.7317	day^{-1}
Number of leptospires ($\times 10^{-3}$) shed per infectious lamb	α_J	2.3323	day^{-1}
Per capita leptospire death rate	ρ	0.02381	day^{-1}
Time	t		days
Removal date of ewes	t_m	90	days
Removal date of lambs	t_r	335	days
End of year	t_y	365	days
Density of the infectious ewe population in a given area (the field) at the beginning of each year	I_{A0}	0	SU ha^{-1}
Density of the immune lamb population in a given area (the field) at the beginning of each year	M_{J0}	N_J	SU ha^{-1}

...Continuation of Table 3.3

Description	**Symbol**	**Value**	**Units**
Density of the susceptible lamb population in a given area (the field) at the beginning of each year	S_{J0}	0	SU ha^{-1}
Density of the free living leptospires ($\times 10^{-3}$) in a given area (the field) at $t = 0$	L_0	10	ha^{-1}

Table 3.3: *Parameters and initial conditions used for sheep model C.*

In model B (section 3.2) a value of 10^3 leptospires per day is chosen for the leptospire shedding rate. This gives a (scaled) α value of 1 day^{-1}. Using $\alpha_J = 1$ day^{-1} in the present model, however, is sub-critical for infection to persist. This is due to the inclusion of the immune compartment, which slows down the speed at which lambs become infectious, as they first have to move into the susceptible compartment. Any leptospires in the field continue to die off while this transition is occurring. With the parameter values used here, lambs become susceptible and then infectious too slowly for the free living leptospires to persist. Therefore, the density at which leptospires are shed into the environment, α_J, is increased to 2.3323 day^{-1}. This allows the proportion of infectious lambs at time of slaughter to be 0.27. That is, $I_J(t_r) = 0.27N_J$. This value is also still within the limits discussed in section 3.1.

The parameter values for N_A, N_J, γ_A, γ_J, H, ρ, t_m, t_r and L_0 are taken from the previous sheep models (section 3.1 and section 3.2).

3.3.4 Numerical Results

Figure 3.30 shows the numerical results for ewes, lambs and leptospires, all over a time period of six years. Steady states of the system are confirmed to be unique and stable by using cobwebbing; however, the graphs are not included here as the results are similar to those in model A (section 3.1). Figure 3.31 shows the bifurcation diagram of they system. The value of ρ_{crit} in this model is $\rho = 0.0293$ day^{-1}. It is not possible to compare this value with that found in the previous model (model B, section 3.2) as the parameter values are not consistent between the models.

3.3.5 Limit Cycle

The limit cycle diagram for this model is very similar to that of model B (section 3.2) and hence in not included here. As there has been no change in the equations for the leptospires in this model, the proof for the existence of a limit cycle is just the same as for model B (section 3.2). Uniqueness follows as well.

The value for the Lyapunov exponent does change; however it is still

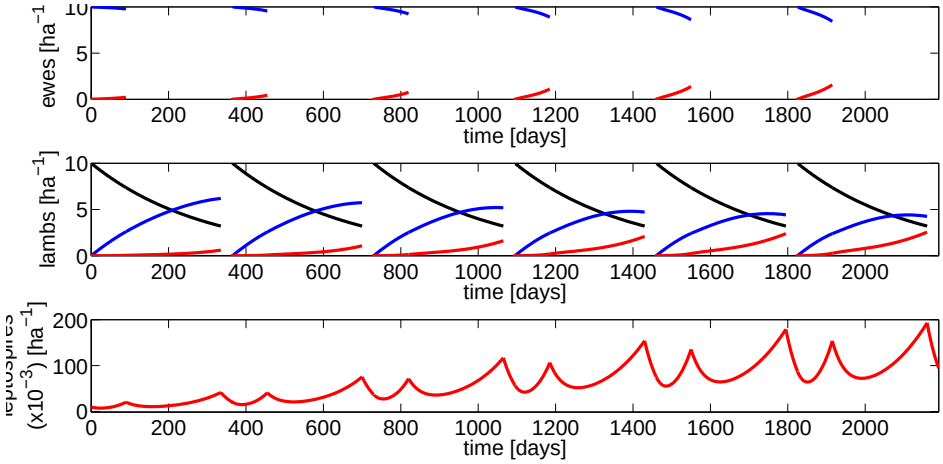

Figure 3.30: *Numerical solutions to sheep model C. Density of susceptible and infectious ewes (top), density of immune, susceptible and infectious lambs (middle), and density of free-living leptospires (bottom) all over time (days). Immune lambs shown in black. Susceptible sheep shown in blue. Infectious sheep shown in red.*

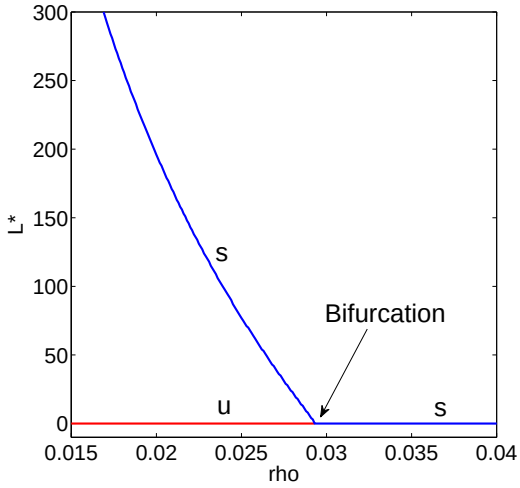

Figure 3.31: *Bifurcation diagram for sheep model C showing the fixed point L^* as ρ is varied from 0.015 to 0.04 day^{-1}. For $\rho > \rho_{crit}$, the stable and only steady state is the trivial fixed point. At $\rho = \rho_{crit}$, the trivial fixed point becomes unstable. A non-trivial stable fixed point exists for $\rho < \rho_{crit}$, as well as the trivial fixed point. In this example, ρ_{crit} occurs at $\rho = 0.0293$ day^{-1}. The diagram is not plotted for $\rho < 0.02$ day^{-1} as the values of L become very large.*

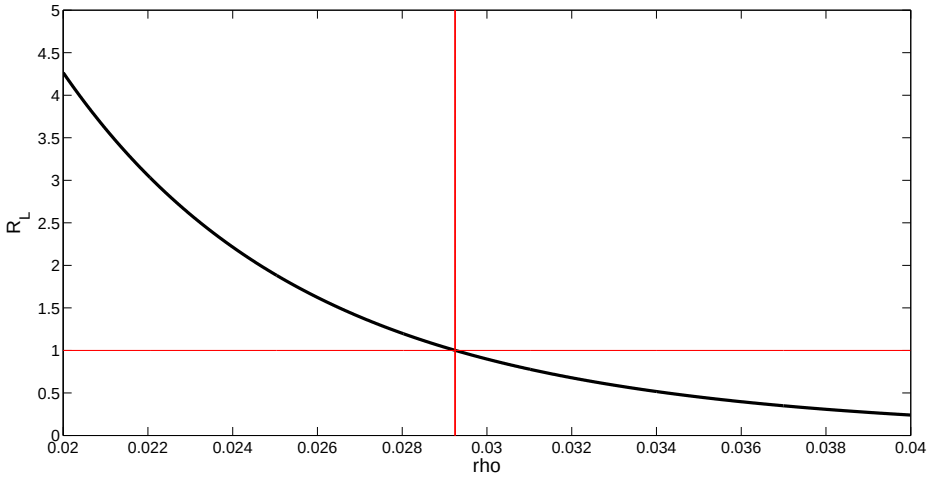

Figure 3.32: *Graph showing R_L as a function of leptospire death rate ρ for sheep model C. $R_L = 1$ is shown with a horizontal red line. The critical value of ρ (ρ_{crit}) is shown with a vertical red line. The graph shows that $\rho = \rho_{crit}$ and $R_L = 1$ coincide and are in agreement with the bifurcation diagram.*

negative and indicates stable behaviour of the limit cycle. The Lyapunov exponent is approximately equal to $\log_2 10^{-3}$.

3.3.6 The Quasi-Basic Reproduction Number, R_L

A quasi-basic reproduction number is again only plotted numerically (figure 3.32). For this model $R_L(\rho_0) = 2.2828$.

3.3.7 Discussion

This model is an extension and more realistic version of model A as presented in section 3.1. Maternally derived immunity is included in the current model while pseudo-vertical transmission is excluded. This expands the compartments of the lamb age class to incorporate an immune compartment. These changes, when using the same parameter values as used in model B (section 3.1), cause the infection to become subcritical, and so the leptospire shedding rate, α_J, is increased. The numerical value of R_L at $\rho = 0.02381$ day^{-1} in this model is approximately 2.

The model presented here assumes that ewes are treated with antibiotics but not vaccinated before lambing each year and are thus free from infection and susceptible. This is not usually the case on New Zealand farms.

3.4 Sheep Model D

3.4.1 Introduction

The final expansion of the sheep model incorporates a non-trivial initial condition for ewes, as well as an additional environment. A second field is introduced into the model to measure the dynamics of infection in ewes while they are not in the field with the lambs. Infection in ewes is then carried over from one year to the next. The fact that ewes do not live indefinitely and part of the flock must, from time to time, be replaced, is also considered. Heat maps, bifurcation diagrams, a limit cycle diagram and a quasi-R_0 diagram are used to examine the system.

As in model C (section 3.3) the system initially begins with a fully susceptible ewe population, $S_A(0) = N_A$, and a fully immune lamb population, $M_J(0) = N_J$. Infection is introduced into the system via free living leptospires in the field hosting the lambs (field one).

The field that the ewes are introduced into after being separated from the lambs (field two), is assumed to be clear of infection at the beginning of each year, $L_z(nt_y) = 0$, where n is the non-negative integer indicating the year and t_y is the end of the year in days. Infection is introduced into field two through the infectious ewes from field one. The dynamics of infection in the ewes is modelled until the end of the year and infection is carried over into the next year. In addition to this change, one can not expect the exact same flock of ewes to be breed indefinitely, so each year, some proportion of the original flock is replaced. The replacement ewes are most likely to be made up of lambs born in the previous year, some of which will be infectious; however, for the sake of simplicity, the new ewes are assumed to be susceptible. This could be achieved by either treating or testing the lambs for infection before they are introduced into the ewe flock. The new flock is introduced to field one, together with their offspring, at the beginning of the next year and the process is repeated.

The system can be described using the following set of differential equations. Note that the set of differential equations describing the system for field one is the same as in model C (section 3.3). It is included here for ease of reference.

Field one

The system before removal of ewes (phase one: $0 < t < t_m$),

$$\begin{aligned}
\frac{dS_A}{dt} &= -\frac{\gamma_A S_A L}{L+H}, \\
\frac{dI_A}{dt} &= \frac{\gamma_A S_A L}{L+H}, \\
\frac{dM_J}{dt} &= -\nu M_J, \\
\frac{dS_J}{dt} &= \nu M_J - \frac{\gamma_J S_J L}{L+H}, \\
\frac{dI_J}{dt} &= \frac{\gamma_J S_J L}{L+H}, \\
\frac{dL}{dt} &= \alpha_J I_J + \alpha_A I_A - \rho L.
\end{aligned}$$

The system after removal of ewes, but before removal of lambs (phase two: $t_m < t < t_r$ and $S_A = I_A = 0$),

$$\begin{aligned}
\frac{dM_J}{dt} &= -\nu M_J, \\
\frac{dS_J}{dt} &= \nu(N_J - S_J - I_J) - \frac{\gamma_J (N_J - M_J - I_J) L}{L+H}, \\
\frac{dI_J}{dt} &= \frac{\gamma_J (N_J - M_J - I_J) L}{L+H}, \\
\frac{dL}{dt} &= \alpha_J (N_J - M_J - S_J) - \rho L.
\end{aligned}$$

The system after removal of both ewes and lambs (phase three: $t_r < t < t_y$ and $S_A = I_A = M_J = S_J = I_J = 0$),

$$\frac{dL}{dt} = -\rho L.$$

Field two

The system after the introduction of ewes into field two (phase two and three: $t_m < t < t_y$),

$$\begin{aligned}
\frac{dS_A}{dt} &= -\frac{\gamma_A(N_A - I_A)L}{L+H}, \\
\frac{dI_A}{dt} &= \frac{\gamma_A(N_A - I_A)L}{L+H}, \\
\frac{dL}{dt} &= \alpha_A I_A - \rho L.
\end{aligned}$$

3.4.2 Model Components

The initial condition for free living leptospires in field two is chosen to be zero, $L_z = 0$. This is done mainly for simplicity, but could be as a result of using a different field for field two each year, or from the free living bacterial infection being treated.

When weaning, it is recommended to move ewes, rather than lambs, as this leaves the lambs in a familiar environment, which ensures that they are able to find food and water and is hence less stressful for them [64]. This strategy is included in the model.

A Brazilian study suggested that sexual transmission in livestock may be possible after finding leptospira in the semen and vaginal fluid of sheep and goats [10]. Director et al, showed that viable leptospira (serovar Hardjo) were present in the vaginal fluid of ewes, which suggests that sexual transmission from ewes to rams may be possible [84]. These authors, however, admitted that it was possible that the positive results were due to contamination. A ewe can expect to be serviced once or twice during a season and as sexual contact would only occur once or twice a year and there do not appear to be any data on sexual transmission coefficients, sexual transmission is ignored here [85].

Description	Symbol	Value	Units
Density of the total ewe population in a given area (the field)	N_A	10	SU ha^{-1}
Density of the susceptible ewe population in a given area (the field)	S_A		SU ha^{-1}
Density of the infectious ewe population in a given area (the field)	I_A		SU ha^{-1}
Density of the total lamb population in a given area (the field)	N_J	10	SU ha^{-1}
Density of the immune lamb population in a given area (the field)	M_J		SU ha^{-1}
Density of the susceptible lamb population in a given area (the field)	S_J		SU ha^{-1}
Density of the infectious lamb population in a given area (the field)	I_J		SU ha^{-1}
Density of the free living leptospires in field one ($\times 10^{-3}$) in a given area (the field)	L_1		ha^{-1}
Density of the free living leptospires in field two ($\times 10^{-3}$) in a given area (the field)	L_2		ha^{-1}
Environmental transmission coefficient for ewes	γ_A	0.02359	day^{-1}
Environmental transmission coefficient for lambs	γ_J	0.02477	day^{-1}
Density of leptospires ($\times 10^{-3}$) at which transmission rate from the environment is 0.5γ	H	10^3	ha^{-1}
Loss of immunity for lambs	ν	3.4×10^{-3}	day^{-1}
Number of leptospires ($\times 10^{-3}$) shed per infectious ewe	α_A	3.7317	day^{-1}
Number of leptospires ($\times 10^{-3}$) shed per infectious lamb	α_J	2.3323	day^{-1}
Per capita leptospire death rate	ρ	0.02381	day^{-1}
Time	t		days
Removal date of ewes	t_e	90	days
Removal date of lambs	t_l	335	days
End of year	t_y	365	days
Density of the infectious ewe population in a given area (the field) at the beginning of each year n	I_{A0}	$\frac{3}{4}I_{A0}(n-1)$	SU ha^{-1}

...Continuation of Table 3.4

Description	**Symbol**	**Value**	**Units**
Density of the immune lamb population in a given area (the field) at the beginning of each year	M_{J0}	N_J	SU ha^{-1}
Density of the susceptible lamb population in a given area (the field) at the beginning of each year	S_{J0}	0	SU ha^{-1}
Density of the free living leptospires ($\times 10^{-3}$) in a given area (field one) at $t = 0$	L_0	10	ha^{-1}
Density of the free living leptospires ($\times 10^{-3}$) in a given area (field two) at $t = nt_y$	L_z	0	ha^{-1}

Table 3.4: *Parameters and initial conditions used for sheep model D.*

Ewes are chosen to be culled or otherwise removed from the breeding flock after four years. This is supported by sources which claim that a ewe is most productive between three and six years of age [65]. Several sources support the culling of ewes at five years of age specifically, with one study finding that culling at five years of age provided the highest economic returns [57, 86, 87]. Culling at five years of age equates to removing the ewes from the flock after four years (they are lambs for the first year). Assuming a regular and fixed turn-over of ewes, this results in 25% of the flock being replaced each year.

All other parameter values are as in section 3.3.

3.4.3 Numerical Results

The numerical solutions for this model are divided roughly by field. Figure 3.33 shows results for lambs and leptospires in field one over a time period of five years. Figure 3.34 shows results for ewes in both fields one and two (field distinguished by colour) and leptospires in field two over the same time period. As in the previous models, repetition of model behaviour is apparent after some time.

3.4.4 Cobwebbing

As in this iteration of the model not only the density of leptospires, but also the density of infectious ewes, is passed from one year to the next, it is not possible to demonstrate the behaviour of the system using cobweb diagrams, as the problem is a mapping from a two dimensional space, $(L_0(n), I_{A0}(n))$, onto another two dimensional space, $(L_0(n+1), I_{A0}(n+1))$. Therefore, a heat map is used to show the behaviour of the system for each pair of initial conditions (L_0, I_{A0}). When a pair of initial conditions (L_0, I_{A0}) results in a pair of end values, (L_y, I_{Ay}), that is far away from the initial condition, that coordinate on the diagram is coloured red and it is far away from a steady state. When the initial condition and end values are close together, that coordinate is coloured blue and it is close to a steady state. Mathematically, a steady state occurs when $L^* = \lim_{n\to\infty} L(nt_y) = \lim_{n\to\infty} L((n+1)t_y)$ and $I_A^* = \lim_{n\to\infty} I_A(nt_y) = \lim_{n\to\infty} I_A((n+1)t_y)$. That is, $L_0(n) = L_0(n+1)$ and $I_{A0}(n) = I_{A0}(n+1)$.

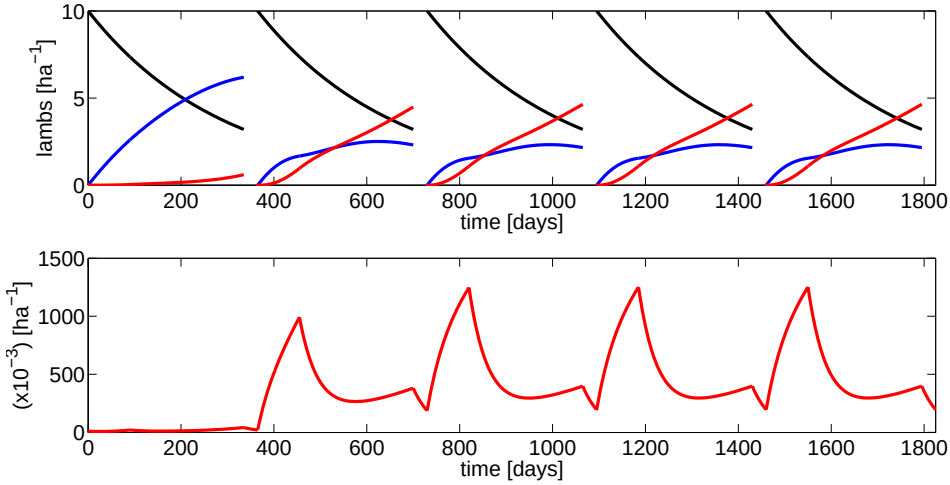

Figure 3.33: *Numerical solutions to sheep model D. Density of immune, susceptible and infectious lambs (top), and density of free-living leptospires in field one (bottom), all over time (days). Immune lambs shown in black. Susceptible lambs shown in blue. Infectious lambs shown in red.*

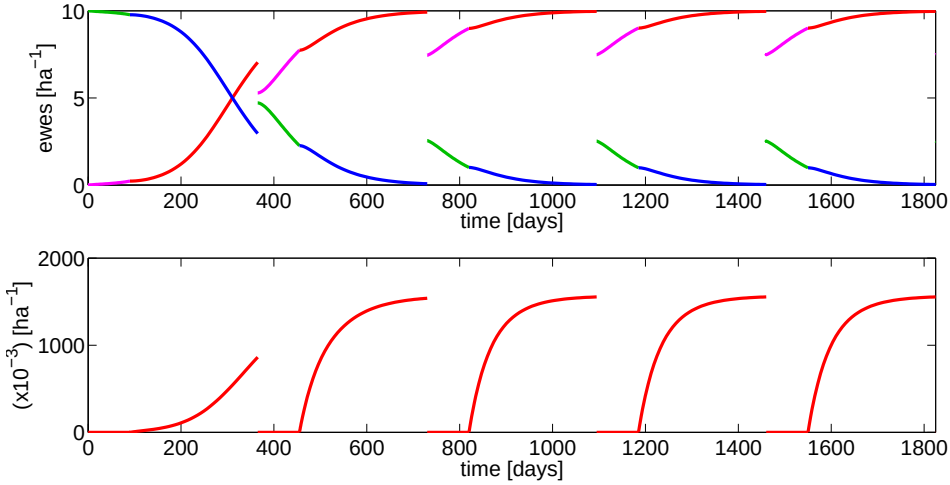

Figure 3.34: *Numerical solutions to sheep model D. Density of susceptible and infectious ewes in field one and two (top), and density of free-living leptospires in field two (bottom), all over time (days). Susceptible ewes while in field one shown in green. Susceptible ewes while in field two shown in blue. Infectious ewes while in field one shown in purple. Infectious ewes while in field two shown in red.*

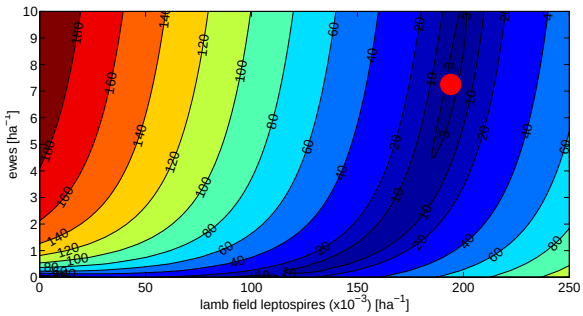

(a) *Cobweb heat map using* $\rho = 0.02381$ day^{-1} *showing the trivial fixed point and a non-trivial fixed point.*

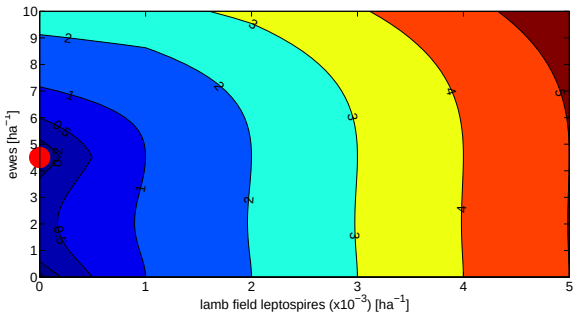

(b) *Cobweb heat map using* $\rho = 0.5$ day^{-1} *showing the trivial fixed point and a quasi-trivial fixed point.*

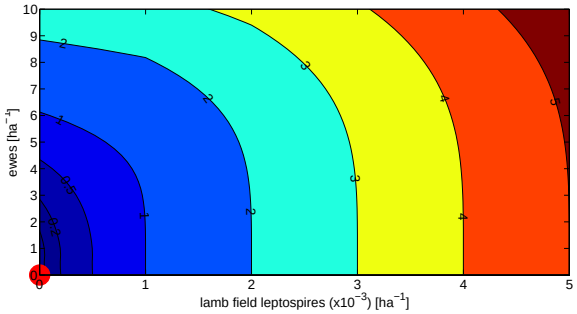

(c) *Cobweb heat map using* $\rho = 1$ day^{-1} *showing only the trivial fixed point.*

Figure 3.35: *Cobweb heat maps for sheep model D using different values of* ρ.

As seen in figures 3.35a, 3.35b and 3.35c, using different leptospire death rates, ρ, produces different types of fixed points. Figure 3.35a shows a unique, non-trivial fixed point as well as a trivial fixed point. Figure 3.35b has a trivial fixed point as well as a quasi-trivial fixed piont. That is, when $\rho = 0.2$ day^{-1}, the system reaches a limit cycle where $L^* = 0$, but $I_A^* \neq 0$.

The quasi-trivial fixed point isn't a true trivial fixed point, as $L > 0$ for some time $nt_y < t < (n+1)t_y$. For a demonstration see figure 3.36, which shows the behaviour of ewes and leptospires in field one over time, when the quasi-trivial fixed point occurs. One can see that while $L = 0$ at $t = nt_y$, $L > 0$ elsewhere. Also, $I_A > 0$ and the behaviour of I_A over the course of the year remains the same from year to year.

Infectious ewes not only shed leptospires into the environment, but also become infectious from it. If this were not the case, the density of infectious ewes would decrease over time as the individual ewes are replaced at the end of the year.

It is not possible to reach a quasi-trivial fixed point where $L^* \neq 0$ and $I_A^* = 0$, as for $I_A^* = 0$ to occur, one must have either $I_A(t) = 0$ and $\dot{I}_A(t) = 0$, or $\dot{I}_A < 0$, for some t. $\dot{I}_A < 0$ is clearly never true and $\dot{I}_A = 0$ at $t = 0$ is possible only if $L_0 = 0$ and $I_A(0) = 0$.

Biologically, to have no infectious ewes at any point, one must either start with no infectious ewes and the ewes do not become infectious, which is not possible as there are free living leptospires in the field, or for ewes to lose infectiousness, which they do not.

Figure 3.35c shows a true trivial fixed point where both L^* and I_A^* are equal to zero.

Note that the contours of the heat maps are not smooth due to the discrete nature of the calculations for the populations studied.

3.4.5 Bifurcation

As this model deals with two initial conditions, the behaviour of the system can not be demonstrated using a single bifurcation diagram. To begin with, one can plot two bifurcation diagrams, one for L^* and another for I_A^*. See figure 3.37. Note that while the curves for both bifurcation diagrams are calculated discretely, the curve for the leptospire bifurcation diagram is fairly smooth, while the curve for the infectious ewe bifurcation diagram is not. This is due to the scaling of each population.

It should also be noted that after the removal of the host from the field, leptospires for all models decay exponentially. This behaviour is accentuated in the current model due to the carriage state in the host population, where infectious ewes are carried over from one year to the next. The exponential decay of leptospires means that as long as the system begins with a positive initial condition, it will never actually reach zero. Thus, the bifurcations are not genuine bifurcations. Calculated bifurcation points are dependent on the arbitrarily chosen numerical tolerance used to distinguish between what is considered a trivial steady state and a non-trivial steady state. In this case, a tolerance of 0.25 ewes for the host and 1 unit of leptospires for the pathogen is used. The results are sensitive to these values, as one can see in figure 3.37, where L^* and I_A^* do not become trivial for simultaneous values of ρ. However, for practical purposes, as it is assumed that less than 1 unit of leptospires is insufficient for infection to spread and new parameters are defined to distinguish ρ_{crit} for L^* and I_A^*. Call ρ_{critL} the value at which L^* moves from the trivial fixed point to the non-trivial fixed point and ρ_{critI} the corresponding value for I_A^*. Here, $\rho_{critL} = 0.1206$ day^{-1}, while $\rho_{critI} = 0.8893$ day^{-1}. Now, the quasi-trivial fixed point is always of type $L^* = 0$, $I_A^* > 0$, so ρ_{critL} will never be larger than ρ_{critI}. The fixed point that occurs when $\rho_{critL} < \rho < \rho_{critI}$ is not a true trivial fixed point as is explained in section 3.4.4. Therefore, the true critical value for ρ is ρ_{critI}. That is, the value of ρ above which the infection truly disappears from the system is $\rho_{crit} = \rho_{critI}$.

3.4.6 Limit Cycle

Figure 3.38 shows the limit cycle of the system on the (L, I_J) plane. The proof of the existence of the limit cycle on this plane is just the same as

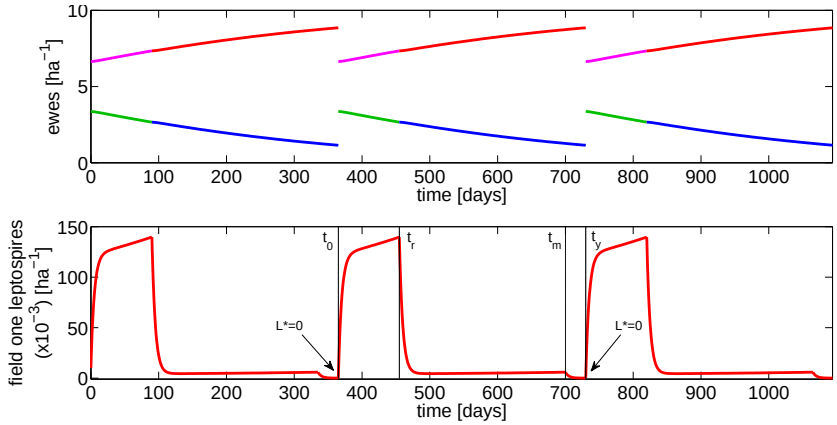

Figure 3.36: *Figure demonstrating the quasi-trivial fixed point for sheep model D. Density of susceptible and infectious ewes (top), and density of free-living leptospires in field one (bottom), all over time (days). Susceptible ewes while in field one shown in green. Susceptible ewes while in field two shown in blue. Infectious ewes while in field one shown in purple. Infectious ewes while in field two shown in red. Here,* $\rho = 0.2$ *day*$^{-1}$*. Note how* $L = 0$ *at* $t = 0$ *and* $t = t_y$*, but not for* $0 < t < t_y$*. Also,* $I_A > 0$ *for all* t*.*

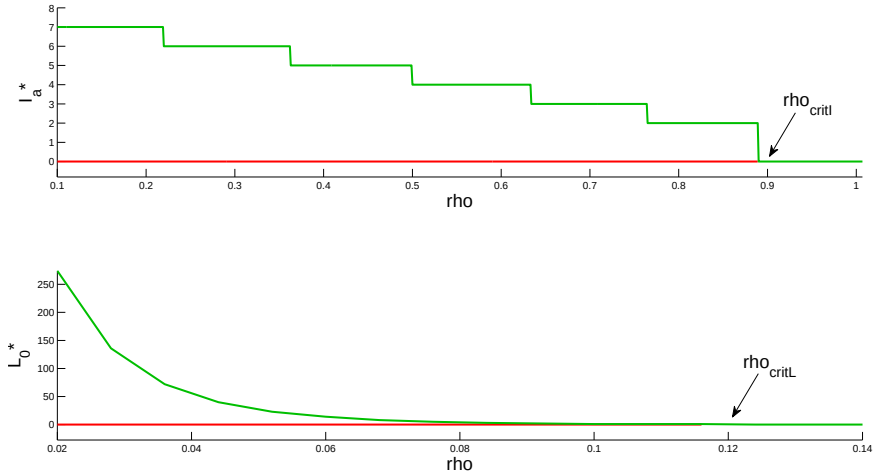

Figure 3.37: *Bifurcation diagrams for sheep model D showing the fixed points* L^* *and* I_A^* *as* ρ *is varied. For* $\rho > \rho_{critI}$*, the stable and only steady state is the trivial fixed point. For* $\rho_{critI} > \rho > \rho_{critL}$*, the quasi-trivial fixed point exists and for* $\rho < \rho_{critL}$ *the non-trivial fixed point exists. In this example,* $\rho_{critL} = 0.1206$ *day*$^{-1}$ *and* $\rho_{critI} = 0.8893$ *day*$^{-1}$*. Note the differing scales of the x-axis on the two graphs.*

the proof for model B (section 3.2), as the difference in this model is in the initial condition for the ewes. The shape of the trajectory in the first year of the limit cycle diagram is similar to that in model B (section 3.2). The behaviour of the trajectory during $0 < t < t_m$ in the remaining years, however, is slightly different. Here, the density of leptospires does not initially decrease as in previous models, but increase. This is due to the presence of infectious ewes in the field. The rate at which the ewes shed leptospires into the environment is enough to replace the leptospires that die off. After ewes are removed from the field, the behaviour of the trajectory follows a similar shape to that in part two.

Figure 3.39 shows the limit cycle diagram on the (L, I_J) phase plane for the quasi-trivial limit cycle.

The limit cycle can also be displayed on the (L, I_A) phase plane. See figure 3.40. The first year streamline, as seen in figure 3.41, behaves in a manner similar to the infectious lamb streamlines in model B (section 3.2). At the end of the first and subsequent years, however, the trajectory of the streamline no longer falls all the way down to the horizontal axis, as 75% of the infectious flock of ewes is carried over from one year to the next. This results in the fixed point for the limit cycle being in two dimensions.

The proof of the existence of a limit cycle in sheep model B (section 3.2) shows that there exists a $\rho_{crit} \in [0, \rho_\infty)$ such that $L_y(\rho_{crit}) = L_0$. This result is still relevant in the current model; however, it does not take I_A into consideration, as in the previous model this was reset to zero at the end of each year. The proof for the current model should include I_A, as part of the infectious ewe population is carried over from one year to the next. An attempt to prove such a result could be approached in a similar manner; however, nothing can be said about the relative sizes of $\dot{I}_A$ at the beginning of the year and $\dot{I}_A$ at end of each year once 25% of the population has been removed. As such, the proof of the limit cycle for this model relies on the proof of the limit cycle for sheep model B (section 3.2) and the fact that the system is "well behaved".

While the change in initial condition for the ewes in this model does cause the proof showing that $L_y(\rho)$ is monotonic decreasing to alter slightly from that in section 3.2, the proof remains almost identical and the limit cycle is still unique.

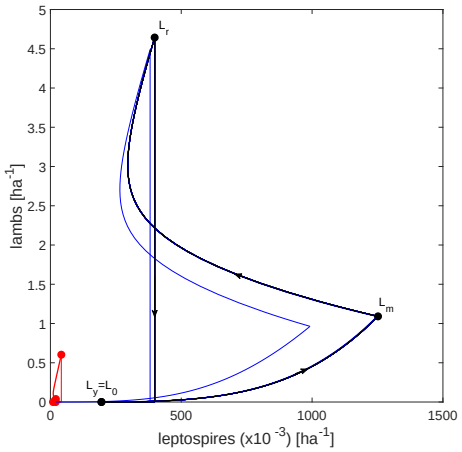

Figure 3.38: *Limit cycle diagram for sheep model D. Phase plane showing the relationship between field one leptospires and lambs. First year shown in red. Limit cycle shown in black. Intermediate years shown in blue.*

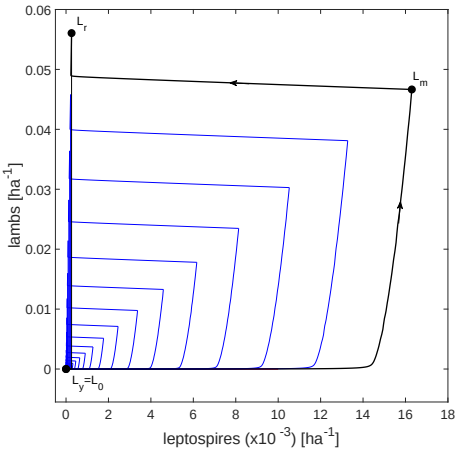

Figure 3.39: *Limit cycle diagram for sheep model D. Phase plane showing the relationship between field one leptospires and lambs. First year shown in red. Limit cycle shown in black. Intermediate years shown in blue. When $\rho = 0.2$ day^{-1} a quasi-trivial limit cycle occurs. This diagram shows that while the leptospire values at the beginning of each year may be zero, this is not always true for the remainder of the year.*

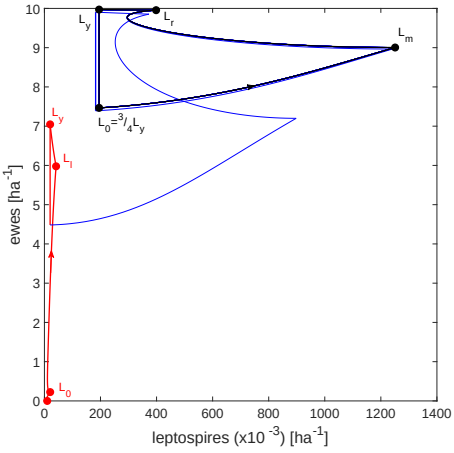

Figure 3.40: *Limit cycle diagram for sheep model D. Phase plane showing the relationship between field one leptospires and ewes. First year shown in red. Limit cycle shown in black. Intermediate years shown in blue.*

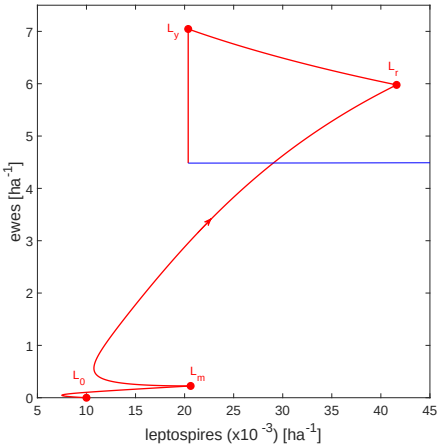

Figure 3.41: *Limit cycle diagram for sheep model D. Phase plane showing the relationship between field one leptospires and ewes. Magnification of first year streamlines.*

The Lyapunov exponent also remains negative. The calculations for this model use the same formula as is subsection 3.1.6; however, the initial condition for infectious ewes is equal to the steady state rather than being set to zero, that is, $I_{A0} = I_A^*$. Here the Lyapunov exponent is approximately equal to $\log_2 10^{-3}$, so the limit cycle is stable.

3.4.7 The Quasi-Basic Reproduction Number, R_L

The quasi-basic reproduction number for this model is just the same as for model C (section 3.3). This is due to the two models being the same, except for the initial conditions. It should be noted, however, that the threshold quantity for the bifurcation diagram for the current model does not result in a quasi-basic reproduction number equal to one. This is due to the inclusion of a carrier state in the model. The infectious ewes, which are carried over from one year to the next rather than being reset to zero at the beginning of each year, act as storage devices for the infection. This results in subcritical persistence of infection. That is, even if R_L is reduced below 1, infection may persist in the population. This is similar to systems with a carrier class for which there is subcritical persistence of infection as presented in [88].

3.4.8 Discussion

The final iteration of the sheep model includes the life cycle and farming practices implemented on New Zealand farms for both lambs and ewes. This model involves two initial conditions and as such heat maps are introduced in place of cobweb diagrams to demonstrate the occurrence of steady states. It is possible, in this case, for the system to reach a quasi-trivial steady state. This is observed in not only the graphs plotting the infectious populations over time, but also the heat maps and in a limit cycle diagram. The usual L^* vs ρ bifurcation diagram is now replaced with a I_A^* vs ρ bifurcation diagram. This is supported by the results of the quasi-basic reproduction number, R_L, which is calculated numerically.

Chapter 4

The Combined Model

The previous two chapters (chapter 2 and chapter 3) consider the spreading of leptospirosis in rats and sheep respectively, independently of one another. In reality, rats and sheep may share an environment, and hence pass leptospiral infection from one population to the other, and back. This chapter considers how rats may act as a reservoir of infection in sheep via a common environment. A variety of models from chapter 2 and chapter 3 are combined for this purpose.

The first model presented is a combination of the simplest rat and sheep models (section 2.1 and section 3.1 respectively) and considers only one environment, namely the field. The second model includes a second environment, the forest, which is occupied only by rats. The third and final model combines the most complex rat and sheep models (section 2.3 and section 3.4 respectively) in two field and one forest environment.

Holt et al showed that, in the absence of seasonal variation, their model for infectious rats and free living leptospires in Tanzania quickly reached a steady state [20]. The models in chapter 2 follow suit. As in the models in this chapter rats share an environment with sheep, whose population has periodic behaviour forced on it, one would expect both the infectious rat and the free living leptospire populations to exhibit periodic behaviour as well. This mimicry of the periodicity of one population by another is observed in the Holt model, with any population without seasonal trends following the behaviour of the population with seasonal trends. Here, the affect of the interaction of the populations in the models on the behaviour of the population dynamics of infectious rats over time is examined.

The Model

In each model, a pasture containing a flock of sheep is assumed to border with New Zealand native forest. Along with infection of the environment via the usual means covered in chapter 3, the field becomes contaminated with leptospires shed by rats. This is assumed to occur at night when the rats enter the pasture to access the water trough provided for the sheep. Rats become infectious with leptospires shed into the field by both sheep and rats, and in the models in section 4.2 and section 4.3, by rat-shed leptospires in the forest.

Due to New Zealand's temperate climate sheep are grazed predominately on pasture without being housed indoors during winter [89, 90]. Leptospiral infection via supplementary feed contaminated with the urine of infectious rats may be possible; however, this only occurs for a short period in the year, if at all, and as such is ignored here [91]. The water trough may provide another transmission route to both sheep and rats, as the rats may shed into it. Leptospires shed into water will theoretically survive indefinitely; however this consideration is not covered here and any infection transmitted from the water supply is grouped together with "environmental transmission". As such, the main route of infection from rats for sheep is assumed to be via the environment.

Climate change is considered as a driving force of infection in the models in this chapter. A report by the New Zealand Ministry of Health found that there was a 300% increase of human leptospirosis cases in New Zealand in 2017, with two thirds being attributed to storms and flooding [92]. Increased rainfall has been shown to increase breeding in mice in Australia due to increased food supply, and precipitation levels are known to influence leptospiral death rate [93]. Therefore, the effective birth rate of rats (in the single age class rat model this is in fact the maturation rate) and the leptospire death rate, ρ, are used as parameter values exploring the possible effects.

Data and Parameter Values

New Zealand has three species of rat; the ship rat (*Rattus rattus*), the Norway rat (*Rattus norvegicus*), and the kiore (*Rattus exulans*). As kiore are neither common, nor found on mainland New Zealand, they are ignored here [94–96]. The Norway rat and black rat are fairly similar in terms of behaviour and so are grouped together in the models presented. The ship rat is distributed fairly uniformly around the country, whereas the spread of the Norway rat is patchy, but often present on farms [26]. Where differences in behaviour do occur, data for the ship rat are given preference as it is more common than the Norway rat.

Measuring rat densities is both time consuming and possibly not particularly accurate. Rat densities, particularly in forests, can vary widely depending on season and environment [26]. As this study focuses on rats in a farming environment, it is assumed that densities are constant. This dovetails nicely with the total rat population in section 2.1 reaching a steady state. Rat densities on islands and forests in New Zealand range from two to 50 rats per hectare [22, 26]. However, it is known that rats can develop large social groups with up to sixty members [24]. Shapira, in her thesis suggested that a population density of 13 Norway rats per hectare is very high [97]. Rat densities are calculated based on the steady states for each independent rat model and depend on various parameter values discussed below.

The birth rate in the literature for the Norway and ship rats is highly variable, with averages ranging from as low as 5.6 pups per female per year, to as many as 72 [23, 26, 27, 98]. This equates to a rate of between 0.01534 and 0.1973 pups per female per day, or between 0.007671 and 0.09863 pups per rat per day, assuming an evenly split gender ratio in the population, and that all adult females are breeding. Values of 0.04603 pups per rat per day for mast years and 0.02360 pups per rat per day for non-mast years could also be chosen. Yet another option is to consider the proportion of rats breeding as a function of population density [28]. A roughly linear relationship was suggested by Blackwell et al with roughly 10% of the population breeding at high densities and 70% at low densities (10.8% for a population of 500 rats and 71.6% for a population close to zero) [28]. For simplicity, and as it is considered in the three age class rat model (section 2.3), the birth rate σ is considered to be constant here. It is assumed that all adult female rats are breeding. The birth rate is increased

when considering the impact of increased rain fall due to climate change on the model. Specific values are discussed on a case by case basis.

Both black rats and Norway rats usually survive for about one year, with annual mortality rate being between 90 and 99% [26, 27]. This is supported by another source claiming that less than 10% of rats will live for more than a year [22]. For this study, a survival time of one year, resulting in a mortality rate of $\mu = 0.0027$ day^{-1}, is chosen.

The serovars of most importance in humans in New Zealand are Hardjobovis, Pomona and Ballum [13]. A study of both urban and rural rats in the Waikato region found that 38.4% and 41.7% respectively were infected with at least two serotypes of leptospirosis, the most common being Copenhageni and Ballum. Both of the two main rat species were included in the study. Of the rats in the study, 39.4% had recently been infected and 33.1% were infectious [99]. Ship rats are a known maintenance host species for Ballum, while a significant proportion of a Norway rat population can be infected if there is a high rat population density [100, 101]. The same study failed to find Hardjo or Pomona in the rat populations and these are the serovars of most importance in livestock [68]. That is, the Waikato study found that the serovars infecting rats were not the same serovars infecting livestock. It may, however, be possible for common rat infecting serovars to host adapt to livestock, introducing a novel transmission route to humans [99, 102]. As such, for the combined livestock/rat model, the serovar of interest is Ballum.

Leptospire shedding rate in rats is calculated in a similar manner to that in sheep in chapter 3. In two studies, *Rattus norvegicus* shed leptospira at a concentration of $10^5 - 10^7$ per ml of urine, where the average weight of the rats was $80 - 110$g in one study and $150 - 190$g in the other [31, 49]. The first of these weight ranges is low in comparison to other sources, which state ranges of $170 - 270$g for Norway rats and $120 - 160$g for ship rats [23, 26]. Preference is taken for the weight range of the Norway rat in this instance, as this is the species specific to the study measuring leptospira in the urine. The data available for amount (in millilitres) of urine shed per 100g of body weight per day (3.3 ml/100g bwt/day) are also Norway rat specific [103]. An average rat weight of 170g is taken. This is the lower end of the range provided by King and the average of the weight range of the rats in the study measuring leptospira in the urine [26]. Then, each rat produces 5.61ml of urine per day (170g x

3.3ml/100g/day= 5.61ml/day). Multiplying this by the range of leptospira concentration per ml of urine results in a range of 5.61 x 10^5 - 5.61 x 10^7 leptospires shed per infectious rat per day. As in chapter 3, the leptospire shedding rate of rats is made to be less than this range. Chosen arbitrarily, $\alpha_R = 0.1$ day^{-1}.

The parameter values for H_S and H_R, the number of leptospires at which transmission rate from the environment is 0.5γ for sheep and rats respectively, are taken from Holt el. al., as are the values of the shape-parameter for density-dependence, c, and the environmental transmission coefficient, γ_R [20]. The environmental transmission coefficient and shedding rate for sheep, γ_S and α_S, are taken from section 3.1 and the leptospire death rate, ρ, and removal times of sheep from the pasture, t_r and t_m, are the same as in chapter 3.

4.1 Wildlife-Livestock Model

In the model presented in this section, the simple livestock (section 3.1) and simple rat (section 2.1) models are combined. Much of the model notation and structure is carried over from the previous models. N_R is the density of the total rat population, I_R is the density of the infectious rat population, I_S is the density of the infectious sheep population and L is the density of free living leptospires, all in a given area.

As in section 2.1, entry into the total rat population occurs at rate σe^{-cN_R} and departure occurs at rate μ, where σ is maximum maturation (effectively the birth rate), c is the shape parameter for density dependence in maturation and μ is the death rate. The total rat population is assumed to be at its steady state $N_R^* = \frac{1}{c}\log(\frac{\sigma}{\mu})$; however, figures involving rats begin at an arbitrary initial condition (for rats) to show the population reaching this steady state. Note also that the steady state value changes as the birth rate σ is varied when considering climate change. The equation for total rat population (equation 4.1) decouples from the infectious subsystem (equations 4.2-4.4, to be shown below).

$$\frac{dN_R}{dt} = \sigma e^{-cN_R} N_R - \mu N_R, \tag{4.1}$$

The equation describing the change in infectious rat population follows equation 2.2 in section 2.1, with rats becoming infectious via density dependent

sexual contacts at rate β and via environmental transmission γ_R, with non-linear saturation expressed in the term $\frac{L}{L+H_R}$. Here H_R is the density of leptospires at which the transmission rate to rats from the environment is $0.5\gamma_R$.

The non-linear saturation term is repeated in the equation describing change in the infectious sheep population (equation 4.2). Here H_S is the density of leptospires at which the transmission rate to sheep from the environment is $0.5\gamma_S$, where γ_R is the environmental transmission coefficient for sheep.

Leptospires are shed into the environment by infectious rats and infectious sheep, at rates α_R and and α_S respectively and die at rate ρ.

Note that parameters shared by both rat and sheep populations (total animal population, infectious animal population, environmental transmission coefficient, density of leptospires at which transmission rate to the population from the environment is half the environmental transmission coefficient and shedding rate) are distinguished with subscripts R and S for rats and sheep respectively.

The system can be described with the following set of differential equations:

The system before removal (phase one: $0 < t < t_r$),

$$\frac{dI_S}{dt} = \frac{\gamma_S(N_S - I_S)L}{L + H_S}, \tag{4.2}$$

$$\frac{dI_R}{dt} = \frac{\beta(N_R - I_R)I_R}{N_R} + \frac{\gamma_R(N_R - I_R)L}{L + H_R} - \mu I_R \tag{4.3}$$

$$\frac{dL}{dt} = \alpha_S I_S + \alpha_R I_R - \rho L. \tag{4.4}$$

The system after removal (phase two: $t_r < t < t_y$ and $N_S = I_S = 0$),

$$\frac{dI_R}{dt} = \frac{\beta(N_R - I_R)I_R}{N_R} + \frac{\gamma_R(N_R - I_R)L}{L + H_R} - \mu I_R$$

$$\frac{dL}{dt} = \alpha_R I_R - \rho L.$$

Description	Symbol	Value	Units
Density of the total rat population in a given area (the field)	N_R	26.1	ha^{-1}
Density of the susceptible rat population in a given area (the field)	S_R		ha^{-1}
Density of the infectious rat population in a given area (the field)	I_R		ha^{-1}
Density of the lamb population in a given area (the field)	N_S	10	SU ha^{-1}
Density of the susceptible lamb population in a given area (the field)	S_S		SU ha^{-1}
Density of the infectious lamb population in a given area (the field)	I_S		SU ha^{-1}
Density of the free living leptospires in the field ($\times 10^{-3}$) in a given area (the field)	L		ha^{-1}
Sexual transmission co-efficient (rat)	β	0.004713	day^{-1}
Environmental transmission coefficient for sheep	γ_S	0.02477	day^{-1}
Environmental transmission coefficient for rats	γ_R	0.005	day^{-1}
Density of leptospires ($\times 10^{-3}$) at which transmission rate from the environment is 0.5γ for sheep	H_S	10^3	ha^{-1}
Density of leptospires ($\times 10^{-3}$) at which transmission rate from the environment is 0.5γ for rats	H_R	10^3	ha^{-1}
Density of leptospires ($\times 10^{-3}$) shed per infectious sheep	α_S	1	day^{-1}
Density of leptospires ($\times 10^{-3}$) shed per infectious rat	α_R	0.1	day^{-1}
Shape parameter for density dependence in maturation for rats	c	0.04	
Maturation/birth rate for rats	σ	0.007671	day^{-1}
Death rate for rats	μ		day^{-1}
Per capita leptospire death rate	ρ	0.02381	day^{-1}
Time	t		days
Removal date of lambs	t_r	335	days
End of year	t_y	365	days

...Continuation of Table 4.1

Description	**Symbol**	**Value**	**Units**
Density of the free living leptospires ($\times 10^{-3}$) in a given area (field one) at $t = 0$	L_0	10	ha^{-1}

Table 4.1: *Parameters and initial conditions used for the wildlife-livestock model.*

4.1.1 Data and Parameter Values

The default rat birth rate, σ, is chosen in relation to the population density steady state for rats $N_R^* = \frac{1}{c}\log(\frac{\sigma}{\mu})$ (refer to section 2.1). For basic figures, to keep the total rat population steady state at an average feasible value, σ is set to 0.007671 day^{-1}. This is the lowest possible value for σ, as mentioned in chapter 4 and the resulting rat population steady state is 26.1 rats per hectare. When considering the impacts of climate change on the model, σ is set to its highest biologically feasible value of $\sigma_{max} = 0.09863$ day^{-1}. The population steady state then becomes 39.1 rats per hectare.

The value for the sexual transmission parameter value, β, used by Holt et. al. ($\beta = 0.01$ day^{-1}) results in undesired behaviour in the model. That is, the proportion of infectious rats out of the total rat population is much higher (76.62%) than observed in a Waikato study in which 33.1% of rats captures were infectious [99]. As such, the value of β is chosen as 0.004713 day^{-1}, which in the model involving rats only (section 2.1), using the parameter values in this section, results in behaviour in the rat population closer to that expected (33.11%). The environmental transmission coefficient, γ_R, could also have been chosen as the varying parameter in order to fit the model to the expected behaviour. This is the parameter chosen in the sheep model in chapter 3. The sexual transmission coefficient is chosen in place of the environmental transmission coefficient as the value used by Holt. et. al. is somewhat larger in terms of order of magnitude when compared to the remaining parameter values than the environmental transmission coefficient.

4.1.2 Numerical Results

As in the livestock models in chapter 3, the seasonal forcing on the sheep population (figure 4.1) causes fluctuations in the leptospire population (figure 4.2). This forcing impacts on the population dynamics of infectious rats as well (figure 4.3), causing oscillations in rat density over time which mirror those in the infectious sheep population. This implies that infection in sheep at least partially drives infection in rats and is confirmed by setting the shedding rate of the rats equal to zero (figure 4.4). In this case, the graphs for leptospires and lambs are the same as for the single age class lamb model (section 3.1); however, oscillations in the infectious rat population still occur despite rats no longer contributing to environmental infection.

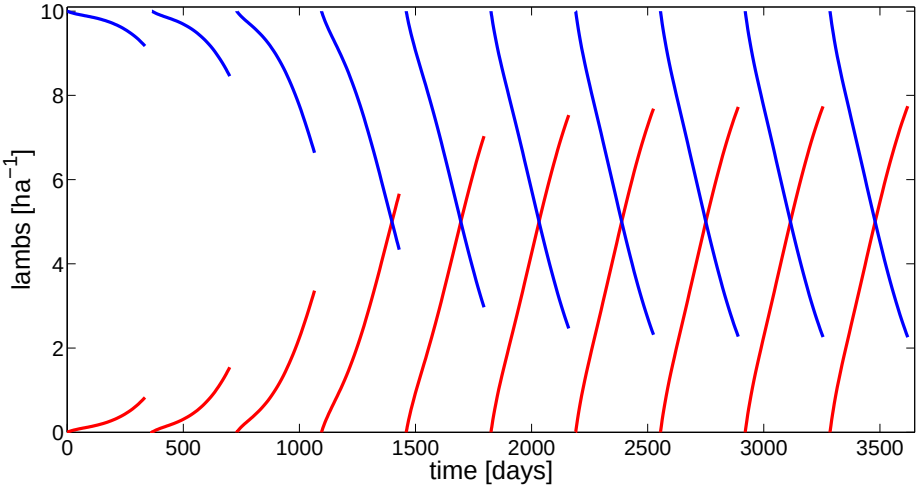

Figure 4.1: *Numerical solutions to the wildlife-livestock model. Density of susceptible and infectious sheep over time (days). Susceptible sheep shown in blue. Infectious sheep shown in red.*

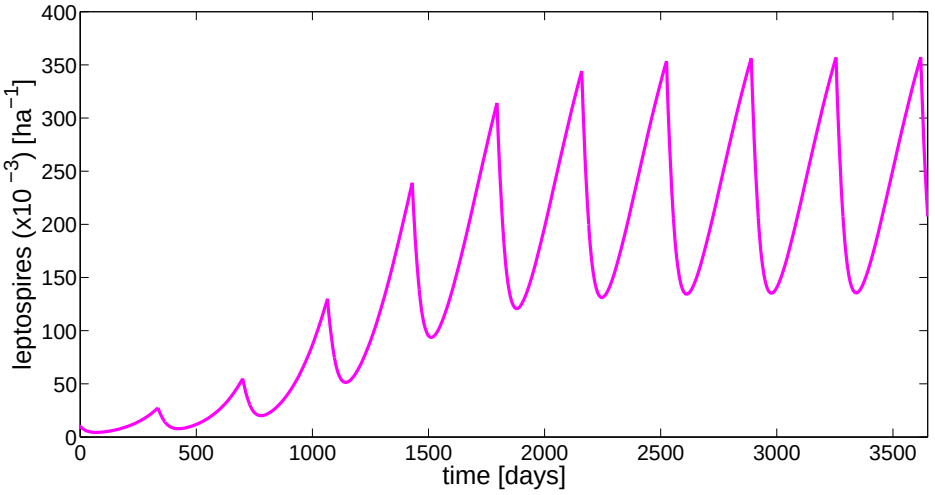

Figure 4.2: *Numerical solutions to the wildlife-livestock model. Density of free living leptospires over time (days).*

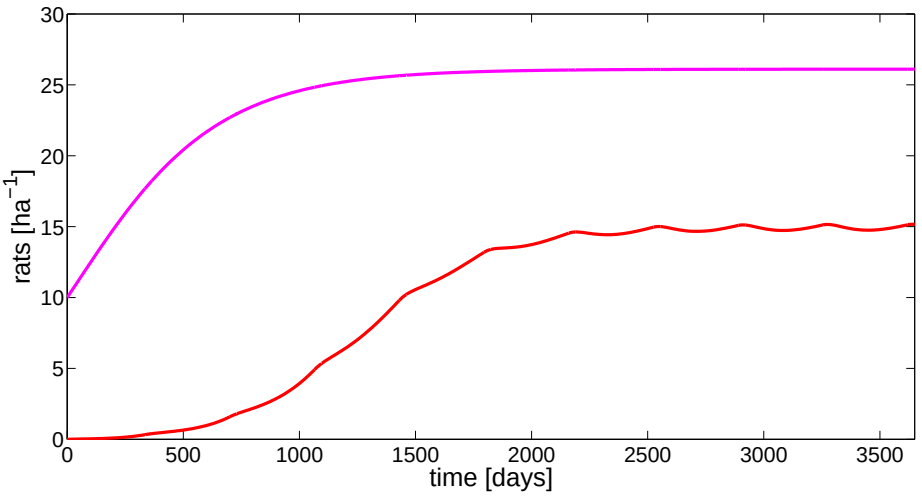

Figure 4.3: *Numerical solutions to the wildlife-livestock model. Density of rats over time (days). Total rats shown in purple. Infectious rats shown in red.*

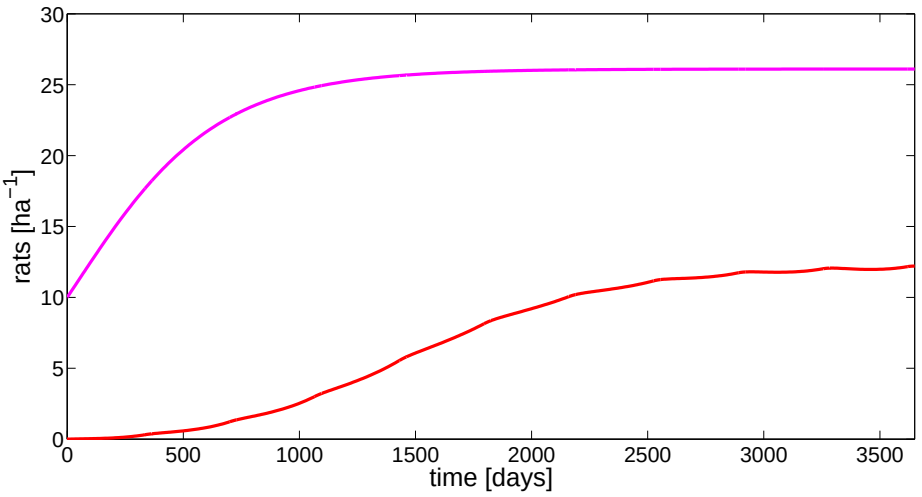

Figure 4.4: *Numerical solutions to the wildlife-livestock model. Density of rats over time (days). Total rats shown in purple. Infectious rats shown in red. All parameter values are as in Table 4.1, except for* $\alpha_R = 0$ *day*$^{-1}$.

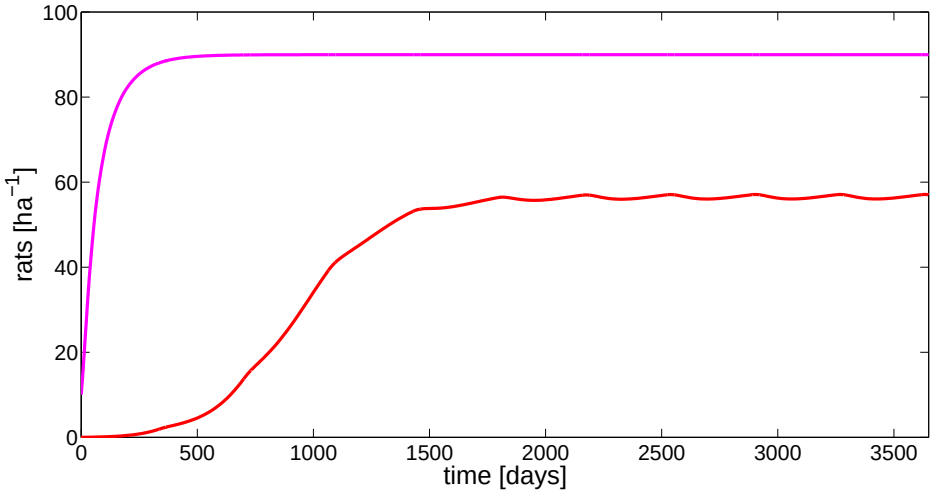

Figure 4.5: *Numerical solutions to the wildlife-livestock model. Density of rats over time (days). Total rats shown in purple. Infectious rats shown in red. All parameter values are as in Table 4.1, except for* $\sigma = 0.09863$ *day*$^{-1}$.

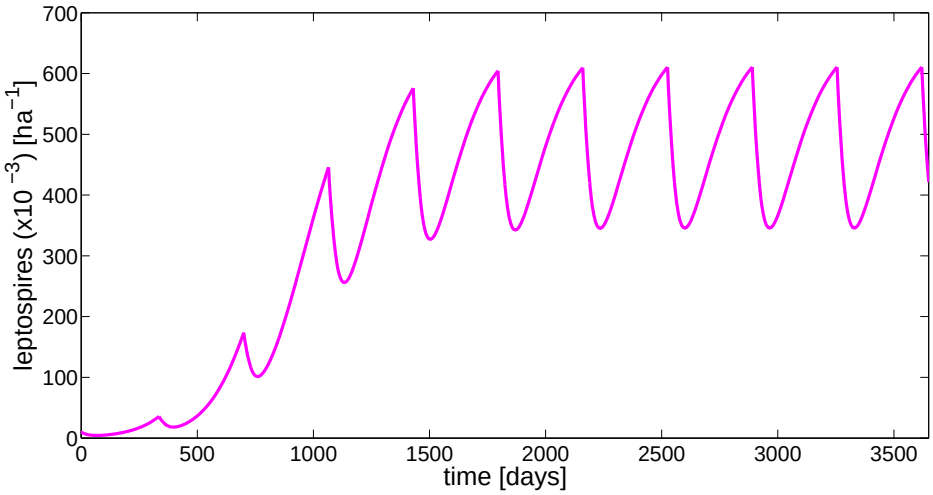

Figure 4.6: *Numerical solutions to the wildlife-livestock model. Density of free living leptospires over time (days). All parameter values are as in Table 4.1, except for* $\sigma = 0.09863$ *day*$^{-1}$.

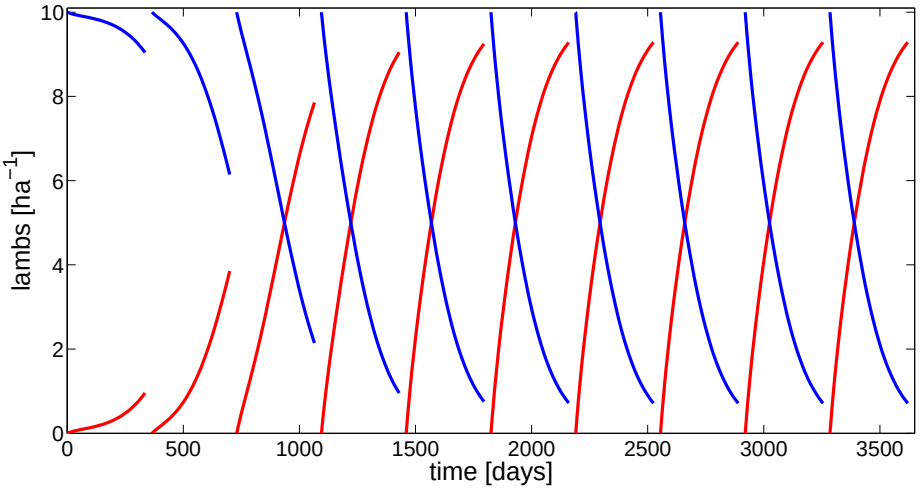

Figure 4.7: *Numerical solutions to the wildlife-livestock model. Density of susceptible and infectious sheep over time (days). Susceptible sheep shown in blue. Infectious sheep shown in red. All parameter values are as in Table 4.1, except for* $\sigma = 0.09863$ *day*$^{-1}$.

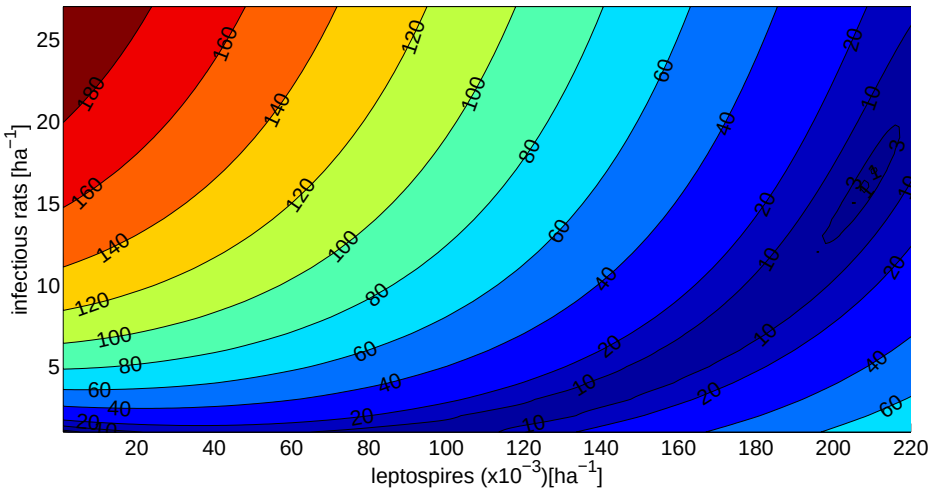

Figure 4.8: *Cobweb heat map for wildlife-livestock model showing the trivial fixed point and a non-trivial fixed point.*

Increasing the rat birth rate σ from 0.007671 to 0.09863 day^{-1} increases the total rat population steady state N_R^* from 26.10 to 89.95 rats ha^{-1} (figure 4.5). This increase in rat density increases the leptospiral load on the environment (figure 4.6) and subsequently the number of infectious lambs being sent to the slaughter house (figure 4.7). As this increase in birth rate is assumed to be due to an increase in rainfall, the leptospire death rate needs to be considered as well, and subsequently decreased. This exacerbates the increase of infection even further (figures not included).

4.1.3 Cobwebbing

As for sheep model D (section 3.4), plotting a cobweb diagram with initial conditions for free living leptospires only, results in a fixed point that doesn't line up with what is seen in the graphs plotting the various population densities over time (figures 4.1-4.3). The initial condition for total rat population density may be set to its steady state; however, the initial condition for the infectious rat population must also be considered. Thus, a heat map is used to display fixed points instead (figure 4.8). Let $L_0(n)$ be the leptospires initial condition, $L_y(n)$ be the leptospires end condition (that is, the density of leptospires at the end of the year), $I_{R0}(n)$ be the infectious rat initial condition and $I_{Ry}(n)$ be the infectious rat end condition, where n is a non-negative integer denoting the year. Then, a range of initial condition pairs $(L_0(n), I_{R0}(n))$ are used to calculate corresponding end condition pairs $(L_y(n), I_{Ry}(n)) = (L_0(n+1), I_{R0}(n+1))$. If the end condition co-ordinate is close to the initial condition co-ordinate, then it is close to a steady state and it is coloured blue. If it is far away, it is coloured red. Mathematically, a steady state occurs when $L^* = \lim_{n\to\infty} L(nt_y) = \lim_{n\to\infty} L((n+1)t_y)$ and $I_R^* = \lim_{n\to\infty} I_R(nt_y) = \lim_{n\to\infty} I_R((n+1)t_y)$. That is, $L_0(n) = L_y(n) = L_0(n+1)$ and $I_{R0}(n) = I_{Ry}(n) = I_{R0}(n+1)$.

4.1.4 Bifurcation

As two parameter values are varied in this model (ρ and σ), a heat map is used in place of a classical bifurcation diagram. For each of the infectious lamb (figure 4.11), infectious rat (figure 4.9) and leptospire (figure 4.10), populations, a heat map is plotted with the leptospire death rate, ρ, on one axis and the maturation/birth rate of rats, σ, on the other. The range of leptospire death rate used, $0.01 < \rho < 0.03$ day^{-1}, is carried over from

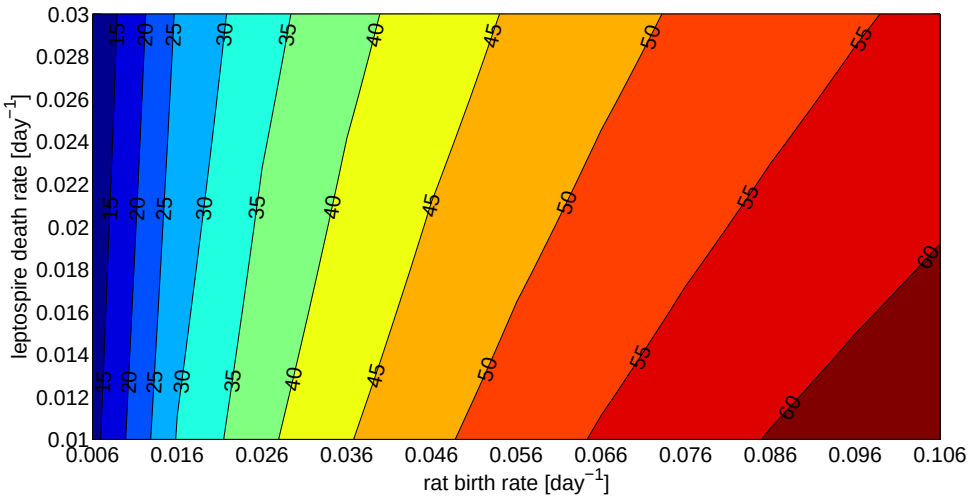

Figure 4.9: *Bifurcation heat map for the wildlife-livestock model showing fixed point values of infectious rats as* ρ *is varied from* 0.01 *to* 0.03 day^{-1} *and* σ *is varied from* 0.006 *to* 0.106 day^{-1}. *Note that no area of the heat map reaches zero.*

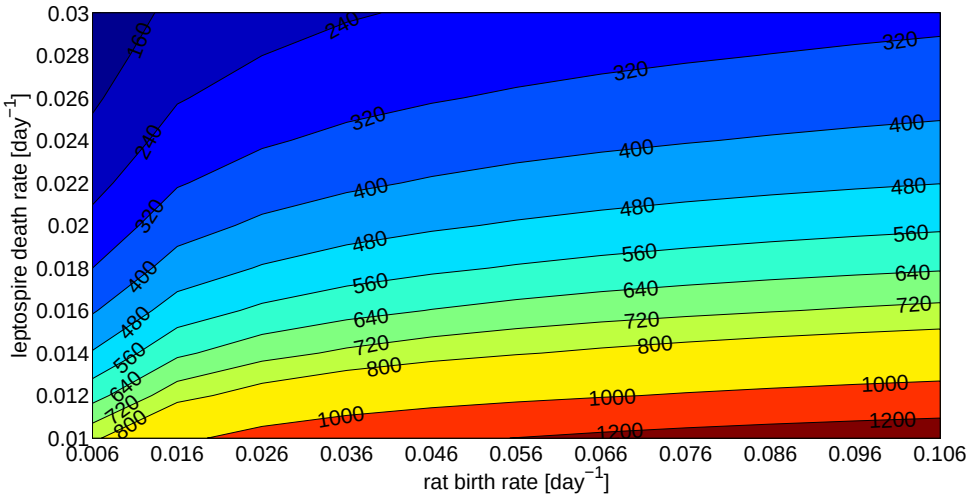

Figure 4.10: *Bifurcation heat map for the wildlife-livestock model showing fixed point values of leptospires as* ρ *is varied from* 0.01 *to* 0.03 day^{-1} *and* σ *is varied from* 0.006 *to* 0.106 day^{-1}. *Note that no area of the heat map reaches zero.*

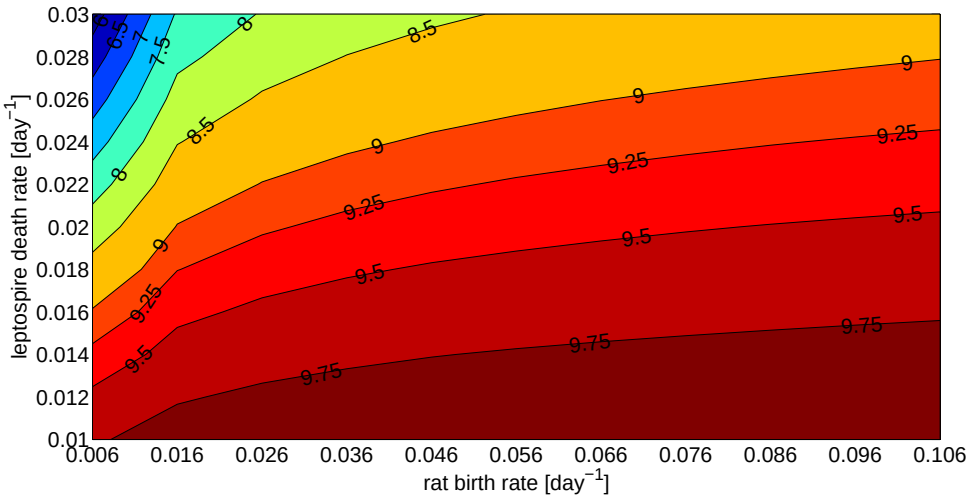

Figure 4.11: *Bifurcation heat map for the wildlife-livestock model showing fixed point values of lambs as ρ is varied from* 0.01 *to* 0.03 *day*$^{-1}$ *and σ is varied from* 0.006 *to* 0.106 *day*$^{-1}$*. Note that no area of the heat map reaches zero.*

section 3.1. The range for maturation rate is chosen from the literature, ranging from the lowest to the highest rates found, $0.007671 < \sigma < 0.09863$ day^{-1}. The size of each population at each coordinate of parameters is indicated by colour. Note that the trivial fixed point is not reached for any combination of the parameters ρ and σ considered. One can see that the topography of all three graphs is similar. That is, as the infectious rat population increases, so do the infectious lamb and leptospire populations.

4.1.5 Limit Cycle

The limit cycle for this model is three dimensional, and thus, the streamlines are displayed as projections. The projection of the limit cycle on the (L, I_S) phase plane (figure 4.12) is similar to those in previous models in chapter 3 (see subsection 3.1.6 for a detailed description of the behaviour of this projection of the limit cycle). The streamline projections on the (I_R, I_S) phase plane (figure 4.13) begin at the origin, as both host populations are assumed to be initially susceptible. Both populations increase in tandem until the time of removal, at which point the streamline falls to the x-axis as the lambs are removed from the system. The rat population continues to increase, moving along the x-axis for the remainder of the year. This process is repeated for the following year. The behaviour of the infectious

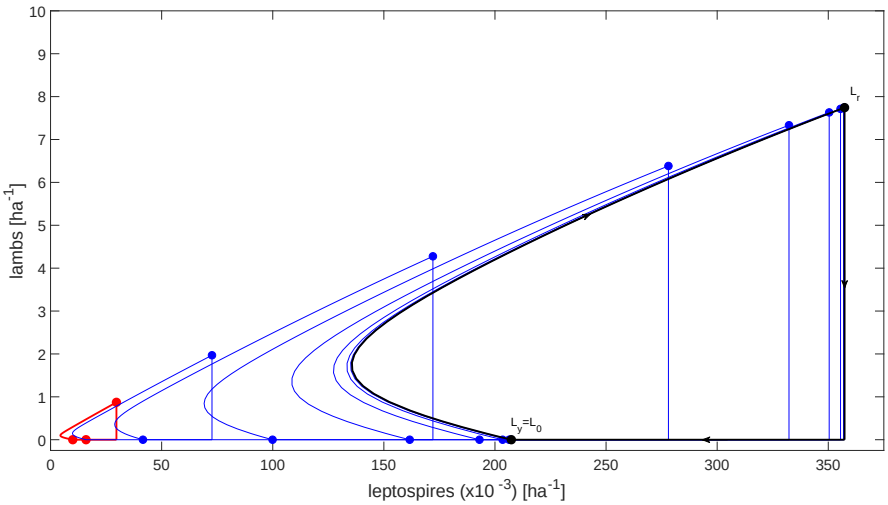

Figure 4.12: *Limit cycle diagram for the wildlife-livestock model. Phase plane showing the relationship between leptospires and lambs. First year shown in red. Limit cycle shown in black. Intermediate years shown in blue.*

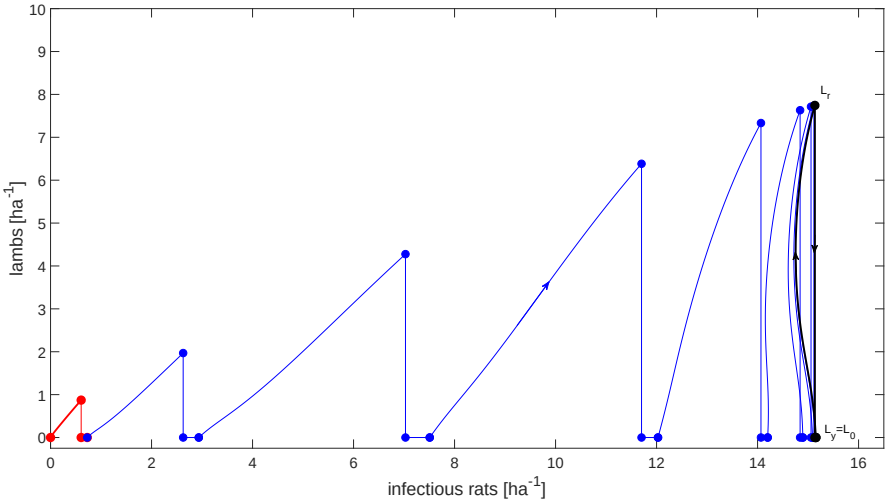

Figure 4.13: *Limit cycle diagram for the wildlife-livestock model. Phase plane showing the relationship between infectious rats and lambs. First year shown in red. Limit cycle shown in black. Intermediate years shown in blue.*

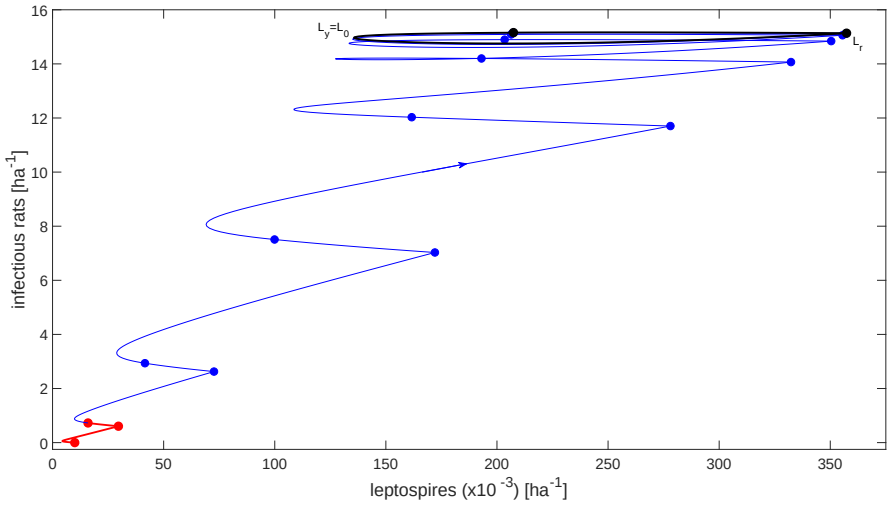

Figure 4.14: *Limit cycle diagram for the wildlife-livestock model. Phase plane showing the relationship between leptospires and infectious rats. First year shown in red. Limit cycle shown in black. Intermediate years shown in blue.*

Limit cycle diagram for leptospires and infectious rats.

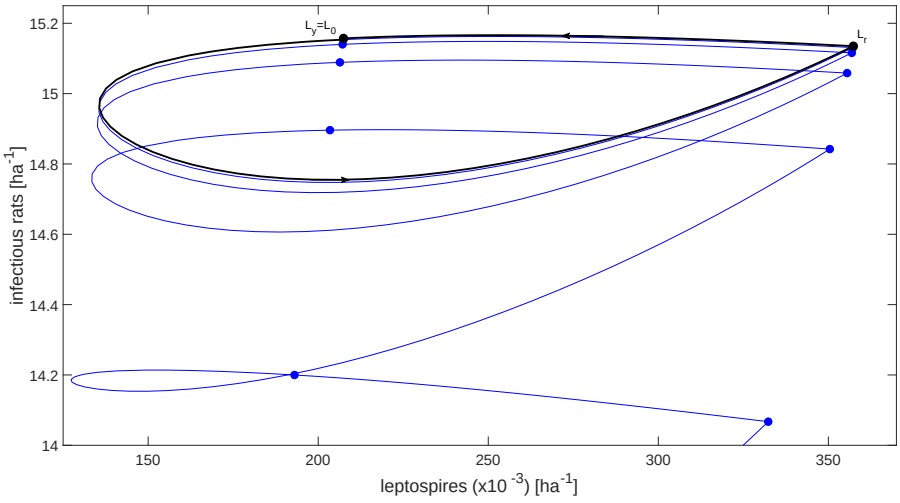

Figure 4.15: *Limit cycle diagram for the wildlife-livestock model. Phase plane showing the relationship between leptospires and infectious rats. Magnification of the limit cycle.*

sheep population (an increase followed by an instantaneous decrease to the x-axis) is repeated indefinitely. The increase in the infectious rat population however, is required to eventually slow down and reverse in order to allow the limit cycle to form. Once reached, the limit cycle begins at the bottom most node and a decrease in infectious rat numbers, followed by an increase, is observed. This behaviour is tied to that of the leptospires during the same time period (see figure 4.12). The number of infectious rats stays fairly constant between the time of removal of the lambs and the end of the year.

The (L, I_R) phase plane projections (figure 4.14) confirm many of the observations seen in the (L, I_S) phase plane. First, the number of infectious rats continues to increase until just before the formation of the limit cycle itself. It is then required to decrease in order for the limit cycle to form. Next, a magnification of the limit cycle (figure 4.15) shows that the height of the limit cycle streamline between the points labelled L_r and $L_0 = L_y$ doesn't change. This relates to the bottom node of the (I_R, I_S) limit cycle. The behaviour of the leptospire component of the streamline follows the same decrease and increase as described in subsection 3.1.6 for the sheep model limit cycles.

An exploration of the three dimensional limit cycle in Matlab confirms, as expected, that streamlines do not cross. Using the same formula as in subsection 3.1.6, with initial conditions for total and infectious rats set to their respective steady state values ($N_{R0} = N_R^*$ and $I_{R0} = I_R^*$), numerical calculations result in a negative Lyapunov exponent of the order of 10^{-4}, confirming that the limit cycle is stable.

4.1.6 Sensitivity

The sensitivity of the leptospire fixed point, L^*, can be examined by plotting it, and its rate of change with respect to the different population densities, against the chosen population. This is done by first calculating L^* over a range of animal densities. The rate of change of L^* is found simply by calculating the slope of the L^* graph at each point of animal density. That is, the rate of change displays how much L^* increases for each increase in animal density. Animal densities are allowed to range from 0 to 50 animals per hectare. As discussed at the beginning of this section, rat densities can reach up to 50 rats ha^{-1}, while stocking densities for sheep in New Zealand reach up to 25 SU ha^{-1} (see chapter 3).

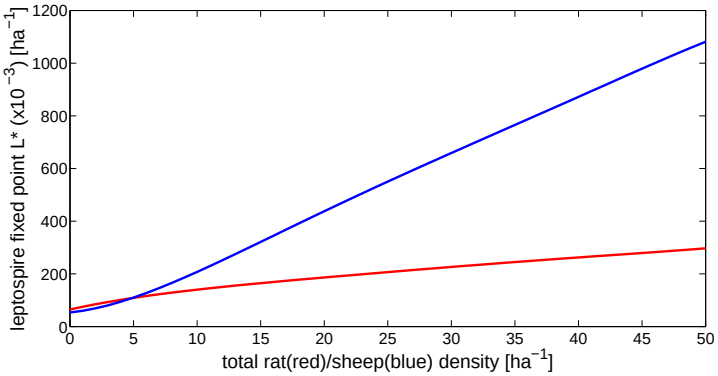

Figure 4.16: *Sensitivity of leptospiral fixed point for wildlife-livestock model by lamb (blue) and rat (red) density.*

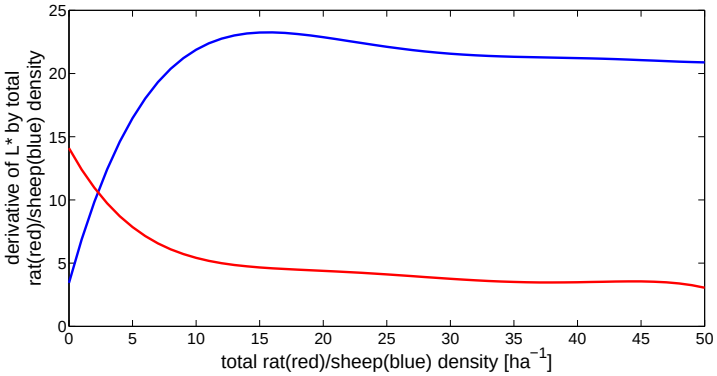

Figure 4.17: *Sensitivity of leptospiral fixed point for wildlife-livestock model by lamb (blue) and rat (red) density (derivatives).*

Figure 4.16 plots the leptospire fixed point, L^*, against densities for both rats (red) and lambs (blue). The densities are used independently of one another (ie. one is varied while the other is fixed at its default value). Clearly, increasing the population density of either animal increases the leptospire density as well. For animal densities above 5 animals ha^{-1}, an increase in lamb density results in a larger increase in the value of the leptospire fixed point than does an increase in rat density. For animal densities below 5 animals ha^{-1} the behaviour is reversed. That is, an increase in rat density results in a larger increase on the leptospire fixed point than does an increase in lamb density.

This behaviour is confirmed in figure 4.17, which plots the derivative of L^* with respect to each animal density, against the respective animal density. Clearly, the curve for lambs (blue), is greater than the curve for rats (red) for values greater than 2 animals ha^{-1}.

4.1.7 The Quasi-Basic Reproduction Number, R_L

The basic reproduction number of the system can be found by calculating the spectral radius of the next generation matrix, K. The next generation matrix can be found most easily by considering its biological interpretation, rather than by using the "recipe" involving the transmission and transition matrices as is used in chapter 2. The next generation matrix of the system is:

$$K = \begin{bmatrix} 0 & 0 & \frac{\gamma_S N_S}{H_S} t_S \\ 0 & \beta t_R & \frac{\gamma_R N_R}{H_R} t_R \\ \alpha_S t_L & \alpha_R t_L & 0 \end{bmatrix}$$

where t_S and t_R are the average times that sheep and rats are infectious respectively, and t_L is the average leptospire survival time. If the rate of change of infection in sheep were constant (ie. $\dot{I}_S =$ some constant), then the average times of infection above could simply be $\frac{t_r}{2}$. If the system were allowed to continue to infinity without interference by the removal of the lambs, each average time of infection could be replaced with the average death rate of the relevant population. In this case, the average times of infection can be calculated by solving the set of equations for the system (equations 4.2-4.4) linearised about the trivial fixed point. This would begin with the following equations:

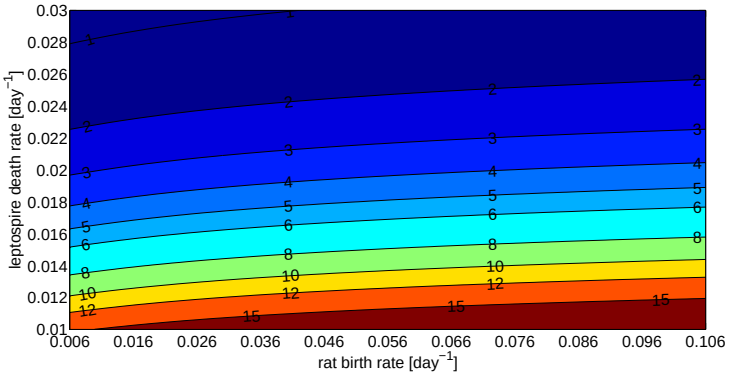

Figure 4.18: *Quasi-basic reproduction number heat map for livestock-wildlife model over a range of σ and ρ values.*

$$\frac{dI_S}{dt} = \frac{\gamma_S N_S L}{H_S}, \tag{4.5}$$

$$\frac{dI_R}{dt} = \beta I_R + \frac{\gamma_R N_R L}{H_R} - \mu I_R, \tag{4.6}$$

$$\frac{dL}{dt} = \alpha_S I_S + \alpha_R I_R - \rho L. \tag{4.7}$$

This is a linear system and so can be solved easily; however, the solution itself is not shown as it involves the solution to a polynomial of degree three, whose expression is somewhat complicated. Once a solution for the system before removal (equations 4.5-4.7) is found, it is used as an initial condition for the system after removal (only equations 4.6-4.7), to find the solution to the system overall. The spectral radius of the next generation matrix can then be calculated to find an analytical expression for the basic reproduction number. Here, however, the quasi-R_0 is calculated numerically using the same definition as is used previously in the thesis. That is,

$$R_L = \lim_{L_0 \to 0} \frac{L_y}{L_0}\bigg|_{I_J(0)=0, I_R(0)=0}.$$

This is plotted as a heat map using both the leptospire death rate, ρ, as well as rat maturation/birth rate, σ, as varying parameters (see figure 4.18). As in sheep model D (see subsection 3.4.7), there is subcritical persistence of infection, where infection in the system persists despite $R_L < 1$.

4.1.8 Discussion

This model combines the most basic of the rat and sheep models. It sets up the structure of the system and corresponding interaction of the two host species for the models that follow. Unlike the models in chapter 2 which borrow parameter values from the Tanzanian based model developed by Holt et. al, where possible, this model incorporates New Zealand specific parameter values for the rat population. As predicted, the rat population is shown to mimic the periodic behaviour forced onto the sheep. The effects of climate change on the rat birth rate and leptospire death rate, and subsequently on infection rates in the system, are explored and shown to be exacerbated with increased rainfall. The system requires the use of heat maps for both cobweb and bifurcation diagrams. It is shown that the behaviour of the bifurcation diagrams are coupled and reflect one another over a range of parameter values of ρ and σ. It is also noted that the trivial fixed point is not reached for any pair of parameter values ρ and σ, even ones outside a feasible region. Therefore, it is concluded that in a multi species system such as the one here, it is not possible to extinguish infection.

4.2 Field-Forest Model

The model in section 4.1 considers only one environment, namely the field. In this iteration of the model, the forest is also considered. The rats now not only shed into both the field and the forest, but can become infectious from both environments as well. The impact of the division of time spent in the various environments by the rats is explored and compared to the single environment model.

4.2.1 Model

In this model, the time rats spend foraging is divided between the field and the forest. As the field is open, unsheltered terrain, it is assumed that rats will spend as little time as possible there in order to protect themselves from predators such as domestic cats, which may venture onto the paddock from a nearby farm house, or wild predators such as feral cats, ferrets, stoats or weasels [104]. These predators will still be present in the forest, but it is assumed that rats are better able to avoid or protect themselves there. The division of time is indicated with a proportion, p, where p is the proportion of time spent in the field, while $1 - p$ is the proportion spent in the forest. The remaining components of the model are as in section 4.1.

The addition of an extra environment into the model results in the environmental transmission term for rats being divided into two; one for each of the two environments. Each term is weighted by the proportion of time spent by rats in each environment. The added environment also requires the introduction of an additional equation into the system for free living forest leptospires, L_2. Shedding of leptospires by rats is divided into the two environments in a similar manner as environmental transmission.

See the system of equations below:

The system before removal ($0 < t < t_r$),

$$\begin{aligned}
\frac{dI_S}{dt} &= \frac{\gamma_S(N_S - I_S)L_1}{L_1 + H_S}, \\
\frac{dI_R}{dt} &= \frac{\beta(N_R - I_R)I_R}{N_R} + \frac{\gamma_R p(N_R - I_R)L_1}{L_1 + H_R} + \frac{\gamma_R(1-p)(N_R - I_R)L_2}{L_2 + H_R} - \mu I_R \\
\frac{dL_1}{dt} &= \alpha_S I_S + p\alpha_R I_R - \rho L_1 \\
\frac{dL_2}{dt} &= (1-p)\alpha_R I_R - \rho L_2.
\end{aligned}$$

The system after removal ($t_r < t < 365$ and $N_S = I_S = 0$),

$$\begin{aligned}
\frac{dI_R}{dt} &= \frac{\beta(N_R - I_R)I_R}{N_R} + \frac{\gamma_R p(N_R - I_R)L_1}{L_1 + H_R} + \frac{\gamma_R(1-p)(N_R - I_R)L_2}{L_2 + H_R} - \mu I_R \\
\frac{dL_1}{dt} &= p\alpha_R I_R - \rho L_1 \\
\frac{dL_2}{dt} &= (1-p)\alpha_R I_R - \rho L_2.
\end{aligned}$$

4.2.2 Data and Parameter Values

Despite the default value of the leptospire death rate, ρ_0, being unlikely to reflect forest conditions, due to lack of forest specific data, the default death rate for leptospira in the forest is set to be the same as that on the pasture. For numerical analysis examining the behaviour of the system for varying leptospire death rate, only the leptospire death rate of the field is considered, with leptospire death rate in the forest remaining constant. This is under the assumption that environmental conditions in the field are likely

to change more rapidly than environmental conditions in the forest.

Due to lack of data available for approximating a proportion p of time spent by rats in the field, the arbitrary value of $p = 0.5$ is chosen for basic numerical results.

All remaining parameter values are carried over from section 4.1 (see table Table 4.1).

4.2.3 Numerical Results

The behaviours of the sheep, leptospire and rat populations over time (figures 4.19-4.21) are similar to those in section 4.1. The inclusion of the extra environment into the model divides the environmental exposure of rats to free living leptospires in two. The two environments differ in that one (the field) has leptospires introduced to it by two populations (both rats and sheep), whereas the other (the forest) has leptospires introduced to it by only one population (rats). As only the proportion of time spent by rats in the field is changed (decreased) as compared to section 4.1, one would expect the environmental load on the field to decrease, as a proportion $1 - p$ of the rats urine is shed into the forest. This is evident in figure 4.20, which displays free living leptospire numbers in both field and forest. The behaviour of the field leptospire population still exhibits the expected periodic behaviour. The forest leptospire population exhibits this behaviour too; however the oscillations are very small. Sheep are exposed to fewer free living leptospires when compared to section 4.1, as rats shed only the proportion p of their total urine into the field and the remainder into the forest. As such, the number of infectious sheep decreases. Rats also are exposed to fewer free living leptospires as when compared to section 4.1 as a proportion $1 - p$ of their time is spent in the forest, which excludes the burden of sheep shed leptospires. Consequently, the infectious rat population is also decreased as compared to section 4.1.

4.2.4 Proportion p

The figures in 4.22 plot population fixed points over the proportion of time spent by rats in the field, p. The populations of infectious sheep (figure 4.22a) and field leptospires (figure 4.22c) increase as p increases, while the population of forest leptospires (figure 4.22d) decreases. An interesting result should be noted in figure 4.22b. One might expect that the infectious

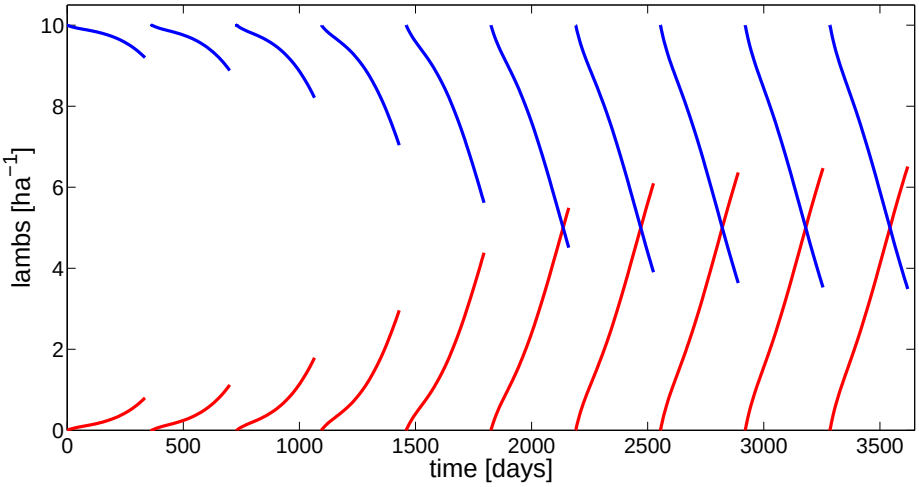

Figure 4.19: *Numerical solutions to the field-forest model. Density of susceptible and infectious sheep over time (days). Susceptible sheep shown in blue. Infectious sheep shown in red.*

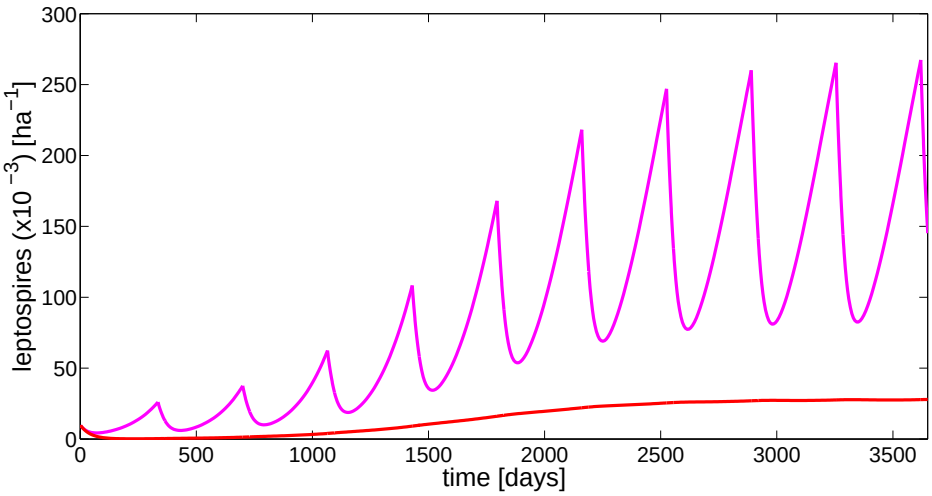

Figure 4.20: *Numerical solutions to the field-forest model. Density of free living leptospires over time (days).*

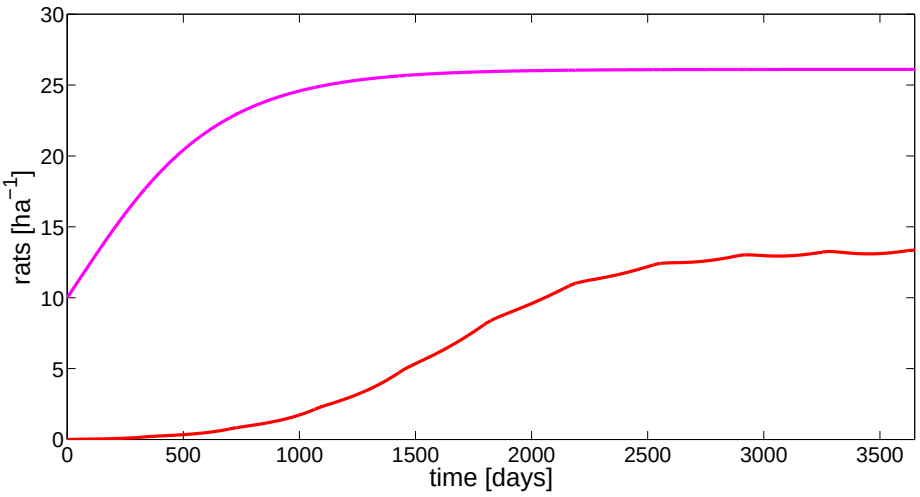

Figure 4.21: *Numerical solutions to the field-forest model. Density of rats over time (days). Total rats shown in purple. Infectious rats shown in red.*

rat population would increase as p increases due to increased exposure to free living leptospiral load; however, this is only true for $p > 0.07$, while the reverse is true for $p < 0.07$.

The shape of these graphs can be altered by varying various parameter values in the model. Leptospire death rate, ρ, and rat birth rate, σ, are the obvious choices for exploring parameter space as they relate well to climate change.

Figure 4.23b shows the curve for infectious rat fixed points with respect to p for default parameter values (black), as well as for $\sigma_{max} = 0.09863$ day^{-1} (red). Clearly, as expected, increasing σ increases the value of the fixed points. It also accentuates the parabolic nature of the curve and moves its minimum to the right. This means that as the birth rate of rats increases, the proportion of time needed for rats to spend in the field in order to minimise their infectious population increases.

An increase in σ increases the values of the other population fixed points as well (figure 4.23). Note that the curves of the sheep and field leptospire graphs meet at $p = 0$, while for the forest leptospire graph the curves meet at $p = 1$. This is due to the fact that at $p = 0$ the field and forest populations

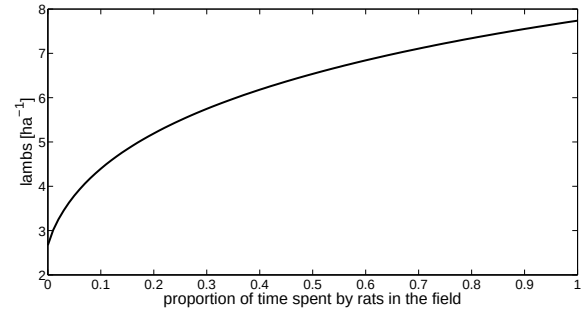

(a) *Lambs.*

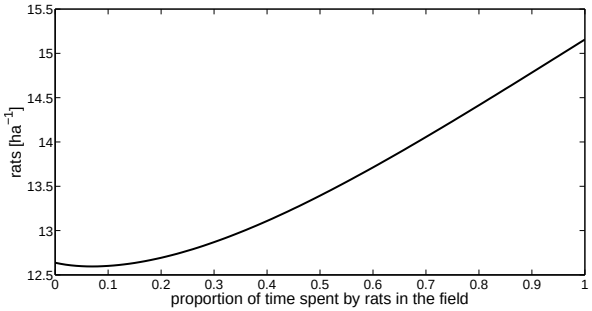

(b) *Infectious rats.*

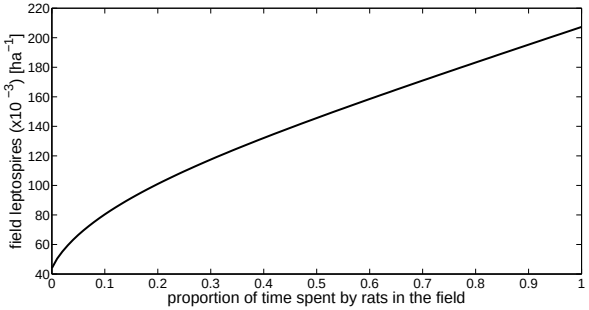

(c) *Field leptospires.*

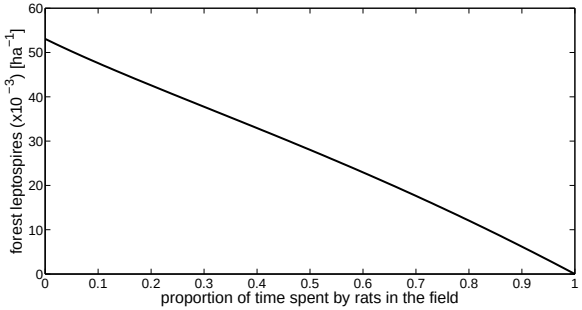

(d) *Forest leptospires.*

Figure 4.22: *Fixed points for the field-forest model as time spent by rats in the field is varied.*

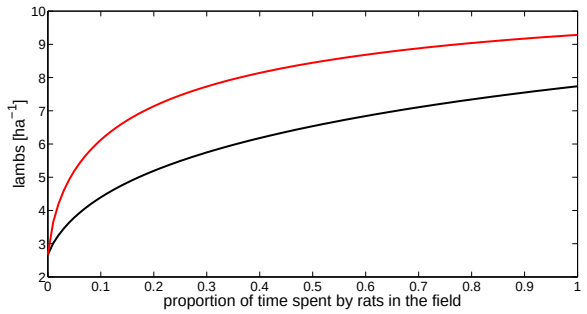

(a) *Lambs.*

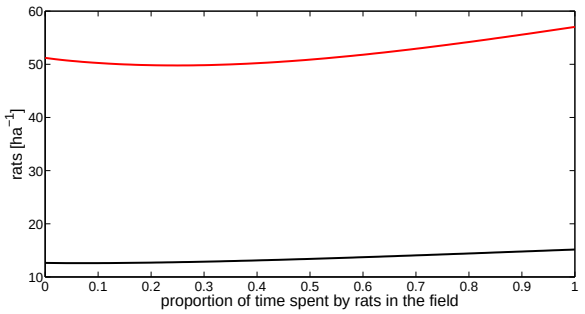

(b) *Infectious rats.*

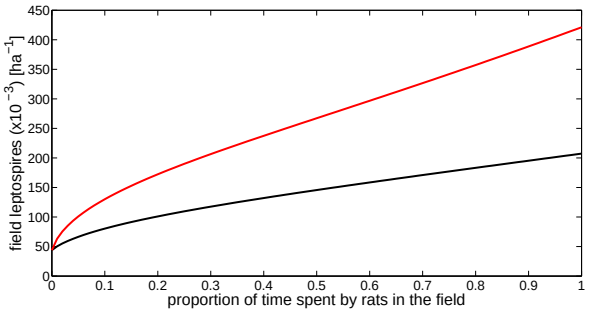

(c) *Field leptospires.*

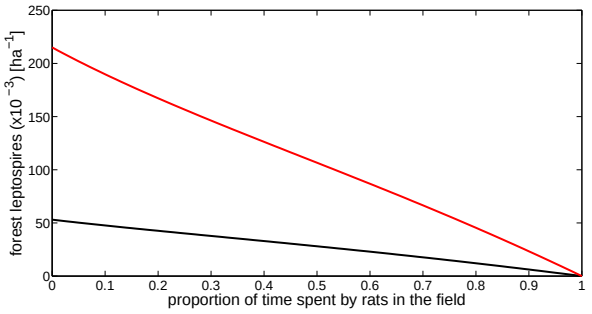

(d) *Forest leptospires.*

Figure 4.23: *Fixed points for the field-forest model as time spent by rats in the field is varied for* $\sigma = 7.671 \times 10^{-3}$ day^{-1} *(black) and* $\sigma = 0.09863$ day^{-1} *(red).*

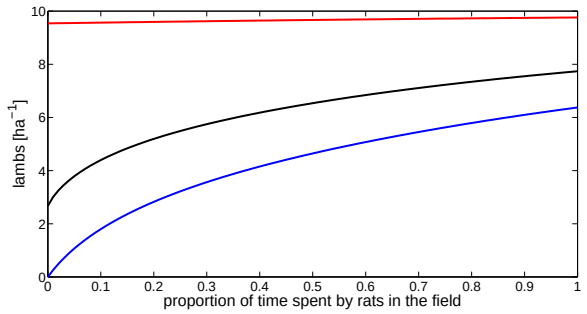

(a) *Lambs.*

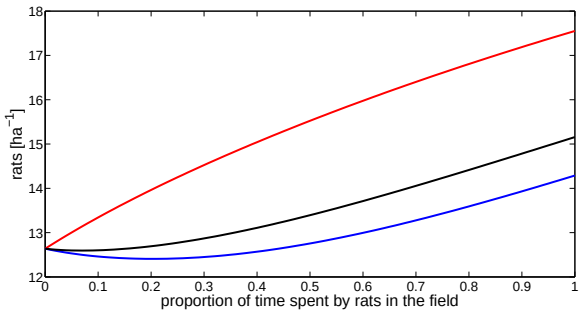

(b) *Infectious rats.*

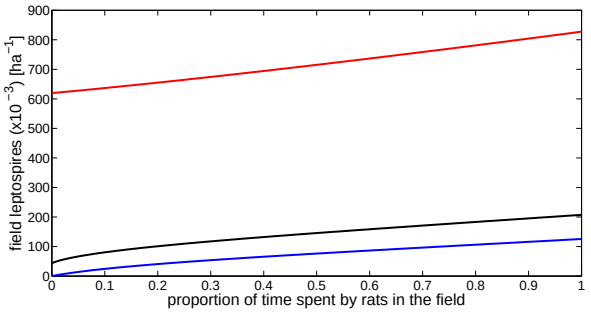

(c) *Field leptospires.*

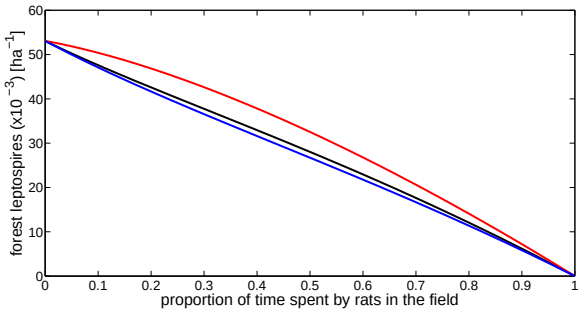

(d) *Forest leptospires.*

Figure 4.24: *Fixed points for the field-forest model as time spent by rats in the field is varied for* $\rho = 0.01$ day^{-1} *(red),* $\rho = \rho_0 = 0.02381$ day^{-1} *(black) and* $\rho = 0.03$ day^{-1} *(blue).*

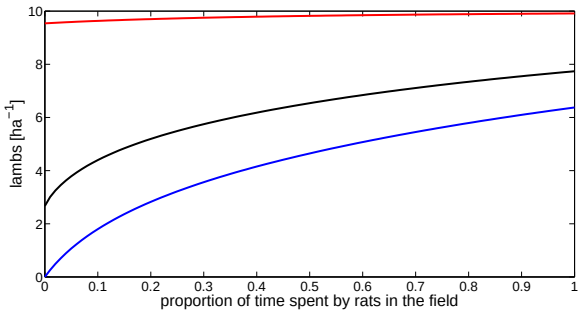

(a) *Lambs.*

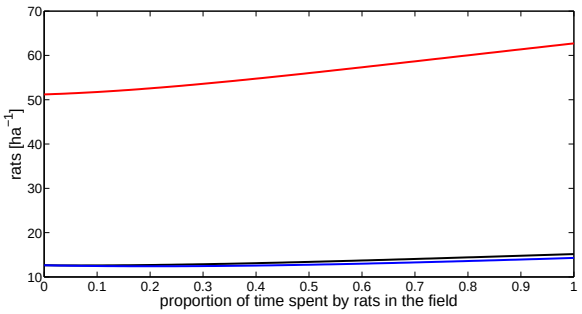

(b) *Infectious rats.*

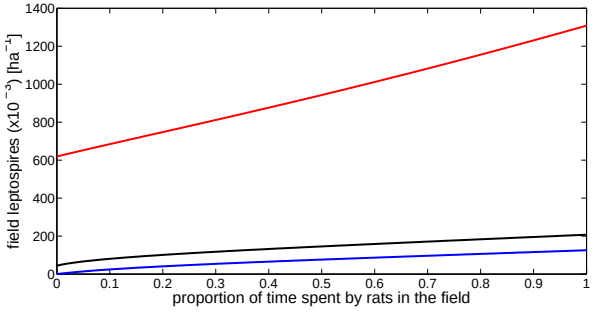

(c) *Field leptospires.*

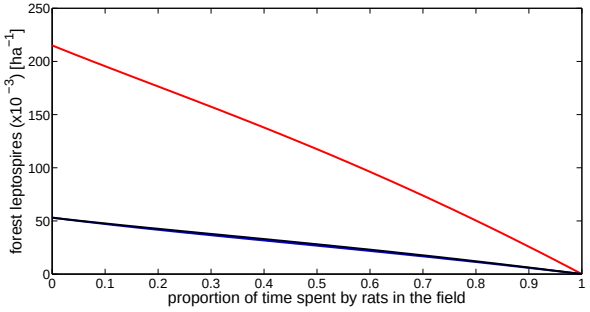

(d) *Forest leptospires.*

Figure 4.25: *Fixed points for the field-forest model as time spent by rats in the field is varied for* $\sigma = 0.007671$ day^{-1} *and* $\rho = 0.03$ day^{-1} *(blue), and* $\sigma = 0.09863$ day^{-1} *and* $\rho = 0.01$ day^{-1} *(red).*

decouple. No rats enter the field and as such their population has no affect on either the sheep or the field leptospire population. Similarly, when $p = 1$, the forest leptospire population decouples for the other populations. Rats spend all their time in the field and as such, their population has no affect on the forest leptospire population.

The figures in figure 4.24 show curves for varying values of ρ with default parameter values in black, $\rho = 0.01$ day^{-1} in red and $\rho = 0.03$ day^{-1} in blue. For field populations (sheep and field leptospires), decreasing ρ increases the height of the curve as well as reducing its slope.

In the forest populations (rats and forest leptospires), when the proportion of time spent by rats in the field if zero ($p = 0$), no changes occur in the infectious populations when varying ρ. Other than the above mentioned end points ($p = 0$ and $p = 1$), as in the field populations, decreasing the value of ρ increases the height of the curve. The curves also move from being concave down to concave up. In the graph for infectious rats, the smaller value of ρ results in a curve that is monotonic increasing.

Combining the changes of both σ and ρ parameter values (figure 4.25) to simulate possible climate change affects results in two extremes; σ is small and ρ is large ($\sigma = 0.007671$ day^{-1} and $\rho = 0.03$ day^{-1}) (blue curve) or σ is large and ρ is small ($\sigma = 0.09863$ day^{-1} and $\rho = 0.01$ day^{-1}) (red curve). The field population figures are more similar to the set of graphs varying ρ than they are to those varying σ, suggesting that in these populations the field leptospire death rate has a stronger affect on the behaviour of the model than the rat birth rate. The opposite is true for forest populations, as one may expect.

4.2.5 Bifurcation

As in section 4.1, bifurcation diagrams are presented as heat maps, with leptospire death rate, ρ, and rat birth rate, σ, used as the parameters of interest. Recall from subsection 4.2.2 that $p = 0.5$ unless specified otherwise. While the height of the contour lines of the bifurcation diagrams for infectious rats (figure 4.26). lambs (figure 4.29) and field leptospires (figure 4.27) changes between the two models, with lower values in the current model, the basic topography of the graphs remains the same. What is of interest is the bifurcation heat map for forest leptospires (figure 4.28). The topography of the heat map follows that of the infectious rat heat map

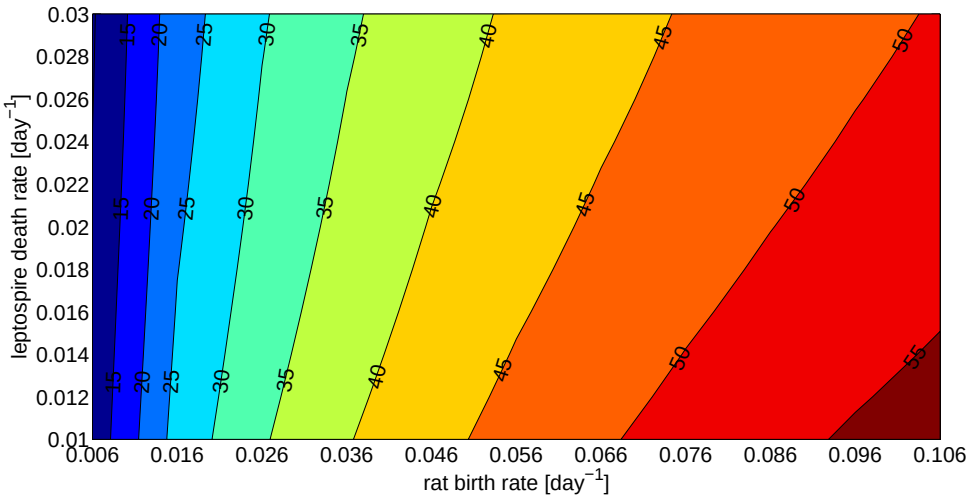

Figure 4.26: *Bifurcation heat map for the field-forest model showing fixed point values of infectious rats as ρ is varied from* 0.01 *to* 0.03 day^{-1} *and σ is varied from* 0.006 *to* 0.106 day^{-1}. *Note that no area of the heat map reaches zero.*

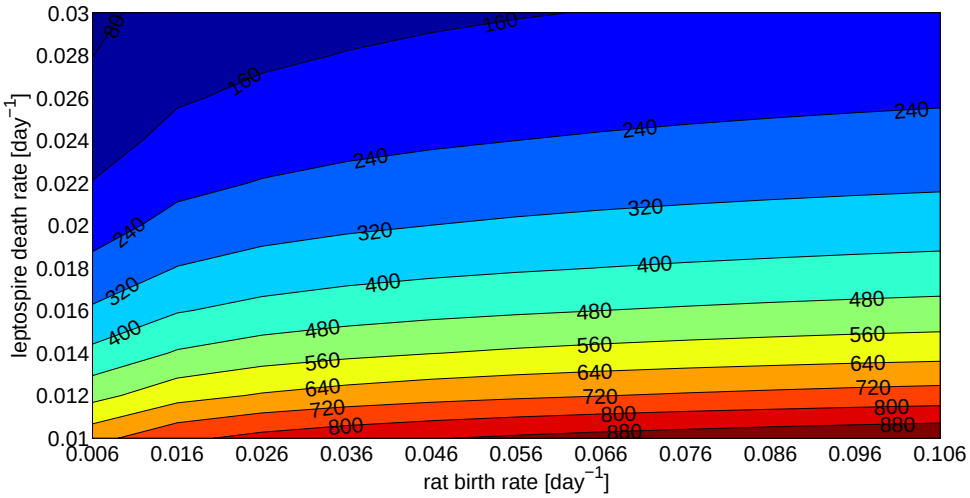

Figure 4.27: *Bifurcation heat map for the field-forest model showing fixed point values of field leptospires as ρ is varied from* 0.01 *to* 0.03 day^{-1} *and σ is varied from* 0.006 *to* 0.106 day^{-1}. *Note that no area of the heat map reaches zero.*

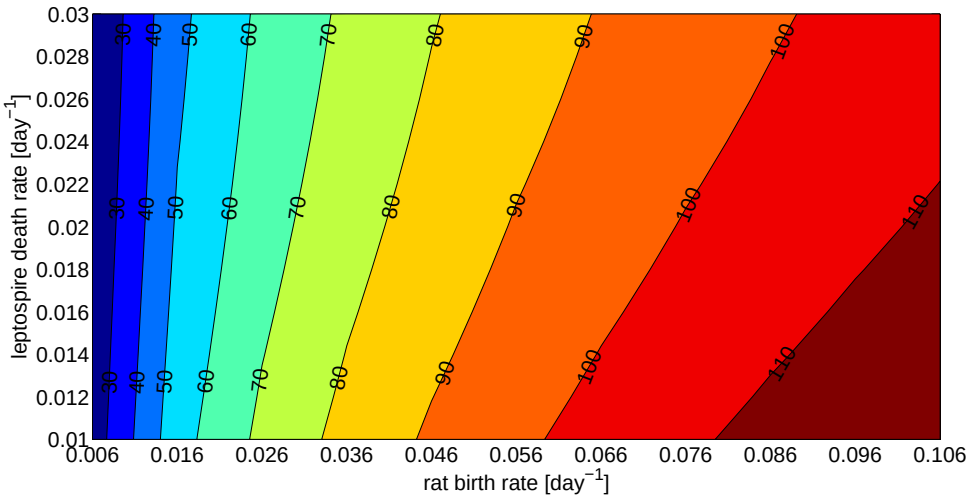

Figure 4.28: *Bifurcation heat map for the field-forest model showing fixed point values of forest leptospires as ρ is varied from 0.01 to 0.03 day^{-1} and σ is varied from 0.006 to 0.106 day^{-1}. Note that no area of the heat map reaches zero.*

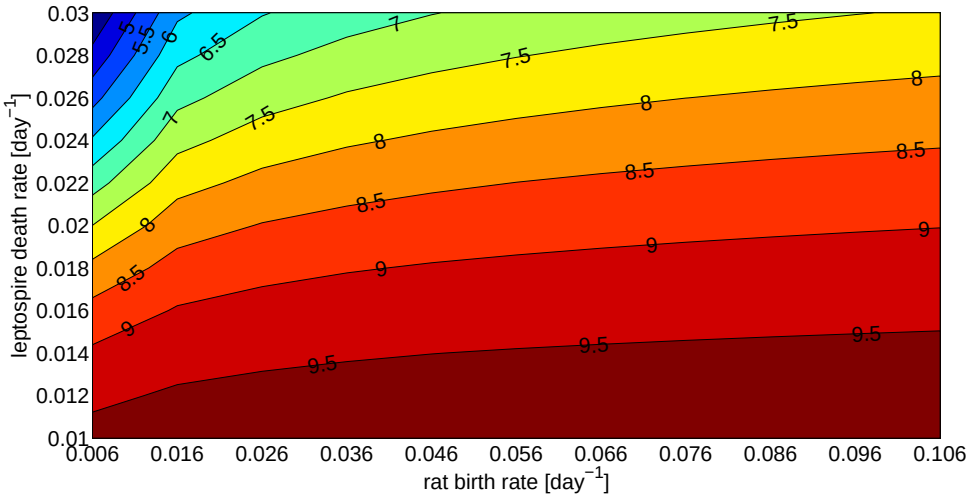

Figure 4.29: *Bifurcation heat map for the field-forest model showing fixed point values of lambs as ρ is varied from 0.01 to 0.03 day^{-1} and σ is varied from 0.006 to 0.106 day^{-1}. Note that no area of the heat map reaches zero.*

more closely than that of the field populations. This is to be expected, as the forest leptospire population is more closely related to the infectious rat population than it is to the field populations.

4.2.6 Limit Cycle

The limit cycle diagrams for the current model are similar to those in section 4.1 in shape; however, with smaller values (see figures 4.30-4.34). An extra limit cycle diagram examining the relationship between infectious rats and forest leptospires is added here to the analysis.

Figure 4.35 shows the streamlines of the system on the (L_2, I_R) phase plane. Colour coding of the graph is the same as in the rest of the thesis. The streamline begins at the system initial condition $(L_2, I_R) = (10, 0)$. As there are very few infectious animals (either rats or sheep) in the system, the number of forest leptospires rapidly decreases, almost reaching the origin. Before the end of the first year, however, an increase in the infectious rat population results in a bend in the curve, followed by subsequent increases in both infectious rat and leptospire populations. This increase initially follows a roughly linear trajectory; however, a small oscillation occurs in the streamline for the sixth year and a sharp corner is visible in the seventh year (see figure 4.36 for a magnification of the limit cycle and streamlines for the few years proceeding it). This corner occurs when $\dot{L}_1 = 0$, that is, when the field leptospires reach a minimum, and eventually results in a loop occurring in the streamlines. While the streamlines do appear to cross, this is not in fact the case as the populations in the phase plane (forest populations) work in tandem with the populations in the field via their mutual population, the rats. This loop eventually forms into the limit cycle, shown in black.

Using the same formula as in subsection 3.1.6, with initial conditions for total rats, infectious rats and forest leptospires set to their respective steady state values ($N_{R0} = N_R^*$, $I_{R0} = I_R^*$ and $L_{20} = L_2^*$), numerical calculations result in a negative Lyapunov exponent in the order of 10^{-4}, confirming that the limit cycles are stable.

4.2.7 The Quasi-Basic Reproduction Number, R_L

In the current iteration of the multi-species model, infection can enter the system via the environment from two different locations, the field or the forest. The next generation matrix below, where L_1 denotes the density of

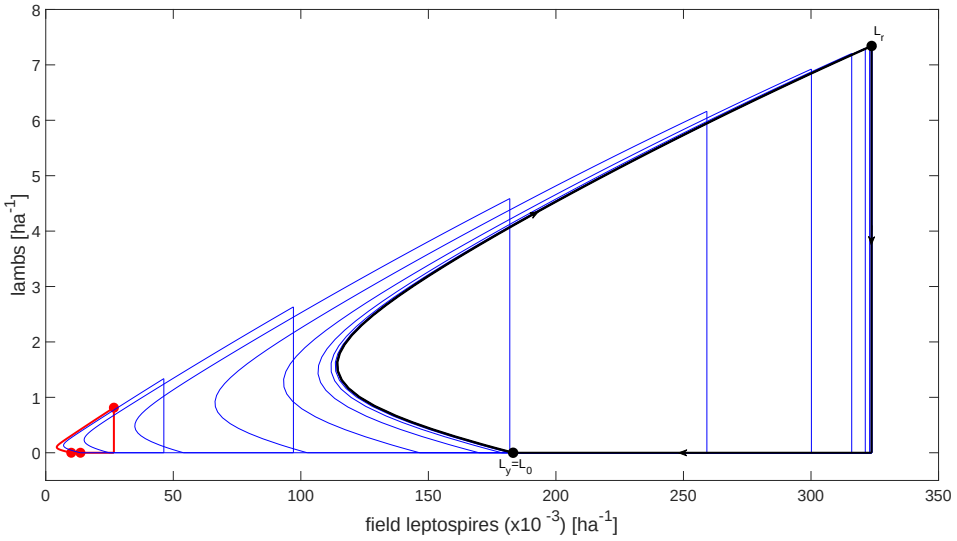

Figure 4.30: *Limit cycle diagram for the field-forest model. Phase plane showing the relationship between field leptospires and lambs. First year shown in red. Limit cycle shown in black. Intermediate years shown in blue.*

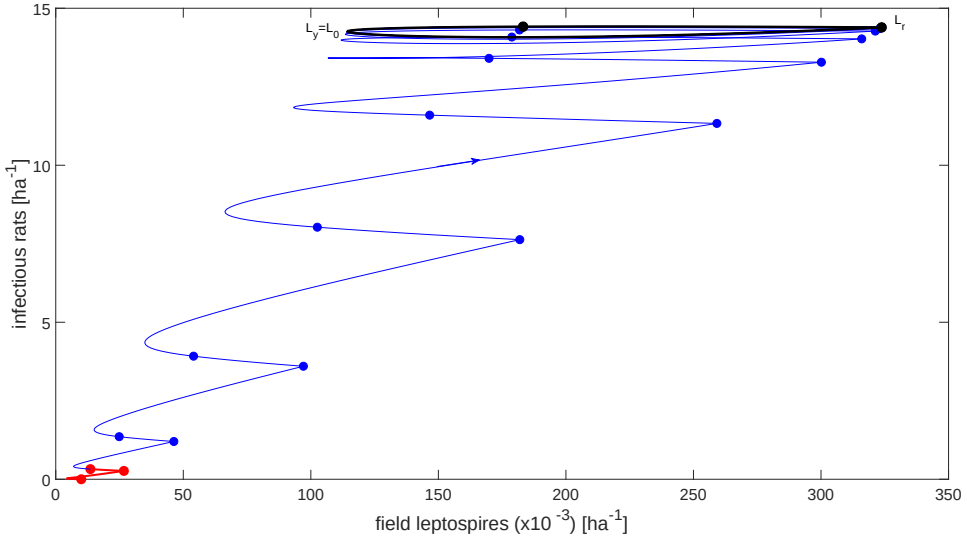

Figure 4.31: *Limit cycle diagram for the field-forest model. Phase plane showing the relationship between field leptospires and infectious rats. First year shown in red. Limit cycle shown in black. Intermediate years shown in blue.*

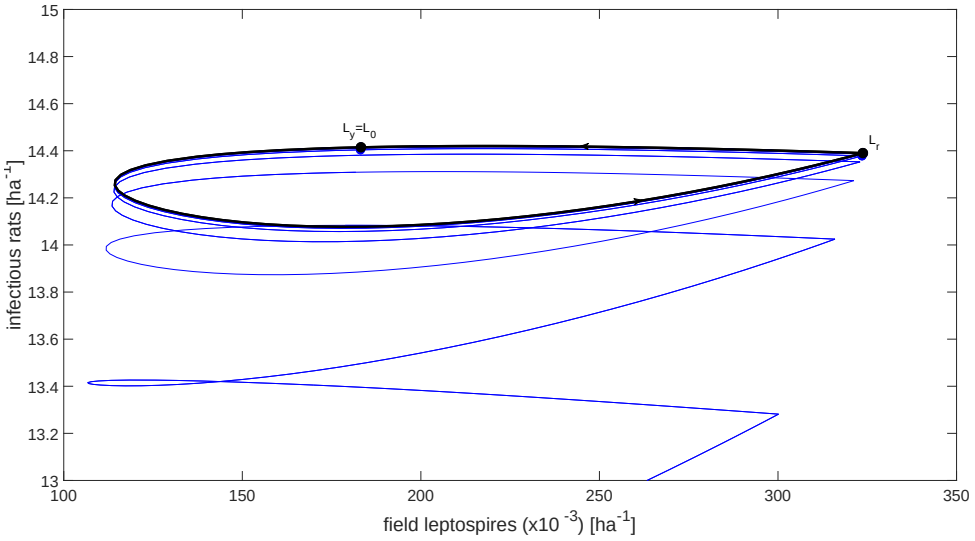

Figure 4.32: *Limit cycle diagram for the field-forest model. Phase plane showing the relationship between field leptospires and infectious rats. Magnification of the limit cycle.*

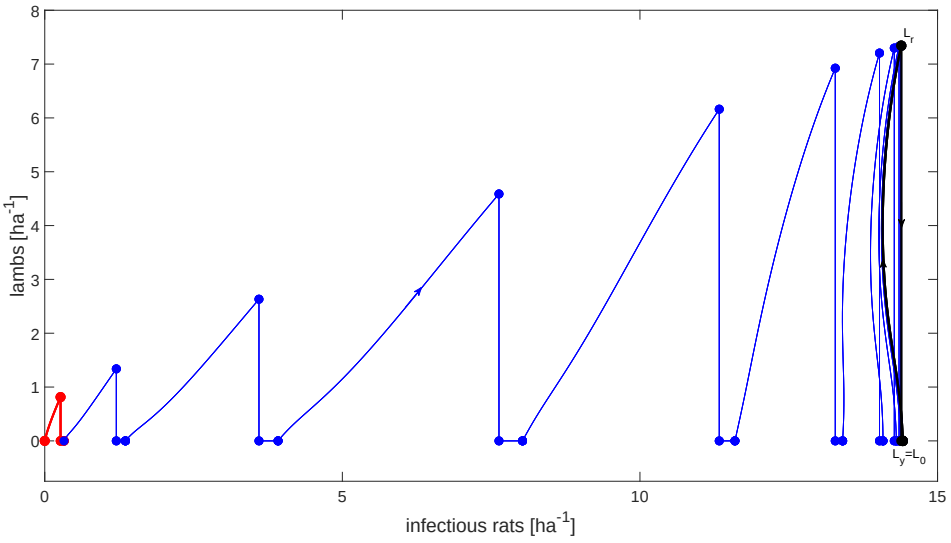

Figure 4.33: *Limit cycle diagram for the field-forest model. Phase plane showing the relationship between infectious rats and lambs. First year shown in red. Limit cycle shown in black. Intermediate years shown in blue.*

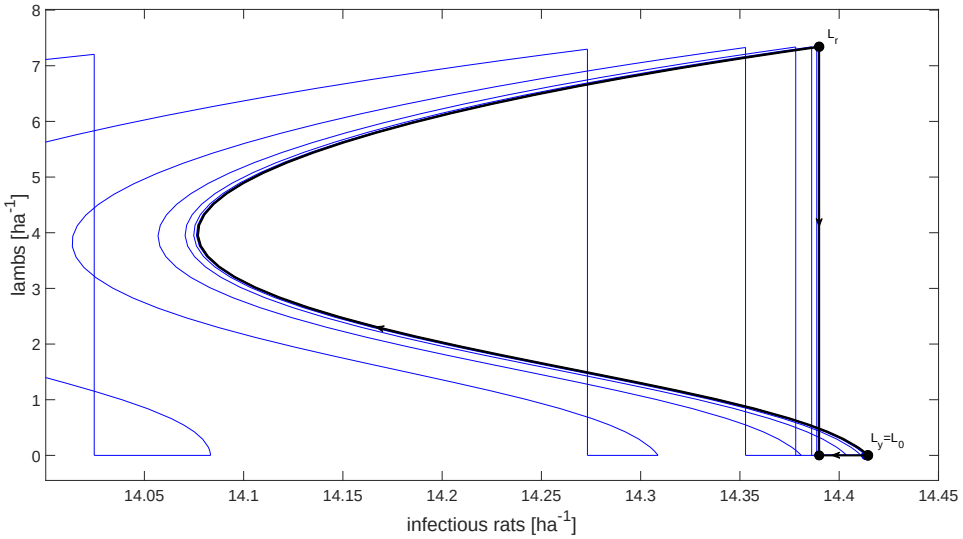

Figure 4.34: *Limit cycle diagram for the field-forest model. Phase plane showing the relationship between infectious rats and lambs. Magnification of the limit cycle.*

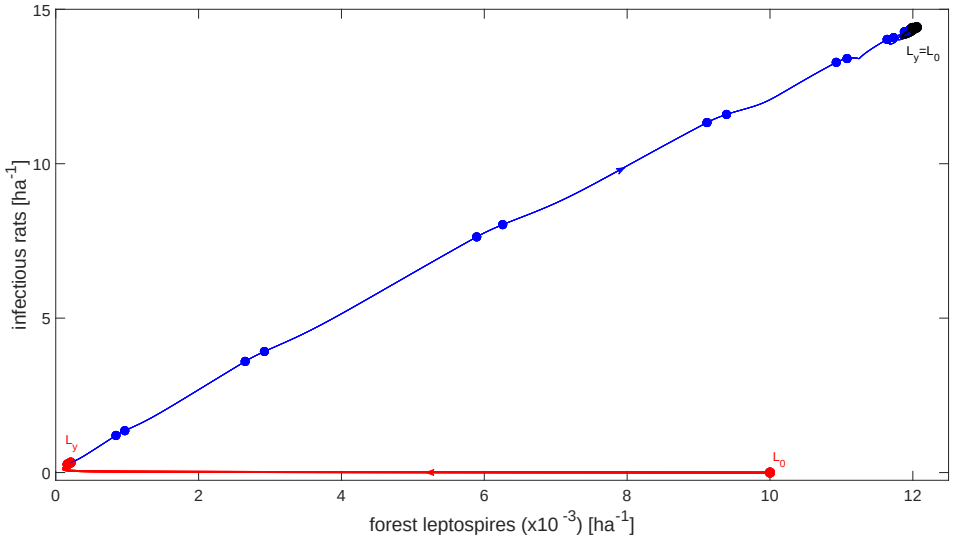

Figure 4.35: *Limit cycle diagram for the field-forest model. Phase plane showing the relationship between forest leptospires and infectious rats. First year shown in red. Limit cycle shown in black. Intermediate years shown in blue.*

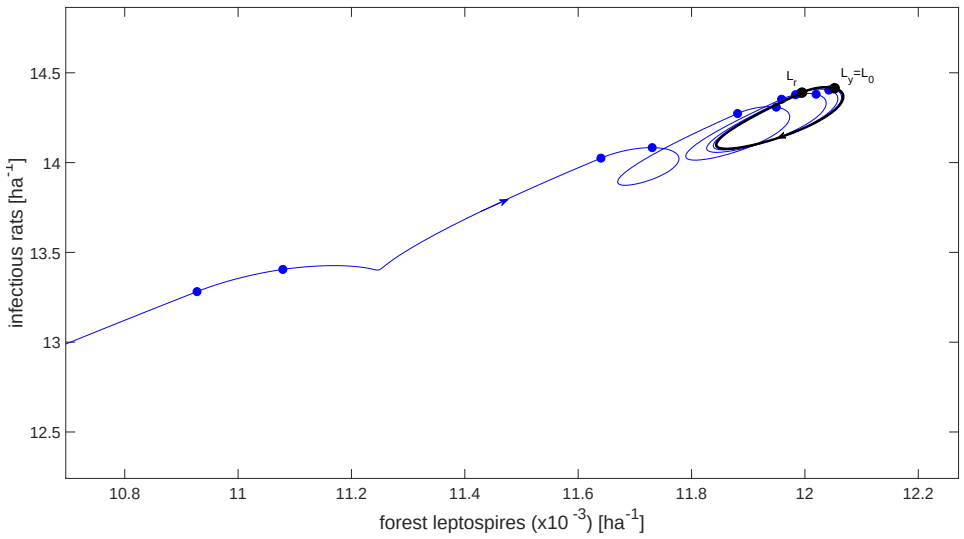

Figure 4.36: *Limit cycle diagram for the field-forest model. Phase plane showing the relationship between forest leptospires and infectious rats. Magnification of the limit cycle.*

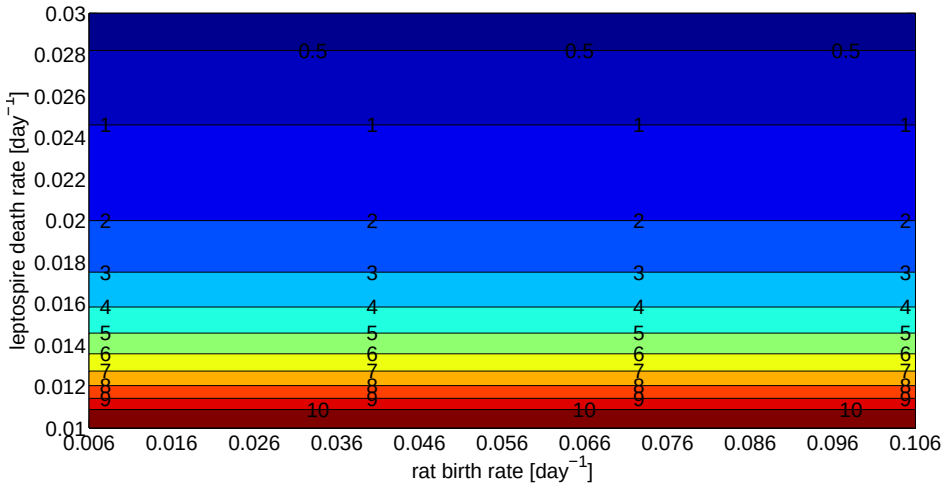

Figure 4.37: *Quasi-basic reproduction number heat map over a range of ρ and σ values for the field-forest model, $p = 0$.*

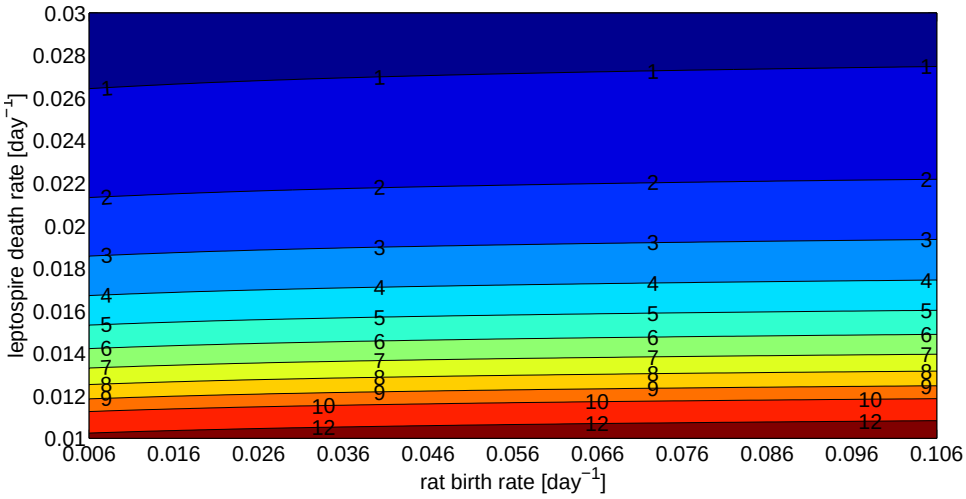

Figure 4.38: *Quasi-basic reproduction number heat map over a range of ρ and σ values for the field-forest model, $p = 0.5$.*

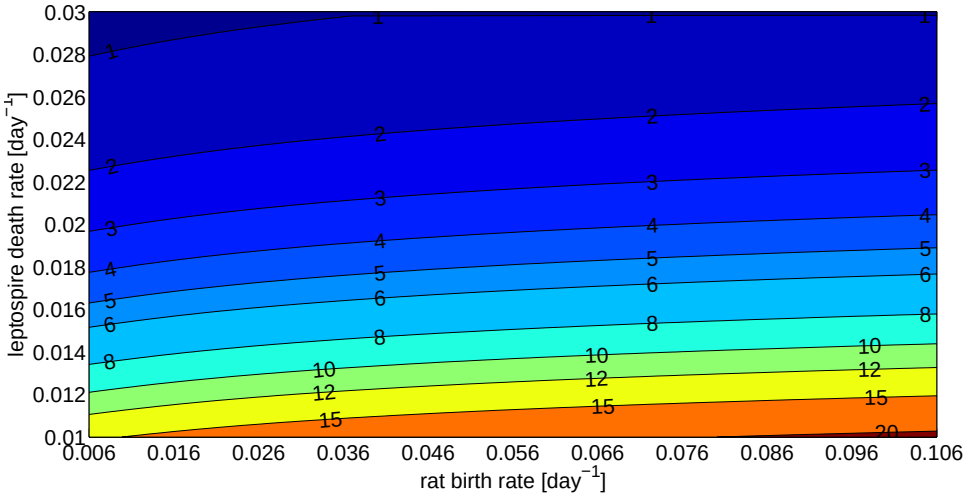

Figure 4.39: *Quasi-basic reproduction number heat map over a range of ρ and σ values for the field-forest model, $p = 1$.*

leptospires in the field, while L_2 denotes the density of leptospires in the forest, considers both potential locations of the initial source of infection into the system.

$$K = \begin{bmatrix} \frac{L_1(t_y)}{L_1(0)} & \frac{L_1(t_y)}{L_2(0)} \\ \frac{L_2(t_y)}{L_1(0)} & \frac{L_2(t_y)}{L_2(0)} \end{bmatrix}.$$

The quasi-basic reproduction number is found by calculating the spectral radius of the next generation matrix. Heat maps are plotted by calculating the quasi-basic reproduction number over a range of leptospire death rate ρ, and rat birth rate σ values, and for a range of p values ($p = 0$, 0.5 and 1. See figures 4.37, 4.38 and 4.39 respectively).

As expected, areas of low altitude occur at high values of leptospire death rate and areas of high altitude occur at low values of leptospire death rate. The contour lines of the heat maps are fairly horizontal over all, indicating that rat birth rate has little effect on infection rates. The heat maps change only marginally as p is increased; however, the contour lines do become less horizontal, indicating an increase of the impact rat birth rate has on the system as rats spend more time in the field. The range of R_L values increases as p is increased. This causes the topography of the heat map to be steeper, thus indicating infection rates in rats become more sensitive to changes in ρ as p increases. An important observation is that the area on the graphs for which $R_L < 1$ decreases as p increases. The system again, as in the wildlife-livestock model, experiences subcritical persistence of infection where infection persists despite $R_L < 1$.

4.2.8 Discussion

Overall, a decrease of the proportion of time spent by rats in the field, p, decreases infection in all populations except for the free living forest leptospire population, for which an increase occurs. The relationship between p and infectious rats is not strictly increasing as one may expect; however, this does not appear to impact on the relationships of p and the other remaining populations.

In general, an increase in rat birth rate, σ, exacerbates infection in all populations, as does a decrease in the leptospire death rate, ρ.

4.3 Complete Combined Model

The final iteration of the livestock-wildlife model combines the most complex of both sheep (section 3.4) and rat (section 2.3) models. The rat component of the model includes a total of seven differential equations; three for the total rat populations, one for each of three age classes (total juveniles, N_{JR}, total sub-adults, N_{SR}, and total adults, N_{AR}), three for the infectious rat populations (infectious juveniles, I_{JR}, infectious sub-adults, I_{SR}, and infectious adults, I_{AR}) and one for the free living forest leptospires, L_3. The sheep component of the model includes another five differential equations; one for the immune lamb population, M_{JS}, one for the susceptible lamb population, S_{JS}, one for the infectious lamb population, I_{JS}, one for the infectious ewe population, I_{AS}, and two for the free living leptospire populations, one each for lamb, L_1, and ewe, L_2, fields. This results in a system of 13 differential equations.

Each of the two host species components of the whole system behave in a similar manner to the models in section 2.3 and section 3.4.

The juvenile rat population increases at birth rate ϕ. Juveniles mature into sub-adults at rate ψ and sub-adults mature into adults at rate $\sigma e^{-cN_{AR}}$. Note that the maturation rate of sub-adults to adults in the current model is used as the birth rate for rats in the previous model (section 4.2). All rat populations, regardless of age class or infection status, decrease at death rate μ.

Total rat population:

$$\frac{dN_{JR}}{dt} = \phi N_{AR} - \psi N_{JR} - \mu N_{JR}, \tag{4.8}$$

$$\frac{dN_{SR}}{dt} = \psi N_{JR} - \sigma e^{-cN_{AR}} N_{SR} - \mu N_{SR}, \tag{4.9}$$

$$\frac{dN_{AR}}{dt} = \sigma e^{-cN_{AR}} N_{SR} - \mu N_{AR}. \tag{4.10}$$

The infection sub-system for rats follows the same structure as the system for the total rat population; however, only a proportion ν of juveniles are born infectious, infection is acquired by adults and sub-adults in a non-linear manner, as described in chapter 1, via the environment at rate γ_R and by adults in a density dependent manner via sexual contacts at rate β.

The rat's time is divided into three proportions, p_1, p_2 and p_3, for lamb field, ewe field and forest respectively. As such, the rats environmental exposure is also divided proportionally by environment. That is, a proportion p_1 of the rats environmental exposure is from the lamb field, a proportion p_2 is from the ewe field and a proportion p_3 is from the forest.

Similarly, the urine shed by non-juvenile rats at rate α_R is also divided proportionally by environment. That is, a proportion p_1 of the rats urine is shed into the lamb field, a proportion p_2 is shed into the ewe field and a proportion p_3 is shed into the forest. Note that $p_1 + p_2 + p_3 = 1$.

The only environment not shared by both animal species (rats and sheep) is the forest. As such, the forest leptospires, L_3, are assumed to be part of the rat component of the model. Leptospires in all environments die off at rate ρ.

Infectious rat population:

$$\begin{aligned}
\frac{dI_{JR}}{dt} &= \nu\phi I_{AR} - \psi I_{JR} - \mu I_{JR}, && (4.11)\\
\frac{dI_{SR}}{dt} &= \psi I_{JR} - \sigma e^{-cN_{AR}} I_{SR} + \frac{p_1\gamma_R(N_{SR} - I_{SR})L_1}{L_1 + H}, \\
&\quad + \frac{p_2\gamma_R(N_{SR} - I_{SR})L_2}{L_2 + H} + \frac{p_3\gamma_R(N_{SR} - I_{SR})L_3}{L_3 + H} - \mu I_{SR}, && (4.12)\\
\frac{dI_{AR}}{dt} &= \sigma e^{-cN_{AR}} I_{SR} + \frac{\beta(N_{AR} - I_{AR})I_{AR}}{N_{AR}} + \frac{p_1\gamma_R(N_{AR} - I_{AR})L_1}{L_1 + H} \\
&\quad + \frac{p_2\gamma_R(N_{AR} - I_{AR})L_2}{L_2 + H} + \frac{p_3\gamma_R(N_{AR} - I_{AR})L_3}{L_3 + H} - \mu I_{AR}, && (4.13)\\
\frac{dL_3}{dt} &= (1 - p_1 - p_2)\alpha_R(I_{SR} + I_{AR}) - \rho L_3.
\end{aligned}$$

The equations for the total rat populations (equations 4.8-4.10) decouple from the rest of the rat system (equations 4.11-4.13) and the total rat population of each subclass can be assumed to be at its steady state as described in section 2.3. Graphs involving rats, however, begin at an arbitrary initial condition and display the rat population(s) as they approach steady state. This is done for demonstrative purposes. The steady states for adults, sub-adult and juveniles are as follows:

$$N^*_{AR} = \frac{1}{c}\log\frac{\sigma(\phi\psi - \mu\psi - \mu^2)}{\mu^2(\psi + \mu)},$$

$$N^*_{SR} = \frac{\psi}{\sigma e^{-cN_A} + \mu} N_{JR},$$

and

$$N^*_{JR} = \frac{\phi}{\psi + \mu} N_{AR}.$$

As in section 3.4, the sheep population (both ewes and lambs) begin each year in field one (the lamb field). Ewes are then separated from their offspring and moved to field two (the ewe field). In section 3.4, at this stage, field two is assumed to be free of infection; however, in this version of the model it is assumed that the field has already been contaminated by the rats and infection is assumed to carry over from one year to the next. This is done due to the presence of rats in the model, which complicates the inclusion of a trivial initial condition in field two (i.e.. one has to consider both shedding and the environmental transmission component for rats into and from field two in the first time phase, during which ewes are absent from the field). Ewes remain in field two until the end of the year and, after 25% of the flock is replaced with susceptible ewes, are reintroduced back into field one at the beginning of the next year.

Lambs are not moved and remain in field one until the time of culling. In the first time phase, when both ewes and lambs occupy field one, free living leptospires are shed into the field by three populations; ewes, lambs and rats. In phase two, when only lambs occupy field one, leptospires are shed by two populations; lambs and rats. In the final time phase only one population sheds into the field; rats.

Regardless of their location, ewes becomes infectious at rate γ_A and shed leptospires at rate α_A. Lambs go through a three stage process; they start off immune (M_{JS}), lose immunity at rate ν to become susceptible (S_{JS}), before finally becoming infectious (I_{JS}) at rate γ_J.

The sheep component of the system before separation of ewes from lambs (phase one: $0 < t < t_m$),

$$
\begin{aligned}
\frac{dL_1}{dt} &= \alpha_{JS} I_{JS} + \alpha_{AS} I_{AS} + p_1 \alpha_R (I_{AR} + I_{SR}) - \rho L_1, \\
\frac{dL_2}{dt} &= p_2 \alpha_R (I_{AR} + I_{AS}) - \rho L_2, \\
\frac{dI_{AS}}{dt} &= \frac{\gamma_A (N_{AS} - I_{AS}) L_2}{L_2 + H}, \\
\frac{dM_{JS}}{dt} &= -\nu M_{JS}, \\
\frac{dS_{JS}}{dt} &= \nu M_{JS} - \frac{\gamma_J S_{JS} L_1}{L_1 + H}, \\
\frac{dI_{JS}}{dt} &= \frac{\gamma_J S_{JS} L_1}{L_1 + H}.
\end{aligned}
$$

The system after separation of ewes from lambs (phase two: $t_m < t < t_r$),

$$
\begin{aligned}
\frac{dL_1}{dt} &= \alpha_{JS} I_{JS} + p_1 \alpha_R (I_{AR} + I_{SR}) - \rho L_1, \\
\frac{dL_2}{dt} &= \alpha_{AS} I_{AS} + p_2 \alpha_R (I_{AR} + I_{SA}) - \rho L_2, \\
\frac{dI_{AS}}{dt} &= \frac{\gamma_A (N_{AS} - I_{AS}) L_2}{L_2 + H}, \\
\frac{dM_{JS}}{dt} &= -\nu M_{JS}, \\
\frac{dS_{JS}}{dt} &= \nu M_{JS} - \frac{\gamma_J S_{JS} L_1}{L_1 + H}, \\
\frac{dI_{JS}}{dt} &= \frac{\gamma_J S_{JS} L_1}{L_1 + H}.
\end{aligned}
$$

The system after removal of lambs (phase three: $t_r < t < 365$),

$$
\begin{aligned}
\frac{dL_1}{dt} &= p_1 \alpha_R (I_{AR} + I_{SR}) - \rho L_1, \\
\frac{dL_2}{dt} &= \alpha_{AS} I_{AS} + p_2 \alpha_R (I_{AR} + I_{SA}) - \rho L_2, \\
\frac{dI_{AS}}{dt} &= \frac{\gamma_A (N_{AS} - I_{AS}) L_2}{L_2 + H}.
\end{aligned}
$$

Note that while infection in the rat population is certainly influenced by infection in the sheep population, unlike the sheep component of the model,

Description	Symbol	Value	Units
Density of the total lamb population in a given area (the field)	N_{JS}	10	SU ha^{-1}
Density of the total ewe population in a given area (the field)	N_{AS}	10	SU ha^{-1}
Density of the immune lamb population in a given area (the field)	M_{JS}		SU ha^{-1}
Density of the susceptible lamb population in a given area (the field)	S_{JS}		SU ha^{-1}
Density of the infectious lamb population in a given area (the field)	I_{JS}		SU ha^{-1}
Density of the susceptible ewe population in a given area (the field)	S_{AS}		SU ha^{-1}
Density of the infectious ewe population in a given area (the field)	I_{AS}		SU ha^{-1}
Density of the free living leptospires in field one ($\times 10^{-3}$) in a given area (the field)	L_1		ha^{-1}
Density of the free living leptospires in field two ($\times 10^{-3}$) in a given area (the field)	L_2		ha^{-1}
Loss of immunity for lambs	ν_S	0.0034	day^{-1}
Environmental transmission coefficient for lambs	γ_{JS}	0.02477	day^{-1}
Environmental transmission coefficient for ewes	γ_{AS}	0.02359	day^{-1}
Number of leptospires ($\times 10^{-3}$) shed per infectious lamb	α_{JS}	2.3323	day^{-1}
Number of leptospires ($\times 10^{-3}$) shed per infectious ewe	α_{AS}	3.7317	day^{-1}
Density of leptospires ($\times 10^{-3}$) at which transmission rate from the environment is 0.5γ	H	10^3	ha^{-1}
Per capita leptospire death rate	ρ	0.02381	day^{-1}
Density of the total juvenile rat population in a given area (the field)	N_{JR}		ha^{-1}
Density of the total sub-adult rat population in a given area (the field)	N_{SR}		ha^{-1}
Density of the total adult rat population in a given area (the field)	N_{AR}		ha^{-1}
Density of the susceptible juvenile rat population in a given area (the field)	S_{JR}		ha^{-1}

...Continuation of Table 4.2

Description	Symbol	Value	Units
Density of the susceptible sub-adult rat population in a given area (the field)	S_{SR}		ha^{-1}
Density of the susceptible adult rat population in a given area (the field)	S_{AR}		ha^{-1}
Density of the infectious juvenile rat population in a given area (the field)	I_{JR}		ha^{-1}
Density of the infectious sub-adult rat population in a given area (the field)	I_{SR}		ha^{-1}
Density of the infectious adult rat population in a given area (the field)	I_{AR}		ha^{-1}
Density of the free living leptospires in the forest ($\times 10^{-3}$) in a given area (the field)	L_3		ha^{-1}
Birth rate of rats	ϕ	0.007671	day^{-1}
Maturation rate of juvenile rats to sub-adult rats	ψ	0.04	day^{-1}
Rat death rate	μ	0.0027	day^{-1}
Sub-adult maturation rate for rats	σ	0.01	day^{-1}
Shape parameter for density dependence in maturation for rats	c	0.4	
Probability of pseudo vertical transmission (transmission of leptospirosis from infectious rat mothers to offspring via suckling)	ν_R	0.01	
Proportion of time spent by rats in the lamb field	p_1	0.3	
Proportion of time spent by rats in the ewe field	p_2	0.2	
Proportion of time spent by rats in the forest	p_3	0.5	
Environmental transmission coefficient for rats	γ_R	0.005	day^{-1}
Sexual transmission co-efficient (rat)	β	0.01	day^{-1}

...Continuation of Table 4.2

Description	**Symbol**	**Value**	**Units**
Density of leptospires ($\times 10^{-3}$) shed per infectious rat	α_R	0.1	day^{-1}
Time	t		days
Removal date of ewes from the lamb field	t_e	90	days
Removal date of lambs	t_l	335	days
End of year	t_y	365	days
Density of the immune lamb population in a given area (the lamb field) at the beginning of each year	M^0_{JS}	N_{JS}	SU ha^{-1}
Density of the susceptible lamb population in a given area (the lamb field) at the beginning of each year	S^0_{JS}	0	SU ha^{-1}
Density of the infectious lamb population in a given area (the lamb field) at the beginning of each year	I^0_{JS}	0	SU ha^{-1}
Density of the infectious ewe population in a given area (the lamb field) at the beginning of each year n	I_{A0}	$\frac{3}{4}I_{A0}(n-1)$	SU ha^{-1}
Density of the free living leptospires ($\times 10^{-3}$) in a given area (the lamb field) at $t = 0$	L^0_1	0	ha^{-1}
Density of the free living leptospires ($\times 10^{-3}$) in a given area (the ewe field) at $t = 0$	L^0_2	0	ha^{-1}
Density of the free living leptospires ($\times 10^{-3}$) in a given area (forest) at $t = 0$	L^0_3	10	ha^{-1}

Table 4.2: *Parameters and initial conditions used for the complete combined model.*

the equations for the rat component of the model (equations 4.8-4.13) don't change over the duration of the year.

4.3.1 Data and Parameter Values

Many of the parameter values used for this model have been used previously. Sheep specific parameter values are carried over from section 3.4, the parameters μ, H, α_R and ρ are carried over from section 4.1 and the parameters ψ, σ, ν, γ_R and β are taken from Holt et. al. [20] (see table Table 4.1).

As in section 4.2, rats are assumed to prefer to spend their time in the forest environment. Hence, the value of $p_3 = 0.5$ is carried over from section 4.2, while the remaining proportions are set arbitrarily at $p_1 = 0.3$ and $p_2 = 0.2$.

The value $\sigma = 7.671^{-3}$ day^{-1} is used in section 4.2 for rat birth rate. Here, however, the parameter σ is no longer assigned to rat birth rate and is instead used as the maturation rate of sub-adults to adults. Hence, the value 7.671^{-3} day^{-1} is now assigned to the birth rate parameter ϕ, while σ is given the new value of $\sigma = 0.01$ day^{-1} (taken from Holt et. al.). Due to this rearrangement of parameters in the model, using the value $c = 0.04$ for the shape parameter for density dependence in rat maturation as taken from Holt et. al. results in unreasonably large values for rat densities. As such, c is increased to $c = 0.4$ in order to fit the total rat population within a biologically plausible range.

Another result of the parameter rearrangement is that, when exploring the parameter space most likely affected by climate change, it is now the parameter ϕ rather than σ being manipulated. Birth rate is varied from the lower end of the biologically feasible range, $\phi = 7.671 \times 10^{-3}$ day^{-1}, to the upper end $\phi_{max} = 9.863 \times 10^{-2}$ day^{-1}.

The other parameter value likely to be affected by climate change is the leptospire death rate ρ. As in section 4.2, only the leptospire death rates in the field environments are altered when considering the influence of climate change on the model, leaving the death rate in the forest environment constant.

4.3.2 Numerical Results

The general shapes of the behaviours of the lamb, ewe and lamb field leptospire populations over time (figures 4.40, 4.41 and 4.42) are similar to those in section 3.4.

As discussed above, the presence of rats in the model complicates the inclusion of a trivial initial condition for the ewe field and as such, this is removed and environmental infection in field two is carried over from one year to the next. The field two leptospire population, shown in figure 4.42 in red, starts with a trivial initial condition. In the first time phase of the first year, leptospire densities increase very slowly as only rats shed into the field. After the introduction of infectious ewes, leptospire densities increases much faster. At the begining of the next year, after ewes are removed from the field, the leptospire population begins to decrease. This is due to the leptospires dying off at rates much faster than the rats are able to shed them into the environment. After reintroduction of ewes at the beginning of the second time phase in the following year, the leptospire population again begins to increase. By the end of the third year the leptospire population appears to begin to plateau before plummeting at the beginning of the next year. This behaviour is then repeated.

Forest leptospire densities, shown in figure 4.42 in black, are much smaller than the field leptospire populations and the periodic behaviour of the forest leptospire population takes longer to become apparent than the other model populations. As such, forest leptospires are plotted in a graph on their own and for a longer time period in figure 4.43.

Figure 4.45 shows the total rat populations with a thick line and the infectious rat populations with a thin line. The juvenile rat population is shown in black, the sub-adults in blue, the adults in red and the global (all age classes combined) shown in green. The behaviour of the rat populations in this model are similar to the behaviour of the rat population in section 4.1 in that the total rat populations reach constant steady states, and infectious rat populations initially increase from zero. The initial behaviour of the total populations differ in that, compared to the initial conditions used for each population, the juvenile and adult total populations decrease to reach their steady states rather than increasing as in section 4.1, and the sub-adult population increases before decreasing. This increase followed by a decrease of the total sub-adult population is due to the interaction of the sub-adult

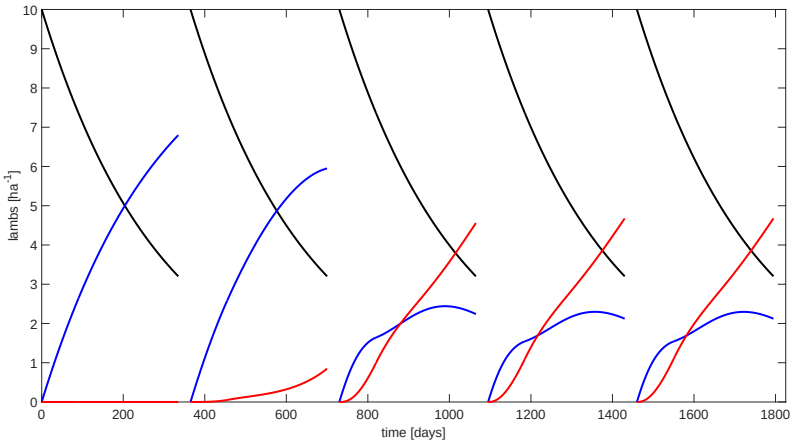

Figure 4.40: *Numerical solutions to the complete combined model. Density of immune, susceptible and infectious lambs over time (days). Immune lambs shown in black. Susceptible lambs shown in blue. Infectious lambs shown in red.*

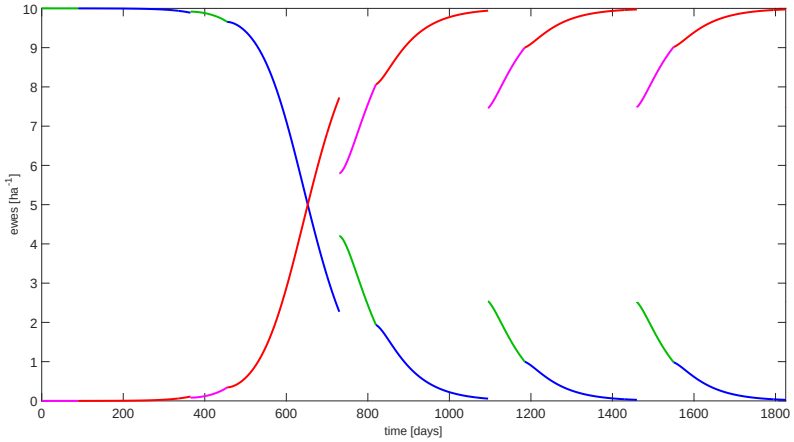

Figure 4.41: *Numerical solutions to the complete combined model. Density of susceptible and infectious ewes in field one and two over time (days). Susceptible ewes while in field one shown in green. Susceptible ewes while in field two shown in blue. Infectious ewes while in field one shown in purple. Infectious ewes while in field two shown in red.*

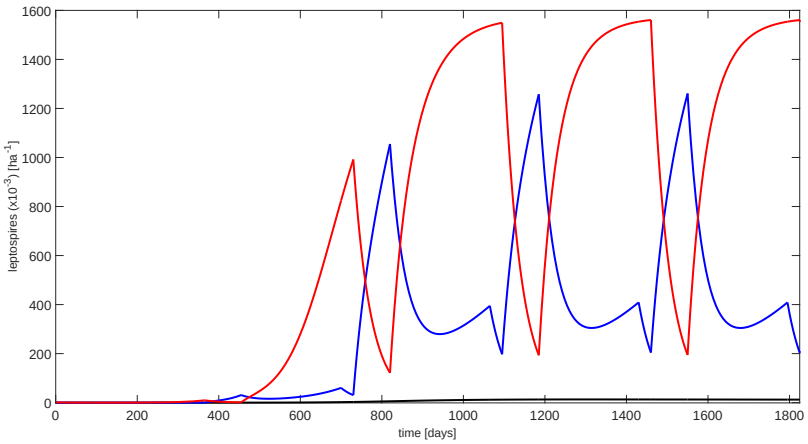

Figure 4.42: *Numerical solutions to the complete combined model. Density of free living leptospires over time (days). Lamb field leptospires shown in blue. Ewe field leptospires shown in red. Forest leptospires shown in black.*

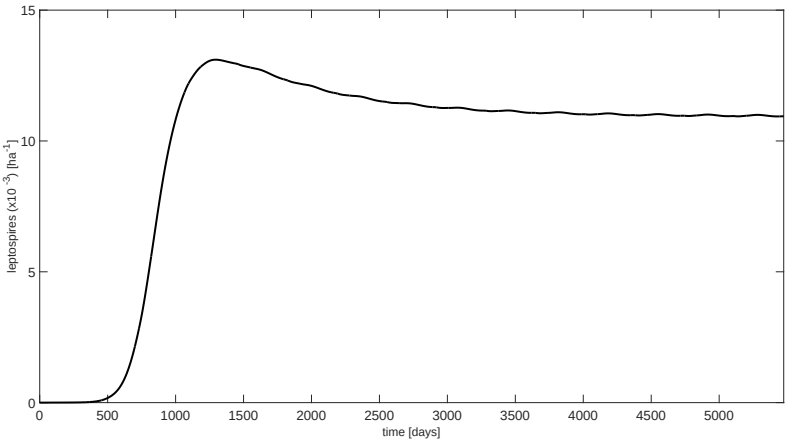

Figure 4.43: *Numerical solutions to the complete combined model. Density of free living forest leptospires over time (days).*

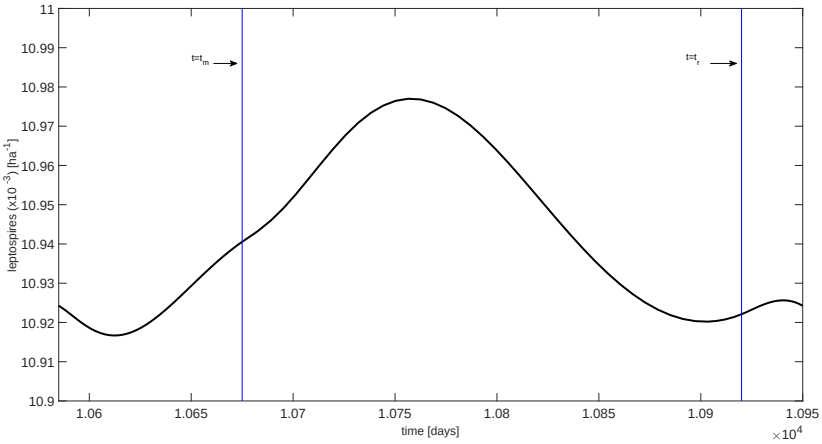

Figure 4.44: *Numerical solutions to the complete combined model. Density of free living forest leptospires over time (days) for one year once the behaviour of the model has begun to repeat.*

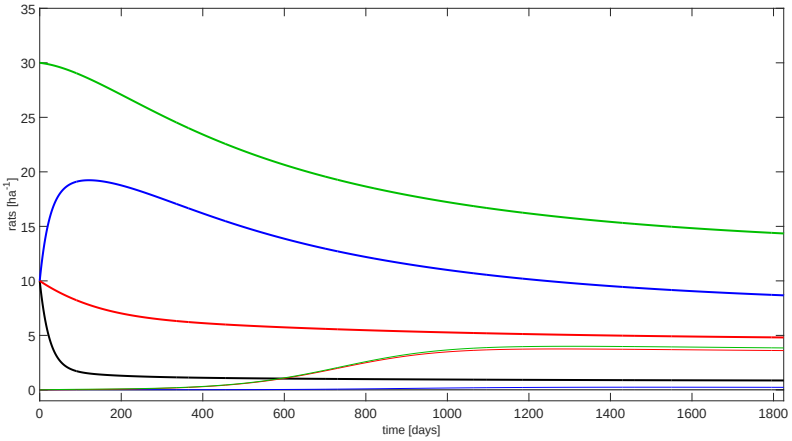

Figure 4.45: *Numerical solutions to the complete combined model. Density of rats over time (days). Total rat populations shown with a thick line. Infectious rat populations shown with a thin line. Adult rats shown in red. Sub-adult rats shown in blue. Juvenile rats shown in black. All age classes combined shown in green.*

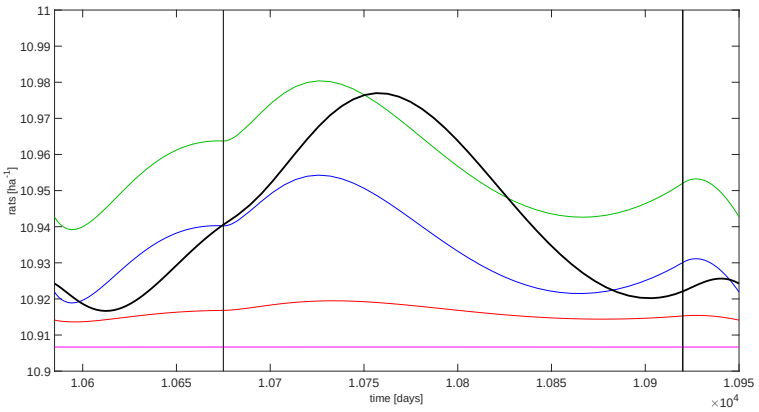

Figure 4.46: *Numerical solutions to the complete combined model. Density of rats and forest leptospires over time (days) for one year once the behaviour of the model has begun to repeat displaying the relationship between the rat and forest leptospire populations. Infectious adult rats shown in red. Infectious sub-adult rats shown in blue. Infectious juvenile rats shown in purple. All infectious age classes combined shown in green. Forest leptospires shown in black. Note that the x-axis is for the leptospire population and as such the rat populations shown are not to scale.*

and adult populations via density dependent maturation. Compared to the rest of time, the adult population is initially "large", resulting in a slow rate of maturation of sub-adults to adults. This results in a build up of rats in the sub-adult class. As the adult population decreases, the maturation rate of sub-adults to adults increases, thus resulting in a decrease in the sub-adult population after some time. This result is largely in part due to the choice of (arbitrary) initial conditions and the behaviour can be altered by varying the proportion of sub-adults, to adults and juveniles.

Figure 4.44 shows a magnification of forest leptospire densities over a period of one year, once the behaviour of the population has begun to repeat itself. The vertical lines show the beginnings of phases two and three respectively. Interestingly, the forest leptospire behaviour appears to exhibit a lag. The turning points of the graph (lowest and highest points) don't line up with the phase changes in the sheep population. This may be related to the periodic behaviour in the rat population. While the infectious rat populations don't initially appear to exhibit periodic behaviour, upon closer inspection it is clear that sub-adult and adult populations do indeed oscillate; however, the amplitude of this behaviour is very small. Figure 4.46

shows the behaviour of the infectious rat populations plotted together with the forest leptospire population. Note that the scaling of the y-axis in this figures is for leptospire density and as such, the curve for the rat populations are not to scale. From here it is quite clear that the sub-adult population has the biggest impact on the periodicity of the total rat population, the adult population appears to very subtly follow that of the sub-adult population and the juvenile population doesn't appear to exhibit periodic behaviour at all. The initial decrease of the total infectious rat population at the beginning of the year makes sense, as the system in the previous time phase (the end of the previous year) has fewer infectious populations in it. That is, the lambs are not contributing to infection in the system as they are not a part of it. As such, infection rates in rats begin to decrease and this trend is carried over into the beginning of the following year. As infection rates in the lamb field begin to increase due to the introduction of a new cohort of lambs, so do infection rates in the rats. As the rate of change in the infectious ewe population slows, so does the rate of change in the field two leptospire population and subsequently the rat population. Despite the separation of the ewes from their lambs, the ewe and lamb field leptospire populations continues to increase, as does the total infectious rat population. The infectious rat population goes through a global (over the course of the year) maximum, followed by a local minimum. The rise in population continues until after the removal of the lambs, before falling again due to the decrease in environmental exposure from the lamb field as a result of their removal. This fall is carried over to the beginning of the next year. The population of the forest leptospires mirrors the behaviour of the total infectious rat population with a small lag.

4.3.3 Proportion p

The graphs showing population fixed points over the proportion of time spent by rats in the various environments as in section 4.2 (Figure 4.22a-Figure 4.25b) must now be plotted as heat graphs. Proportions p_1 and p_2, time spent by rats in the lamb and ewe fields respectively, are chosen for this purpose. Recall that $p_1 + p_2 + p_3 = 1$, hence, only the bottom left triangle of each figure is feasible.

Heat maps are plotted for the following populations: infectious lambs, lamb field leptospires, infectious ewes, ewe field leptospires, total infectious rats and forest leptospires (figures 4.47a-4.48b). Apart from the forest leptospire heat map, the region of low altitude for all graphs is for both

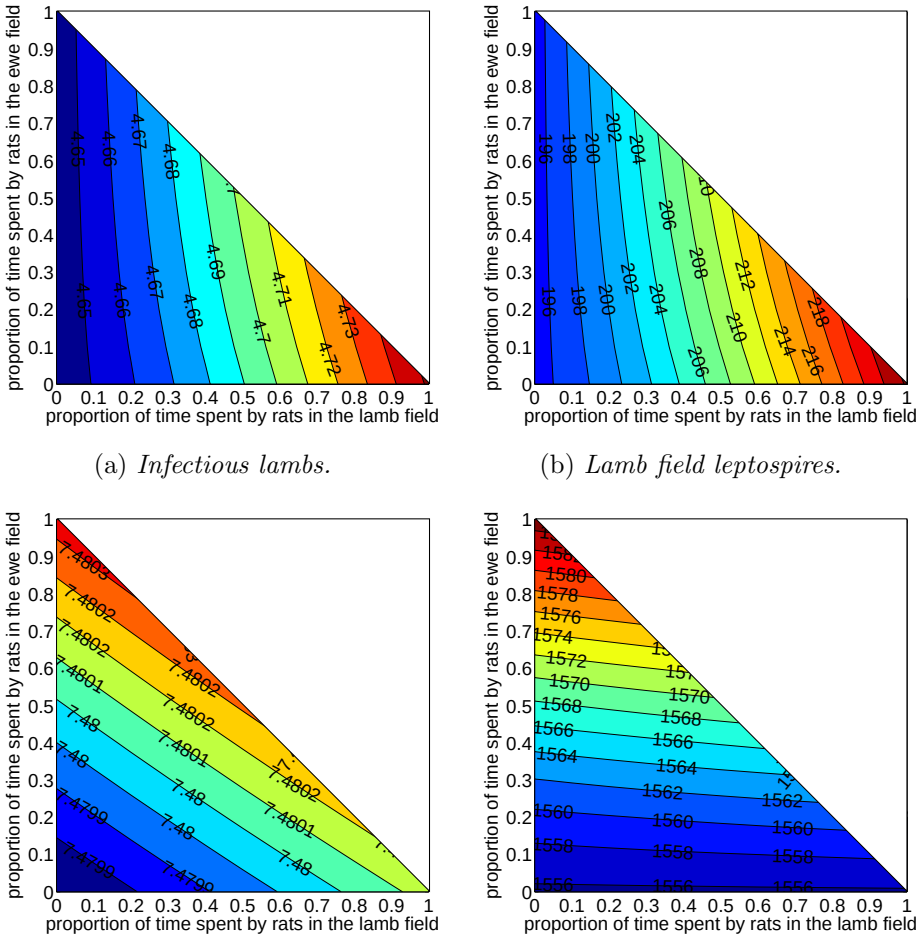

(a) *Infectious lambs.* (b) *Lamb field leptospires.*

(c) *Infectious ewes.* (d) *Ewe field leptospires.*

Figure 4.47: *Fixed points of infectious sheep and field leptospire populations for the complete combined model as time spent by rats in different environments is varied.*

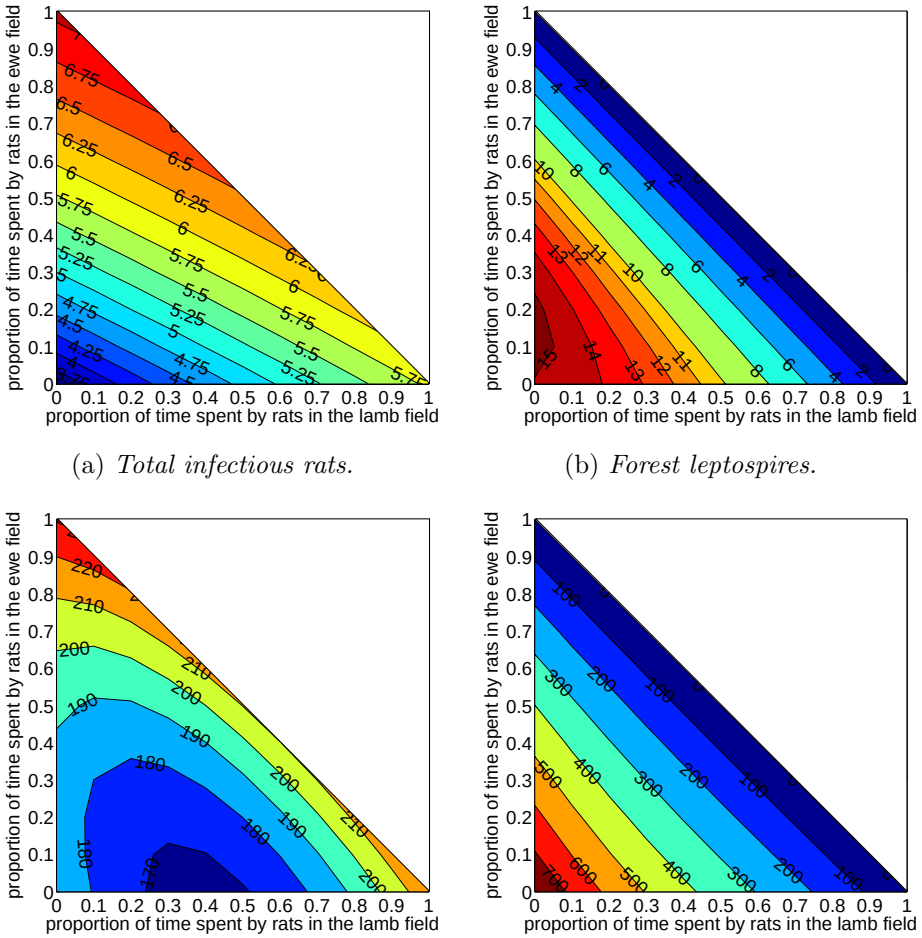

(a) *Total infectious rats.* (b) *Forest leptospires.*

(c) *Total infectious rats, $\phi = \phi_{max}$.* (d) *Forest leptospires, $\phi = \phi_{max}$.*

Figure 4.48: *Fixed points of infectious rats and forest leptospire populations for the complete combined model as time spent by rats in different environments is varied.*

p_1 and p_2 small. This implies that the less time rats spend in environments shared with livestock, the lower infection rates are overall. This relationship is clearly reversed for the forest leptospires, which increase as rats spend more time in that environment. The angle contour lines make when measured from the horizontal axis (with zero degrees pointing left) reveals which proportion, p_1 or p_2, has a stronger effect on infection rates. If the angle is greater than 45 degrees, then p_1 is stronger, and if the angle is less than 45 degrees, then p_2 is stronger. In the heat map for infectious rats the angle is greater then 45 degrees implying that more time spent in the lamb field results in higher rates of infection in the rats. As expected, this in turn results in higher infection rates in the forest as well. Interestingly, a higher proportion of time spent by rats in the lamb field results in a decrease in lamb infection rates, coupled with a decrease in lamb field leptospires and an increase in ewe infection rates, coupled with an increase in ewe field leptospires.

As in section 4.2, the leptospire death rate, ρ, and rat birth rate, ϕ are used as varying parameters to explore the possible effects of climate change. These graphs are not included, however, as they are very similar to the ones already shown.

As the leptospire death rate, ρ, is increased, fixed point values become smaller, as expected, and the range of fixed point values decreases, resulting in terrain in the heat map which is less steep and implying that the proportion of time spent by rats in each environment becomes less important as ρ increases. Varying ρ has only minor effects on the heat maps of all populations, and hence, only figures for default values of ρ are shown.

The default value of the birth rate ϕ is at the lower end of the range used. Increasing ϕ to the maximum value considered over all increases the value of the fixed points in each population and, as with increasing ρ, decreasing the range. Thus, as ϕ increases, the proportion of time spent by rats in each environment becomes less important.

For most of the heat maps, contour lines run parallel to one another. The heat map for forest leptospires differs from the others in that for small values of p_1 and p_2, the contour lines curve in such a way that the lowest point on the heat map is not at the origin, or running along one axis, but is instead bunched around the point $p_1 \approx 0.15$ and $p_2 = 0$. This behaviour is similar to that occurring in the figure showing infectious rat density over proportion of

time spent by rats in the field in section 4.2 (figure Figure 4.22b). At ϕ_{max} (see figure 4.48d) this behaviour is lost and instead appears in the infectious rat heat map (figure 4.48c); however, on the opposite axis.

The two parametric extremes which could be caused by climate change, namely, ρ small paired with ϕ large and ρ large paired with ϕ small, result in figures similar to figures plotted with large values of ϕ and figures plotted using default values respectively, hence they are not included here.

4.3.4 Bifurcation

Bifurcation diagrams for the current model (figures 4.54-4.54) plot population steady states, with leptospire death rate, ρ, and rat birth rate, ϕ, as varying parameters. Overall, an increase in birth rate increases the values of the infectious population steady states, as does a decrease in leptospire death rate. The topography of bifurcation diagrams is paired by location. That is, the bifurcation diagram of the host population mirrors the diagram of the leptospire population in the same environment. The field environment populations (figures 4.54-4.52) are more sensitive to changes in the leptospire death rate than to the rat birth rate as indicated by the angle of the contour lines, while the opposite is true for the forest populations (figures 4.53-4.54). This makes sense as sheep have a more direct relationship with changes in the field leptospire death rate than do rats, while rats have a more direct relationship to rat birth rate than do sheep. Steady state values here are much higher than in section 4.2. This is to be expected, as even though the stocking density has remained the same, the number of livestock has effectively doubled as each stocking unit is now a pair of sheep rather than a lone sheep, hence resulting in a greater bacterial burden on the environment.

4.3.5 Limit Cycle

The current model is represented by a system of 13 differential equations. This could result in a cumbersome number of projections of the limit cycle. Therefore, only a handful of projections are considered here. The limit cycle projections for infectious rats against lamb field (figure 4.55-4.56), ewe field (figures 4.57-4.58) and forest (figure 4.59-4.60) leptospires are plotted, as are the projections of total sheep against infectious rats (figures 4.63-4.64) and the field leptospire populations (figures 4.61-4.62).

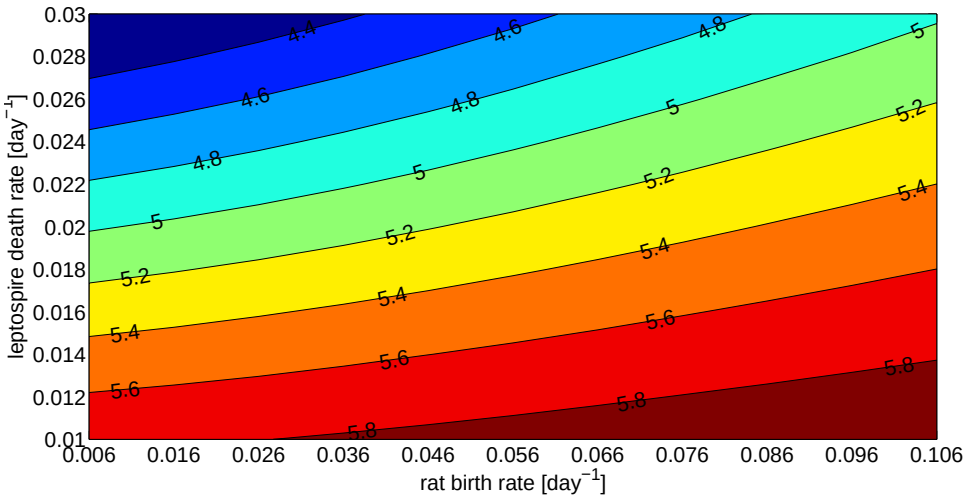

Figure 4.49: *Bifurcation heat map for the complete combined model showing fixed point values of lambs as ϕ is varied from* 0.006 *to* 0.106 day^{-1} *and ρ is varied from* 0.01 *to* 0.03 day^{-1}. *Note that no area of the heat map reaches zero.*

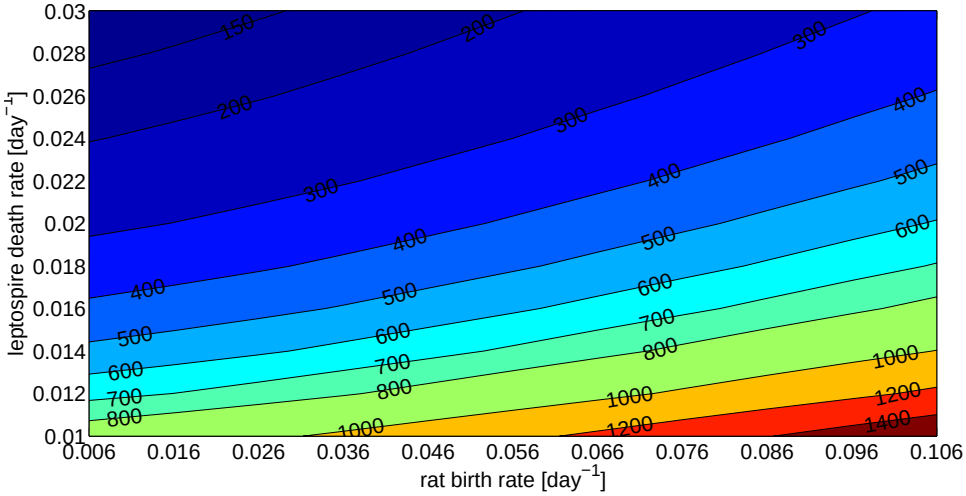

Figure 4.50: *Bifurcation heat map for the complete combined model showing fixed point values of lamb field leptospires as ϕ is varied from* 0.006 *to* 0.106 day^{-1} *and ρ is varied from* 0.01 *to* 0.03 day^{-1}. *Note that no area of the heat map reaches zero.*

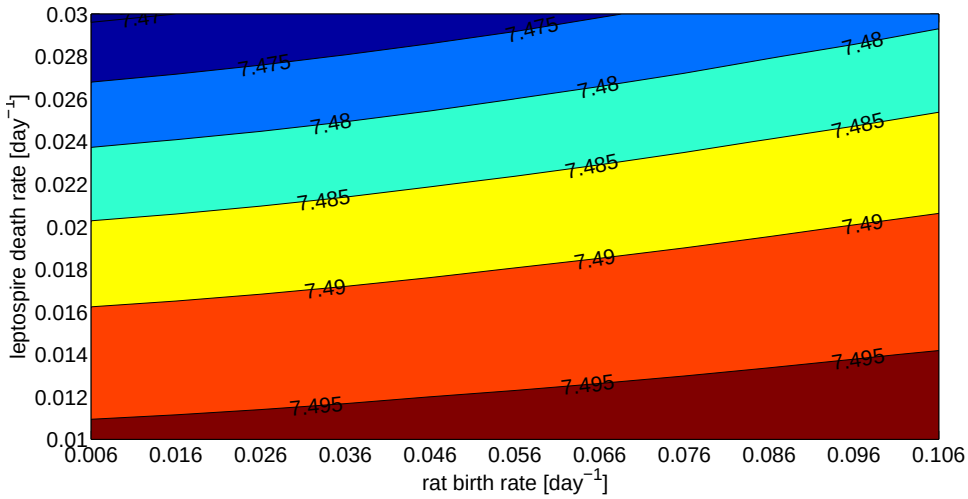

Figure 4.51: *Bifurcation heat map for the complete combined model showing fixed point values of ewes as ϕ is varied from* 0.006 *to* 0.106 *day*$^{-1}$ *and ρ is varied from* 0.01 *to* 0.03 *day*$^{-1}$*. Note that no area of the heat map reaches zero.*

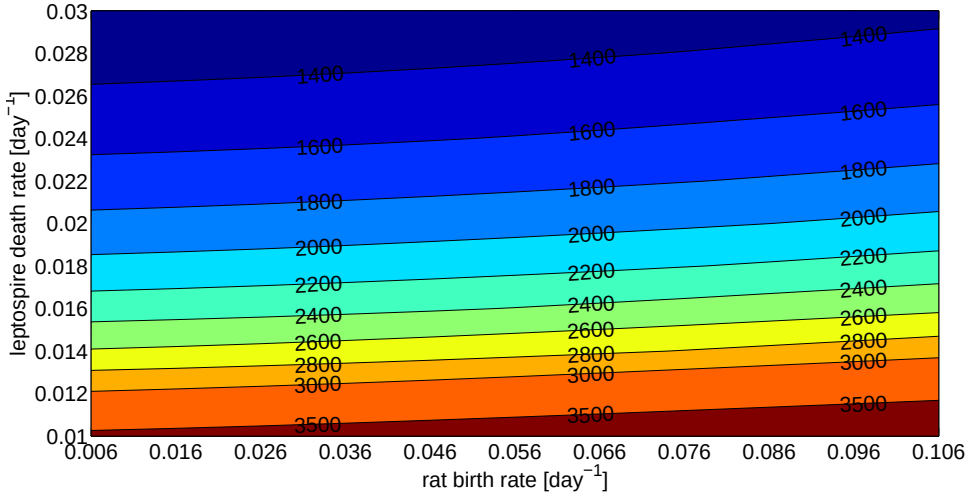

Figure 4.52: *Bifurcation heat map for the complete combined model showing fixed point values of ewe field leptospires as ϕ is varied from* 0.006 *to* 0.106 *day*$^{-1}$ *and ρ is varied from* 0.01 *to* 0.03 *day*$^{-1}$*. Note that no area of the heat map reaches zero.*

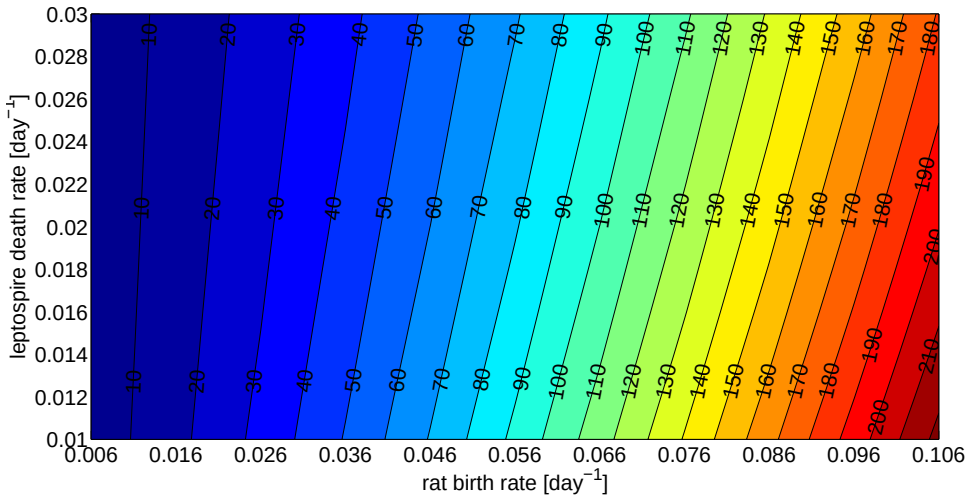

Figure 4.53: *Bifurcation heat map for the complete combined model showing fixed point values of infectious rats as ϕ is varied from* 0.006 *to* 0.106 *day^{-1} and ρ is varied from* 0.01 *to* 0.03 *day^{-1}. Note that no area of the heat map reaches zero.*

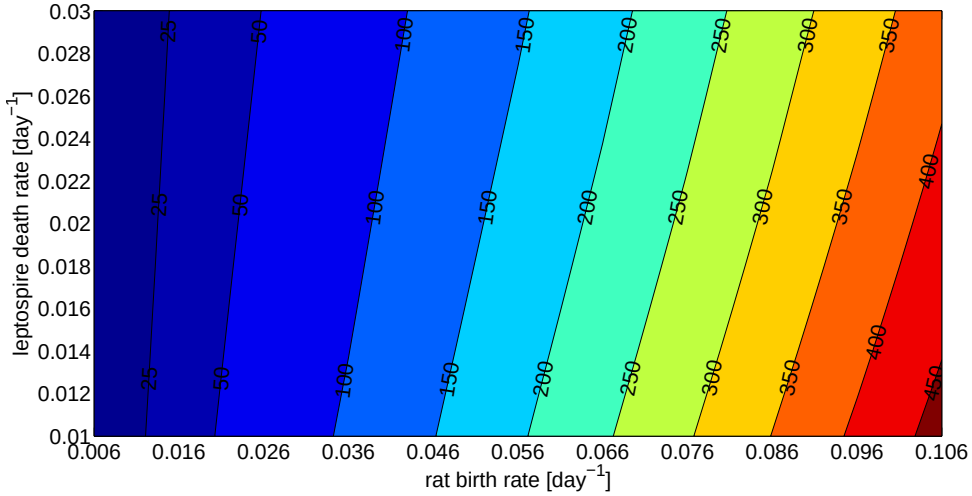

Figure 4.54: *Bifurcation heat map for the complete combined model showing fixed point values of forest leptospires as ϕ is varied from* 0.006 *to* 0.106 *day^{-1} and ρ is varied from* 0.01 *to* 0.03 *day^{-1}. Note that no area of the heat map reaches zero.*

The general shapes of the limit cycle diagrams of rats against the two field leptospire populations are fairly similar. Both start off near the origin, with the limit cycle itself oscillating between a small range of infectious rats and a large range of leptospires, resulting in a limit cycle that appears as a straight line. Upon closer inspection, both limit cycles follow loops of intriguing shapes; however, note that the range of densities for rats in both limit cycles is very small (figures 4.56 and 4.58).

The limit cycle for the lamb field leptospires begins at the left most corner of the limit cycle and runs in a counter-clockwise direction. Each subsequent corner corresponds to the beginning of the next time phase (removal of ewes, removal of lambs and end of the year respectively). The ewe leptospire limit cycle begins at the bottom right corner and runs clockwise.

The rat vs forest leptospire limit cycle is similar to the one in section 4.2. The global picture of the streamlines has leptospires plummeting towards the origin from the positive initial condition for leptospires, while the number of infectious rats increases at a slow pace. Both rats and leptospires then increase, initially without any decreases in population. The limit cycle diagram in section 4.2 reaches its limit cycle without any apparent decreases in either population (when looking globally), while the limit cycle diagram for the current model does decrease with respect to both populations. Neither population is directly impacted by the management practices implemented on livestock and so the streamlines are smooth, with no corners. The limit cycle starts at the node labelled t_y and runs clockwise (figure 4.60).

The limit cycle diagrams for the sheep differ to those in the rest of the thesis due to the combination of lamb and ewe populations in the diagrams. The limit cycle for sheep against lamb field leptospires begins at the left most bottom corner and runs counter-clockwise (figure 4.61). At the beginning of the limit cycle, as the number of infectious sheep increases so do the leptospires. At the first node, ewes are removed from the lamb field and moved to the ewe field. The total infectious sheep population continues to increase; however, as the ewes are no longer shedding into the lamb field, the number of leptospires begins to decrease. This continues until the number of infectious lambs has increased to a point where the shedding rate balances out with the leptospire death rate and the leptospires begin to increase again. Lambs are removed from the system at the node t_{rl} and the streamline falls suddenly. The lamb field is now empty of livestock and the leptospire population decreases as the shedding rate of rats is not enough

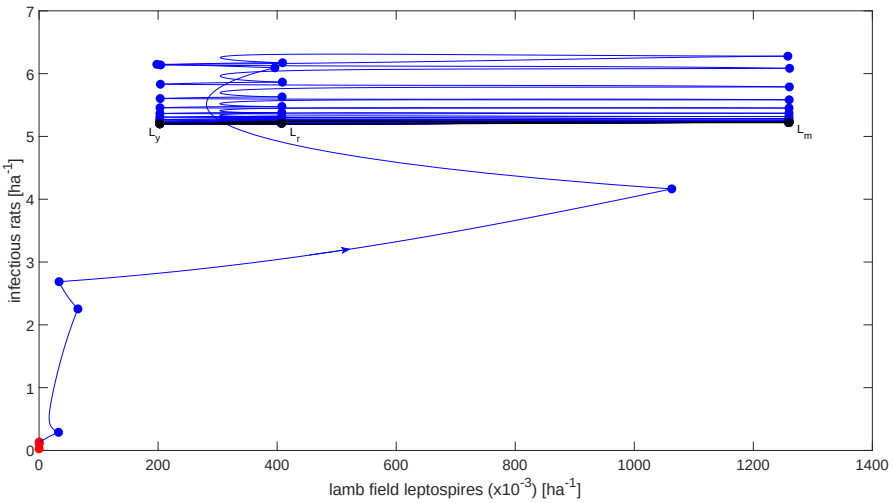

Figure 4.55: *Limit cycle diagram for the complete combined model. Phase plane showing the relationship between lamb field leptospires and infectious rats. First year shown in red. Limit cycle shown in black. Intermediate years shown in blue.*

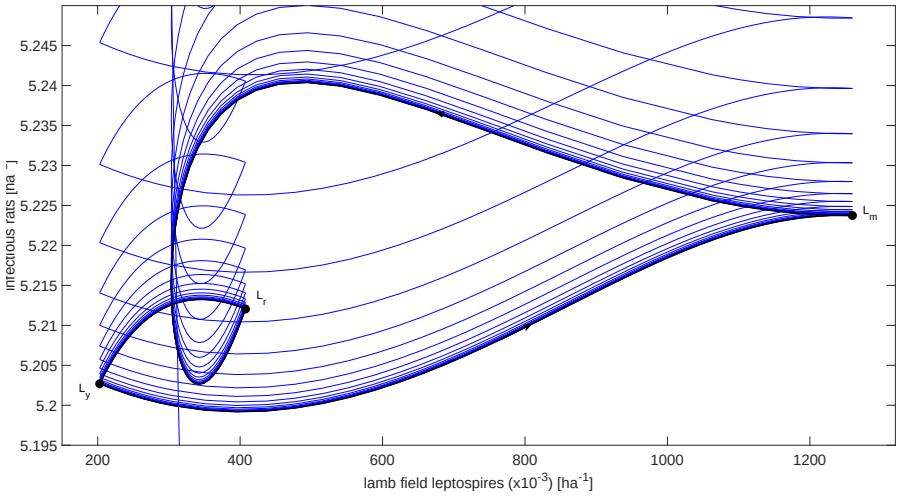

Figure 4.56: *Limit cycle diagram for the complete combined model. Phase plane showing the relationship between lamb field leptospires and infectious rats. Magnification of the limit cycle.*

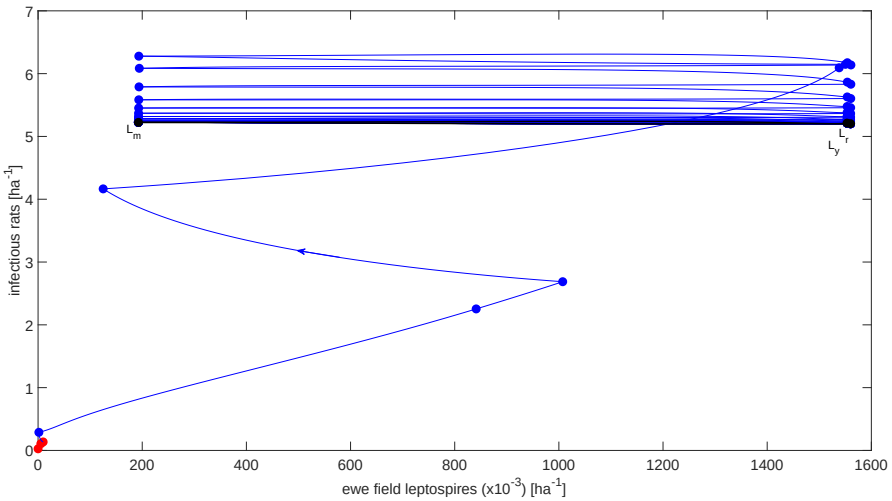

Figure 4.57: *Limit cycle diagram for the complete combined model. Phase plane showing the relationship between ewe field leptospires and infectious rats. First year shown in red. Limit cycle shown in black. Intermediate years shown in blue.*

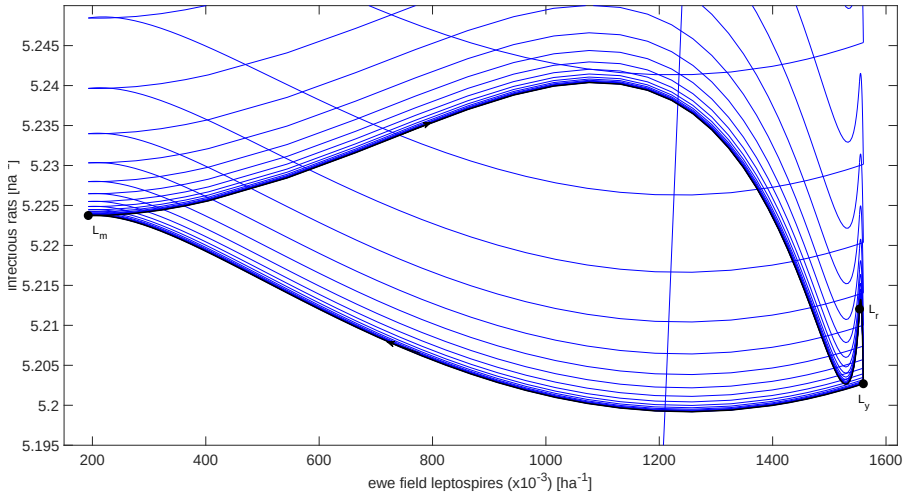

Figure 4.58: *Limit cycle diagram for the complete combined model. Phase plane showing the relationship between ewe field leptospires and infectious rats. Magnification of the limit cycle.*

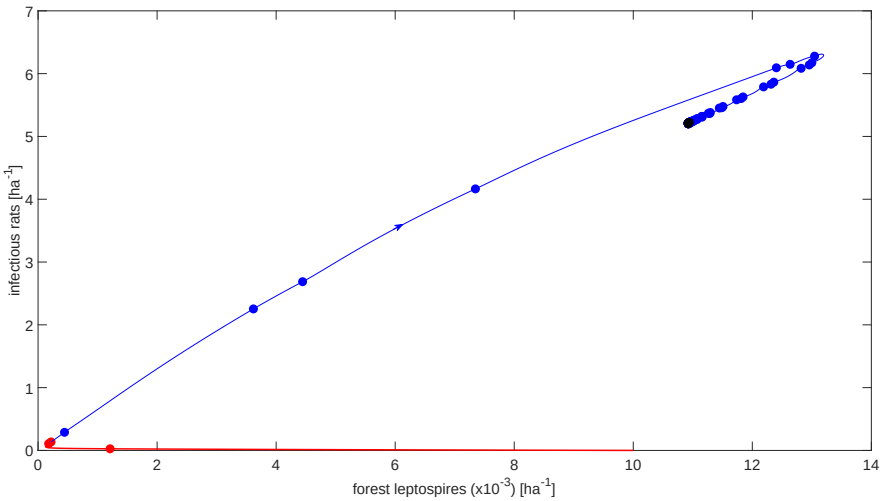

Figure 4.59: *Limit cycle diagram for the complete combined model. Phase plane showing the relationship between forest leptospires and infectious rats. First year shown in red. Limit cycle shown in black. Intermediate years shown in blue.*

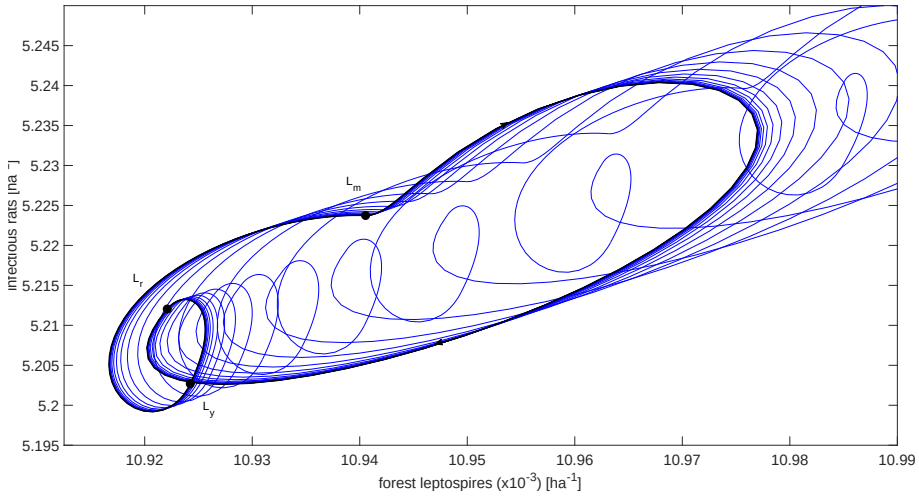

Figure 4.60: *Limit cycle diagram for the complete combined model. Phase plane showing the relationship between forest leptospires and infectious rats. Magnification of the limit cycle.*

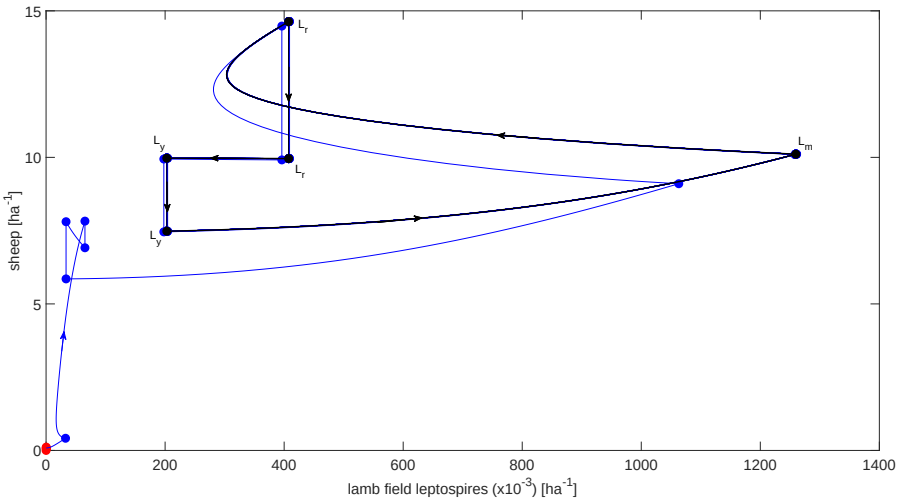

Figure 4.61: *Limit cycle diagram for the complete combined model. Phase plane showing the relationship between lamb field leptospires and sheep. First year shown in red. Limit cycle shown in black. Intermediate years shown in blue.*

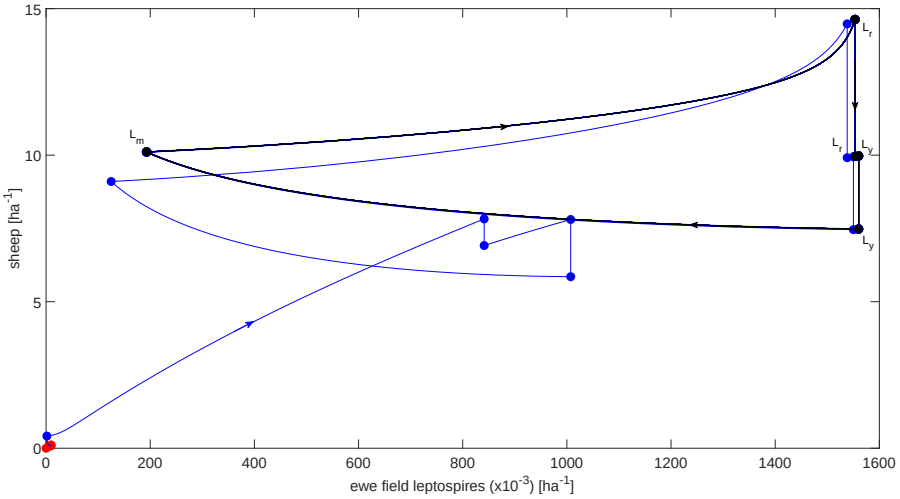

Figure 4.62: *Limit cycle diagram for the complete combined model. Phase plane showing the relationship between ewe field leptospires and sheep. First year shown in red. Limit cycle shown in black. Intermediate years shown in blue.*

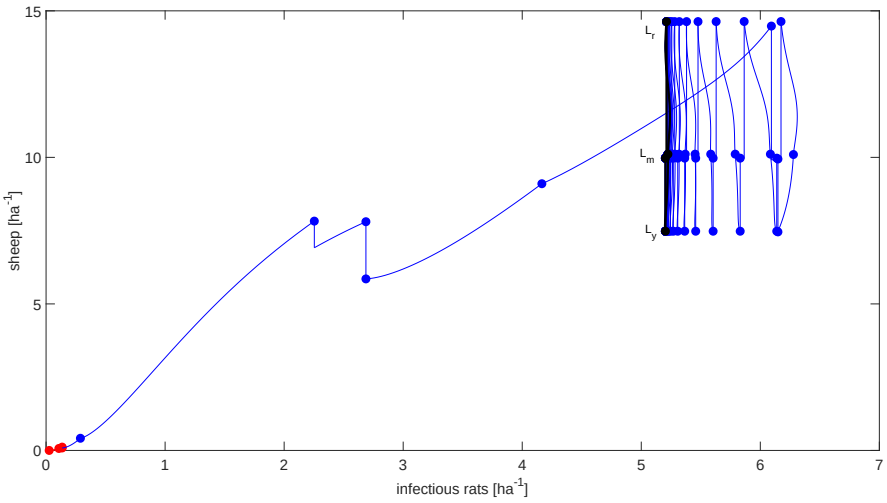

Figure 4.63: *Limit cycle diagram for the complete combined model. Phase plane showing the relationship between infectious rats and sheep. First year shown in red. Limit cycle shown in black. Intermediate years shown in blue.*

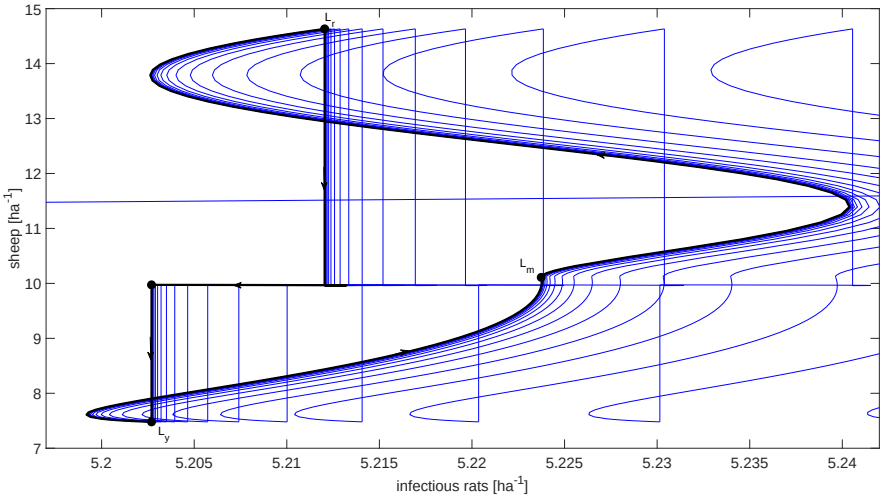

Figure 4.64: *Limit cycle diagram for the complete combined model. Phase plane showing the relationship between infectious rats and sheep. Magnification of the limit cycle.*

to sustain its population. At the final node, part of the ewe population is removed from the system and replaced with susceptible ewes causing a drop in the streamline and the cycle begins again.

The limit cycle diagram for the ewe field (figure 4.62) begins in the right most bottom corner and runs clockwise. Even though the infectious sheep population rises in the first time phase, none of the sheep are present in the field and the rate at which rats shed into the environment isn't enough to sustain the leptospire population, therefore the number of leptospires decreases until the first node. At the first node ewes are introduced into the field and the number of leptospires begins to increase. Lambs are removed from the system at the next node and the number of infectious sheep plummets suddenly; however, the number of sheep in the ewe field does not change and so the leptospire population continues to increase until the end of the year at which time part of the ewe flock is replaced with susceptible ewes and the sheep population again plummets, reaching the beginning of the limit cycle.

Using the same formula as in subsection 3.1.6, with all initial conditions except for field one leptospires (L_0) set to their respective steady state values, numerical calculations result in a negative Lyapunov exponent in the order of 10^{-3}, confirming that the limit cycles are stable.

4.3.6 The Quasi-Basic Reproduction Number, R_L

The quasi-basic reproduction number heat map is found in a similar manner as in section 4.2; however, now the leptospires in the ewe field are considered as an initial source of infection as well. The next generation matrix is as follows, where L_1 denotes the density of leptospires in the lamb field, L_2 denotes the density of leptospires in the ewe field and L_3 denotes the density of leptospires in the forest.

$$K = \begin{bmatrix} \frac{L_1(t_y)}{L_1(0)} & \frac{L_1(t_y)}{L_2(0)} & \frac{L_1(t_y)}{L_3(0)} \\ \frac{L_2(t_y)}{L_1(0)} & \frac{L_2(t_y)}{L_2(0)} & \frac{L_2(t_y)}{L_3(0)} \\ \frac{L_3(t_y)}{L_1(0)} & \frac{L_3(t_y)}{L_2(0)} & \frac{L_3(t_y)}{L_3(0)} \end{bmatrix}.$$

The quasi-basic reproduction number is found by calculating the spectral radius of the next generation matrix. This calculation is performed over a

range of parameter values, with the resulting heat map (figure 4.65) similar to those in the field-forest model (section 4.2). Low values of leptospire death rate result in high rates of infection and high values of leptospire death rate result in low rates of infection. The leptospire death rate is still a stronger control parameter than is rat birth rate; however, the rat birth rate appears to have a larger influence on the complete combined model than on the field-forest model. For this model, the range of parameter values used in the calculations do not allow the quasi-basic reproduction number to fall below one. This can be achieved by increasing the leptospire death rate to at least 0.0407 day^{-1}; however, this is outside the range considered here.

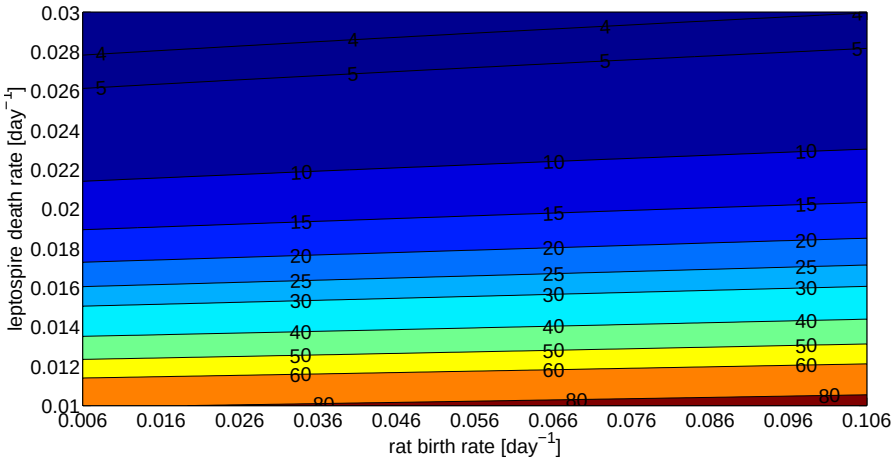

Figure 4.65: *Quasi-basic reproduction number heat map over a range of ρ and σ values for the complete combined model.*

4.3.7 Discussion

In this section, the previously explored combined rat-sheep model is expanded for each species population to incorporate their full age class structure. The construction of the model requires changes to the sub-models not covered in previous chapters. While some numerical results are similar to those previously covered, novel results have also appeared, such as the lag in the increase in forest leptospires after increases in infectious rats, and the continuation of the leptospire population in the ewe field from one year to the next. The heat maps showing population fixed points with respect to different combinations of time spent by rats in the various environments

reveal how the behaviour of rats can influence infection in livestock and may be a factor when considering the impacts of climate change. More direct parameters likely to be influenced by climate change are the leptospire death rates in the field environments, and the birth rate for rats. These effects are explored in the bifurcation diagrams. Limit cycle diagrams, as in previous chapters, show the cyclical behaviour of the system, also revealing that changes in the infection rate of rats over the year is minimal. The quasi-basic reproduction number heat map is again plotted using the next generation matrix; however, in this iteration of the model, this involves three environments. No area of the heat map considered has quasi-basic reproduction number values of less than one.

4.4 Conclusion

The first model in this chapter helps to establish a basis for the system. It shows that infection rates in rats mimic infection rates in sheep, and the behaviours of the two populations line up with one another. It is also shown that an increase in rat birth rate results in an increase in infection rates in lambs. The area of the heat map for which the basic reproduction number is less than one is quite small, indicating that infection is difficult to eliminate.

The second model improves on the first by including an environment specifically for rats. This improves the realism of the model as the first model assumes the rats spend all their time in the field. This model introduces the concept of division of time by rats in various environments, and due to the decrease of time spent by rats in the field, results in a decrease in infectious lamb and leptospire populations as compared to the first model. An interesting result is noted in that the relationship between the proportion of time spent by rats in the field and infection rates in rats, isn't monotonic increasing. Exploring the relationships of the various infectious populations with the proportion p as either the rat birth rate or the leptospire death rate is varied shows that in general the rat birth rate is more important for forest populations, while the leptospire death rate is more important for field populations. The results for the quasi-basic reproduction number, while calculated in a slightly different manner to that of the first model, are similar to those of the first model.

The final multi-species model incorporates the most realistic of both rat and sheep models. The inclusion of an extra age class in sheep results

in higher steady state values throughout, as the number of livestock is effectively doubled. The model shows that unlike in the multi-species single age class models, oscillations in rat infection rates are very small and lag behind infectious sheep rates. Exploration of the proportion of time spent by rats in the various environments show that less time spent by rats in the fields lowers infection rates overall. More time spent by rats in the lamb field as opposed to the ewe field decreases infection in the lamb environment populations, while increasing infection in the ewe environment populations. This may influence decision making in response to which population poses a greater threat to humans. For example, abattoir workers process lambs on a more regular basis than they do ewes, therefore, a farmer may like to sacrifice infection rates in ewes, by placing the ewe field closer to forests, in order to protect lamb flocks from exposure to rats. The non-linear behaviour seen in the relationship between the proportion of time spent by rats in each environment, with infection rates in rat environment populations, as seen in the field forest model, is again seen here. The quasi-basic reproduction numbers are calculated in a similar manner to those in the second model; however, in the complete combined model the quasi-basic reproduction number values are greater than one in the entire heat map indicating that it is not possible to eliminate infection.

Chapter 5

Risk to Humans

Humans acquire leptospirosis when material contaminated with the bacteria comes into contact with broken skin, mucous membranes or is ingested internally [105]. This can occur in a multitude of different ways, from direct contact with host species, such as one might see in farming or veterinary work, to indirect contact with infected animal urine, such as when wading in contaminated flood waters. Person to person transmission also appears to be possible; however, it is exceedingly rare [106]. This chapter examines likely New Zealand specific risk factors of human leptospirosis, how they may be exacerbated and how the models covered earlier in the thesis may be expanded to include humans. The impacts of the disease on infected individuals, employers and the medical system is considered, as well as possible prevention strategies.

5.1 New Zealand Specifics

New Zealanders have a unique exposure to and risk from leptospirosis. Overseas studies on human leptospirosis do not necessarily reflect local conditions due to differences in climate, cultural norms and religious practices. Factors associated with leptospirosis overseas, that are unlikely to reflect conditions in New Zealand, include; the presence of slums, prevalence of keeping animals at home, presence of livestock in the community, unvaccinated pets, availability of running water in the home, prevalence of walking barefoot, poverty, personal hygiene, high cattle density, working in rice fields, hunting rodents for food etc. [107, 108]. Overseas risk factors that may be relevant to local conditions are living close to a large river, particularly if the home is downstream of a livestock

farm and direct contact with rodents [107]. Interestingly, while the presence of rodents is considered a risk factor in New Zealand, a Fijian study found that antibody presence was not found to be associated with the presence of rodents [107].

5.2 Local Risks to Humans

The majority of leptospiral risk to humans in New Zealand is due to the livestock industry [109]. Many common occupations, such as farming, abattoir and veterinary work, put individuals in close contact with animals with potential leptospiral infection [105]. Livestock farms may result in secondary risk factors as well, with run off contaminating local water ways which people may swim in, hence acquiring infection via indirect means [105, 109].

Wildlife also provides sources of infection to domestic animals, as well as to humans, and this source may be exacerbated by climate change. Drought may force wildlife into urban areas in search of food and water, while flood waters can carry and spread free living leptospira from one environment to another; however, there are no data available on New Zealand specific rates for these [14, 110].

New Zealand also has very high rates of pet ownership compared with the rest of the world. Approximately 64% of households keep pets [111]. While domesticated pets may be yet another source of infection for humans, of the two most common pets, cats and dogs, dogs are commonly vaccinated against leptospirosis, whereas cats appear to be quite resistant to it [111]. Pet ownership, however, may decline in future, as New Zealand's housing crisis pushes more people to rent or flat, due to decreasing affordability of home ownership. This makes it difficult to keep a pet due to landlord's general unwillingness to accommodate animals on the premise [112]. Therefore, in future, pets may play an even smaller role in the spreading of infection than they do now.

5.3 Exacerbating Factors

Factors that may exacerbate the spreading of leptospiral infection include climate change and increased urbanisation. As the effects of climate change intensify, our climate may more closely reflect the environmental

conditions of our Northern neighbouring island countries. Suitable living conditions for leptospires may increase with an increase in warm, wet weather. As mentioned above, both drought and flooding may change wildlife behaviours, while increases in rainfall may increase food availability for wildlife in native forests, thereby causing an increase in wildlife population. This may result in increased wildlife population density and hence the spreading of infection.

Wildlife population density may also increase as a result of increased urbanisation. An increase in human population may result into fewer habitats suitable for wildlife, thus forcing them into smaller areas. Some types of wildlife, such as rats, will readily adapt to urban areas where there is an abundance of food available to them via human food waste. Another result of increased urbanisation may be the development of slums. The Auckland region of New Zealand is currently experiencing a housing crisis and there are concerns of the development of slums in the region, which have been shown to be a risk factor for leptospiral infection [107, 113, 114].

On a more global scale, increases in world population may create more demand for meat and other animal products, resulting in a higher number of New Zealanders being recruited into the livestock industry, thus exposing more people to infection. An increase in livestock production will exacerbate not only climate change, but may also worsen the pollution of our waterways due to livestock run off. This in turn may increase exposures due to recreational activities such as swimming in local water ways.

The New Zealand government has pledged to improve New Zealand's water quality and their proposed plans include the suggestion to remove livestock from waterways; however, they have come under scrutiny and been criticised for not being effective enough [115–118]. Thankfully, businesses as well as individuals are also making strides to improve water quality by planting native plants along waterways. This strategy may reduce run off from neighbouring farms by allowing somewhere for water to drain into the soil rather than running directly into streams after rainfall [119, 120].

While cleaning up waterways is certainly a positive move in terms of the environment and enjoyability of locals, leptospira actually prefer clean water over polluted water and if farmers and others are not careful to

prevent bacteria getting into local waterways this may in fact exacerbate the issue. Several businesses are providing water meters which allow water monitoring [121]. Technologies such as these may be useful in monitoring free living bacteria in streams, which may help farmers make informed decisions about farming practices ie. fencing off contaminated waterways, and perhaps helping to identify where their particular farm may be contributing to bacterial pollution.

5.4 Mathematical Models

The models covered in this thesis consider only animal host species, together with free living leptospires. Humans can be incorporated into the models in a variety of ways. These are discussed on a chapter by chapter basis.

The model in chapter 2 considers only rats as its animal species. Infection can be passed directly from rats to humans; however, direct contact with rats is unusual in New Zealand except for a very small minority of people (pest control workers and occasionally hunters, trappers, farmers and people working in the bush). Rats are more likely to cause infection via indirect contact through the environment. In the rat models, this infection risk comes from the free living leptospire population. The rat models could be expanded to include a susceptible human class from which people would move into an infectious class. This transition should include an environmental transmission term similar to that in the rat components of the model. A recovery term should also be included as many people infected eventually overcome the disease without any medical intervention. Those not recovering and requiring medical attention could move into an inpatient class, from which they could either recover, or be removed from the population; however, mortality as a result of infection is largely uncommon in New Zealand. Recovered humans might move into an immune compartment, as humans are believed to develop immunity to the infection-causing serovar [1, 122]. Note that this applies for models considering one serovar type only. A model considering multiple serovars would increase in complexity. The immune class, as well as the fact that humans live for much longer than the rodents considered in the model do, requires the time scale for the human class to be much slower than that of rats.

The only animal host species considered in chapter 3 are sheep. Both direct and indirect contact is likely between livestock and humans and it is possibly the most important transmitting population. Veterinarians can gain infection directly when treating all age classes of sheep, but in particular when caring for pregnant or birthing sheep. Abattoir workers commonly gain infection from infectious lambs at the slaughter house, either via urine splatter when stunning the sheep, or directly when working with the carcass. Farm workers are likely to pick up infection from sheep and free living leptospires. As for the rat model, the livestock model could be extended to include humans. Multiple subclasses of humans could be included to consider the different types of transmission commonly experienced by different professions as discussed above. The various human subclasses could include weighted transmission terms depending on where infection is likely to come from and at which strength, or include only particular types of transmission. Recovered and inpatient classes should also be included. A similar differentiation between human and animal time scales, as mentioned for the rat model, should be considered.

When considering the human component of the combined sheep-rat model in chapter 4, all the factors mentioned above should be included: multiple sub-groups for humans dependent on the likelihood of different transmission types, an infectious class, an inpatient class and an immune class. A sub-group considering only environmental transmission to humans may be divided further into two sub-groups, one for rat derived free living leptospires in a forest environment, and another for livestock derived free living leptospires in a farming environment. The leptospires in these two populations may combine in a flooding event, reaching groups of people not previously included in the human subgroups, which could expand the model even further.

5.5 Serovars

The models considered in this thesis consider only one serovar type. New Zealand has six different leptospiral serovars, from two different species. *Leptospira borgpetersenii* Hardjobovis and Ballum and *Leptospira interrogans* Pomona are the serovars most associated with human disease. The remaining three serovars, *Leptospira borgpetersenii* Balcanica and Tarassovi and *Leptospira interrogans* Copenhageni, are not commonly found in humans [4]. *L. borgpetersenii* Tarassovi is a serovar not commonly

Genospecies	**Serovar**	**Maintenance Host(s)**	**Accidental Hosts**
L.borgpetersenii	Hardjobovis	Cattle, sheep, deer	Cattle, humans
	Balcanica	Possum	Cattle, humans
	Ballum	Mouse, black rat, hedgehog	Cattle, humans
L.interrogans	Tarassovi	Pigs	Cattle, humans, dogs
	Pomona	Pigs	Cattle, sheep, humans
	Copenhageni	Norway rat	Cattle, dogs, horses

Table 5.1: *Maintenance and accidental host species of New Zealand endemic leptospire serovars. Adapted from [123].*

found in livestock either and as such it is not currently included in livestock vaccines for cows. A recent study, however, found this strain to be present in very high numbers in local dairy herds [92]. Regardless of the reason for this change, whether it is changes in weather patterns or simply as a result of bacterial adaptation, this serovar may eventually adapt to human hosts as well as livestock, providing an extra serovar of infection in humans.

Along with new exposures to humans by different serovar types, the distribution of the various serovars in humans may change. Variations in the distribution of infection of different leptospiral species have been found, with *L. interrogans* found in humid environments only, whereas *L. borgpetersenii* was present in both humid and non-humid environments [108]. The authors point out that some serovars of *L.interrogans* are well suited to survive outside a host, whereas some serovars of *L. borgpetersenii* (Hardjo) are not. Changes in the New Zealand ecosystem could have profound effects on the balance, disease dynamics and spread of the different leptospiral species. For serovars of type *L. borgpetersenii*, vertical transmission among animals via direct contacts, such as breeding, as well as pseudo-vertical transmissions via the placenta or through suckling, may have more dominant influences than horizontal transmissions.

Future models constructed to examine the dynamics of leptospiral infection in humans should consider the various serovar types and their interactions within the system and within the host. One such within system interaction is that of virulence. Different serovar types may have different virulence strengths for different host species. Infection with

multiple leptospire serovars may weaken the host's immune system, making them more likely to succumb to infection from yet more serovars or even other diseases [92].

5.6 Human impacts

While on one end of the scale, leptospiral infection may not result in any apparent form of illness at all, on the other end, the disease can result in fatalities. These are uncommon in New Zealand; however, the disease can none the less result in long term disability and causes a financial burden on the country, as well as individuals, due to medical expenses and lost productivity [90].

On an individual level, clinically ill individuals may be required to cover part, or all, of their medical costs. Time taken away from work results in lost income, the individual may be unable to return to their line of work due to complications acquired due to the disease, or may be unable to return to work at all. Additional expenses may be incurred to take care of a person's other responsibilities while they are either in hospital or recovering. These may include caring for children, family members or pets. Extra expenses may come from transportation costs, the cost of buying ready prepared food or from hiring a cleaner, if one is unable to drive, cook or clean.

Even if an individual's medical expenses are covered by insurance or the state, medical providers must shuffle resources, that could otherwise be spent elsewhere, towards treating those ill with leptospirosis. These resources might include blood needed for the dialysis of the patient, doctor's time and diagnostic resources. Another concern is that of the use of antibiotics used during the treatment of leptospirosis. Antibiotics not only eradicate the digestive microbiome of the individual, but also contribute towards the development of antibiotic resistance.

Employers of ill individuals, such as abattoir workers or farmers, may be required to continue to pay an employee who is on sick leave, as well as paying a replacement worker. Replacement workers may take time to find and they may need to be trained to do the job of the unwell individual. This can not only delay work tasks being completed, but also takes time and resources away from the person conducting the training. Upon the ill

individuals return to their place of employment, they may not be as productive as before the onset illness.

Leptospirosis can also financially impact farmers by resulting in slower growth rates in animals and a lower carcass weight at time of slaughter. In deer, this can equate to a two to four kilogram difference in carcass weight, which when added up over the animals in a herd, can result in substantial losses in profit [124]. Abortions can also occur as a result of infection, further exacerbating financial loss.

Human illness with leptospirosis can last from just a few days, to months [125]. Flu like symptoms are usually experienced; however, psychological changes may also occur. These may include depression, confusion, aggression, schizophrenia, psychosis and personality changes which can persist for months after the onset of illness [125]. Other mid to long term effects, experienced by approximately a third of patients, can include fatigue, headaches, eye pain and vision problems, dementia, muscle pain, dizziness, bronchitis, abdominal pain, myocarditis, general malaise and a weakened immune system, which may result in even more time spent on sick leave due to less severe, secondary illness such as colds [92, 126].

Haemorrhaging, internal bleeding and heart infections may occur in more severe forms of the disease and patients may need to be put on a ventilator. Long term disability or illness may be due to damage to the liver or kidneys, or due to the triggering of autoimmune reactions due to infection; however, these (autoimmune reactions) are rare and the majority of patients are believed to recover fully [126, 127]. Mild forms of infection may cause long or mid-term medical problems as well; however, this is not known [126].

5.7 Preventing Disease

The number of males who acquire leptospirosis is greater than the number of females; however, this appears to be behaviour related rather than an innate resistance on part of females. Therefore, behavioural changes, some of which are discussed below, are an important factor in preventing the disease [127].

Occupational hygiene recommendations, possibly one of the most

important prevention strategies on an individual basis, are beyond the scope of this thesis. The booklet entitled, "Prevention and Control of Leptospirosis: Good Practice Guidelines", produced by Work Safe New Zealand, however, is an excellent resource [90]. For persons working in direct contact with potentially infectious animals, personal protective equipment is important to use. For the general public, hand washing, dressing broken skin with waterproof dressings, gardening only with gloves on, avoiding waterways potentially contaminated with leptospirosis, wearing appropriate attire when cleaning up after floods, and wearing shoes, are helpful strategies to implement [105].

At risk individuals may consider getting genetic testing. Individuals with certain genetic makeup are more susceptible to acquiring the disease, as are older people and those with weakened immune systems [127]. Breastfeeding may also be a transmission route, as well as transmission through the placenta, hence, breastfeeding or pregnant women who participate in high risk activities should take care [127]. The individuals mentioned above in particular may like to pay strict attention to appropriate safety measures and keep an eye out for symptoms of leptospirosis. This requires a greater awareness of the disease in at-risk occupations, as well as in the medical community. While not necessarily preventing disease, increased awareness may prevent the disease from progressing to a point where complications occur and hospitalisation is necessary.

On a recreational level, extra care should be taken when travelling to poor, lesser developed countries or to tropical areas. These may include "South and Southeast Asia, Australia, the Caribbean, Central America, Latin America, Hawaii, Barbados, East Sub-Saharan Africa and the Andes" [128]. Water sports undertaken in untreated water, such as swimming, caving and rafting etc. are also risk factors during which care should be taken. Broken or otherwise compromised skin should be protected with waterproof coverings and showering after swimming is advised [128].

Sexual intercourse is an uncommon transmission route for leptospirosis in humans; however, as with other sexually transmitted infections, proper precautions should be taken. In general, individuals should work at improving their overall health and strengthening their immune systems, allowing them to better fight off and recover from possible infection.

From an animal perspective, upkeep of vaccinations in both livestock, as well as working dogs, plays an essential role in protecting humans against those serovars covered in the vaccine [92, 109, 129]. While human vaccines are available overseas, they are not currently in use in New Zealand. This is possibly due to the difficulty of developing a vaccine with great efficiency [130]. Therefore, exposure should be lowered at an animal level.

5.8 Conclusion

The risk of leptospirosis to humans is a multifaceted hazard with humans becoming infected via a variety of means. The consequences of the illness can be damaging on a financial level, for both individuals and the country, and the medical outcomes can span from benign to fatal. The picture of leptospiral infection is complex and continually evolving. Current preventative measures still result in a disproportionate number of human cases and these cases are likely to increase as our local climate changes as a result of greenhouse gas emissions. More research into prevention strategies needs to be done, not only at a human level, but also at an animal and environmental level.

Chapter 6

Conclusion

This chapter provides an overview of the three model types presented in this thesis. An explanation of the model structure and the inclusion of various sub-models is provided. Each model is critiqued and suggestions for improvements are made.

6.1 Wildlife Models

In chapter 2, three rat models with one, two and three age classes respectively are examined. Each model includes five variations, a summary of which is provided below. Each variation considers a different combination of possible transmission sources in rats, as well as different environmental conditions. Each variation not only has biological significance, but also provides a gentle progression into the analysis of the rat model as presented by Holt et. al. [20].

Simplification 1 The first simplification results in the most basic version of each of the age class models. It removes the environment as a source of transmission and assumes that infection is spread within the rat population via sexual contacts only. Bacteria are still shed into the environment via infectious individuals and these free living leptospires could, in a multi-species model, infect members of other animal species. One reason that pest rat populations are difficult to control and eradicate is that they are exceptionally skilled at avoiding harmful substances, one of which may be leptospira contaminated materials, thus justifying the use of this simplification [131].

Simplification 2 The second simplification removes sexual contacts as a source of transmission and considers environmental transmission only. Transmission rates of infectious diseases, especially in wildlife, are difficult to estimate and the parameter values used in the model, based on those in the paper by Holt. et. al., are educated guesses. This simplification considers the possibility that the majority of infections are gained via the environment and few are caused by sexual transmission. It also keeps the leptospire population at steady state, which helps to simplify the analysis of the model.

Simplification 3 The third simplification includes both sexual and environmental transmission sources of infection within the population but keeps the free living leptospire population at steady state. This simplification is useful in not only examining the effect the inclusion of sexual transmission has on the model by comparing it to simplification two, but also as a comparison to simplification five, which is the same as simplification three, but with the free living leptospire population allowed to vary.

Simplification 4 The fourth simplification is a more realistic version of simplification two in that it allows the leptospire population to fluctuate. The comparison of these two models can be used to determine whether complicating the model by allowing free living leptospire populations to vary has an impact on the system.

Simplification 5 The fifth simplification includes all components of the model.

In general, the complexity of the models and subsequent analysis increases from simplification one through to simplification five, and from the single age class model through to the three age class model. Where possible, it is found, using trapping regions and Dulac's criterion, that the models are biologically feasible. For each simplification, fixed points and the conditions under which they are feasible are found, stability is analysed, a bifurcation diagram is produced and the next generation matrix and R_0 are found.

Each variation has three fixed points, a trivial fixed point, where all compartment values are at zero, an 'infection free' fixed point, where the total rat populations are at their non-trivial fixed points, but the infectious

rat populations are at zero, and an 'infected' fixed point where all the fixed points of each equation of the system are positive. Each case produces a transcritical bifurcation diagram with bifurcation point at $R_0 = 1$. That is, the infection free fixed point is stable when $R_0 < 1$ and unstable otherwise, while the infected fixed point is unstable (or does not exist/is not feasible) when $R_0 < 1$ and stable otherwise. The use of various mathematical techniques is required through the progression of the models; however, in some cases results need to be calculated numerically.

Where possible, the rat models produce analytical results for sub-models of the model presented by Holt. et. al. These models are used as a basis for the models presented in chapter 3 and the compression of the model into fewer age classes prepares simpler versions of the rat model to be included in the introductory versions of the multi-species model in chapter 4.

A criticism of the model by Holt may be the assumption that infectious and susceptible rats die at the same rate. This is not necessarily an invalid assumption here, as in all the host population considered in the thesis, the infecting serovars are assumed to be host adapted.

An improvement that could be made to the model is the inclusion of seasonality in breeding, as is included in the original model by Holt, or by including birth pulses as experienced in New Zealand forest rats during mast years.

When implementing the models in chapter 2, the impact each transmission type and age class has within the rat population must be weighted out and a decision must be made in regards to which aspects of the model are required and which are not. This will depend mainly on the available literature and comparable sizes of the various parameter values for the rat population in the location of interest.

6.2 Livestock Models

A variety of models for the spreading of leptospiral infection in livestock, namely sheep, is established in chapter 3. Various components of the model in chapter 2 are used in the livestock models. These include the non-linear saturation term $\frac{L}{L+H}$ which is used in the term for environmental transmission and the structure of the differential equation

for free living leptospires.

The major difference between the two models is that the total livestock population density is fixed by the farmer, whereas the rat population is allowed to come to a steady state naturally. The sheep population also has periodic forcing imposed on it.

Four livestock models of increasing complexity are presented and each model addresses different aspects of the system as discussed on a case by case basis below.

The leptospire death rate is used as the main control parameter in all models and it is found that increases in the leptospire death rate reduce infection rates, while decreases increase it. While this approach is appropriate in the context of climate change, there are not currently any practical control strategies in place that use this tactic. It may require the development of new products which may be costly to the farmer and may also negatively impact not only the environment, but also the sheep themselves. The ingestion of novel products could result in unexpected side effects for the sheep, including decreased weight gain, reduced immunity, birth defects and the like. Testing new chemicals for safety is not only costly, but also time consuming. With the encroaching effects of climate change, a timely strategy for environmental leptospiral control would be prudent. However, perhaps a better understanding of the effects of climate change should be explored before attempting to make changes to farming practices, as these may be nullified or diluted with changes in weather and climate patterns. In this way, the leptospire death rate is a sensible choice for control parameter as it is one likely to vary not only seasonally, but also as a result of climate change. As such, future work should allow the seasonal varying of leptospire death rate over the course of the year.

Another criticism of the models is that they assume a homogeneous environment. On a macro level, farming practices vary across the country. The livestock load on a paddock, for example, changes depending on the topography of the paddock and the part of the country the farm is located in. Soil type and local weather conditions vary across the country as well and these impact on the leptospire death rate. On a micro level, sheep may not graze homogeneously across a paddock. They may, for example, cluster around a watering trough or a stream, around which bacterial survival may be enhanced, or they may seek shelter from winds behind a

grove of trees. This argument is especially applicable for the combined rat-sheep chapter (chapter 4) which specifically assumes that rats enter the field for the purposes of accessing water.

Finally, data for parameter values overall are exceptionally difficult to find and it is impossible to consider all variables in a real world scenario. The environmental transmission coefficient for example is found numerically and has no data available for it and the default parameter value for leptospire death rate used is based on a minimum survival time. While these are the best data currently available, they may underestimate how long the bacteria survive in the environment.

6.2.1 Sheep Model A

Sheep model A (section 3.1) considers only one field and one age class. The advantage of considering only one environment is that it allows the model to remain simple. It can be assumed that the size of the field remains constant and so the density of sheep allowed to graze on it is also constant. The model focusses on leptospires in only one environment, rather than complicating the model by allowing multiple sources as in models C and D (section 3.3 and section 3.4).

In practice, a farmer is likely to have more than one field, moving the flock of sheep from one field to another as the pasture is consumed and replenished over time. Pasture requires time to recover after having been grazed and this time may vary depending on the time of year and location. Livestock are also commonly grazed with members of a different species, for example, sheep and cows together.

Sheep model A is unrealistic in that it ignores the fact that there is a period of time during which lambs must be with their mothers. Model A, however, is simply a foundational model upon which models B, C and D build, and a way to introduce various concepts. These include the absence of the host population during part of the year, the resetting of the host population at the beginning of each year, cobweb diagrams as a technique to find fixed points used in bifurcation diagrams, the concept of the limit cycle and the notion of the quasi-basic reproduction number. The simpler system allows for a simpler proof of the existence, stability and uniqueness of the limit cycle, which is the main result for the chapter.

Several variations of the system are considered, all of which could be used as future avenues of research. The first variation considered is the inclusion of recovery in the model. While this is not supported by the literature, not all the animals in a flock appear to be infectious [53]. This may be due to some inherent immunity, which is included for lambs in sheep models C and D, but it could also be as a result of recovery. Even though the value for the recovery parameter is small, it significantly reduces infection rates in both field and flock. The general behaviour of the recovery model does not differ much from the basic model other than in the size of the infectious population densities. This line of research could be followed in the event that evidence supporting recovery emerges. Currently, however, there are no data to support naturally occurring recovery and recovery as a result of human intervention would likely be implemented via vaccination at a flock, rather than an individual level.

Another section is dedicated to removal time, with preliminary results looking promising. This may have been a good line of inquiry to pursue, as the strategy can be implemented immediately by farmers without having to rely on the development of new products. It requires no special equipment and is easy to implement and understand, all the while resulting in a substantial decrease in infection rate. As mentioned in section 3.1, removing lambs from the field a little over a week early can stifle the spreading of infection completely. The issue with this approach is that it requires the lambs to be removed before a very specific time. The farmer prefers to send livestock to the abattoir when the meat is likely to fetch a premium price and the live weight of the animal is at its highest. The timing most ideal for the prevention of leptospiral spreading may not suit the farmer, who is trying not only to increase his profit margins, but also likely juggling multiple flocks and a barrage of other farming tasks. In a system involving only sheep, this approach may be useful to implement for a limited number of years to eliminate infection from an already infected farm, after which the removal date could be pushed back while other preventative strategies could be put in place to prevent the reinfection of the farm.

The final variation considered in sheep model A is turning the equations for the first time phase into a second order differential equation. This provides a convenient method to explore the system mathematically. It is proved that the turning point of the system is a minimum, rather

than a maximum, revealing the general conduct of infection. One of the possible short comings of all the models is the value of the parameter value H in the non-linear saturation term $\frac{L}{L+H}$. H is the density of leptospires at which transmission from the environment is half the environmental transmission coefficient. Finding a realistic value for this parameter is biologically challenging and the one used may not reflect real world conditions. Two cases are considered for H at extreme values when compared to L ie. H is very small or very large in comparison to L. When H is very small the second order differential equation reduces to one for which an analytical solution can be found and when H is very large the whole system is expected to tend to zero.

6.2.2 Sheep Model B

Model B expands on model A by including an extra age class. This increases the realism of model A by acknowledging that until the time of weaning, lambs are hosted in the field together with their mothers and as such, the environmental burden of leptospires in the field is greater. Unlike the other models in chapter 3 this model includes pseudo-vertical transmission from mother to offspring and would be good base model in the event that this transmission route were confirmed in the future.

The model considers and compares various ewe and leptospire initial conditions. The cases considering the trivial initial condition for infectious ewes assumes antibiotic treatment of ewes at the beginning of each year while cases considering a fixed number of infectious ewes at the beginning of each year reflect real life data. While longitudinal infection rates are unavailable, infection rates during a snapshot in time are at least accurate. This set up results in higher rates of infection overall as compared to the trivial initial condition case for infectious ewes and could encourage farmers to regularly treat infectious livestock. The issue with this scenario is that it would be sensible to vaccinate sheep in concert with antibiotic treatment and this is not included in the model.

When the initial condition for infectious ewes remains the same and the initial condition for the environment is varied, the behaviour of the system is very similar over time indicating that the initial condition of infectious ewes each year is a more powerful indicator of the behaviour of the system when compared to the leptospiral initial condition. This is also reflected in the cobweb diagrams of the model considering non-trivial initial conditions

for infectious ewes. As a consequence of this scenario, only a single fixed point is allowed for the system, revealing that infection rates in ewes are a strong driving force of infection in the system and require greater decreases in the leptospire death rate to reduce infection rates in the system to the trivial fixed point as compared to the trivial ewe initial condition case. This would encourage the promotion of flock treatments over environmental treatments.

Two of the cases considered in the section allow infectious proportions of ewes to carry over from one year to the next. This increases realism in that there is continuity of infection in the flock; however, it ignores the period of time in which the behaviour of infection in the ewe population is not modelled while they are absent from the field. This shortcoming is remedied in model D which introduces an additional field into the model. The latter of the two continuity cases mentioned includes a recovery term which is quite useful in allowing infection to carry over from one year to the next without allowing infection rates to approach carrying capacity, which has been shown to be inaccurate when considering data on infection rates.

Most of the parameter values used in model B are carried over from model A. As such, any unreasonable or ill-considered values are also passed across. No data on pseudo vertical transmission for sheep are available and so the value taken for this parameter is taken from Holt et. al. and is a rat parameter which could be very different to sheep. The term stocking unit refers to one ewe and her lamb. As model B considers both of these populations, this model embodies the real definition of the stocking unit and as such is an improvement on model A which essentially considers only half the number of animals.

The general recommendation for weaning time for sheep is 90 days. This is a fixed term in the model; however, allowing this parameter to vary and exploring the spreading of infection in concert with lamb growth rates and the resulting liveweight at time of slaughter would be an important avenue of research which considers the financial concerns of the farmer.

Environmental transmission in lambs is taken as a fixed value which is based on the average value of consumption over time. In reality, lambs gradually increase the amount of grass they eat while decreasing the amount of milk they eat until the time of weaning during which time milk

consumption is suddenly stopped. This would suggest including two inversely related functions to the model, the lamb environmental transmission term and the pseudo-vertical transmission term.

The added realism of the model also adds complexity with does not allow an analytical expression for the quasi-basic reproduction number R_L to be found.

6.2.3 Sheep Model C

Sheep model C improves model B in that it includes maternally derived immunity which is supported by the literature, and excludes pseudo-vertical transmission for which the evidence is conflicting.

When using the same parameter values as in model B, the added step required to infect lambs in the form of the added immune compartment results in infection not taking off. In order to simulate infection in the model, the shedding rate of lambs (and thus by extension ewes) is increased. If an immune compartment were allowed for ewes as well as lambs, infection rates could again reduce to subcritical levels. This could be a very important control strategy for New Zealand sheep flocks and is one which is already supported in part by the success in using vaccination in pig and dairy herds. The vaccination of ewes, particularly before lambing, could have added beneficial effects to the immunity of the lambs as well, as antibodies may be passed from mother to offspring not only via colostrum, but also transplacentally. The stumbling block of immunity to the progression of the disease could also be enforced onto lambs by farmers directly via vaccination after birth.

6.2.4 Sheep Model D

In sheep model C ewes are considered to be susceptible at the beginning of each year. This arrangement is unrealistic in that even if there is some interference by the farmer in the infection of the animals, it is likely to be vaccination in combination with treatment, not simply treatment alone. Sheep model D improves on this scenario by allowing (some proportion of) the infectious ewe population to be passed from one year to the next. This requires the model to follow the growth of the infectious ewe population during the time that they are separated from their lambs and this is

achieved by introducing a second environment into the system.

The model also improves on the realism of the system by considers the lifespan of sheep. A certain proportion of the ewe population is removed from the system each year and replaced with an equal number of susceptible ewes. Model D assumes a steady turnover of ewes where 25% of the flock is replaced each year. In reality a farmer may replace whole flocks every four years instead, or have some other arrangement and these differing farming practices should be considered. As mentioned in the discussion to model C, ewes should also be introduced into the population as immune, rather than susceptible, and this should be included in future models as well.

In order to prevent the system from becoming too complex, the ewes are removed from field one and placed into a sterile (from leptospires) environment. As explained in section 3.4, this could be achieved by using a different field for the ewes each year, or by treating the environment. This may not be an option on all farms, however. Fields are often grazed by other livestock, which may host the same or different leptospire serovar types and contamination may also be introduced into the environment by wildlife (consider in chapter 4).

Despite attempts to maintain simplicity, some complexity in the analysis of the model is introduced. Firstly, cobweb diagrams must consider two initial conditions and so are turned into heat maps in order to display steady states. An unusual result is discovered when plotting cobweb heat maps for different values of ρ. As one increases ρ, the non-trivial steady state reaches a quasi-trivial state before reaching the true trivial steady state. This quasi-trivial steady state is one where the leptospire population in field one reaches zero at the beginning/end of each year, whereas the number of infectious ewes does not. This result could be misleading if one were to ignore the behaviour of leptospires during the remainder of the year.

The two dimensionality of the initial conditions leads to the examination of two bifurcation diagrams as well. However, as is discussed in the section on the bifurcation diagram in section 3.4 (subsection 3.4.5), only the bifurcation diagram involving the infectious ewes is required. This, as well as the results found in sheep model B (section 3.2) which found that the livestock initial condition has a stronger effect on the

behaviour of the model than free living leptospires, suggests that the focus of future work could be on infectious livestock, rather than free living leptospires.

Another result of the added complexity in the model is difficulty in proving the existence of a limit cycle. While numerical results clearly display that the system does indeed reach repetitive behaviour, the analytical proof of such results is not trivial. It can at least be proved that $L_y(\rho)$ is monotonic decreasing and the Lyapunov exponent finds the limit cycle to be stable. Despite the minor shortcomings of this model in terms of analytical results, the numerical results presented are revealing of the behaviour of infection in the system and may prove to be a useful tool in future research and policy making.

6.3 Combined Models

The final chapter involving a mathematical model combines a variety of models from each of the two previous chapters (chapter 2 and chapter 3). This final set of models explores the interaction of the two host species through their mutual environment, and how infection rates in one host population influences those of the other. As the models in chapter 4 are a compilation of ones previously discussed in the present chapter, many of the same comments and criticisms apply. The multi-species model chapter begins by combining a pair of the most simple of the rat and sheep models in order to construct a base model upon which the more complex models are built.

As in the sheep models, increases in leptospire death rate decrease infection rates, and decreases increase it. This control parameter is now paired with an additional aspect of the system, namely, rat birth rate. This is done in order to simulate climate change. In general, increases in rat birth rate increase infection rates, while decreases decrease it. This results in two extremes of infection at opposite ends of parameter space. Low leptospire death rate paired with high rat birth rate results in high rates of infection, and high leptospire death rate paired with low rat birth rate results in low rates of infection. These parameter value pairs are likely to occur as a result of increased and decreased rainfall respectively. A moderate increase in rainfall may result in increased breeding among rats due to an increase in food availability while at the same time supporting

environmental leptospire survival. Conversely, a major decrease in rainfall resulting in drought would reduce food availability, thus reducing rat birth rate, as well as exacerbating leptospire death as the bacteria dry out in the arid conditions. These results are apparent in bifurcation and quasi-R_0 heat maps across all the models in the chapter.

A parameter introduced into the multi-environment models as a result of the interaction of the two host species is the proportion of time spent by rats in various environments. This is another parameter value which may be influenced by climate change; however, results involving this parameter cannot be generalised in concert with results involving the leptospire death rate and rat birth rate. Therefore, results involving the proportion of time spent by rats in the various environments are considered separately.

An example of how climate change may influence the proportion of time spent by rats in each environment is a major increase in rainfall. This may, for example, force ground dwelling Norway rats to higher ground, which, depending on topography, may either limit their access to nearby fields, or force them to spend more time in them. The black rat, which is an excellent climber, may spend more time tree bound as a result of high rainfall. A major decrease in rainfall resulting in drought on the other hand could increase the parameter value by forcing rats to enter the pasture more often in search of water. None-the-less, heat maps showing the behaviour of infectious steady states over a range of proportions of time spent by rats in the various environments show that the less time spent by rats in the livestock environments, the less infection there is in the system overall. This should encourage farmers to attempt to deter rats from entering the livestock environments as a strategy to reduce infection rates in livestock and the field.

A concern for the combined models is the host shedding rate. These are taken arbitrarily and to be less than the total number of leptospires shed per infectious host per day, as not all leptospires shed are assumed to remain on the surface of the pasture. It should be noted that the number of leptospires shed per animal per day is not proportional by body weight betweem species. Rats shed between 10^5 and 10^7 leptospires per day. This is a huge range, with a 100 fold difference between the lower and upper limits. Lambs on the other hand shed between 10^6 and 10^9 leptospires per day, which has an even wider range than that of rats. One should also note that according to this data, a rat shedding at a high rate (10^7 leptospires per day) is able to shed

more than a lamb shedding at a low rate (10^6 leptospires per day). This is despite rats being on average approximately 230 times smaller than lambs. The bodies of sheep are also high up off the ground and urine is likely to land on the surface of the grass, which is then likely to be consumed by the same, or another, sheep. Rats, being close to the ground, are unlikely to shed onto grass that will be consumed, and more likely to shed directly onto the dirt, where the leptospires have a chance to seep into the soil. So the scaling of the shedding rates between host types is likely to be inaccurate, as sheep may be less likely to become infectious by rat shed leptospires than by sheep shed leptospires, while rats are likely to become infectious by both. This scenario occurs, of course, in the absence of precipitation, which may bring leptospires which have been absorbed into the soil up to the surface of the pasture and into contact with both host species. The overall effect cannot be clarified until further data are available in the literature.

6.3.1 Wildlife-Livestock Model

The wildlife-livestock model combines the most simple of the rat and sheep models and forms the basis for the models that follow. The use of the rat birth rate as a control parameter for infection is introduced and the influence of the periodic nature of the sheep population is shown to be reflected in infection in the rat population. This model also shows that a trivial steady state cannot be reached in the multi-species model.

The sensitivity analysis for this model of the leptospire steady state with respect to animal density points towards the use of reducing animal density as a tactic for reducing leptospiral load on the environment, and subsequently the host species. The thesis considers only the reduction of rat densities when considering control; however, a decrease of a single sheep could have far greater effects. This makes sense, as the number of leptospires shed per infectious sheep is far greater than that of infectious rats; however, a strategy of this kind would also have economic implications which may outweigh the benefits, and so this line of exploration is not followed further.

6.3.2 Field-Forest Model

In the livestock-wildlife model rats are assumed to spend all their time in the field, whereas in reality they are likely to divide their time, and hence shedding and environmental exposure, among different environments. The wildlife-livestock field-forest model improves on this by introducing an

environment especially for rats. This enhancement in the realism of the model results in lower infection rates than those in the wildlife-livestock model due to the division of time into two environments. An interesting result should be noted in that the relationship between the density of infectious rats and the proportion of time spent by rats in the field is not monotonic increasing as one would expect and as are the other model populations; however, this anomaly does not impact on infectious lamb rates.

Due to the presence of two environments, each with the ability to introduce infection into the system, the quasi-basic reproduction numbers are found by numerically calculating the spectral radius of the next generation matrix involving the two environments. The quasi-basic reproduction numbers appear to be more sensitive to leptospire death rate than to rat birth rate, regardless of the amount of time spent by rats in the field. A common result apparent in the heat maps is the reduction of infection as leptospire death rate is increased. The system is found to become more sensitive to this parameter value as the time spent by rats in the field is increased.

6.3.3 Complete Combined Model

The final model in the thesis combines the most complex of both rat and sheep models. This requires the reassignment of various rat specific parameter values, as well as some other adjustments to values so that the system behaves in a biologically plausible manner. The rat's time is now divided among three environments, with proportions chosen arbitrarily due to the lack of available data in the literature. The initial condition for the ewe field must now be set to be non-trivial, with infection in ewes being carried over from one year to the next. This both complicates the system and makes it more realistic.

The behaviour of the model is as one may expect. Bifurcation diagrams reveal that as compared to the previous model, this model is more sensitive to rat birth rate. The graphs showing the total population of rats over time shows the behaviour of the different age classes over time as well. If rat birth rate were allowed to vary over the course of the year, this behaviour would change, potentially impacting on infection rates in sheep, as sub-adult rat populations have been shown to oscillate at a higher amplitude than adult and juvenile populations.

Some non-monotonic increasing behaviour in relation to the proportion of time spent in each environment, as for the field-forest model, is apparent in the infectious rat and forest leptospire populations as well, and in which population this appears depends on the rat birth rate.

Infection rates in each population are sensitive to the amount of time spent by rats in either the lamb field or the ewe field. Those more sensitive to the lamb field are: infectious rats, ewes and ewe field leptospires. Those more sensitive to the ewe field are: lambs, lamb field and forest leptospires.

An exploratory option for this system is to assume that rats do not enter the ewe field until the ewes are introduced into it. This could reflect efforts by the farmer to cover watering troughs, thus removing incentive for rats to enter the field. This would, of course, make the parameters for proportions of time spend by rats in each of the environments change for each time phase over the course of the year, thus complicating the system.

In this chapter, each model is both defended and scrutinised for its choices, and suggestions for developments and alternative lines of research for future work are made. Overall, each model attempts to consider a variety of scenarios for each host species while keeping the system as simple as possible. While each model dabbles in an assortment of different areas, the impact of climate change is a major consideration when varying parameters and it is found that the two climatic extremes New Zealand and the world are expected to experience have profound impacts on infection rates in the models. The models, unfortunately, only consider constant values for the parameters likely to be influenced, and so future work should consider fluctuations in these values over time.

Bibliography

[1] Leptospirosis. Fact sheet, World Health Organization, Regional Office for South-East Asia, 2003.

[2] G. Pappasa, P. Papadimitrioua, V. Siozopouloua, L. Christoub, and N. Akritidisc. The globalization of leptospirosis: worldwide incidence trends. *International Journal of Infectious Diseases*, 12(4):351–357, July 2008. `https://www.sciencedirect.com/science/article/pii/S1201971207001956#tbl2`.

[3] World Economic Situation and Prospects. Technical report, United Nations, New York, 2014.

[4] *Leptospirosis overview*. Leptospirosis.org.nz. Accessed: 2018-09-30, from `http://leptospirosis.org.nz/Leptospirosis.aspx`.

[5] *Leptospirosis: Reducing the impact on New Zealand workplaces*. Department of Labour, Wellington, 2007. ISBN: 978-0-478-28142-2.

[6] C.N. Thornley, M.G. Baker, P. Weinstein, and E.W. Maas. Changing epidemiology of human leptospirosis in New Zealand. *Epidemiol. Infect.*, 128(1):29–36, Feb 2002.

[7] M.P Ward. Seasonality of canine leptospirosis in the United States and Canada and its association with rainfall. *Preventive Vetinary Medicine*, 56:203–213, 2002.

[8] A. Florence, B. Victoriano, L.D. Smythe, N. Gloriani-Barzaga, L.L. Cavinta, T. Kasai, K. Limpakarnjanarat, B.L. Ong, G. Gongal, J. Hall, C.A. Coulombe, Y. Yanagihara, S. Yoshida, and B. Adler. Leptospirosis in the Asia Pacific region. *BMC Infectious Diseases*, 9(147), September 2009.

[9] A.F. Victoriano, L.D. Smythe, N. Gloriani-Barzaga, L.L. Cavinta, T. Kasai, K. Limpakarnjanarat, B.L. Ong, G. Gongal, J. Hall, C.A. Coulombe, Y. Yanagihara, S. Yoshida, and B. Adler. Leptospirosis in the Asia Pacific region. *BMC Infect. Dis.*, 9:147–155, Sep 2009.

[10] W. Lilenbaum, R. Varges, F.Z. Brandão, A. Cortez, S.O. de Souza, P.E. Brandão, L.J. Richtzenhain, and S.A. Vasconcellos. Detection of Leptospira spp. in semen and vaginal fluids of goats and sheep by polymerase chain reaction. *Theriogenology*, 69:837842, 2008.

[11] Factsheet about leptospirosis. Fact sheet, European Centre for Disease Prevention and Control , June 2017.

[12] Accident Compensation Corporation. *Leptospirosis in New Zealand, An overview of clinical best practice* (ACC Review 54). Technical report, May 2014. Accessed: 2016-12-30, from `www.acc.co.nz`.

[13] Institute of Environmental Science and Research Limited, Porirua. *Notifiable and other diseases in New Zealand,* Annual Report 2012.

[14] C. Heuer, J. Benschop, L. Stringer, J. Collins-Emerson, J. Sanhueza, and P. Wilson. *Leptospirosis in New Zealand - Best Practice Recommendations for the use of vaccines to prevent human exposure.* Report by Massey University. Prepared for the Zealand Veterinary Association, June 2012.

[15] Leptospirosis cost could top $130 million. *NZ Farmer*, December 2014.

[16] *Antibiotics and resistance.* New Zealand food safety. Accessed: 2018-12-07, from `https://www.mpi.govt.nz/food-safety/whats-in-our-food/chemicals-and-food/agricultural-compounds-and-residues/antibiotics-and-resistance/`.

[17] S.C. Hathaway. Leptospirosis in the possum *Trichosurus* Vulpecula. *Proceedings of the First Symposium on Marsupials in NZ*, 1981.

[18] M. G. Roberts and J. A. P. Heesterbeek. Characterizing the next-generation matrix and basic reproduction number in ecological epidemiology. *J. Math. Biol.*, 2012.

[19] O. Diekmann, J.A. Heesterbeek, and J.A. Metz. On the definition and the computation of the basic reproduction ratio R_0 in models

for infectious diseases in heterogeneous populations. *J. Math. Biol.*, 4(28):365–82, 1990.

[20] J. Holt, S. Davis, and H. Leirs. A model of leptospirosis infection in an African rodent to determine risk to humans: Seasonal fluctuations and the impact of rodent control. *Acta Tropica*, 99:218–225, 2006.

[21] C. Heuer, R.M. Mitchell, Y.H. Schukken, Z. Lu, C. Verdugo, and P.R. Wilson. Modelling transmission dynamics of paratuberculosis of red deer under pastoral farming conditions. *Prev. Vet. Med.*, 106(1):63–74, Sep 2012.

[22] Predator traps. Accessed: 2017-07-18.

[23] J.G. Innes, C.M. King, M. Flux, and M.O. Kimberley. Population biology of the ship rat and Norway rat in Pureora Forest Park, 198387. *New Zealand Journal of Zoology*, 28:57–78, 2001.

[24] NZ Landcare Trust. *Northland Pest Control Guidelines*. 2016.

[25] G.A. Harper and N. Bunbury. Invasive rats on tropical islands: Their population biology and impacts on native species. *Global Ecology and Conservation*, 3:607–627, Jan 2015.

[26] C.M. King, editor. *The handbook of New Zealand Mammals*. Oxford University Press, 2 edition, 2005.

[27] M.J. Daniel. Bionomics of the ship rat (*Rattus r. rattus*) in a New Zealand indigenous forest. *New Zealand Journal of Science*, 15(3):313–341, 1972.

[28] G.L. Blackwell, M.A. Potter, and E.O. Minot. Rodent and predator population dynamics in an eruptive system. *Ecological Modelling*, 25:227–245, 2001.

[29] A.R. Spickler and K.R. Leedom Larson. Leptospirosis. Fact sheet, The Center for Public Security and Health, Aug 2013.

[30] M.J. Caimano, S.K. Sivasankaran, A. Allard, D. Hurley, K. Hokamp, A.A. Grassmann, and et al. A model system for studying the transcriptomic and physiological changes associated with mammalian host-adaptation by *Leptospira interrogans* Serovar Copenhageni. *PLoS Pathog*, 10(3), 2014.

[31] A.M. Monahan, J.J. Callanan, and J.E. Nally. Proteomic analysis of *Leptospira interrogans* shed in urine of chronically infected hosts. *Infect. Immun.*, 76(11):4952–4958, Nov 2008.

[32] S.H. Strogatz. *Nonlinear Dynamics and Chaos*. Perseus Books Publishing, Reading, MA, United States, 1994.

[33] D.A. Sánchez. *Ordinary differential equations and stability theory: An introduction*. W. H. Freeman and Company, 1968.

[34] J.A.P. Heesterbeek, O. Diekmann, and M.G. Roberts. The construction of next-generation matrices for compartmental epidemic models. *Journal of The Royal Society Interface*, 7:873–885, 2010.

[35] B. Shulgin, L. Stone, and Z. Agur. Pulse vaccination strategy in the SIR epidemic model. *Bull. of Math. Bio.*, 60:1123–1148, 1998.

[36] C. Verdugo. *Epidemiology of Mycobacterium avium subspecies paratuberculosis infection on sheep, beef cattle and deer farms in New Zealand: A thesis presented in partial fulfilment of the requirements for the degree of Doctor of Philosophy at Massey University*. PhD thesis, Institute of Veterinary, Animal and Biomedical Sciences, Massey University, Palmerston North, New Zealand, 2013.

[37] R.C. Johnson. *Medical Microbiology*, volume 4. Galveston (TX): University of Texas Medical Branch at Galveston, 1996.

[38] World Health Organization. *Guidelines for safe recreational water environments: Volume 1 - Coastal and fresh waters*. World Health Organization Geneva, 2003. ISBN 92 4 154580 1.

[39] *Survival of leptospires in the environment*. Leptospirosis information, 2011. Accessed: 2017-09-18, from `http://www.leptospirosis.org/survival-of-leptospires-in-the-environment-2/`.

[40] S. Baron. *Medical Microbiology*, volume 4th edition. University of Texas Medical Branch at Galveston, Galveston, Texas, 1996.

[41] A. Shimshony. A closer look at leptospirosis - part 1. *Infect. Dis. News*, November 2009.

[42] G. Trueba, S. Zapata, K. Madrid, P. Cullen, and D. Haake. Cell aggregation: a mechanism of pathogenic leptospira to survive in fresh water. *Int. Microbiol.*, 7(1):35–40, Mar 2004.

[43] J.S. Hellstrom and R.B. Marshall. Survival of *Leptospira interrogans* serovar Pomona in an acidic soil under simulated New Zealand field conditions. *Res. Vet. Sci.*, 25(1):29–33, Jul 1978.

[44] J. Dymond. *Ecosystem Services in New Zealand: Conditions and Trends*. Manaaki Whenua Press, Lincoln, New Zealand, 2013.

[45] Ministry of Agriculture and Forestry. *Northland Sheep and Beef: Pastoral Monitoring*. Report by Ministry of Agriculture and Forestry, August 2011.

[46] *National sheep and beef: Farm Monitoring*. Ministry for Primary Industries, August 2012. ISBN 978-0-478-40425-8.

[47] Farmlands Co-operative Society Limited. *Farmlands lifestyle guide*, 2016. Retrieved from `https://issuu.com/farmlands/docs/farmlands_lifestyle_guide`.

[48] *A guide to feed planning for sheep farmers*. Beef and Lamb New Zealand, June 2012. ISBN 0 - 908768 - 25 7.

[49] E. Jarlath, J.E. Nally, A.M. Monahan, I.S. Miller, R. Bonilla-Santiago, P. Souda, and J.P. Whitelegge. Comparative proteomic analysis of differentially expressed proteins in the urine of reservoir hosts of leptospirosis. *PLOS One*, October 2011.

[50] P. Rojas, A.M. Monahan, S Schuller, I.S. Miller, B.K. Markey, and J.E. Nally. Detection and quantification of leptospires in urine of dogs: a maintenance host for the zoonotic disease leptospirosis. *Eur J Clin Microbiol Infect Dis.*, 29(10):1305–9, Oct 2010.

[51] S. Weis, A. Rettinger, M. Bergmann, J.R. Llewellyn, N. Pantchev, R.K. Straubinger, and K. Hartmann. Detection of leptospira DNA in urine and presence of specific antibodies in outdoor cats in Germany. *Journal of Feline Medicine and Surgery*, February 2016. online.

[52] S. Subharat. *Epidemiology, diagnosis and vaccination control of leptospirosis in farmed deer in New Zealand*. PhD thesis, Institute of Veterinary, Animal and Biomedical Sciences, Massey University, Palmerston North, New Zealand, 2010.

[53] J.S. Hellstrom. *Studies on some aspects of the epidemiology of bovine leptospirosis*. PhD thesis, Veterinary Pathology and Public Health, Massey University, Palmerston North, New Zealand, 1978.

[54] F.C. Leonard, P.J. Quinn, W.A. Ellis, and K. O'Farrell. Association between cessation of leptospiruria in cattle and urinary antibody levels. *Research in Veterinary Science*, 55:195–202, 1993.

[55] World Health Organization. *Guidelines for leptospirosis control*. World Health Organization Geneva, 1982. ISBN 92 4 170067 X.

[56] M.A. Ayanegui-Alcerreca. *Epidemiology and control of leptospirosis in farmed deer in New Zealand*. PhD thesis, Veterinary and Clinical Sciences, Massey University, Palmerston North, New Zealand, 2006.

[57] G.J. Cruickshank, B.C. Thomson, and P.D. Muir. *Modelling management change on production efficiency and methane output within a sheep flock*. Final Report for Ministry of Agriculture and Forestry, On-Farm Research Ltd, June 2008.

[58] S.E. Fielder. *Urine Volume and Specific Gravity*. Merck Manuals. Accessed: 2016-05-18, from `http://www.merckvetmanual.com/mvm/appendixes/reference_guides/urine_volume_and_specific_gravity.html`.

[59] K. Vinod Kumar, C. Lall, R. Vimal Raj, K. Vedhagiri, and P. Vijayachari. Coexistence and survival of pathogenic leptospires by formation of biofilm with azospirillum. *FEMS Microbiol Ecol.*, 91(6):218–225, Jun 2015.

[60] M.D. Weir, J. Hass, and F.R. Giordano. *Thomas' Calculus*. Perseus Books Publishing, Boston, MA, United States, 11 edition, 2005.

[61] M. G. Roberts and J.A.P. Heesterbeek. The dynamics of nematode infections of farmed ruminants. *Parasitol.*, 110(4):493–502, May 1995.

[62] Fact sheet: Lactation, lamb growth and the lamb weaning decision. Fact sheet, Beef+Lamb New Zealand, August 2009.

[63] L. Genever. *Lamb briefing: Nutrition at weaning*. AHDB Beef and Lamb, June 2015. Accessed: 2017-04-06, from `beefandlamb.ahdb.org.uk`.

[64] M. Barkley. Weaning practices limit stress to ewes and lambs. *Penn State Extension*, June 2014. Accessed: 2017-04-06, from `http://extension.psu.edu/animals/sheep/news/2014/weaning-practices-limit-stress-to-ewes-and-lambs`.

[65] S. Schoenian. *Sheep 201: A beginner's guide to raising sheep*. Sheep201, February 2014.

[66] G. E. Ricketts. Weaning management of lambs and ewes is important. *Illinois Livestock Trail by University of Illinois Extension*, January 1999. Accessed: 2017-04-06, from `http://livestocktrail.illinois.edu/sheepnet/paperdisplay.cfm?contentid=667`.

[67] P.R. Kenyon. *Hogget Performance - Unlocking the potential*. Beef and Lamb New Zealand, February 2012.

[68] Anou Dreyfus. *Leptospirosis in humans and pastoral livestock in New Zealand*. PhD thesis, Institute of Veterinary, Animal and Biomedical Sciences, Massey University, Palmerston North, New Zealand, 1 2013.

[69] World Health Organization. *Human leptospirosis : guidance for diagnosis, surveillance and control.* World Health Organization, Malta, 2003.

[70] J.D. Hoski. *Update on babesiosis, leptospirosis in dogs: Reviewing means of transmission, latest diagnosis and treatment protocols*. DVM360 Magazine, Jul 2008. Accessed: 2016-09-20, from `http://veterinarynews.dvm360.com/update-babesiosis-leptospirosis-dogs`.

[71] K.F. Lunn. *Overview of Leptospirosis*. Merck Manuals, 2015. Accessed: 2016-08-20, from `http://www.merckvetmanual.com/mvm/generalized_conditions/leptospirosis/overview_of_leptospirosis.html`.

[72] D. Herenda. *Human leptospirosis : guidance for diagnosis, surveillance and control.* Food and Agriculture Organization of the United Nations Rome, 1994.

[73] A.M.K. Mohan Rao. Preventive measures for leptospirosis: Rodent control. *Indian J Med Microbiol*, 24(4):325–328, 2006.

[74] S.P. Rodning, M.A. Edmondson, J.A. Gard, and A.S. Lovelady. Leptospirosis in cattle. *Alabama Cooperative Extension System*, Mar 2012.

[75] Factsheet: Leptospirosis. *New South Wales Public Health Bulletin*, 14(11-12):230–231, Nov-Dec 2003. Accessed: 2016-08-30.

[76] S. Rusbridge, G. Caldow, M. Crawshaw, and G. Gunn. *Leptospira hardjo infection in cattle*. SAC Consulting, Mar 2004.

[77] J.C. Murphy and R. Jensen. Experimental pathogenesis of leptospiral abortion in cattle. *Am. J. vet. Res*, 30:703–713, 1969.

[78] Leptospirosis: Working with dairy cattle - information sheet. Information sheet, Work Safe New Zealand, June 2016.

[79] S. R. R. Haskell, editor. *Blackwell's Five-Minute Veterinary Consult: Ruminant*. Food and Agriculture Organization of the United Nations Rome, 1994.

[80] S. Niewiesk. Maternal antibodies: Clinical significance, mechanism of interference with immune responses, and possible vaccination strategies. *Front. Immunol.*, 5:446, September 2014.

[81] E. Valle, C. Heuer, J.M. Collins-Emerson, J. Benschop, and P.R. Wilson. Serological patterns, antibody half-life and shedding in urine of leptospira spp. in naturally exposed sheep. *N Z Vet J.*, 63(6):301–12, Nov 2015.

[82] F. Fang. *Leptospirosis diagnostics and exposure at the human and animal interface in New Zealand*. PhD thesis, Institute of Veterinary, Animal and Biomedical Sciences, Massey University, Palmerston North, New Zealand, 2014.

[83] R. Wesselink, K.J. Stafford, D.J. Mellor, S. Todd, and N.G. Gregory. Colostrum intake by dairy calves. *New Zealand Veterinary Journal*, 47:31–34, 1999.

[84] A. Director, B. Penna, C. Hamond, A.P. Loureiro, G. Martins, M.A. Medeiros, and W. Lilenbaum. Isolation of *Leptospira interrogans* Hardjoprajitno from vaginal fluid of a clinically healthy ewe suggests potential for venereal transmission. *Journal of Medical Microbiology*, 63:12341236, 2014.

[85] C. Dalton. *Sheep Farm Husbandry - Reproduction and the ram*. Woolshed1, 2009. Accessed: 2016-11-26, from `http://woolshed1.blogspot.co.nz/2009/01/sheep-farm-husbandry-reproduction-and.html`.

[86] A. Fall, M. Diop, J. Sandford, Y.J. Wissocq, J. Durkin, and J.C.M. Trail. *Evaluation of the productivities of Djallonke sheep and N'Dama cattle at the Centre de Recherches Zootechniques, Kolda, Senegal - ILCA Research Report No. 3.* Food and Agriculture Organization of the United Nations - International Livestock Centre for Africa, Sept. 1982.

[87] T.G. Harvey and R.L. Baker. Performance of visually or objectively culled ewe hoggets. *Proceedings of the New Zealand Society ofAnimal Production*, 49:215–219, 1989.

[88] M. G. Roberts. The pluses and minuses of R_0.

[89] Factsheet: Shelter. Fact sheet, Beef+Lamb New Zealand, May 2017.

[90] Work Safe New Zealand. *Prevention and Control of Leptospirosis: Good Practice Guidelines.* August 2015. ISBN 978-0-908-33603-6 (online).

[91] Leptospirosis: Working with sheep - information sheet. Information sheet, Work Safe New Zealand, June 2016.

[92] A Cook. 'Alarming' spike in leptospirosis infection. *Radio New Zealand*, July 2017.

[93] P.R. Brown and G.R. Singleton. Rate of increase as a function of rainfall for house mouse *Mus domesticus* populations in a cereal-growing region in southern Australia. *Journal of Applied Ecology*, 36:484–493, 1999.

[94] *Rats.* Kiwicare. Accessed: 2017-05-22, from `http://www.kiwicare.co.nz/help/problem/?sid=pests-rats`.

[95] *Rats.* Department of Conservation, 2017. Accessed: 2017-05-22, from `http://www.doc.govt.nz/nature/pests-and-threats/animal-pests/rats/`.

[96] *Rat facts.* Predator Free NZ, 2016. Accessed: 2017-05-22, from `http://predatorfreenz.org/whats-the-story-about-rats/`.

[97] S. Idan. *Behavioural ecology of New Zealand invasive rodents (Rattus norvegicus and Mus musculus) : implications for rodent control.* PhD thesis, Ecology, Massey University, Auckland, New Zealand, 2013.

[98] Introduced rodents. Factsheet: Rs0023, Department of conservation, Christchurch, 2006.

[99] M.E. Carter and D.O. Cordes. Leptospirosis and other infections of *Rattus rattus* and *Rattus norvegicus*. *New Zealand Veterinary Journal*, 28(3):45–50, Mar 1980.

[100] R.E. Brockie. Leptospiral infections of rodents in the North Island. *New Zealand Veterinary Journal*, 25(4):89–96, 1977.

[101] S.C. Hathaway. *Leptospirosis in free-living animals in New Zealand, with particular reference to the possum (Trichosurus Vulpecula)*. PhD thesis, Massey University, Palmerston North, New Zealand, 1978.

[102] B. Adler, editor. *Current Topics in Microbiology and Immunology: Leptospira and Leptospirosis*, volume 387. Springer, 2015.

[103] John Hopkins University. *Animal Care and Use Committe - The Rat*. Accessed: 2018-06-22, from `http://web.jhu.edu/animalcare/procedures/rat.html`.

[104] *Animal pests A - Z*. Department of Conservation. Accessed: 2018-01-15, from `http://www.doc.govt.nz/nature/pests-and-threats/animal-pests/`.

[105] Leptospirosis. Fact sheet, Community and Public Health (CDHB), April 2017.

[106] *How do people get leptospirosis?* Leptospirosis.org.nz. Accessed: 2018-09-30, from `http://leptospirosis.org.nz/Leptospirosis/Human.aspx`.

[107] C.L. Lau, C.H. Watson, J.H. Lowry, M.C. David, S.B. Craig, S.J. Wynwood, and et al. Human leptospirosis infection in Fiji: An eco-epidemiological approach to identifying risk factors and environmental drivers for transmission. *PLoS Negl Trop Dis*, 10(1), 2016.

[108] J.F. Cosson, M. Picardeau, M. Mielcarek, C. Tatard, Y. Chaval, Y. Suputtamongkol, and S. Morand. Epidemiology of leptospira transmitted by rodents in Southeast Asia. *PLoS Neglected Tropical Diseases*, 8(6):e2902, 2014.

[109] Wellington: Ministry of Health. *Communicable Disease Control Manual*, May 2018.

[110] V. Tapaleao. Fun in the sun for rodent pests. *NZ Herald*, Mar 2013.

[111] Companion Animals in New Zealand 2016. Technical report, New Zealand Companion Animal Council Inc., June 2016.

[112] N Barnett. Why the fall in cat and dog ownership? *Stuff.co.nz*, June 2017.

[113] N. Pryor. Slum warning over Auckland CBD. *Radio New Zealand*, Sept 2014.

[114] Auckland's homeless problem could turn areas into slums. *Newstalk ZB*, May 2016. `https://www.newstalkzb.co.nz/news/national/aucklands-homeless-problem-could-turn-areas-into-slums/`.

[115] Newshub. The seven steps to healthier New Zealand waterways. *newshub.co.nz*, Jun 2017.

[116] J. Morton. Campaign to clean up waterways. *NZ Herald*, Jan 2016.

[117] Govt plans to make 90% of NZ waterways swimmable by 2040. *Radio New Zealand*, Feb 2017.

[118] *Clean rivers for future generations*. Labour, 2018. Accessed: 2018-11-18, from `https://www.labour.org.nz/water`.

[119] Why should you pay to clean up New Zealands waterways? *Million Metres Streams Project*, Mar 2018.

[120] R. Clayton. Group collaborates to clean up waterways and restore native bush. *Stuff.co.nz*, Mar 2018.

[121] J. Clark. New technologies helping clean up NZ's waterways. *NZTech*, Aug 2018.

[122] Paul N. Levett. Leptospirosis. *Clinical Microbiology Reviews*, 14(2):296–326, 2001.

[123] Leptospirosis in New Zealand dairy herds. Technical bulletin, Schering-Plough Animal Health. `http://www.msd-animal-health.co.nz/binaries/21628_leptavoid_tech_bulletin_v1_1__tcm51-37432.pdf`.

[124] K. Taylor. Leptospirosis could affect dairy growth. *NZ Farmer*, November 2014.

[125] *Leptospirosis information: Overview of human leptospirosis guide for the public.* Leptospirosis Information Center, 2011. Accessed: 2018-09-18, from `http://www.leptospirosis.org/human-leptospirosis-guide/`.

[126] A. Spichler, D. Athanazio, A.C. Seguro, and J.M. Vinetz. Outpatient follow-up of patients hospitalized for acute leptospirosis. *International Journal of Infectious Diseases*, 15(7):e486 – e490, Jul 2011.

[127] D. A. Haake and P. N. Levett. Leptospirosis in humans. *Current Topics in Microbiology and Immunology*, 387:65 – 97, 2015.

[128] C. Nordqvist. Leptospirosis: What you need to know. *Medical News Today*, Aug 2018.

[129] *Which animals can infect people with leptospirosis?* Leptospirosis.org.nz. Accessed: 2018-09-18, from `http://leptospirosis.org.nz/Leptospirosis/Pets.aspx`.

[130] T. R. Fraga, A. S. Barbosa, and L. Isaac. Leptospirosis: Aspects of innate immunity, immunopathogenesis and immune evasion from the complement system. *Scandinavian Journal of Immunology*, 73(5):408–419, 5 2011.

[131] G. Naheed and J.A. Khan. Poison-shyness and bait-shyness developed by wild rats (*Rattus rattus* L.). I. Methods for eliminating shyness caused by barium carbonate poisoning. *Applied Animal Behaviour Science*, 24(2):89–99, 1989.